REPORT UAG - 24
PART II

WORLD DATA CENTER A
for
Solar-Terrestrial Physics

DATA ON SOLAR - GEOPHYSICAL ACTIVITY ASSOCIATED WITH THE MAJOR GROUND LEVEL COSMIC RAY EVENTS OF 24 JANUARY AND 1 SEPTEMBER 1971

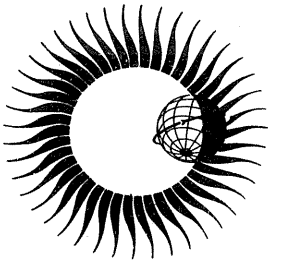

DECEMBER 1972

WORLD DATA CENTER A

National Academy of Sciences
2101 Constitution Avenue, N. W. Washington, D. C. U.S.A., 20418

World Data Center A consists of the Coordination Office

and eight subcenters:

World Data Center A
Coordination Office
National Academy of Sciences
2101 Constitution Avenue, N.W.
Washington, D. C., U.S.A. 20418
Telephone (202) 961-1478

Solar and Interplanetary Phenomena, Ionospheric Phenomena, Flare-Associated Events, Geomagnetic Variations, Magnetospheric and Interplanetary Magnetic Phenomena, Aurora, Cosmic Rays, Airglow:
World Data Center A
for Solar-Terrestrial Physics
National Oceanic and Atmospheric Administration
Boulder, Colorado, U.S.A. 80302
Telephone (303) 499-1000 Ext. 6467

Geomagnetism, Seismology, Gravity (and Upper Mantle Project Archives):
World Data Center A:
Geomagnetism, Seismology and Gravity
Environmental Data Service, NOAA
Boulder, Colorado, U.S.A. 80302
Telephone (303) 499-1000 Ext. 6311

Glaciology:
World Data Center A:
Glaciology
U. S. Geological Survey
1305 Tacoma Avenue South
Tacoma, Washington, U.S.A. 98402
Telephone (206) 383-2861 Ext. 318

Longitude and Latitude:
World Data Center A:
Longitude and Latitude
U. S. Naval Observatory
Washington, D. C., U.S.A. 20390
Telephone (202) 698-8422

Meteorology (and Nuclear Radiation):
World Data Center A:
Meteorology
National Climatic Center
Federal Building
Asheville, North Carolina, U.S.A. 28801
Telephone (704) 254-0961

Oceanography:
World Data Center A:
Oceanography
National Oceanic and Atmospheric Administration
Rockville, Maryland, U.S.A. 20852
Telephone (202) 426-9052

Rockets and Satellites:
World Data Center A:
Rockets and Satellites
Goddard Space Flight Center
Code 601
Greenbelt, Maryland, U.S.A. 20771
Telephone (301) 982-6695

Tsunami:
World Data Center A:
Tsunami
National Oceanic and Atmospheric Administration
P.O. Box 3887
Honolulu, Hawaii, U.S.A. 96812
Telephone (808) 546-5698

Notes:

(1) World Data Centers conduct international exchange of geophysical observations in accordance with the principles set forth by the International Council of Scientific Unions. WDC-A is established in the United States under the auspices of the National Academy of Sciences.
(2) Communications regarding data interchange matters in general and World Data Center A as a whole should be addressed to: World Data Center A, Coordination Office (see address above).
(3) Inquiries and communications concerning data in specific disciplines should be addressed to the appropriate subcenter listed above.

WORLD DATA CENTER A
for
Solar-Terrestrial Physics

REPORT UAG - 24 PART II

DATA ON SOLAR - GEOPHYSICAL ACTIVITY ASSOCIATED WITH THE MAJOR GROUND LEVEL COSMIC RAY EVENTS OF 24 JANUARY AND 1 SEPTEMBER 1971

compiled by

Helen E. Coffey and J. Virginia Lincoln
WDC-A for Solar-Terrestrial Physics
Boulder, Colorado

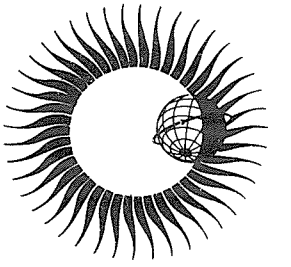

Prepared by World Data Center A for
Solar-Terrestrial Physics, NOAA, Boulder, Colorado
and published by

U.S. DEPARTMENT OF COMMERCE
NATIONAL OCEANIC AND ATMOSPHERIC ADMINISTRATION

ENVIRONMENTAL DATA SERVICE
Asheville, North Carolina, USA 28801

DECEMBER 1972

SUBSCRIPTION PRICE: $9.00 a year; $2.50 additional for foreign mailing; single copy price varies.* Checks and money orders should be made payable to the Department of Commerce, NOAA. Remittance and correspondence regarding subscriptions should be sent to the National Climatic Center, Federal Building, Asheville, NC 28801, Attn: Publications.

*PRICE THIS ISSUE $2.00

TABLE OF CONTENTS

		Page
PART I	JANUARY EVENT	
	FOREWORD	
1.	INTRODUCTION AND BACKGROUND DATA	1
2.	SOLAR REGION OF JANUARY 1971	7
3.	SOLAR RADIO EVENTS	61
4.	SPACE OBSERVATIONS	100
5.	COSMIC RAYS	134
6.	IONOSPHERE	200
7.	AURORA	247
8.	GEOMAGNETISM	261
PART II	SEPTEMBER EVENT	
1.	INTRODUCTION AND BACKGROUND DATA	299
2.	SOLAR REGION OF SEPTEMBER 1971	303
3.	SOLAR RADIO EVENTS	318
4.	SPACE OBSERVATIONS	362
5.	COSMIC RAYS	370
6.	IONOSPHERE	404
7.	AURORA	443
8.	GEOMAGNETISM	446
	ACKNOWLEDGEMENTS	456
	ALPHABETICAL INDEX	456
	AUTHOR INDEX	461

Table of Contents (Continued)

		Page	
PART II			
1.	INTRODUCTION AND BACKGROUND DATA	299	
2.	SOLAR REGION OF SEPTEMBER 1971		
	"Sunspots and H-alpha Plage in McMath Region #11482" (Patrick S. McIntosh)	303	
	"Large-Scale Magnetic Field and Activity Distribution Connected with the Proton-Flare of September 1, 1971 Region" (V. Bumba and J. Sýkora)	311	
3.	SOLAR RADIO EVENTS		
	"Early Development of Radio Emission from MMH 11482" (D. S. Lund)	318	
	"The Microwave Sun at the Time of the Cosmic Ray Increase of September 1, 1971" (J. H. Deuter and R. N. Bracewell)	325	
	"Centimeter Wavelength Observations of the Behind-the-Limb Flare of 1 September 1971" (Fred L. Wefer)	327	
	"On the S-Component and Noise Storms in September, 1971" (A. Böhme and A. Krüger)	334	
	"Millimeter Wave Spectroheliograms Associated with the September 1, 1971 Solar Terrestrial Event" (Larry E. Telford)	338	
	"Dynamic Radio Spectra of the Solar Flare of 1971 September 1 1930 UT" (A. Maxwell)	346	
	"September 1, 1971 Solar Radio Burst Observations" (W. R. Barron)	348	
	"Analysis of the Polarization of the Solar Radio Emission at 237 MHz, during the Period 17-31 August 1971, Coming from the McMath Region 11482, Responsible for the Event of September 1, 1971" (Paolo Santin)	349	
	*"The Slowly Varying Component of the Frequencies of 2695 MHz, 606 MHz and 536 MHz during the Period of the Proton Flare Events of January 24 and September 1, 1971" (A. Tlamicha and J. Olmr)	77	Part I
	"Radio Bursts Associated with Solar Proton Flare on September 1, 1971" (Kunitomo Sakurai)	353	
	"VLF and Solar Observations during the Event of September 1, 1971" (S. Ananthakrishnan, D. Basu, L. R. Piazza and M.E.Z. Mellone)	358	
4.	SPACE OBSERVATIONS		
	"Solar X-ray and Ultraviolet Emission on September 1, 1971" (D. M. Horan, R. W. Kreplin and R. G. Taylor)	362	
	*"IMP V Observations on the Solar Flare Particle Events of January 24 and September 1, 1971" (M. Van Hollebeke, J. R. Wang and F. B. McDonald)	102	Part I
	"Proton and Alpha Particle Fluxes Measured Aboard OV5-6" (G. K. Yates, J. G. Kelley, B. Sellers and F. A. Hanser)	365	
	"Solar Wind Plasma Observations Subsequent to the Solar Proton Event of September 1, 1971" (H. C. Howe, J. H. Binsack and H. S. Bridge)	367	
5.	COSMIC RAYS		
	"Tables of Neutron Monitor Data and Selected Graphs for the September 1, 1971 Event" (Helen E. Coffey)	370	
	"Relativistic Solar Cosmic Rays from the Invisible Disk on September 1-2, 1971" (S. P. Duggal and M. A. Pomerantz)	389	
	"The Flare of Cosmic Rays on September 1, 1971" (N. P. Chirkov, A. M. Novikov, G. V. Skripin, G. G. Todikov and A. T. Filippov)	396	
	*"Upper Cutoff in the Proton Spectrum of January 24 and September 1, 1971 Events" (Dj. Heristchi, J. Perez Peraza and G. Trottet)	182	Part I

* Article covers both the January and September events.

Table of Contents (Continued)

	Page
"The Ground Level Cosmic Ray Increase of September 1, 1971 Recorded by the Neutron Monitor in Bergen, Norway" (R. Amundsen and H. Trefall)	400
"Scintillation Monitor, Bologna, Italy, 15-Minute Observations" (M. Galli, L. Fiandri and M. R. Attolini)	401
6. IONOSPHERE	
"The September 1, 1971 Solar Cosmic Ray Event" (A. J. Masley)	404
"30 MHz Riometer Data for September 1971 Solar Particle Event" (Raymond J. Cormier)	406
"Polar Cap Absorption of September 1, 1971 by Riometer Data in the Arctic and Antarctic" (V. M. Driatsky and V. A. Ulyev)	407
"Ground Based Ionospheric Observations from the Danish Geophysical Observatories in Greenland during the September 1 Event 1971" (J. Taagholt and V. Neble Jensen)	410
"Ionospheric Observations in Kiruna of the PCA Event of 1 Septmeber 1971" (C. Jurén and J. Svennesson)	417
"Effects of the September 1971 Solar Particle Event on Polar VLF Propagation" (John P. Turtle)	424
"Mid-Latitude Total Electron Content during Cosmic Ray Event September 1-2, 1971" (J. A. Klobuchar and M. J. Mendillo)	426
"Polar Cap Disturbances of September 1, 1971, Observed on the Phase of VLF Waves" (Y. Hakura, T. Ishii, T. Asakura and Y. Terajima)	427
"Report on Ionospheric and Whistler Activity at the Panská Ves and Průhonice Observatories on September 1, 1971" (F. Jiricek, J. Lastovicka and P. Triska)	430
"Solar Particle Events in the Ionosphere during the Period of September 1-8, 1971" (P. Velinov and G. Nestorov)	432
"The Effects of a Solar Proton Event and Associated Geomagnetic Disturbance on the Phase of VLF Signals Received at Leicester, UK" (J. W. Chapman and R. E. Evans)	440
7. AURORA	
"The Auroral-zone Effects of the September 1 Event Over Cola Peninsula" (B. E. Brunelli, L. S. Evlashin, S. I. Isaev, L. L. Lazutin, G. A. Loginov, G. A. Petrova, V. K. Roldugin, N. V. Shulgina, G. V. Starkov, G. F. Totunova and E. V. Vasheniuk)	443
8. GEOMAGNETISM	
"K-Indices for August 23 - September 11, 1971" (D. van Sabben)	446
"Provisional Equatorial Dst" (M. Sugiura)	450
*"Solar Wind Velocities and Geomagnetic Activity Associated with the Cosmic Ray Increases of January 24 and September 1, 1971" (S. Krajcovic)	264 Part I
*"Recurrent Tendencies in Geomagnetic Activity at the Time of Increased Cosmic Radiation at the Earth's Surface on 24 January and 1 September, 1971" (Jaroslav Halenka)	268 Part I
"Geomagnetically Active Plages and Flares Observed during the Interval Including September 1, 1971" (M. C. Ballario)	451
*"Comments on the Special Intervals of January 24 and September 1, 1971" (Bohumila Bednárová-Nováková)	277 Part I
*"On Geomagnetic Pulsations at the Time of Solar-Terrestrial Events of January 24, 1971 and September 1, 1971 at the Budkov Observatory" (Karel Prikner)	283 Part I

* Article covers both the January and September events.

1. INTRODUCTION AND BACKGROUND DATA

by

Helen E. Coffey
World Data Center A for Solar-Terrestrial Physics
NOAA, Boulder, Colorado 80302

General Activity

The sun on September 1, 1971 was relatively quiet. Since no large flare occurred on the visible solar disk, it is proposed that a large flare occurred in McMath Region 11482, a very active region which passed over the West limb three days earlier. Figure 1 shows this region at central meridian passage (August 23.8). Figure 2 shows the activity on the visible disk on September 1, 1971.

An historical review of McMath Region 11482 is given in Table 1:

Table 1

McMath Region 11482 CMP Date 23.8 Return of Region 11445 Rotation 2

				Calcium Page Data						Sunspot Data								9.1 cm	
YR	MO	DA	MC NO.	LAT	CMD	L	AREA	INT	MW NO.	LAT	CMD	L	MAG.	H	AREA	CNT	C	INT	FLUX
71	8	17	11482	S13	E85	268	900	3.5	18538	S13	E80	272	(αp)	4	310	7	H	29	9
		18		S13	E71	269	2000	4.0		S13	E70	269	(βp)	4	470	47	F	58	18
		19		S13	E58	268	3500	3.5		S13	E58	268	(δ)	6	180	40	F	69	21
		20		S13	E43	270	4000	3.5		S13	E42	270	(δ)	6	240	67	F	99	31
		21		S12	E30	269	4800	3.0		S12	E26	270	(δ)	6					
		22		S12	E17	270	4700	3.5		S12	E15	270	(βp)	6					
		23		S12	E04	270	4800	3.5		S12	E01	271	(βγ)	6	610	23	F	84	26
		24		S12	W08	268	4400	3.5		S12	W12	271	(δ)	6	530	36	F	96	29
		25		S12	W20	268	4600	3.5		S12	W25	270	(βp)	6	180	26	E	83	25
		26		S12	W35	269	4400	3.5		S13	W39	270	(βγ)	5	0	29	F		
		27		S12	W50	270	4600	3.5		S13	W52	271	(βγ)	5	900	63	F	70	22
		28		S12	W63	269	4500	3.0		S13	W65	270	(βp)	5	730	52	F		
		29		S12	W74	269	3800	2.5		S12	W78	270	(βp)	5					
		30		S11	W88	270	3000	2.5		S14	W88	268		0					

The final Relative Sunspot Numbers (R_z) and the observed 2800 MHz flux (S_a) for the period August 29 - September 5, 1971 are given below; the monthly means for September are: $\overline{R}_z$ = 50.2, $\overline{S}_a$ = 105.1.

	R_z	S_a		R_z	S_a
Aug. 29	29	112.0	Sept. 2	19	90.1
30	21	103.3	3	26	92.5
31	21	96.3	4	29	92.6
Sept. 1	22	90.3	5	42	95.2

A small confirmed grouped flare, Group 40225, occurred at 2045 UT on September 1 in Region 11496. This, however, was not considered large enough to be responsible for the cosmic ray ground-level increase around 2200 UT.

AUGUST 24, 1971 (P = 18.71, B_o = 7.00, L_o = 266.61)

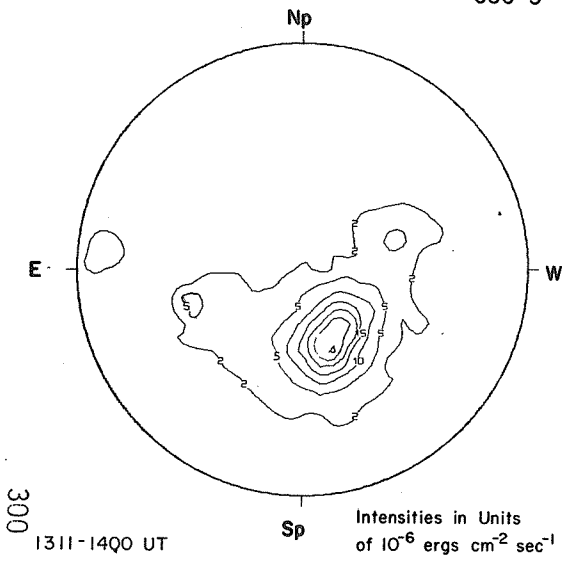

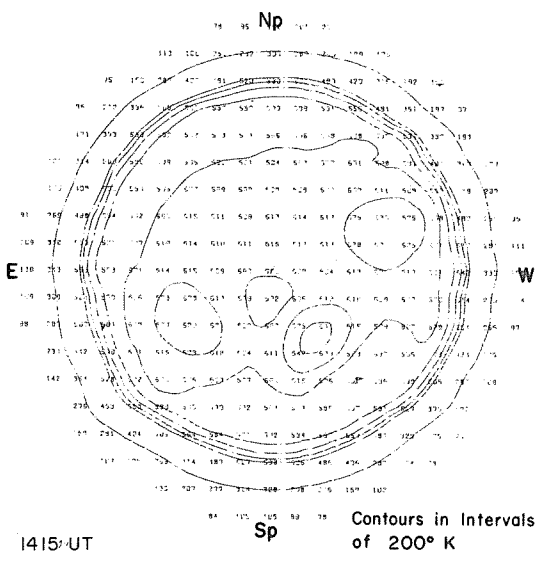

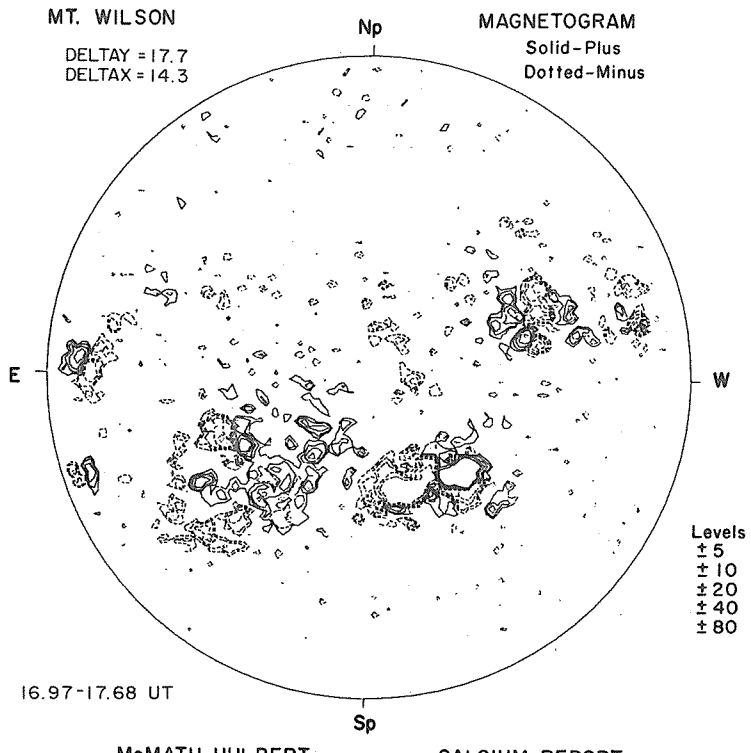

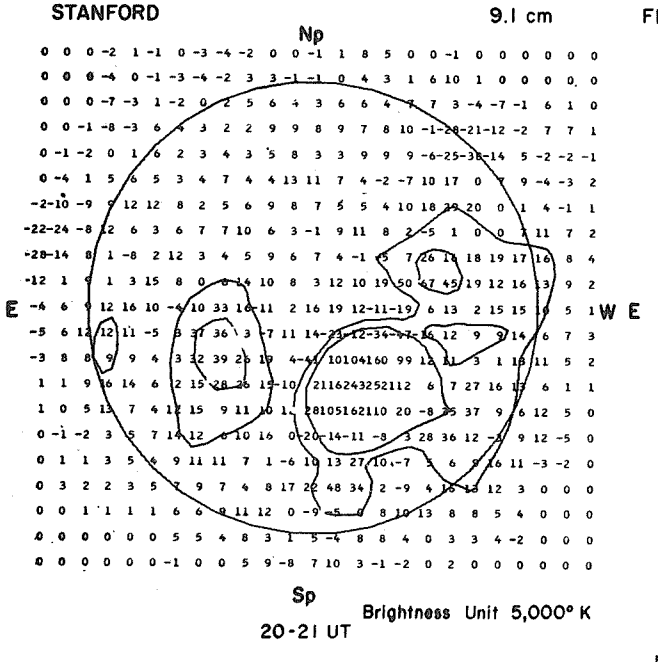

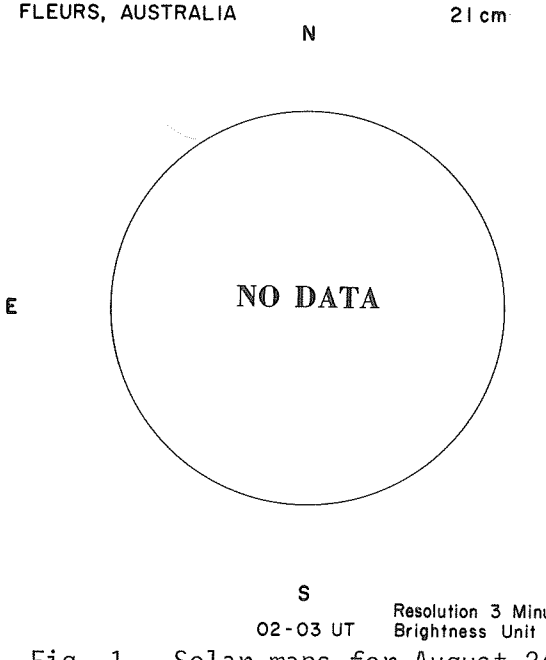

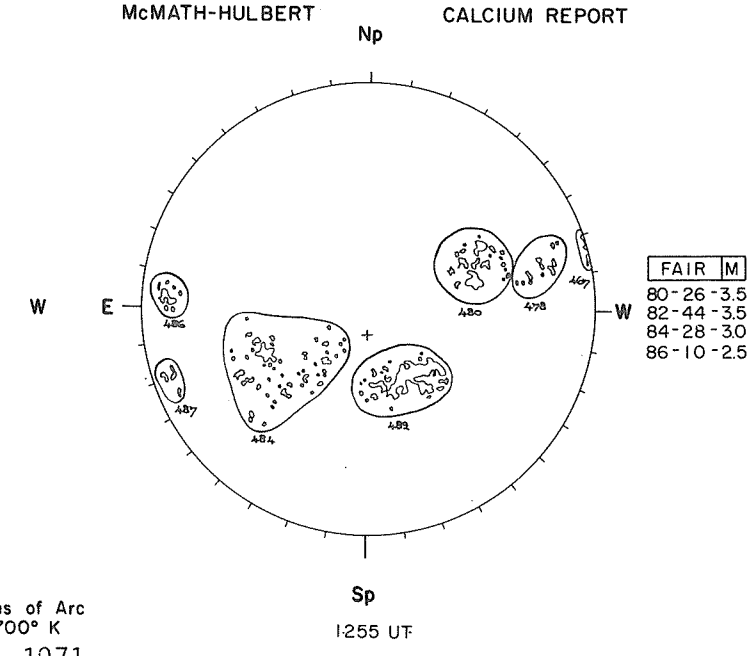

Fig. 1. Solar maps for August 24, 1971.

SEPTEMBER 1, 1971 (P = 20.95, B_o = 7.19, L_o = 160.92)

UNIV. COLLEGE LONDON
LEICESTER UNIV.
X-RAY
OSO-5

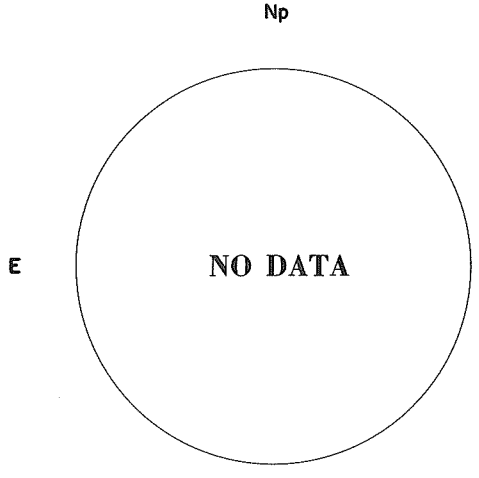

Intensities in Units of 10^{-6} ergs cm^{-2} sec^{-1}

PROSPECT HILL
AFCRL
8.6 mm

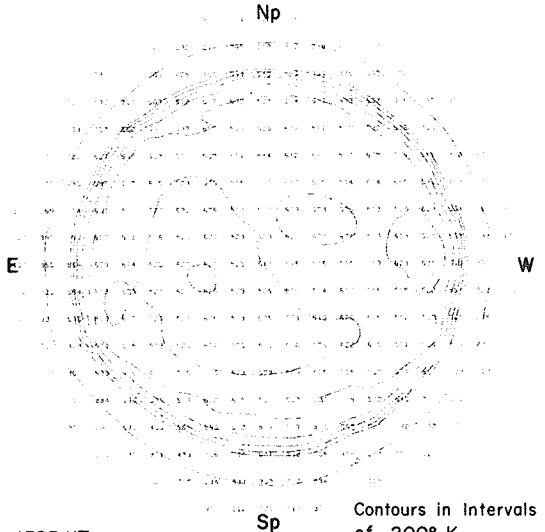

1525 UT

Contours in Intervals of 200° K

MT. WILSON
MAGNETOGRAM
Solid-Plus
Dotted-Minus

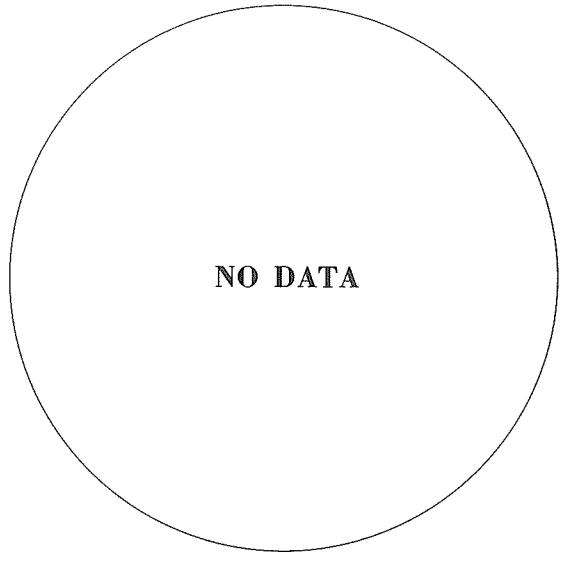

Levels
±5
±10
±20
±40
±80

STANFORD
9.1 cm

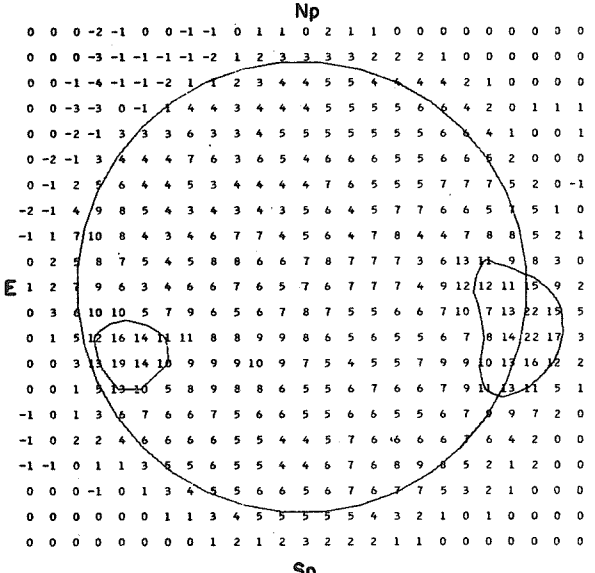

20-21 UT

Brightness Unit 5,000° K

FLEURS, AUSTRALIA
21 cm

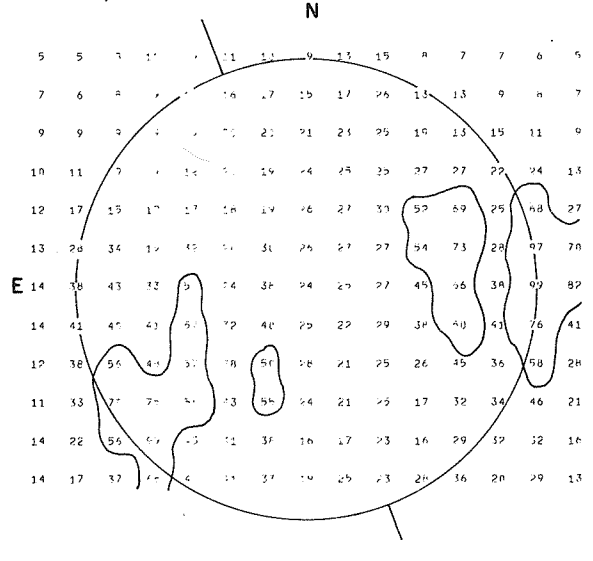

02-03 UT

Resolution 3 Minutes of Arc
Brightness Unit 1,700° K

McMATH-HULBERT
CALCIUM REPORT

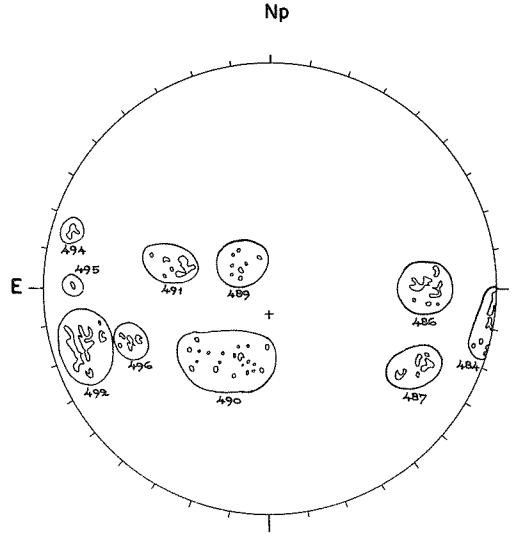

V POOR	M
86-13-3.0	
92-25-2.5	

1340 UT

Fig. 2. Solar maps for September 1, 1971.

Spectral observations at the time of the ground-level increase are as follows:

SOLAR RADIO EMISSION
SPECTRAL OBSERVATIONS
SEPTEMBER 1971

SEP. 1971	TIMES OF OBSERVATION START UT	TIMES OF OBSERVATION END UT	STATION	EVENTS: CENTIMETRIC BAND START UT	CENTIMETRIC BAND END UT	CENTIMETRIC BAND INT.	DECIMETRIC BAND START UT	DECIMETRIC BAND END UT	DECIMETRIC BAND INT.	METRIC BAND START UT	METRIC BAND END UT	METRIC BAND INT.	DEKAMETRIC BAND START UT	DEKAMETRIC BAND END UT	DEKAMETRIC BAND INT.	SPECTRAL TYPE
01	1300	2400	HARV				1934		1	1933.8	1948	3	1934.8	1946	3	II
	1230	2400	BOUL							1934.2	1935.4	2	1934.2	1935.4	2	III
	0953	2304	SGMR										1934.2	1936.3	2	IIIG
			HARV				1934.5	1950	2							IV
			SGMR										1937.0	1946.9	2	IV
			BOUL							1937.5	2009.5	2	1937.5	2009.5	2	IV
			SGMR										1950.2	2002.3	1	CONT
	2033	2400	CULG							2034	2037	1				I
02	0000	0129	CULG													
	0000	0130	BOUL													
	0000	0101	HARV													
	0204	0731	CULG													
	0520	1730	HEIS													
	0938	2313	SGMR													
	1230	2400	BOUL													
	1300	2400	HARV													
	2032	2400	CULG													

Outstanding solar radio emission occurrences on September 1-2, 1971 are shown in Table 2.

Table 2

SOLAR RADIO EMISSION
OUTSTANDING OCCURRENCES
SEPTEMBER 1971

SEP. 1971	FREQUENCY STATION	TYPE	STARTING TIME UT	TIME OF MAXIMUM UT	DURATION MINUTES	FLUX DENSITY 10^{-22} Wm^{-2} Hz^{-1} PEAK	FLUX DENSITY MEAN	INT	REMARKS
1	2800 OTTA	29	1950		40	13.8	3.9		
	7000 SAOP	29	1953		12				
	18 BOUL	48	1958	2005	11			3	
	18 MCMA	48	1958	2004	15			3	
	1415 SGMR	29	2000.7	2000.7	32.7	15.4	7.7		
	606 SGMR	29	2000	2000	37	14.7	7.3		
	2695 SGMR	29	2002.2	2002.2	27.8U	13.0	5.5		
	960 PENN	29	2010	2010	110 D	5.8	2.9		
	2700 PENN	29	2012.1	2012.1	135 D	9.8	4.9		
	2695 BOUL	40	2125.5	2127	3.5	30.0			
	2695 BOUL	40	2156	2156.5	5.5	108.0			
	184 BOUL	42	2226	2248	125			1	
2	930 BORD	40	0931	0932.2	2	11.0	2.0		
	930 BORD	45	0940	0940.8	1	7.0	2.0		
	930 BORD	3	1015	1016	1	11.0	1.0		
	536 ONDR	5	1205.5E	1212	6.5	60.0			
	808 ONDR	1	1210	1212	2.5				
	930 BORD	40	1400	1401.4	2	7.0	2.0		
	184 BOUL	42	1936	2107	106			2	
	2695 BOUL	41	2243.5	2245.5	4.5	36.0			

Magnetic activity is indicated in the following chart. An sc followed by a magnetic storm occurred at 1646 UT on September 4, 1971, reported by 22 stations (ssc: 22[A: 3; B: 13; C: 6]; si: A: 2). Storm data follows:

PRINCIPAL MAGNETIC STORMS
SEPTEMBER 1971

DATE 1971 MO DA	STORM TIME UT START	STORM TIME UT END MO DA HR	OBS	GEO-MAG LAT.	SUDDEN COMMENCEMENT TYPE	AMPLITUDES D(')	AMPLITUDES H(γ)	AMPLITUDES Z(γ)	C FIGURE DEGREE OF ACTIVITY	MAXIMAL ACTIVITY ON K-SCALE 0 TO 9 MO DA	3-HOUR PERIOD	K INDEX	RANGES D (')	RANGES H (γ)	RANGES Z (γ)	STORM NUMBERS
09 04	1646	09 05 22	COLL	64.6N	SC *	+ 1	+16	- 8	MS	09 05	4.5.6	6	101	890	480	37
	1646	09 05 16	MBOR	21.3N	SC *	- 0.4*	+36	- 4		09 04	8	4	3	45	7	37
	1645	09 05 22	HYDE	7.6N	SC	- 0.1	+10	- 1	M	09 04	8	4	6	72	33	37
	1646	09 05 14	AABA	5.4N	SC	- 0.3	+11	- 3.5	-	-- --	-	-	---	---	---	37
	1646	09 05 21	HRMN	33.3S	SC	--	+ 5	--	M	09 04	8	5	14	67	67	37

2. SOLAR REGION OF SEPTEMBER 1971

Sunspots and H-alpha Plage in McMath Region #11482

by

Patrick S. McIntosh
NOAA Environmental Research Laboratories
Boulder, Colorado 80302

The ground-level cosmic ray event of 1 September 1971 occurred two days after the west-limb passage of McMath Region #11482, and since no active centers crossed east limb for five days following this activity, we must associate the GLE event with this region. This report presents the evolution of the active center as viewed in white light and H-alpha from observations obtained at NOAA-Boulder, Gran Canary Island (NASA/NOAA SPAN), Carnarvon, West Australia (NASA/NOAA SPAN), Culgoora, New South Wales (C.S.I.R.O.), Ramey Air Force Base, Puerto Rico (U.S.A.F. Air Weather Service), and the Sacramento Peak Observatory (Air Force Cambridge Research Laboratories) at Sunspot, New Mexico.

This active center, located at S12 and Carrington longitude 270, was formed on the visible disk during the previous solar rotation as McMath Region #11445. The small group was born on 25 July near the low-latitude terminus of a large quiescent filament and exhibited some growth on 30 July. The region returned to east limb on 17 August as a giant spot group still increasing in area. Maximum area was reached on 21 August at about 1700 millionths of the solar hemisphere. The central meridian aspect of this naked-eye group is presented in Figure 1 below.

It is well known that only a few of the very large sunspot groups are associated with particle-producing solar flares. In looking for some distinguishing characteristic for this region, we are attracted to the conspicuous sunspot motions that were visible during the entire disk passage of the region. This author has noted that unusually large motions of sunspots and sunspot rotation are characteristics that may be peculiar to particle-producing active regions [McIntosh, 1969, 1970]. The regions from which this conclusion was made were also notable for having complex magnetic field configurations, usually with the "delta" configuration of two large spots of opposite polarity enclosed in a common penumbra. We cannot identify such a complex configuration for this active center.

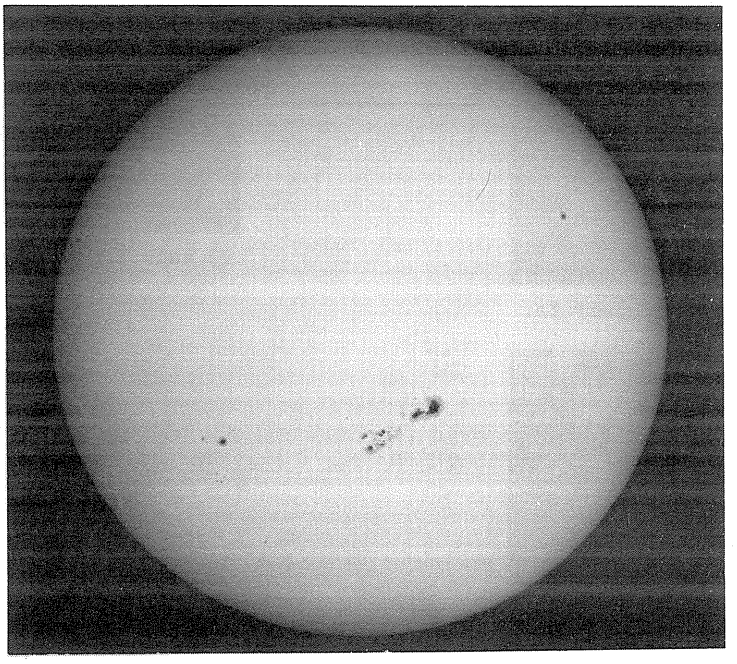

Fig. 1 The white-light patrol photograph from Culgoora, New South Wales (C.S.I.R.O., Australia) for 23 August 1971 at 2246 U.T. with the sunspots of McMath Region #11482 at central meridian. The orientation is geocentric with west to the right.

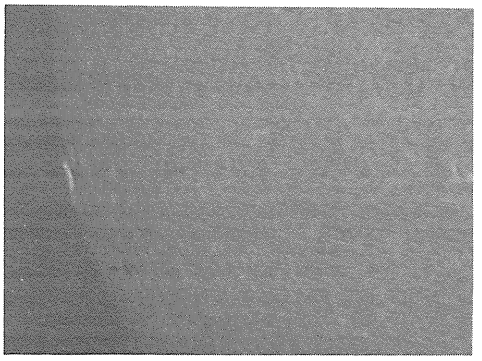

17 Aug. 71 1349 U.T. Ramey AFB

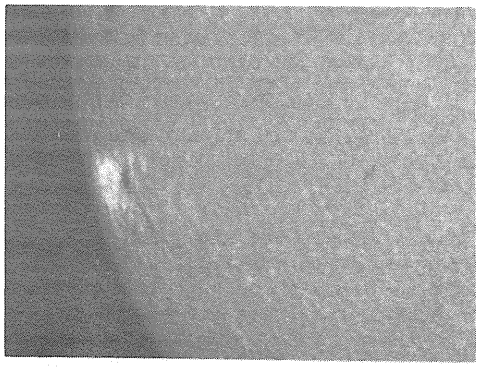

18 Aug. 71 1112 U.T. Ramey AFB

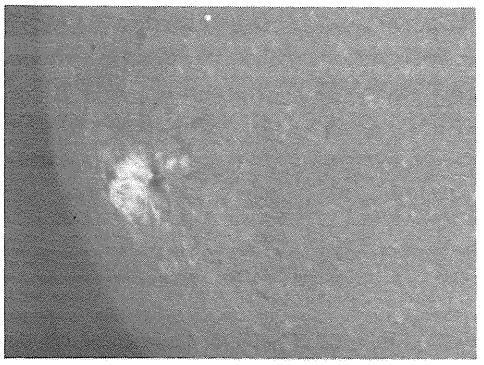

19 Aug. 71 0925 U.T. Canary Is.

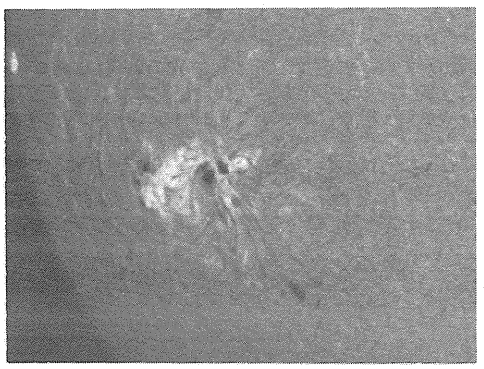

20 Aug. 71 0908 U.T. Canary Is.

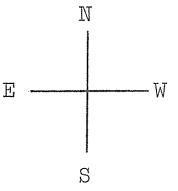

Heliographic

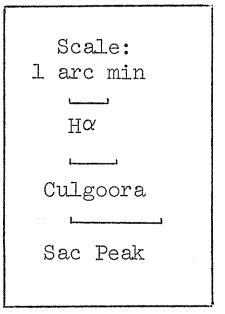

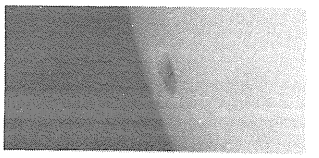

18 Aug. 71 0100 U.T. Culgoora

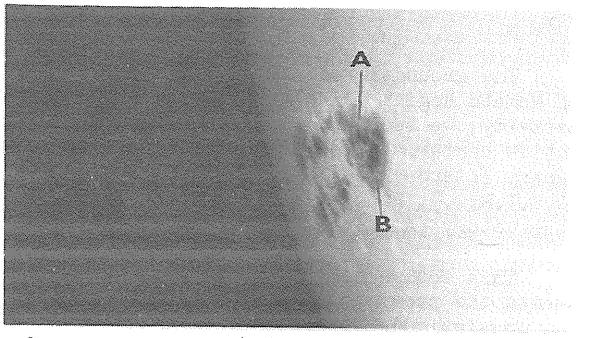

18 Aug. 71 1438 U.T. Sac Peak

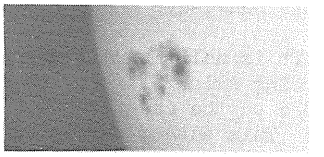

18 Aug. 71 2240 U.T. Culgoora

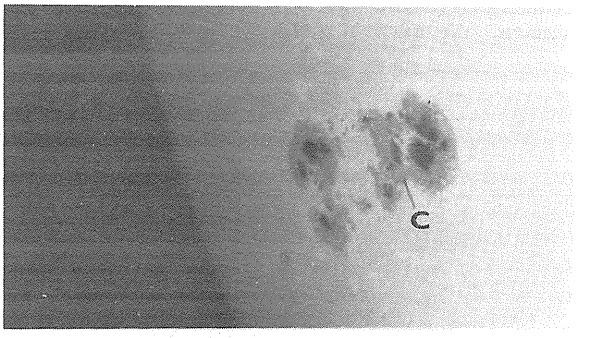

19 Aug. 71 1345 U.T. Sac Peak

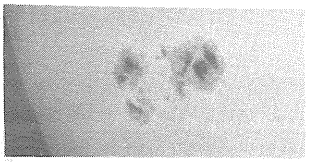

19 Aug. 71 2400 U.T. Culgoora

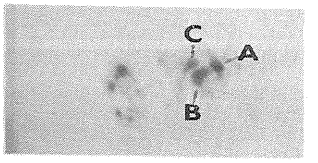

20 Aug. 71 0909 U.T. Canary Is.(Hα+1Å)

Fig. 2 H-alpha (left) and white light (right) patrol photographs for 17-20 August 1971 showing an expanding fibril field and sunspot rotation, respectively.

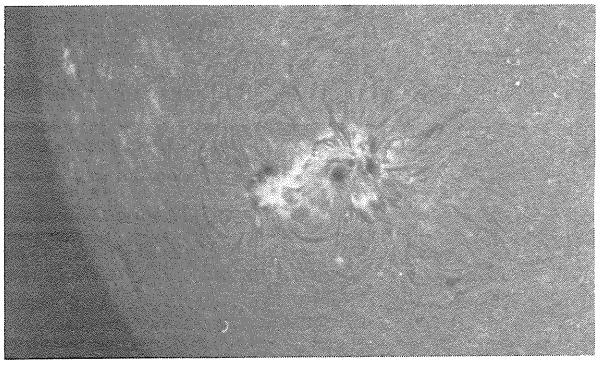

21 Aug. 71 0821 U.T. Canary Is.

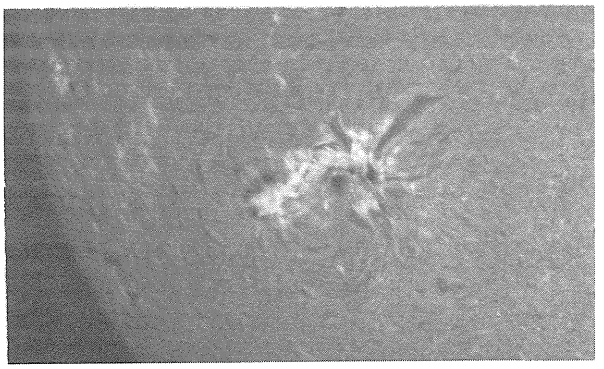

21 Aug. 71 1050 U.T. Ramey AFB

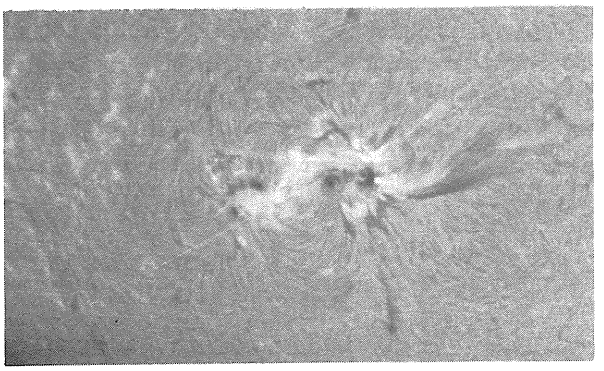

22 Aug. 71 0835 U.T. Canary Is.

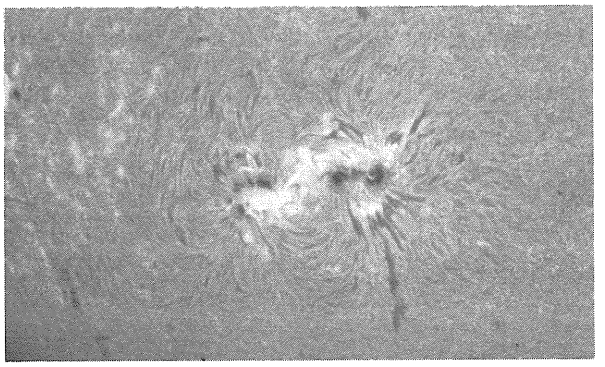

22 Aug. 71 1127 U.T. Ramey AFB

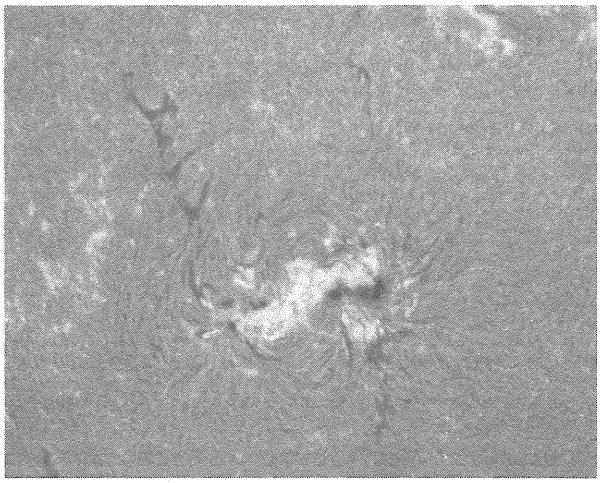

23 Aug. 71 1059 U.T. Ramey AFB

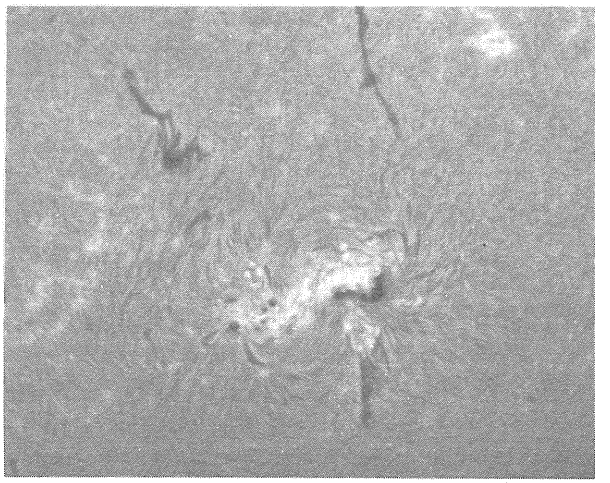

24 Aug. 71 1519 U.T. Ramey AFB

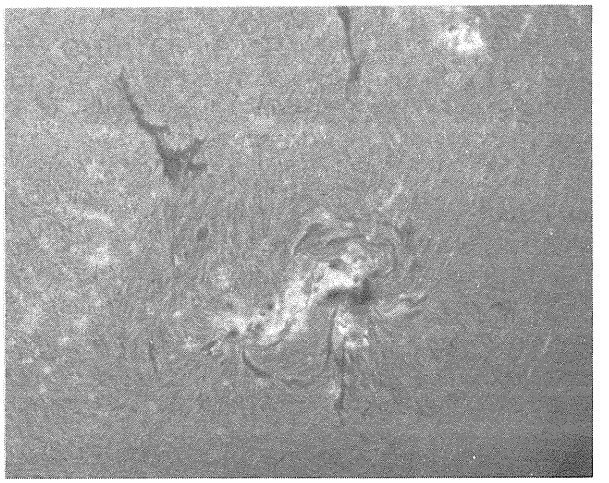

25 Aug. 71 1133 U.T. Ramey AFB

Fig. 3 Dark surge activity (left) and active filaments (right) were associated with the region in H-alpha observations.

20 Aug. 71 1600 U.T. Boulder

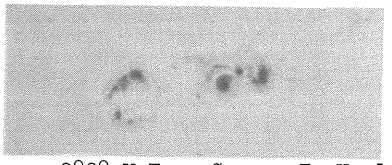

21 Aug. 71 0828 U.T. Canary Is. Hα+1Å

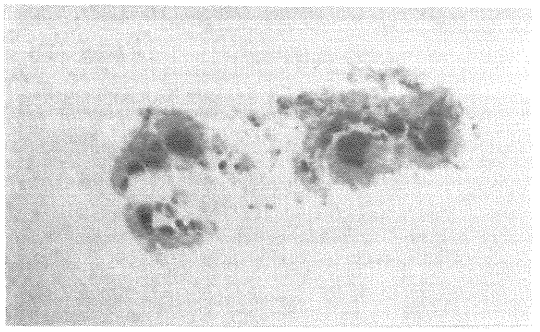

21 Aug. 71 1355 U.T. Sac Peak

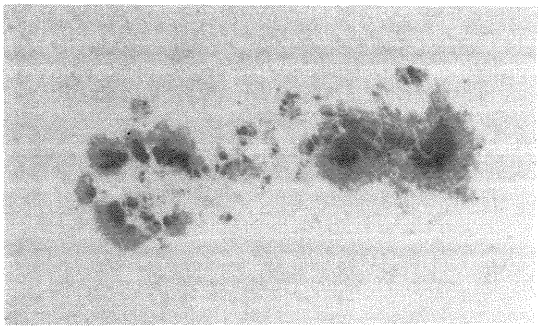

22 Aug. 71 1320 U.T. Sac Peak

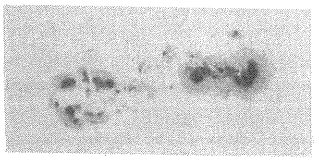

22 Aug. 71 2245 U.T. Culgoora

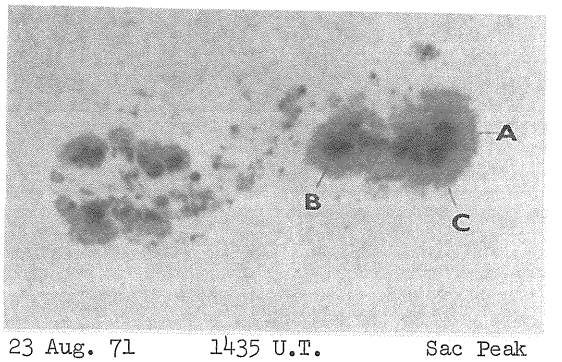

23 Aug. 71 1435 U.T. Sac Peak

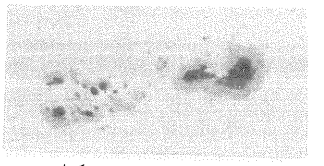

23 Aug. 71 2246 U.T. Culgoora

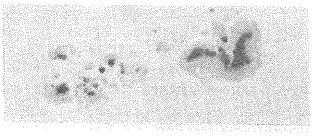

24 Aug. 71 2335 U.T. Culgoora

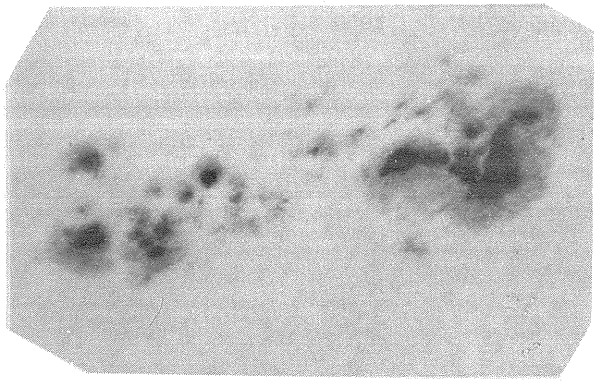

25 Aug. 71 0730 U.T. W. M. Baxter

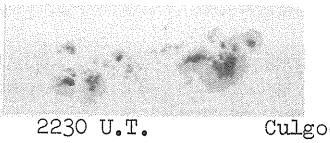

25 Aug. 71 2230 U.T. Culgoora

Fig. 4 Sunspot evolution during 20-25 August 1971 was highlighted by the movement of spot C over the same path covered by spot A during the previous two days. Spot C penetrates spot A on 22 August, becoming surrounded by photospheric and chromospheric bright material (see also Fig. 3). After this collision a portion of spot A is ejected from the leader penumbra, becoming detached by the end of the 25th.

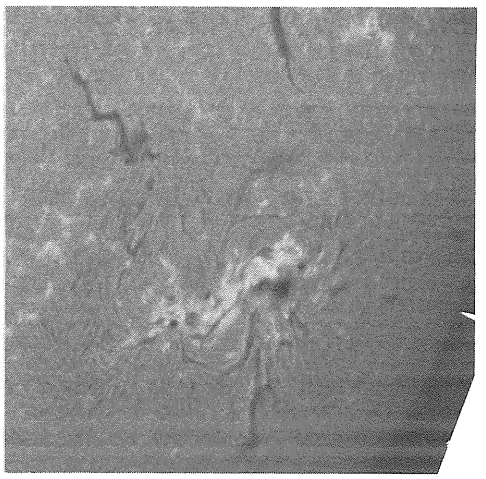

26 Aug. 71 1116 U.T. Ramey AFB

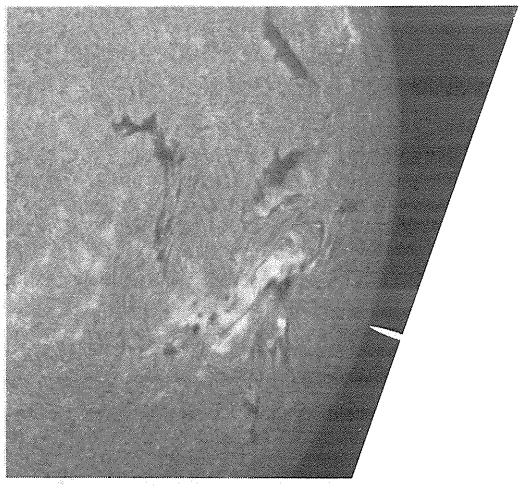

27 Aug. 71 1115 U.T. Ramey AFB

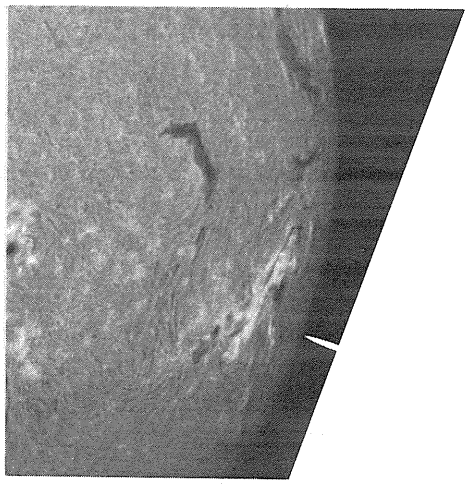

28 Aug. 71 1111 U.T. Ramey AFB

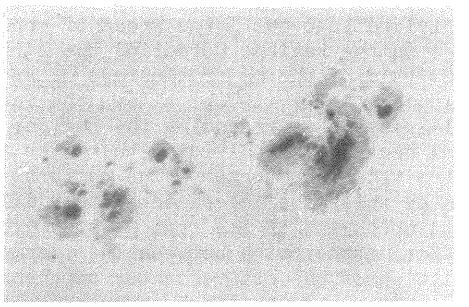

26 Aug. 71 1345 U.T. Sac Peak

27 Aug. 71 1435 U.T. Sac Peak

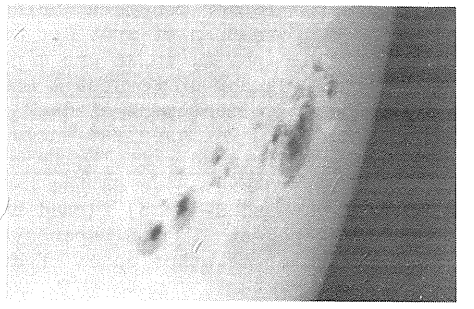

28 Aug. 71 1600 U.T. Sac Peak

Fig. 5 H-alpha (left) and white light (above) observations as the region approached the west limb. The scales are the same as in Fig. 2. The only notable activity during this interval seemed to be increased filament activity north of the main spot, both within the plage and further north near, and north of, the solar equator. The spots were decreasing steadily in area.

The magnetic field distribution in an active region can be studied either as part of the large-scale magnetic field patterns over much of the visible sun, or in a restricted view of just the internal parts of the active region. The latter view was presented for McMath Region #11482 by Livingston [1972, Fig. 4]. This high resolution subtraction magnetogram gives the impression that the region was basically divided into two large areas of opposite magnetic polarity, but with considerable mixing of polarities in the regions bordering the large leader spot and in the vicinity of the longitudinal neutral line dividing the major clusters of spots. The interpretation of H-alpha structures as magnetic fields, [McIntosh, 1972a, 1972b] allows the integration of this close-up view with the large-scale magnetic field patterns surrounding the region. The plage corridor within the bright plage mapped the longitudinal neutral line dividing the major spots, coinciding with the general polarity division seen on the subtraction magnetogram. The patterns of fibrils immediately outside the plage permits the continuation of this line to connect with a filament channel to the east of the region and to connect with filaments northwest of the region, even crossing the solar equator. These connections reveal a large-scale physical association between the flaring region and filament activity viewed in Figs. 3 and 5. The evolution of the active center apparently affected large-scale "quiet" solar features, or both the active center and the large-scale chromospheric patterns were responding to a common evolutionary force. The sunspot motions in this region suggest that the common evolutionary force was mass motions in the photosphere.

The sequence of sunspot photographs in Fig. 2 shows considerable sunspot movements even early in the disk passage of the region. A line connecting spots A and B rotated clockwise through nearly 90 degrees during the 48 hours from 18 August to 20 August. Careful measurement of the absolute heliographic coordinates of these spots revealed that both A and B were in motion, spot A moving west and spot B moving east, during the early part of this interval. Spot B came to rest early on the 20th, but spot A continued its westward motion and moved slightly south in latitude. This motion continued during the 21st and 22nd, as seen in Fig. 4, placing spots A and B at equal latitude at opposite ends of a large penumbra for the remainder of the disk passage. The motion of spot A can be considered as an arc with the center of radius approximately located in spot B, as if spot B were the center of a vortex of Coriolis-type mass motion in the photospheric gases. The direction of motion, clockwise as viewed in "sky" directions, agrees with southern hemisphere atmospheric motions in a planetary atmosphere. The observation of vortical motions of opposite senses in opposite hemispheres has been reported for solar structures by Hale [1927], Richardson [1941], Sakurai [1967], and McIntosh [1969, 1970, 1972c].

The sunspot photographs of Fig. 2 also show the movement of a sunspot from the follower cluster of spots toward the leader penumbra during 18-19 August. This spot became attached to the leader penumbra at the time of formation of spot C. Spot C then moved during 19-22 August over almost the identical path followed by spot A, in an arc centered on spot B. On 22 August, a very significant event took place as spot C caught up to spot A and penetrated through spot A! As spot C approached spot A there was a pronounced commencement of dark surge activity surrounding the western perimeter of the leader penumbra (Fig. 3). The greatest surge activity occurred during the 22nd, as spot C moved into spot A. The surges were directed radially from the point of contact between the merging spots (see photograph at 22/0835 U.T. in Fig. 3). As the two spots came into contact, a bright ring of material (visible in both white light and H-alpha) formed around spot C. This ring is easily seen in Figs. 3 and 4 and in the sunspot photograph in the paper by Bumba and Sykora elsewhere in this compilation. This observer has noted a number of other cases of bright rings surrounding spots that were in the process of coalescing. It is important to note that these cases of coalescence, including our region of interest here, involved spots of the same magnetic polarity.

The proper motion velocities of spots A and C, measured with respect to Carrington coordinates, were 0.20 km/sec and 0.35 km/sec, respectively, during the period 19-21 August. The southern hemisphere proton-flare region of October 30, 1968 also contained a spot moving in an arc about a larger spot, both of leader polarity (like our case here). The measured proper motion velocity in that case was 0.12-0.20 km/sec [McIntosh, 1970].

On the 23rd of August, spot C had fully penetrated spot A, apparently splitting A into two parts. Late on the 24th, the northern portion of spot A formed a satellite umbra which separated and detached from the leader penumbra by the end of the 25th (Fig. 4). This satellite spot appears related to the development of complex absorption features north of the leader during the days just prior to west-limb passage.

The spots in the following portion of the region formed a configuration of a ring. The motions among these spots had a pattern of movement south (to higher latitude) then westward along the lower border of the ring. The movements of spots in leader and follower together depicted a continuous line of movement in the shape of the letter "S" from latitudes above the follower to latitudes between the leader and the solar equator. The line of motion paralleled the longitudinal neutral line. The spot motions then suggest the transport of momentum from higher latitudes to lower latitudes, in agreement with the mass motions required by recent dynamo theories of the solar cycle.

The most rapid sunspot motions occurred close to the time of greatest sunspot growth (early in the disk passage) and also during the time of most frequent flare activity detected from the earth. The reasons for the occurrence of a great event two days past west-limb passage are not obvious. Close

study of the H-alpha photographs provided some clues. The motions of the spots were paralleled with a gradual alteration of the shape of the line of polarity reversal inferred from the H-alpha structures. The curvature of the S-shaped line became more pronounced as the region approached west limb, as if the mass motions deduced from the spot motions resulted in the transport of follower-polarity magnetic fields to a position between the leader and the solar equator. An accumulation of follower magnetic field strength might be inferred by the increase in plage brightness and the appearance of filaments north of the leader spot just prior to west-limb passage (Fig. 5). If this trend is extrapolated there may have formed sufficient field strength by the time of the proton flare to create a configuration like the "delta" configuration. Our extrapolation would give an increasing gradient in the longitudinal magnetic field across a neutral line that was oriented east-west. Such a configuration is especially common in proton-flare regions.

Another subtle evolution in H-alpha structures may be part of the explanation for the proton flare. The inferred longitudinal neutral line in the center of the region was positioned midway between leader and follower spots for most of the disk passage. Beginning about four days before west-limb passage, the position of this line began to shift westward toward the leader spots, implying an increase in magnetic field gradient. Foreshortening of our view of the region interfered with careful measurements during the last two days before west-limb passage, so an extrapolation to the time of the flare is not reliable. Perhaps the magnetic field gradient increased throughout the longitudinal neutral line positioned over a 90-degree arc north and east of the leader spot, and thereby increased the potential for a proton flare.

The return of the region on 13 September as McMath Region #11516 showed a bright plage with a relatively small, but complex, sunspot group. The configuration of the inferred longitudinal neutral line was almost identical to the configuration inferred just prior to west-limb passage two weeks earlier, with a six-degree westward shift in Carrington longitude. The neutral line was still S-shaped, with an east-west oriented section directly north of the old leader spot. The plage on the north side of the returning leader sunspot was brighter than when the region was last seen two weeks earlier, and a narrow plage corridor extended east-west through this plage. This tends to confirm the speculation above that magnetic field strengths may have increased in the vicinity of the leader just beyond the west limb, with a resulting increase in magnetic field gradient across a longitudinal neutral line.

In summary, we are missing the most important observations pertinent to explaining the occurrence of the proton flare of 1 September 1971 because the region was out of view for two days before the event. The evolution of the sunspots and H-alpha structures suggest that large-scale photospheric mass motions in this region may have led to the formation of a magnetic field configuration favorable for the generation of the proton flare. The extrapolation of these observations to the time of the flare, and therefore our conclusions, must remain speculative.

Acknowledgements

We are grateful for the loan of observational material from several observatories, making it possible to monitor active center evolution in greater detail than in most previous studies. Special thanks are given to the late W. M. Baxter, Director of the Solar Section of the British Astronomical Association until his untimely death. Mr. Baxter volunteered his sunspot photograph published here, one of the last to be taken before his death. The white light patrol films from the Sacramento Peak Observatory (Air Force Cambridge Research Labs) were provided by L. Gilliam and copied into large-scale internegatives [McIntosh, 1972d]. Other observations are the courtesy of Capt. J. Smith (USAF) at the solar observatory at Ramey Air Force Base, Puerto Rico, J. Hirman at the NASA/NOAA S.P.A.N. observatory on Gran Canary Island (Spain), R. Giovanelli of the C.S.I.R.O. Culgoora Solar Observatory, and the several observers at the NOAA observatory in Boulder, Colorado.

The study was performed under NASA Contract G.O. #H-42710A for the purpose of flare forecasting technique development.

REFERENCES

HALE, G. E. 1927 The Fields of Force in the Atmosphere of the Sun, Nature, 119, 708.

LIVINGSTON, W. C. 1972 Measuring Solar Photospheric Magnetic Fields, Sky and Telesc., 43, 344-349.

McINTOSH, P. S. 1969 Sunspots Associated with the Proton Flare of 23 May 1967, World Data Center A, Upper Atmosphere Geophysics Report UAG-5, 14-19, February 1969.

McINTOSH, P. S. 1970a Sunspots Associated with the Proton Flares of Late October 1968, World Data Center A, Upper Atmosphere Geophysics Report UAG-8, 22-29, March 1970.

McINTOSH, P. S. 1972a Solar Magnetic Fields Derived from Hydrogen-alpha Filtergrams, Topical Review in Reviews of Geophysics and Space Physics, 11,

McINTOSH, P. S. 1972b Inference of Solar Magnetic Polarities from H-alpha Observations, in Solar Activity Observations and Predictions, edited by P. S. McIntosh and M. Dryer, Volume 30 of Progress in Astronautics and Aeronautics series, Martin Summerfield, series editor, MIT Press, pp. 65-92.

McINTOSH, P. S. 1972c Sunspots and H-alpha Plage Associated with the GLE Event of 24 January 1971, this compilation.

RICHARDSON, R. S. 1941 The Nature of Solar Hydrogen Vortices, Astrophys. J., 93, 24.

SAKURAI, K. 1967 Solar Cosmic Ray Flares and Related Sunspot Magnetic Fields, Report of Ionos. and Space Res. in Japan 21, 113-124.

Large-Scale Magnetic Field and Activity Distribution Connected with the Proton-Flare of September 1, 1971 Region

by

V. Bumba
Astronomical Institute
of
The Czechoslovak Academy of Sciences, Ondrejov

and

J. Sýkora
Astronomical Institute
of
The Slovak Academy of Sciences, Skalnaté Pleso

1. Introduction

The relation of particle-emitting flares to a characteristic large-scale configuration of solar magnetic fields has been described in the previous paper concerning the proton-flare of January 24, 1971 [Bumba, Sýkora, present compilations] as well as in some other papers [Bumba, 1971 a, b; Bumba et al., 1972]. We demonstrate in this short note that the studied proton-flare from September 1, 1971 developed in a similar large-scale magnetic and activity situation. The same kinds of observational data as in the previous paper are used. These include the Mt. Wilson daily magnetic maps, Fraunhofer Institute, Freiburg, daily activity "Maps of the Sun", "Daily Geomagnetic Character Figures" from the Institut für Geophysik, Göttingen and the "Magnetic Field of Sunspots" published by the Pulkovo Observatory of the U. S. S. R. Academy of Sciences.

2. Development of the Large-scale Situation in which the Studied Proton-flare Took Place

It is noted that the proton-flare from September 1, 1971 occurred in the same magnetic stream as the proton-flare of January 24, 1971 (in the Carrington network tilted by the 27 day rotation, therefore, with a difference of about 40° to the West in heliographic longitude). The only difference is that this time it developed in the southern hemisphere while the first one took place in the northern solar hemisphere. The large-scale situation in more detail is shown in Figure 1 which represents the series of consecutively mounted synoptic charts (with two consecutive maps overlapped for integration). These describe separately the negative and positive polarity magnetic fields, geomagnetic activity (with four days shift) and calcium plages, filaments and sunspot group activity. Although it is more difficult to find in these magnetic synoptic charts the characteristic large-scale patterns of the supergiant drop-shaped body with which the proton-flare regions are correlated, the skilled observer may agree that at least some indications of this characteristic feature may be found in the negative polarity distribution having its head again about 90° to the West. Again the faster redistribution of the negative polarity fields in comparison with the relatively more stable (or still more pronounced) positive polarity fields following the proton-flare occurrence are seen.

The development of photospheric and chromospheric activity which precedes and follows the appearance of the proton-flare region is also shown.

The enhanced periods of the geomagnetic activity correlate this time in the upper left corner (western half of the Figure 1d) and in the middle lower part with the negative polarity fields. The recurrent geomagnetic events in the western half of the Figure 1d form the prolongation of the recurrent geomagnetically enhanced intervals connected with the older negative polarity magnetic fields which are westward of the proton-flare of January 24, 1971. In the lower right hand corner (eastern part of the Figure 1d) the recurrent enhanced geomagnetic activity correlates with the magnetic stream of positive polarity as in preceding years of activity.

3. Development of the Proton-flare Region

From Figure 1c we see that one rotation before the proton-flare region developed, a small β type group is observed in its central meridian passage. From the form of calcium plage one rotation after the proton-flare, we judge that the plage represents the remains of at least two active regions (or spot groups), the new one being east of the original group.

Studying the development of the huge sunspot group in which the flare took place we notice its fast growth just after it appears from behind the eastern limb. This growth proceeds from the central part of the group (from the close-vicinity of the dividing line between the field polarities), but this process reaches its maximum sometime around August 23, 1971 (see Figure 2 representing the photographs of this group on August 22, 1971) and then the area as well as the activity of the group diminishes very fast as the group approaches to the western solar limb.

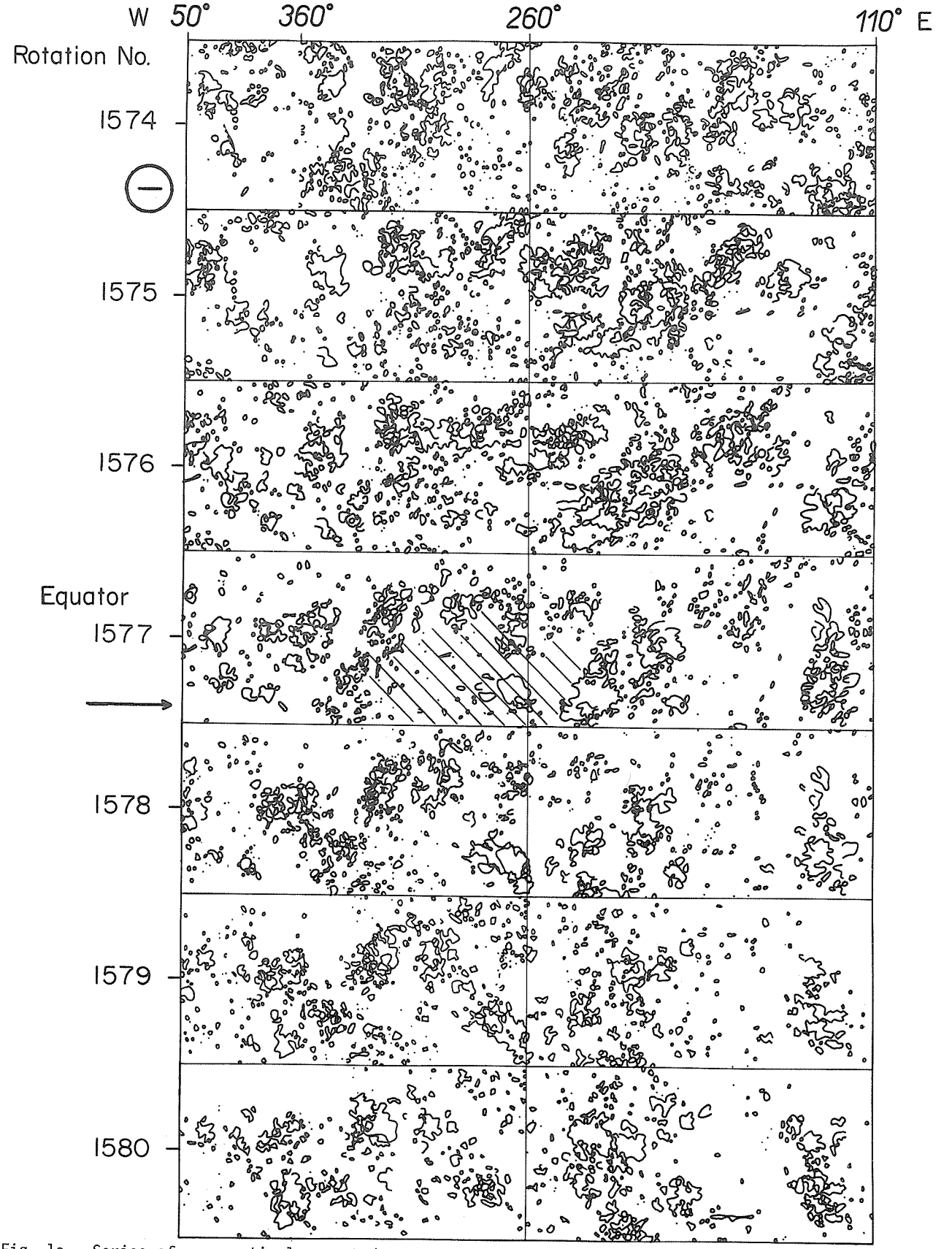

Fig. 1a. Series of consecutively mounted magnetic synoptic charts (within the heliographic latitudes ± 40°) of negative polarity for rotations Nos. 1574-1581. For integration two consecutive maps, one of which is repeated are overlapped. The rotation with the proton-flare which occurred close to the indicated heliographic longitude 260° (south from the equator) is shown by an arrow.

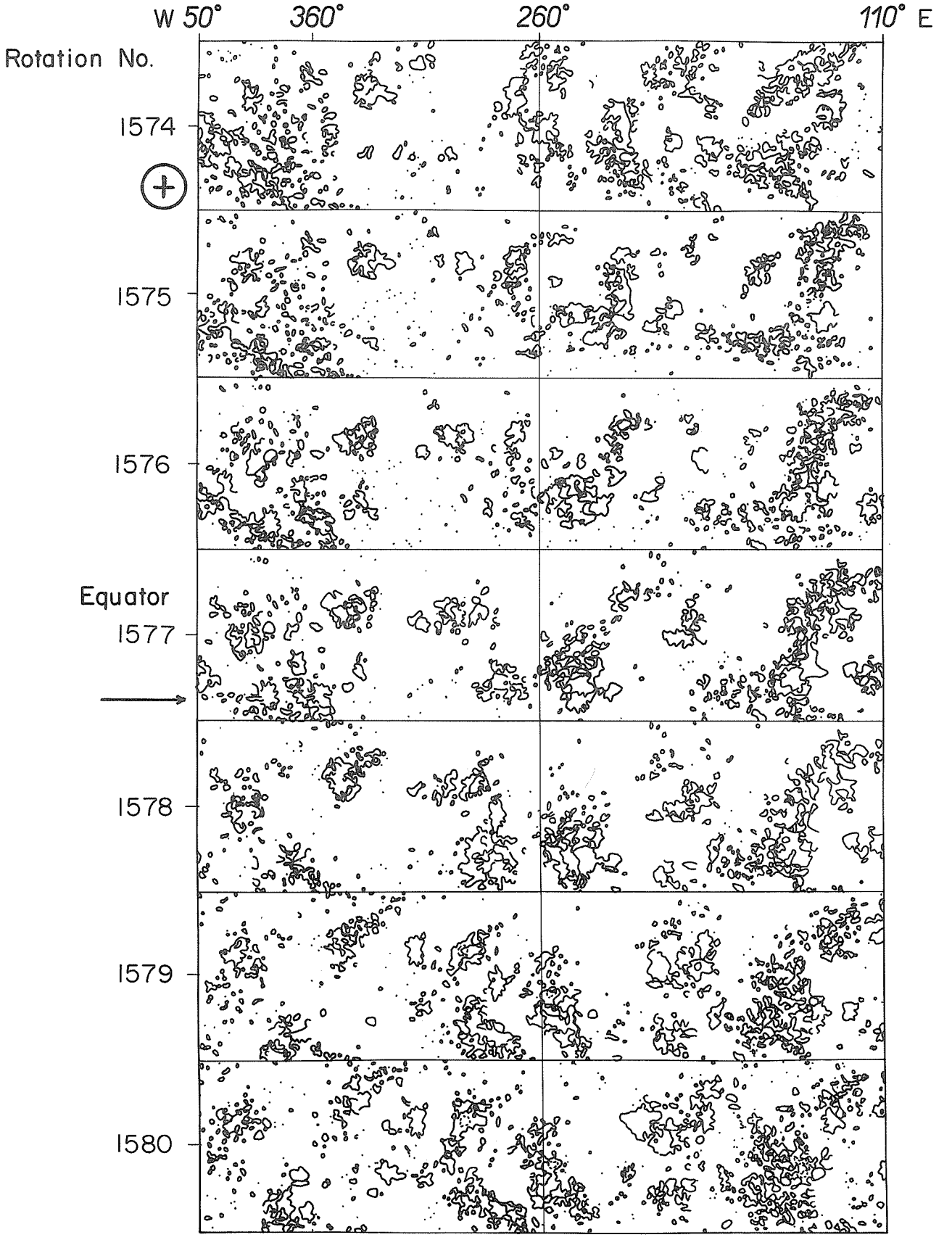

Fig. 1b. The same series of consecutively mounted magnetic synoptic charts for positive polarity fields as in Figure 1a.

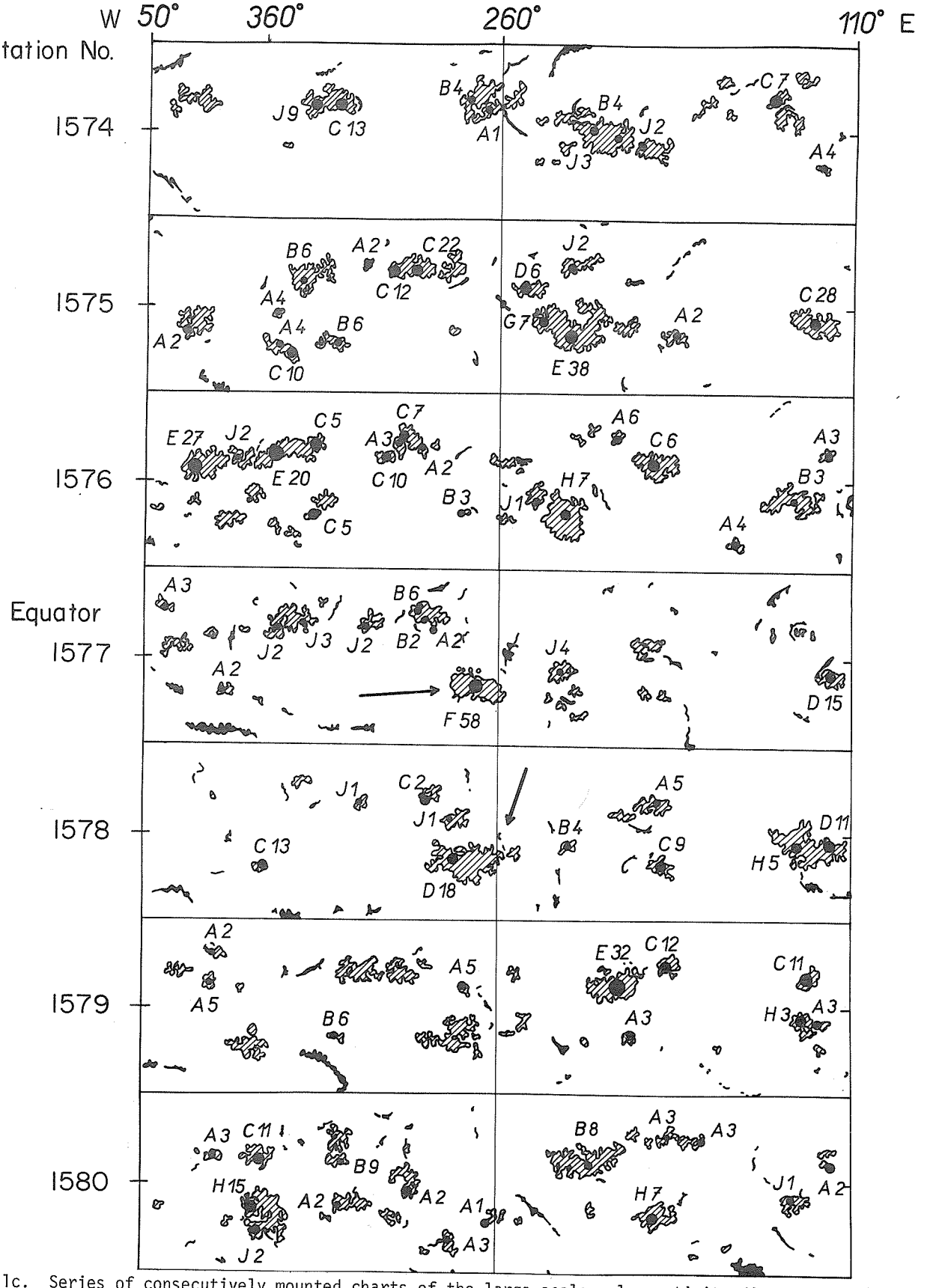

Fig. 1c. Series of consecutively mounted charts of the large-scale solar activity distribution (Fraunhofer Institute, Freiburg) without the overlapping of maps for rotations Nos. 1575-1581. The studied active region F 58 as well as the calcium plage remains of the probable newly developed group in the following rotation are indicated by an arrow.

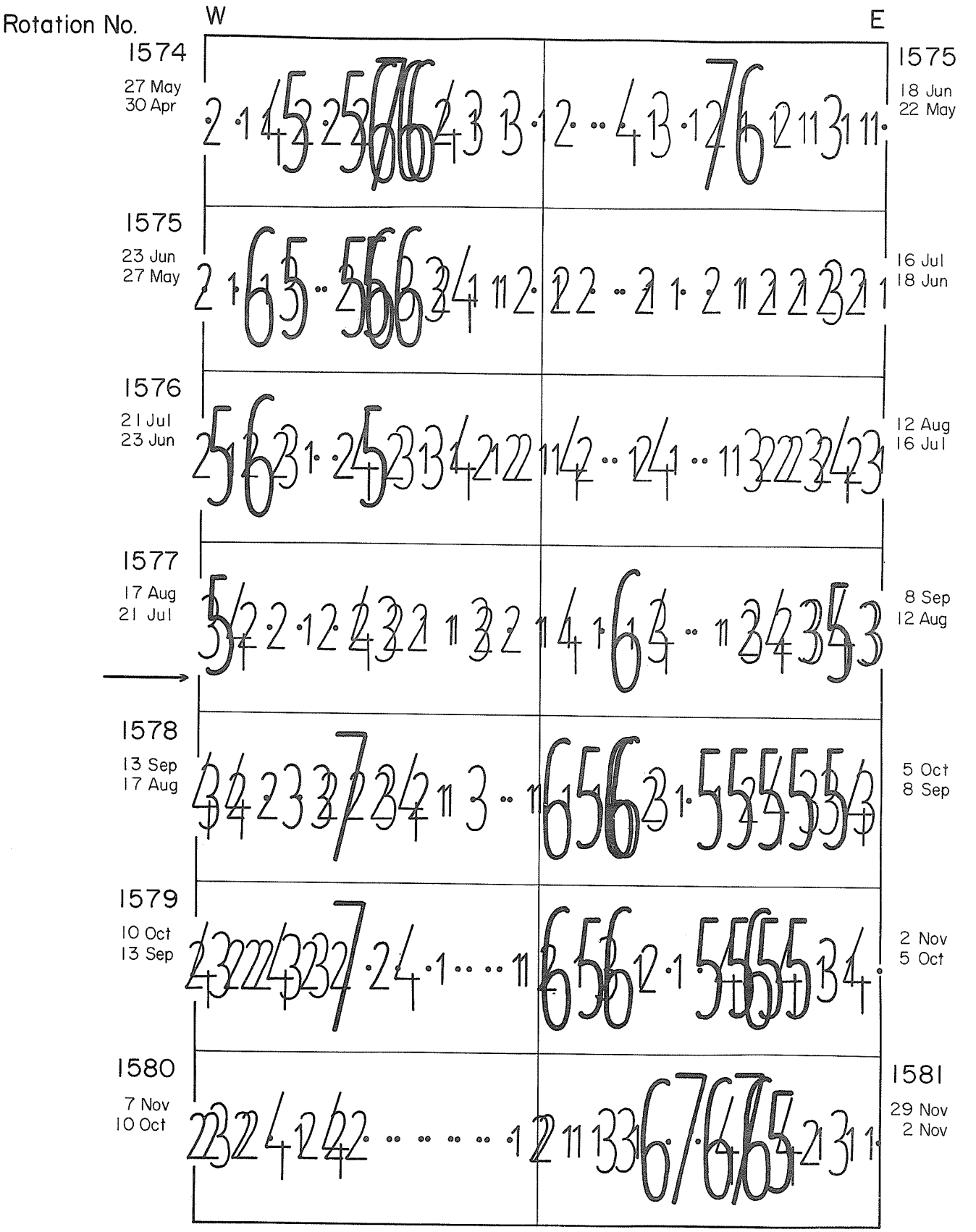

Fig. 1d. Series of consecutively mounted charts of geomagnetic activity distribution (Institut fUr Geophysik, Göttingen) for the same time interval with the same overlapping of charts. The four days, needed by the particles to arrive at the Earth, are taken into account.

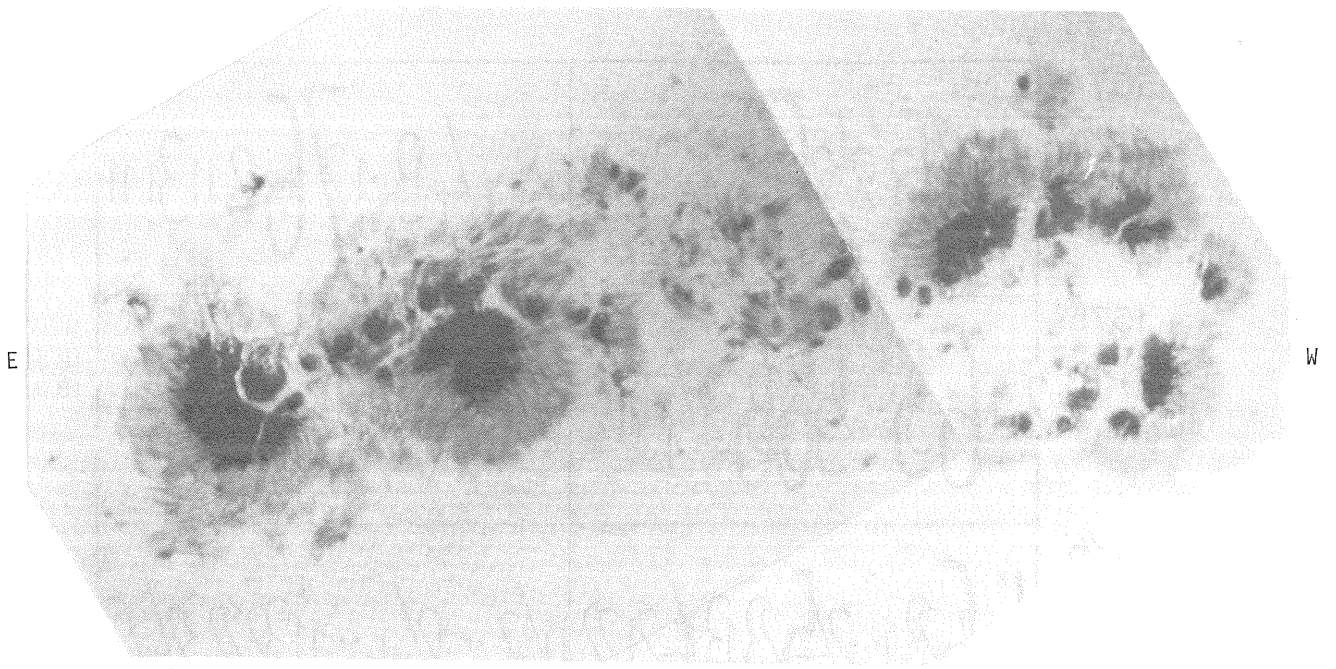

Fig. 2. Photograph of the studied sunspot group from August 22, 1971 obtained at the Astronomical Institute of the Slovak Academy of Sciences, Skalnaté Pleso with the objective lens having the diameter of 16 cm and focal length 304 cm. West is to the right, North to the top of the Figure. The exposure time of the right hand part: $5^h36^m57^s$ UT; of the left hand part: $6^h37^m50^s$ UT.

From all that has been said it is very difficult to make some conclusions about what happened during the two days the region was behind the limb. Probably new activity developed (see the form of the plage the next rotation) in the closest neighborhood of the described group, although no sign of such renewal of activity is seen in the photosphere or in the chromosphere before the group disappears behind the limb.

4. Coronal Situation Above the Proton-flare Region

Again not enough observational material exists for construction of synoptic charts demonstrating the green corona large-scale distribution. In Figure 3 the coronal situation development as was observed above the proton-flare region is shown. We see in the corona the enhanced level of green (λ5303 Å) emission during the western limb passage of the studied longitudinal interval in the preceding rotation, where the photospheric activity was very low, which signals the future development of larger activity. On the eastern and still more on the western limb during the main rotation with the large developed sunspot group the level of green coronal emission is very high. It seems even higher at the beginning of the rotation following the proton-flare occurrence, although the whole figure is not drawn because of the lack of observational data. But later a fast decrease of emission is observed.

REFERENCES

BUMBA, V. and J. SÝKORA 1972 Development of the Large-Scale Situation in which the Proton-Flare of January 24, 1971 Took Place, present compilation, p. 43.

BUMBA, V. 1971 a Large-Scale Negative Polarity Magnetic Fields on the Sun and Particle-Emitting Flares, Submitted to the Proceedings of the Solar Wind Conference, Asilomar, Pacific Grove, California, March 21-26, 1971.

BUMBA, V. 1971 b Large-Scale Regularities in Solar Magnetic Field Distribution and Occurrence of Large Flares, Submitted to the Proceedings of the 6th Regional Consultation on Solar Physics, Gyula, Hungary, September 6-11, 1971.

BUMBA, V., L. KRIVSKÝ and J. SÝKORA 1972 Development and Spatial Structure of Proton-Flares near the Limb and Coronal Phenomena. IV Proton-flare from Nov. 2, 1969 and its Active Region, Bull. Astr. Inst. Czech., 23, 85.

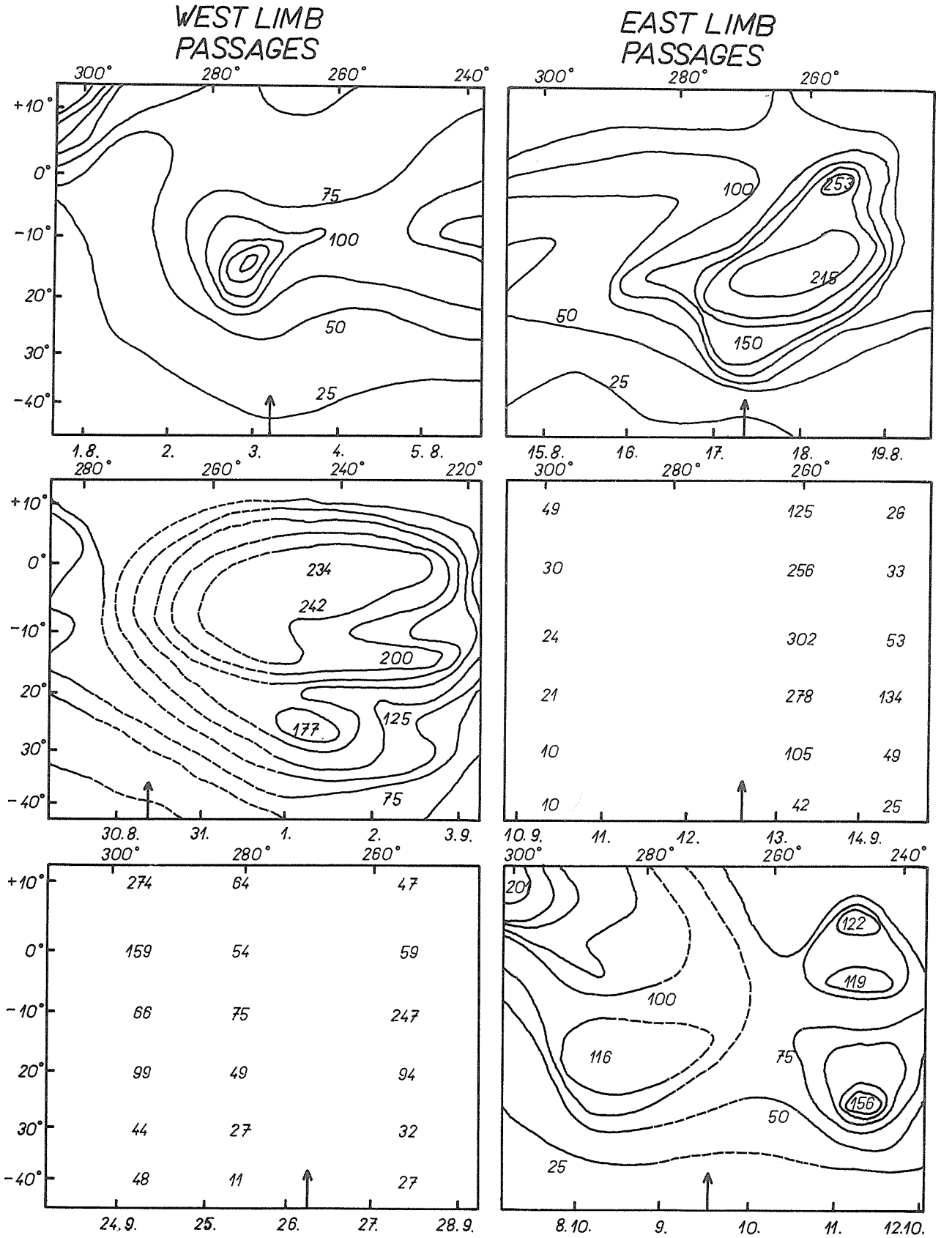

Fig. 3. Coronal situation above the proton-flare region for the preceding, main and the following rotations. Lines of equal mean intensity or the values of the intensity of the green (λ5303 Å) coronal emission in absolute coronal units are shown. Heliographic coordinates are indicated. Also the passages of the region on the eastern and western limb are shown by the data and the arrows.

3. SOLAR RADIO EVENTS

Early Development of Radio Emission from MMH 11482

by

D. S. Lund
NOAA Environmental Research Laboratories
Boulder, Colorado 80302

Introduction

In a previous volume in this series, we reported on our efforts to apply synchrotron emission theory to flare-associated radio spectra [Lund, 1970]. Our interest was in rapid diagnosis of physical conditions within the flare region which would be premonitory of energetic particle arrival in the near-earth environment. Since that time, we have been studying the radio spectra of active centers, as observed well before major flare activity, and we will now apply some of our results to the observations of McMath-Hulbert Region Number 11482. Although a thorough explanation of active-center emission requires discussion of the radiative transfer equation, with a source function that includes gyroemission and gyroabsorption, we will defer such discussion and will here comment on a number of aspects which do not require such rigorous derivation.

Microwave observations of active center emission may be of several types: the spectrum may be inferred from whole-sun measurements, or the spectrum may be derived from observations which seek to isolate the individual center of activity. In this note, we shall confine our attention to the latter class. Further the spectrum may be described in terms of its polarization. Observations at Pulkovo [Gel'freikh and Peterova, 1970] indicate that bipolar regions often display a circular polarization excess which maximizes near the limbs, and is nearly zero close to the central meridian (CM), with sense inverting near CM passage. Unipolar regions show a simple maximum near CM passage. Unfortunately, this type of data was not available to us during the research we are reporting. Thus we must discuss the spectrum of one linearly polarized component, and see what (if anything) can be deduced about development of either the coronal extension of the active region, or the chromosphere-to-corona interface, during the period before the flare of September 1, 1971.

Discussion of Observations

In Figure 1, we show a schematic spectrum of the radio emission from an active center, representing the spectral flux density in one polarized component, integrated (spatially) over the entire active center, and viewed close to the central meridian. At the longer wavelengths (10 to 50 centimeters) the spectral flux density varies as λ^{-2}, and corresponds to a brightness temperature of one or two million degrees. In this portion of the spectrum (marked A in the Figure), the corona is optically thick, and the emission at the several observed wavelengths is born in a thin shell; thin enough that thermal

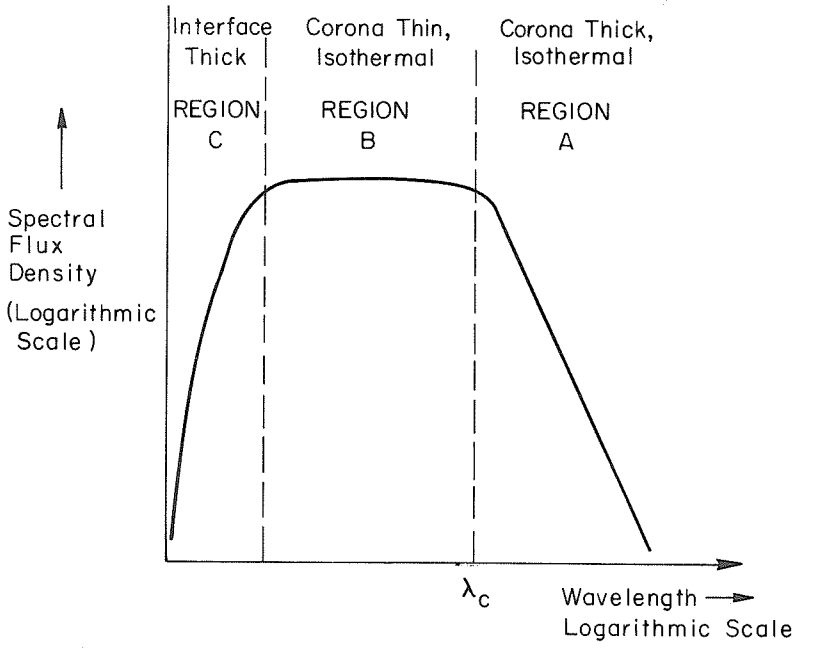

Fig. 1 Idealized Spectrum of an Active Center

gradients in the corona are unimportant. By this we mean that the kinetic temperature is nearly the same for small and large optical depths. In Region B, the corona is optically thin, comparatively speaking, but still isothermal in the sense defined above. Despite the coronal transparency, the coronal temperature is sufficiently high as to provide most of the flux. If the electron density and temperature were constant, then the flux would be independent of wavelength, and Figure 1 would be flat. We have sketched it in this way on the basis of Drago's [1970] observations, although the evidence we will show doesn't support such interpretation. At the shortest wavelengths, in Region C, the interface between corona and chromosphere is opaque, while the corona itself is quite transparent. The shorter the wavelength, the deeper within the active region is the origin of the radiation. Deeper portions are cooler, hence the source function decreases at the shorter wavelengths in this oversimplified view.

Two further observational facts are needed later: the first that the spectral flux density, as observed at a fixed frequency in active centers that are not changing rapidly, seems to follow a cosinusoidal dependency on apparent longitude [Christiansen et al., 1957; Gutmann and Steinberg, 1957; Khangil'din, 1964, present the evidence at various wavelengths]. This result appears valid over the wavelength range 0.8 to 20 centimeters, and offers a crude way of distinguishing spatial and temporal variations. The absence of wavelength dependence in this experimental result leads us to expect that the entire spectrum should increase and decrease in magnitude, but not be deformed (i.e. change slope), as the region is carried across the visible disk by solar rotation. The second empirical result we shall need relates to the 'size' of active centers. Neglecting for the moment the question of structure within the active center [the 'core and halo' of Kundu, 1959; the aureole structure of Khangil'din, op. cit.], it appears from eclipse observations [Straka, 1970; Drago, op.cit.] that the angular extent of the emission region is less than the beamwidth of the antennas in use at the Fleurs, Stanford and Prospect Hill observatories. For this reason we shall treat the emission region as if it were an unresolved source.

In the context of the previous paragraphs, we can now examine the observational evidence contained in the spectroheliograms published in "Solar-Geophysical Data." Pertinent maps at wavelengths 0.8, 9.1 and 21 centimeters have been drawn from this source during the visibility of MMH 11482 on the disk. We have supplemented these data with our own observations at 3.2 centimeters. During the period 17-31 August, 1971, observations were obtained with a prototype polarimeter installed at prime focus of a sixty-foot-diameter antenna. During that time, only linearly-polarized components were observed, thus making our results comparable with those from the other observatories. In Table I, we list the solid angle to half beamwidth (Ω_A) of the several observatories, together with the factors $\frac{2k\Omega_A}{\lambda^2}$, which when applied to the reported temperatures represent the conversion factors to flux. We note in passing that a relatively poor antenna pattern in our own measurements has been compensated for by integrating the antenna pattern and deriving a Gaussian function of equivalent area.

Table 1.

	Ω_A	$\frac{2k\Omega_A}{\lambda^2}$
Fleurs	$(1.27 \times 10^{-6})^{*}$	7.96×10^{-28}
Stanford	$(8.95 \times 10^{-7})^{*}$	2.97×10^{-27}
Boulder	$(1.77 \times 10^{-5})^{**}$	4.89×10^{-25}
Prospect Hill	1.49×10^{-6}	5.02×10^{-25}
	Steradians	Watts Meter^{-2} Hertz^{-1} Degree^{-1}

*Adjusted for beamwidth in δ coordinate

**Equivalent Gaussian FWHM

In Figures 2, 3 and 4 the daily spectra are shown for the entire passage of the active center across the visible disk. Comparing these Figures with earlier published results [Christiansen et al., 1960; Kakinuma and Swarup, 1962; Swarup et al., 1963; Tsuchiya and Takahashi, 1968; Straka, op. cit.; Drago, op. cit.] we find general agreement with the earlier results. However, our results are the first showing the effects of rotation and region development.

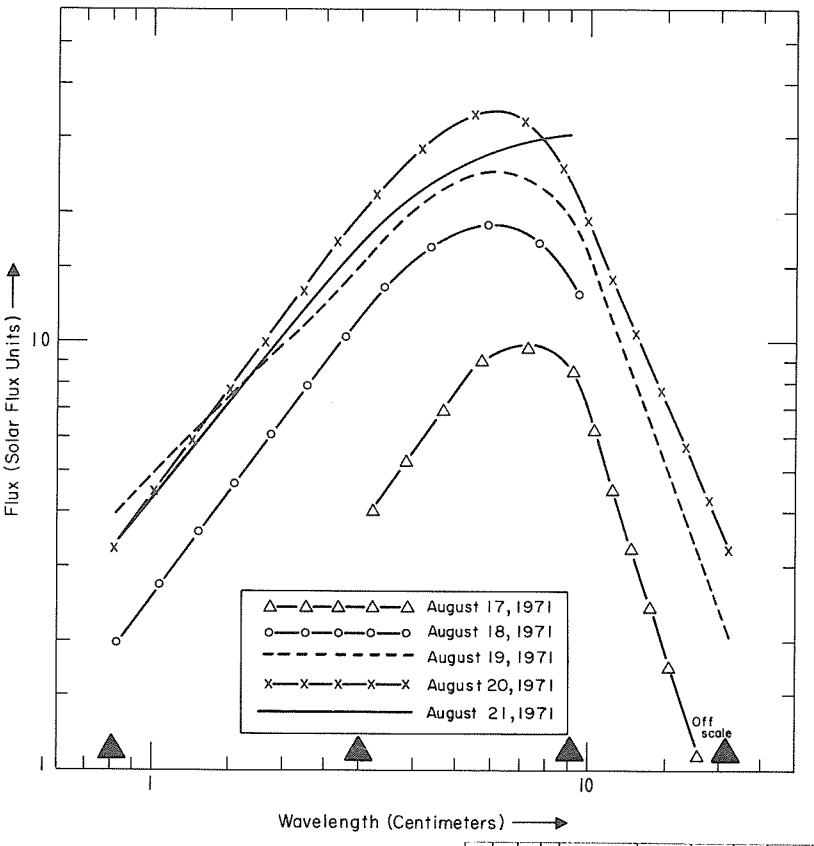

Fig. 2

Observed Spectra from MMH 11482 (east limb toward CM)

▲ denotes observed wavelengths. Smooth curve drawn through observations.

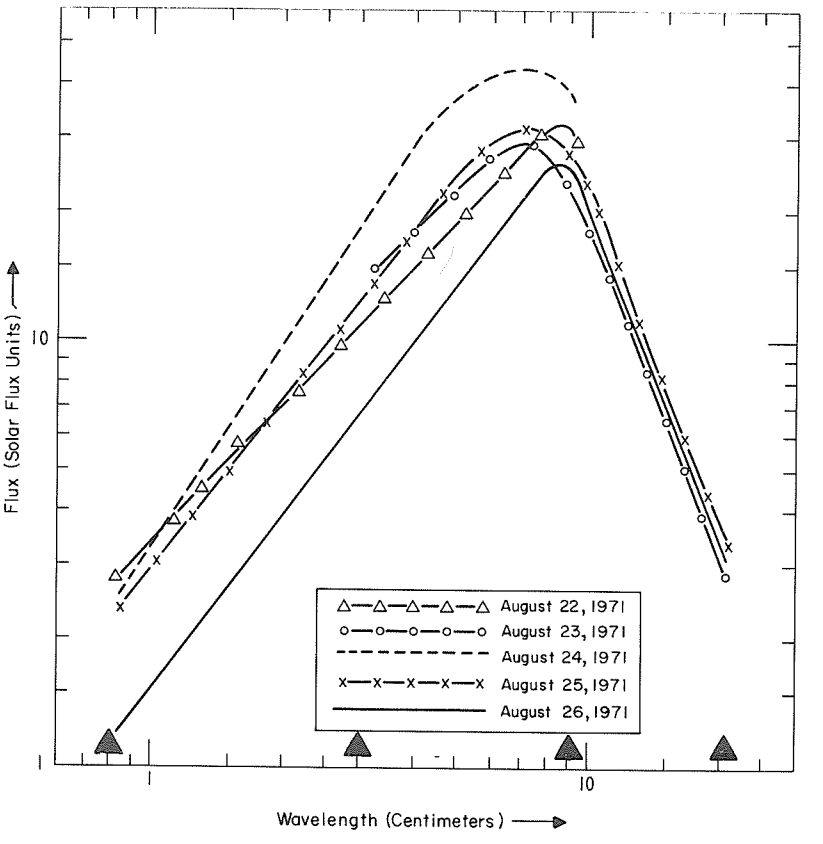

Fig. 3

Observed Spectra from MMH 11482 (before and after CMP).

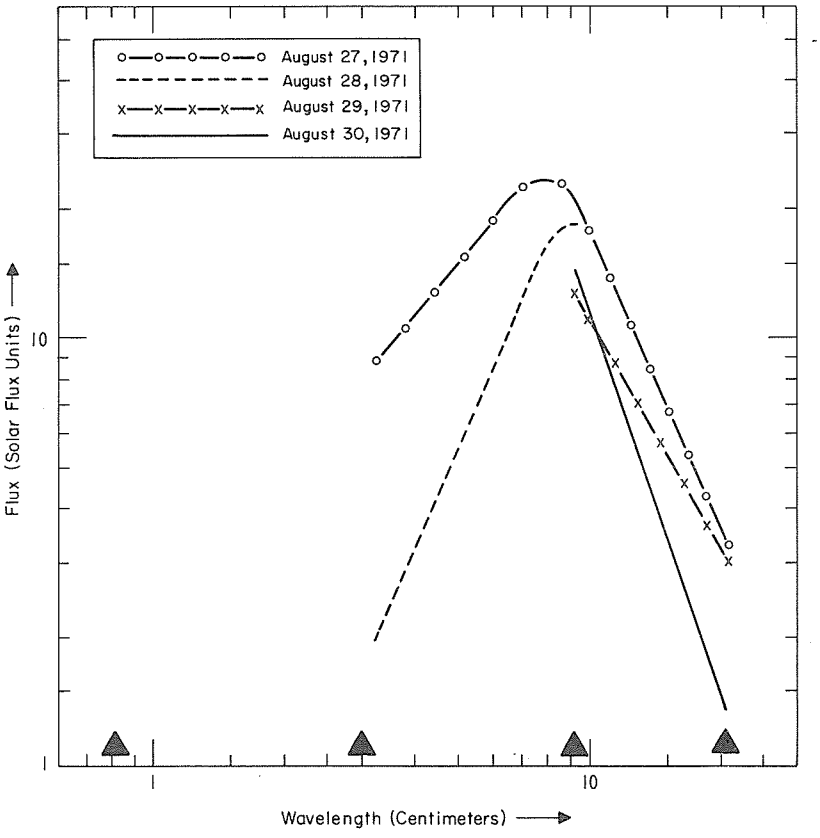

Fig. 4 Observed Spectra from MMH 11482 (CMP to West limb)

Analysis and Conclusions

A careful examination of Figures 2-4 will show three points of interest, which deal with a) coronal development, b) developments in the interface region, and c) a curious change in the spectrum as the active center progresses toward West Limb (and the flare which is the subject of this volume). We will expand on each of these items separately.

Consider the longer-wavelength portions of the spectra shown in Figures 2-4. These correspond to Region A of Figure 1. Of the nine days for which data are available at both 9.1 and 21 cm., eight show a spectral index of about 2. Recalling that spectral index (α) is defined as $S \propto \lambda^{-\alpha}$, where S denotes spectral flux density, a spectral index of 2 is characteristic of thermal emission from a quasi-isothermal region. Formally, if S_∞ is a constant

$$S = S_\infty \lambda^{-\alpha} \text{ (long wavelengths)}$$

seems a valid description of the long-wavelength spectrum with $\alpha \sim 2$. The transition between Regions A and B occurs at a critical wavelength λ_c, where

$$S = \left(1 - \frac{1}{e}\right) S_\infty \lambda_c^{-\alpha}$$

which may be taken as a definition of the wavelength at which the coronal extension of the active region is close to unit optical depth. Unit optical depth means

$$\tau = \int_{\text{outside}}^{S^*} \frac{0.16\, N_e^2\, \lambda_c^2}{c^2 T_e^{3/2}}\, ds = 1$$

Where the c in the denominator is the velocity of light, and N_e and T_e are electron density and temperature. In Figure 5 we plot λ_c as a function of time.

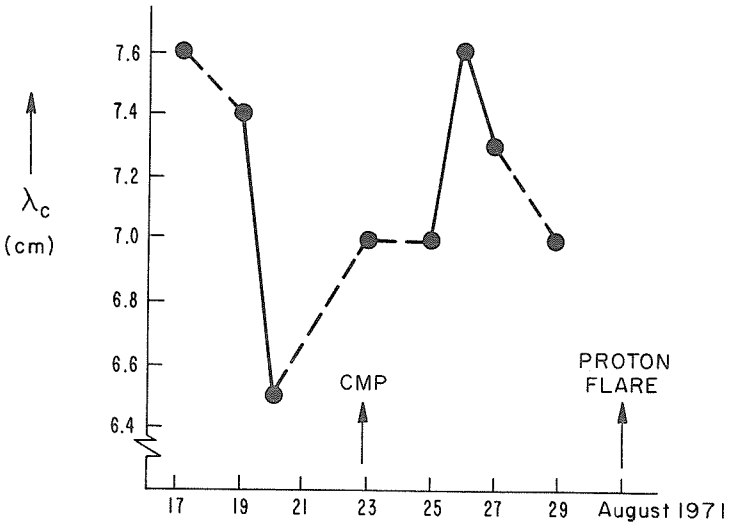

Fig. 5 Critical wavelength of spectra (as a function of time).

Considering the crudeness of our spectra, the relative constancy of λ_c is surprising, for if λ_c is indeed constant then

$$\int N_e^2 \, T_e^{-3/2} \, ds \neq f(\theta, t)$$

where θ is the angle between the line of sight and the outward normal from the active center. Thus, to the limits of accuracy of our data, we find no evidence for pumping of material (enhanced N_e) into the corona in advance of the proton flare, such as would increase λ_c.

Turning now to the short wavelengths, there is a wealth of information about the interface between chromosphere and corona, that may be gained by studying Region C of Figure 1. However, such studies are very difficult. One of the difficulties is coronal contamination of the observations: we have argued that the coronal portion of the active center has unit optical depth at around 7 cm., and if the optical depth varies as λ^2, one might expect an optical depth of 10^{-2} from just the active corona at 8 mm. Since this results in a brightness temperature an order of magnitude greater than enhancements observed at 8 mm., we conclude that coronal contamination may be severe at the shorter wavelengths. Another difficulty is that the source function in the interface region must include a non-negligible contribution from gyroemission, and this is not well understood. Because of these, and other, difficulties let us discuss the short-wavelength information in qualitative fashion. Although there is no theoretical reason for believing that a power-law spectrum represents the correct dependence of flux on wavelength (Region C), we have calculated such a spectral index from the ratio of 0.8/3.2 cm. flux. In Figure 6 spectral indices derived from short-, and long-wavelength slopes are shown, as functions of time, together with the Daily Flare Indices. It may be easily seen from Figure 6 that there were anomalies in the short-wavelength spectral index on the 19th, 24th, 28th and 29th. The last two will be discussed in the next paragraph. The softening on the 19th corresponds to an increase in the 0.8 cm. flux, which did not presage major activity, either in the optical or the X-ray portions of the spectrum. The hardening of the short-wavelength portion of the spectrum on the 24th, which can be seen in the enhanced fluxes at 3.2 and 9.1 cm., is thought to be associated with a slow rise and fall of the X-ray emission from the region beginning at about 12 hours (GMT) and ending at about 23 hours. This X-ray 'gradual rise and fall' can be clearly seen in the Solrad 9 data. In summary, then, if $\partial S/\partial \lambda$ at the short wavelengths is truly indicative of physical conditions in the interface region, then there is little evidence of change within that region.

Initial examination of Figures 3 and 4 might make one speculate that the active center began decaying on the 26th. However, no decay is evident at the longer wavelengths, and optical observations of the lower-lying portions of the active center offer further evidence that the region was not decaying. Another explanation is that the region was displaying the limb darkening we have described previously. However, comparison of Figures 2 and 4 show that this explanation is incorrect. One explanation that is consistent with the evidence is that the spectral changes are due to obscuration. Examine the H_α pictures of the region as reproduced in the optical section of this volume. Note the

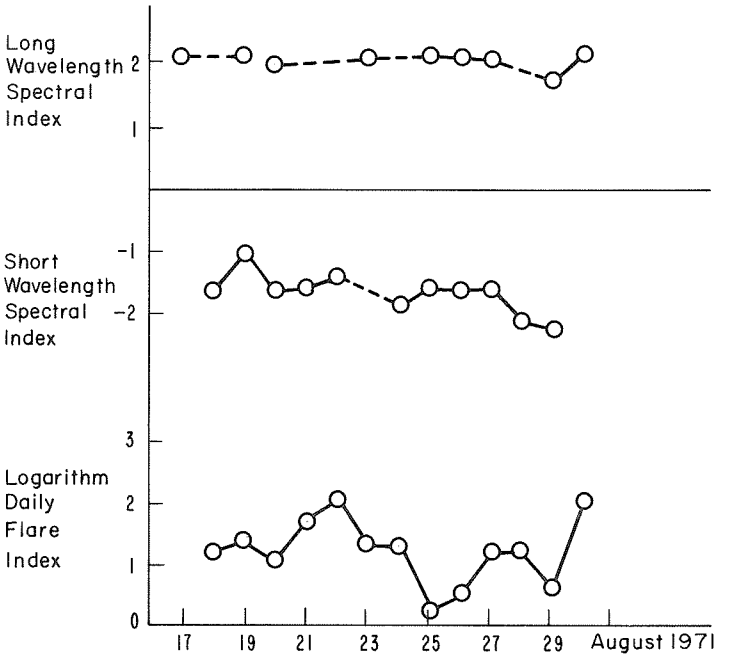

Fig. 6 Comparison of Spectral Indices with Flare Activity

extensive filamentary system trailing the region, and especially observe that the filament crosses the equator of the sun. Such systems are, on occasion, associated with 'coronal holes'. Further evidence for this speculation may be found by examining the radio maps, and noting that as the region approached west limb, the center of gravity of the radio emission was increasingly displaced from the optical plage. Further, the effect was greater at 21 cm. than at 9 cm. We offer this as evidence that the region was progressively occulted at the shorter wavelengths, and that refraction at the longer wavelengths was responsible for the displacement between optical and radio positions.

Let us quickly summarize our conclusions:

a) The radio evidence indicates that temporal changes in the corona either were nonexistent, or proceeded with a time scale of hours.

b) The observations suggest a coronal structure of possible high density and low temperature trailing behind the active region.

c) There is no evidence for substantial changes in the interface region, although the obscuration noted makes this conclusion weak.

REFERENCES

CHRISTIANSEN, W. N., J. A. WARBURTON and R. D. DAVIES — 1957 — The Distribution of Radio Brightness Over the Solar Disk at a Wavelength of 21 Centimeters, IV. The Slowly Varying Component, Aust. J. Phys., 10, 491-514.

CHRISTIANSEN, W. N., D. S. MATHEWSON, J. L. TAWSEY, S. F. SMERD, A. BOISCHOT, J. F. DENISSE, P. SIMON, T. KAKINUMA, HELEN DODSON-PRINCE and JOHN FIROR — 1960 — A Study of a Solar Active Region Using Combined Optical and Radio Techniques, Ann. d'Ap., 23, No. 1, 75-101.

DRAGO, F. C. — 1970 — Radio Spectrum of Two Active Regions, Solar Physics, 13, 357-371.

GEL'FREIKH, G. B., and N. G. PETEROVA — 1970 — Polarization of Local Sources of Solar Radio Emission at 4.4 cm., Astronomicheskii Zh., 47, No. 4, 689-701.

GUTMANN, M., and J. L. STEINBERG — 1957 — Resultats Preliminaires Obtenus avec L'Interferometre a 8 Antennes sur 3 Cm de Longeur d'Onde, in Paris Symposium on Radio Astronomy, R. N. Bracewell (ed), pp. 123-124, Stanford University Press, Stanford, California.

KAKINUMA, T., and G. SWARUP — 1962 — A Model for the Sources of the Slowly Varying Component of Microwave Solar Radiation, Ap. J., 136, 975-994.

KHANGIL'DIN, U. V. — 1964 — Characteristics of Solar Active Regions Obtained from Observations on Millimeter Wavelengths, Astronomicheskii Zh., 41, No. 2, 302-312.

KUNDU, M. R. — 1959 — Structures et Proprietes des Sources d'Activite Solaire sur Ondes Centimetriques, Ann. d'Ap., 22, No. 1, 1-100.

LUND, D. S. — 1970 — Radio Burst Spectra Associated with Proton Flux Increases, Upper Atmosphere Geophysics Report UAG-8, 103-111.

STRAKA, R. M. — 1970 — Microwave Spectral Observations of Coronal Condensations, AFCRL-70-0241, 1-24.

SWARUP, G., T. KAKINUMA, A. E. COVINGTON, GLADYS A. HARVEY, R. F. MULLALY and J. ROME — 1963 — High-Resolution Studies of Ten Solar Active Regions at Wavelengths of 3-21 cm., Ap. J., 137, 1251-1267.

TSUCHIYA, A., and TAKAHASHI, K. — 1968 — Spectrum of Slowly Varying Component of Solar Radio Emission on Millimeter Wavelengths, Solar Physics, 3, 346-348.

The Microwave Sun at the Time of the Cosmic Ray Increase of September 1, 1971

by

J. H. Deuter and R. N. Bracewell
Radio Astronomy Institute
Stanford University
Stanford, California

Between 2000 and 2100 UT on the day of September 1, 1971 the microwave solar emission at a wavelength of 9.1 cm was distributed as shown in Figure 1. Equal brightness temperatures are represented by contours; the outermost contour is for 10,000°K and the contour interval is 10,000°K. The photospheric disk is shown by a circle. The north pole of the sun is at the top and east is at the left. The contours presented here refer to a smoothed map in which each observation is replaced by the mean of the nine values centered on it. Details regarding the instrument can be obtained from Bracewell and Swarup [1961], and further details about the presentation are given in the annually published Descriptive Text that accompanies "Solar-Geophysical Data".

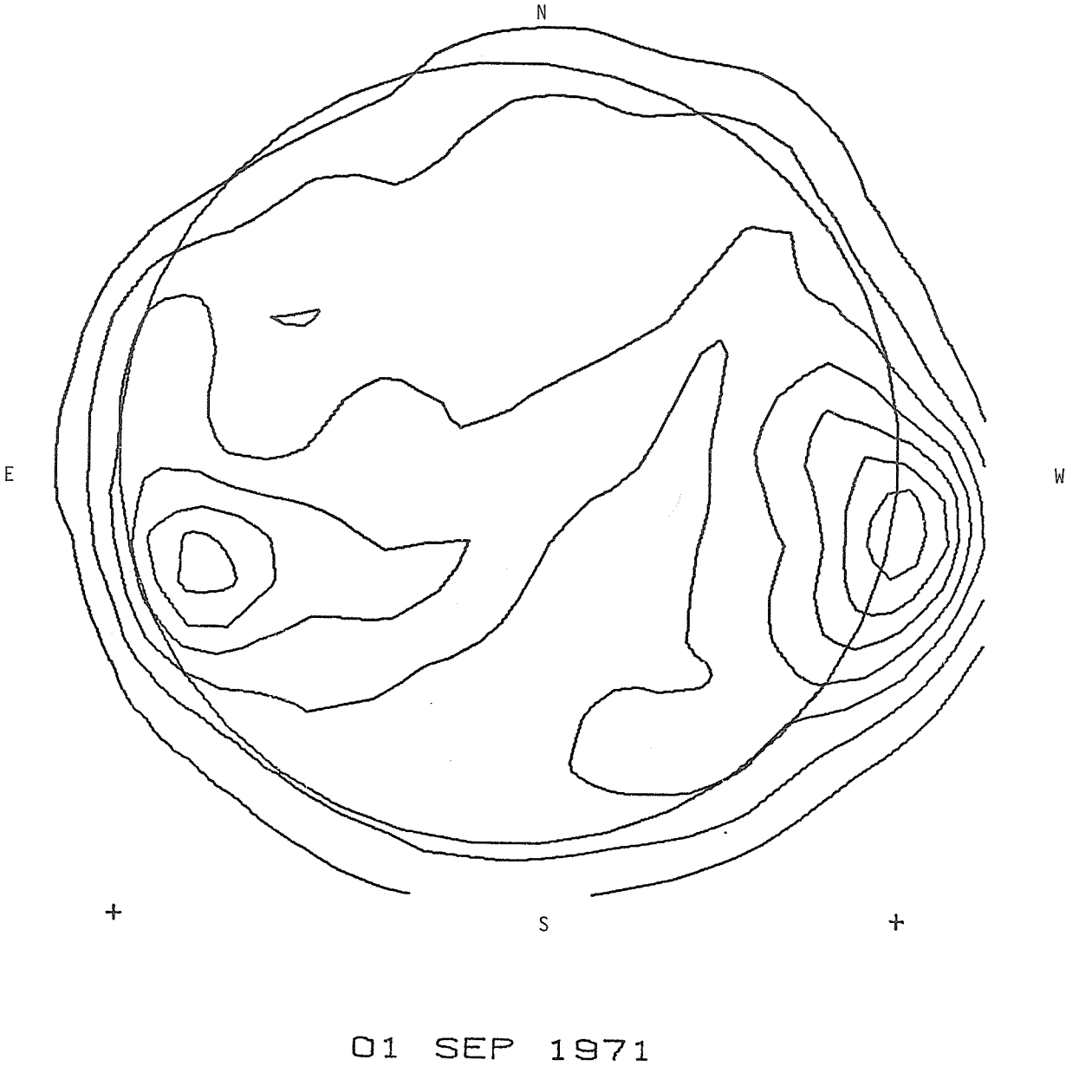

Fig. 1. Stanford 9.1 cm solar emission between 2000 and 2100 UT, September 1, 1971.

A microwave burst was recorded just before the map was taken, as shown in Figure 2. Records of this type are made as the sun moves through the fan beams of the east-west arm of the instrument. The beam width is 2.3 minutes of arc and the spacing of successive fringes is 41 minutes of arc when the source is near the meridian, as in this case.

The burst occurred on the west limb. It was not in existence at 1928 UT but had acquired considerable strength by 1931 UT. After a further increase a maximum was reached between 1936 and 1939 and by 2000 UT, when observations were started for Figure 1, recovery was not quite complete.

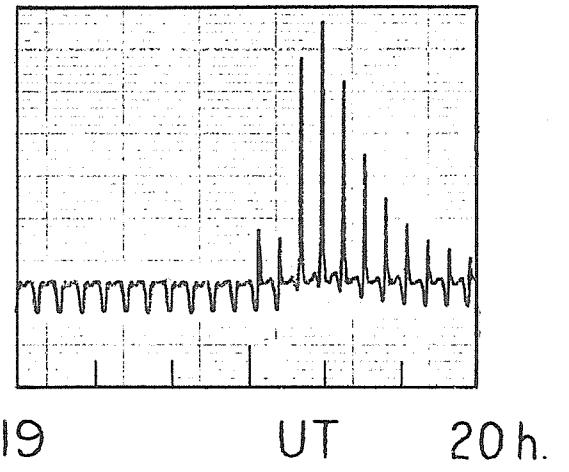

Fig. 2. Microwave burst between 1900 and 2000 UT, September 1, 1971.

Acknowledgement

This research was supported by the Air Force Office of Scientific Research under Contract AF44620-70-C-0076.

REFERENCE

BRACEWELL, R. N. and G. SWARUP 1961 The Stanford Microwave Spectroheliograph Antenna, a Microsteradian Pencil Beam Interferometer, Trans. I.R.E., Vol. AP-9, 22-30.

"Centimeter Wavelength Observations of
the Behind-the-Limb Flare of 1 September 1971"

by

Fred L. Wefer
Department of Astronomy
The Pennsylvania State University
University Park, Pennsylvania

Introduction

The data pertaining to the behind the limb event of 1 September 1971 presented below are from observations made at The Pennsylvania State University Radio Astronomy Observatory (PSURAO) with fixed frequency radiometers operating at 10.7 GHz, 2.70 GHz and 960 MHz. The radiometers and their calibration have been discussed in detail by Hagen and Wefer [1971]. A brief discussion of the radiometer systems is given in Solar-Geophysical Data [1972]. The radiometers are operated primarily as a burst patrol. The behavior of the background solar flux density with radio frequency during a two month period centered on 1 September 1971 is first discussed. Then detailed data on the microwave flare of 1 September 1971 are presented.

Background Solar Flux Density

It has been fairly well established that the proton event of 1 September 1971 was a behind-the-limb-event [Solar-Geophysical Data, 1971b]. Additional evidence for this can be gained from a study of the behavior of the undisturbed or background solar flux density. The unpublished measurements made at PSURAO, combined with the published values at other frequencies from AFCRL [Solar-Geophysical Data, 1971a and 1971c], provide values of the background solar flux density at nine frequencies in the range 245 MHz through 15.4 GHz during the period 1 August through 30 September 1971.

In Figure 1 is shown the fractional change in the background solar flux density as a function of radio frequency and time, in the form of a contour map. The contour interval is 0.1, the zero contour being indicated by tic marks on the downward (negative) side. The single ambiguity on the map is that the region just to the left of the asterisk is a depression rather than a hump. The fractional change is defined by

$$\zeta_\nu(t) = \frac{S_\nu(t) - \overline{S}_\nu}{\overline{S}_\nu}$$

where $\zeta_\nu(t)$ = fractional change in background solar flux density at frequency ν and time t,

$S_\nu(t)$ = background solar flux density at frequency ν and time t, and

$\overline{S}_\nu$ = average value of $S_\nu(t)$ over the time interval of interest.

The quantity $\zeta_\nu(t)$ is used instead of $S_\nu(t)$ directly for three reasons. It is the change in $S_\nu(t)$ with time which is of interest here, not the actual values of $S_\nu(t)$. The time average of $\zeta_\nu(t)$ is zero at each frequency, yielding a contour map much easier to interpret than a contour map of $S_\nu(t)$. Finally the values of $\zeta_\nu(t)$ are independent of errors in the values of the antenna effective areas used to compute $S_\nu(t)$, thus eliminating one of the largest sources of error in the data.

Focusing attention on frequencies above 600 MHz, it is seen that during the period 1 through 17 August 1971 the background solar flux density remained within about 10% of the two month average. The value of $\zeta_\nu(t)$ increased on 18 August at 5 GHz, the increase spreading to both higher and lower frequencies on 19 and 20 August. These increases correspond to the appearance on the east limb on 17 August

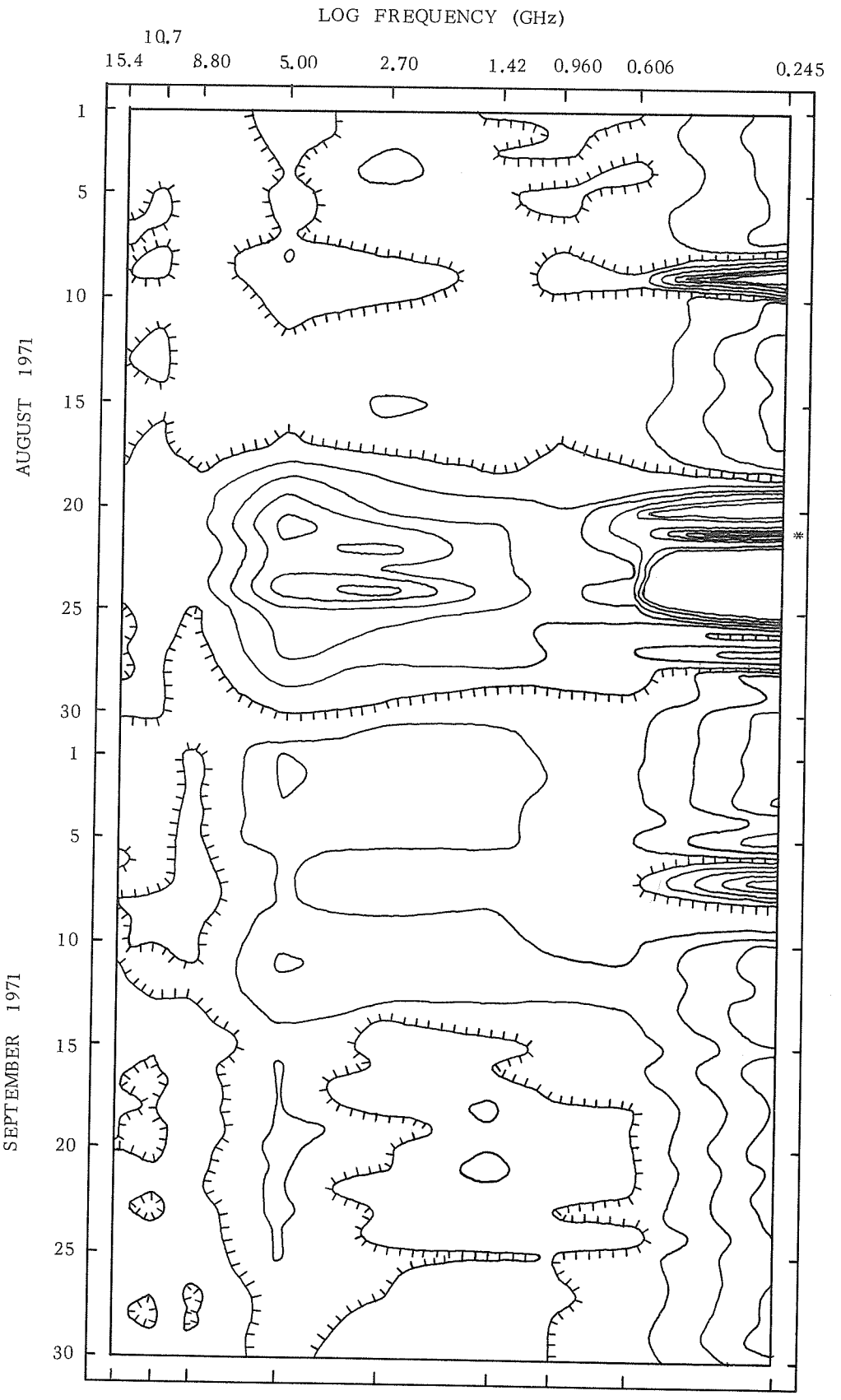

Figure 1. Contour map in the time-frequency plane of the fractional change in the background solar flux density during the period 1 August through 30 September 1971. The contour interval is 0.1, the zero contour being indicated by tic marks on the downward (negative) side.

of Mt. Wilson sunspot region 11445 (McMath Region 11482) [Solar-Geophysical Data, 1971d]. While there were a number of other regions on the visible surface of the sun, the increase in ζ did not begin until McMath region 482 appeared on the east limb. The center of region 482 crossed the central meridian on 23 August, near the center of the broad peak in ζ. The fractional change in the background solar flux density reached a peak value of 0.54 at 2.70 GHz on 24 August. Following this, ζ steadily declined, reaching a level of 0.1 at 5 GHz on 29 August, when region 482 began west limb passage. While there were a number of regions remaining on the visible surface of the sun, ζ decreased as region 482 approached the west limb. The 9.1 cm Stanford and 21 cm Fleurs spectroheliograms [Solar-Geophysical Data, 1971d] substantiate that the increase in ζ was caused almost entirely by region 482. McMath region 482 was, therefore, the most "active" by far of the various regions on the sun during this period.

The values of ζ were low and relatively constant during the month of September. When region 482 (McMath region 11516) reappeared on the east limb on 13 September, only a slight increase in the values of ζ was observed. The Stanford and Fleurs spectroheliograms also showed much reduced brightness temperatures associated with the region at this time.

McMath region 482 is thus seen to be the most likely candidate for the seat of the proton event of 1 September 1971.

The Microwave Flare

The microwave outbursts associated with the proton event of 1 September 1971 began at 19:26.3 UT, 19:28.6 UT and 19:31.8 UT at 2.70 GHz, 960 MHz and 10.7 GHz, respectively. The radiometer chart records of these events were digitized in preparation for the construction of the dynamic spectrum of the microwave flare. These digitized records are plotted in Figure 2. The flux density scale is the same for the three records. The 2.70 GHz and 960 MHz traces have been offset by 40 fu and 80 fu, respectively, in an attempt to improve clarity. The time is marked at ten minute intervals along the lower abscissa; tic marks appear every minute along the upper abscissa.

Three things should be noted in the figure. In spite of the above mentioned offsets, the 2.70 GHz and 960 MHz traces cross twice. The peak of the 2.70 GHz burst went slightly off-scale on the high gain channel causing the apparent 1.2 minute long flat maximum. Finally, the two minute long gaps in the traces beginning at 20:01 UT are caused by the automatic hourly calibration of the radiometers.

The recordings at the three frequencies are presented again in Figure 3, with the peaks of the traces normalized to unity. The two lower frequencies have again been offset to improve clarity. This figure shows the striking similarity of the shapes of the burst at the three frequencies.

While it is normally risky to attempt to construct dynamic spectra of microwave flares from only three single frequency records, the AFCRL observations [Solar-Geophysical Data, 1971e] indicated that the flare was quite regular and smooth in the frequency range 960 MHz through 10.7 GHz. The dynamic spectrum constructed from the PSURAO data alone is shown in Figure 4. The contours are logarithmic in their spacing, successive contour levels differing by a factor of two. The shape of the 128 fu contour line indicates that the peak flux density of the microwave flare occurred somewhere between 2.70 GHz and 1.42 GHz.

Hagen and Wefer [1972] have analyzed this microwave flare in some detail and were able to show that the spectrum of the peak flux densities is consistent with synchrotron radiation due to 3 Mev electrons interacting with a magnetic field of approximately 50 Gauss at a level of about 150,000 km above the photosphere.

REFERENCES

Hagen, J. P. and Wefer, F. L. 1971 A Catalog of Distinct Solar Radio Events for Fixed Frequency Observations Made at The Pennsylvania State University Radio Astronomy Observatory During the Period 1 July 1964 through 30 June 1970, The Penna. State University, Dept. of Astronomy Scientific Report No. 023.

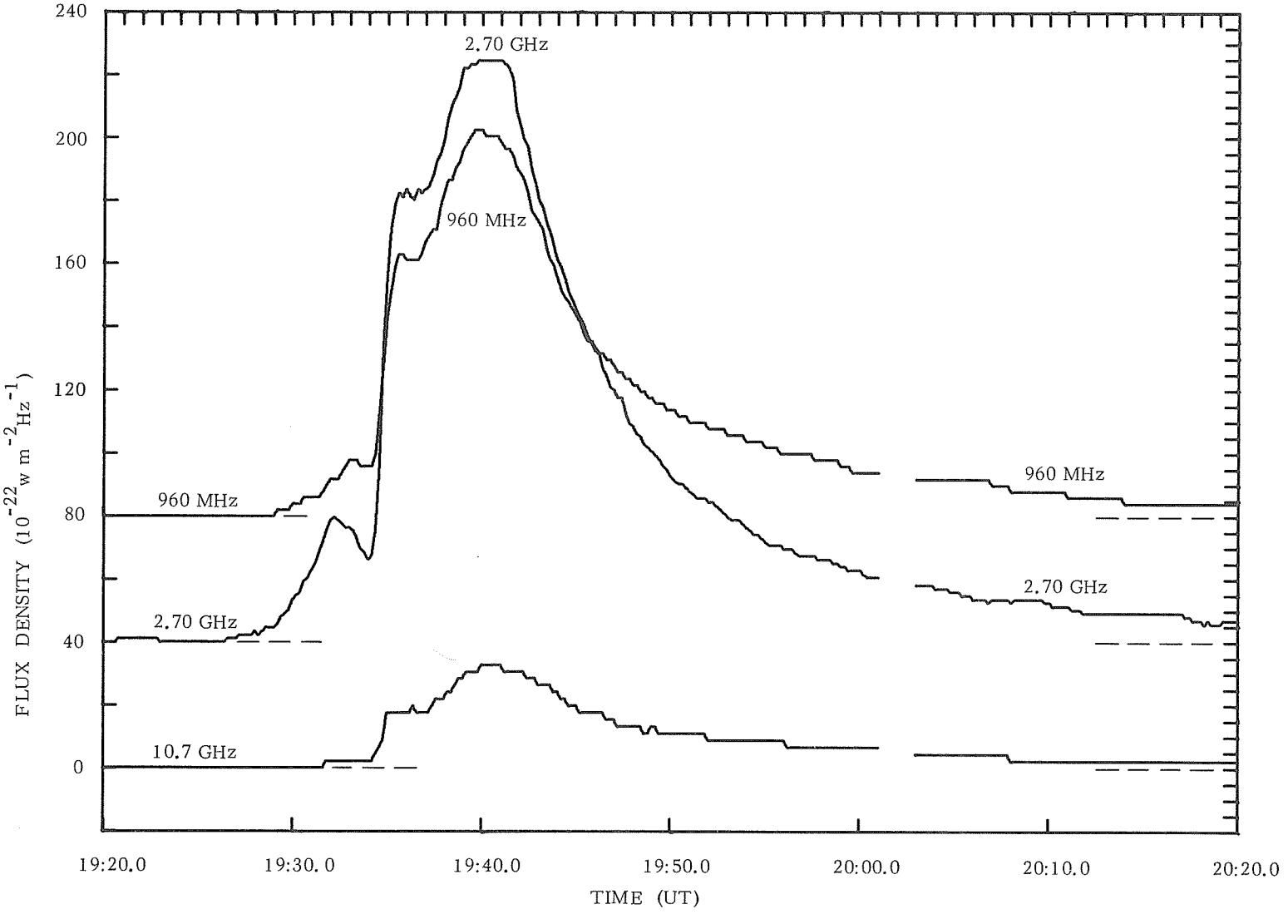

Figure 2. Plots of the digitized radiometer records of the behind-the-limb flare of 1 September 1971.

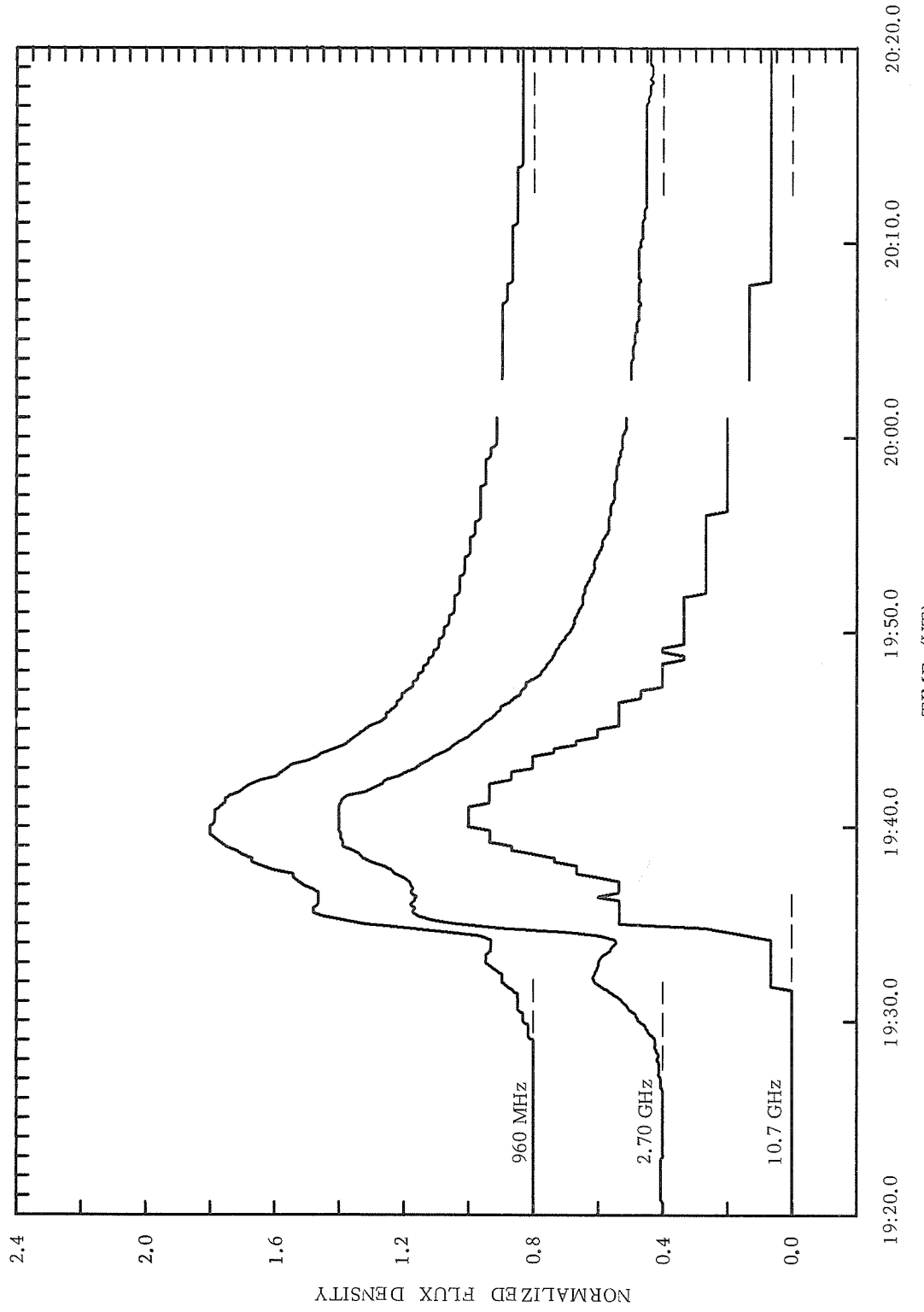

Figure 3. Plots of the digitized radiometer records with the peak flux densities normalized to unity, for the 1 September 1971 behind-the-limb flare.

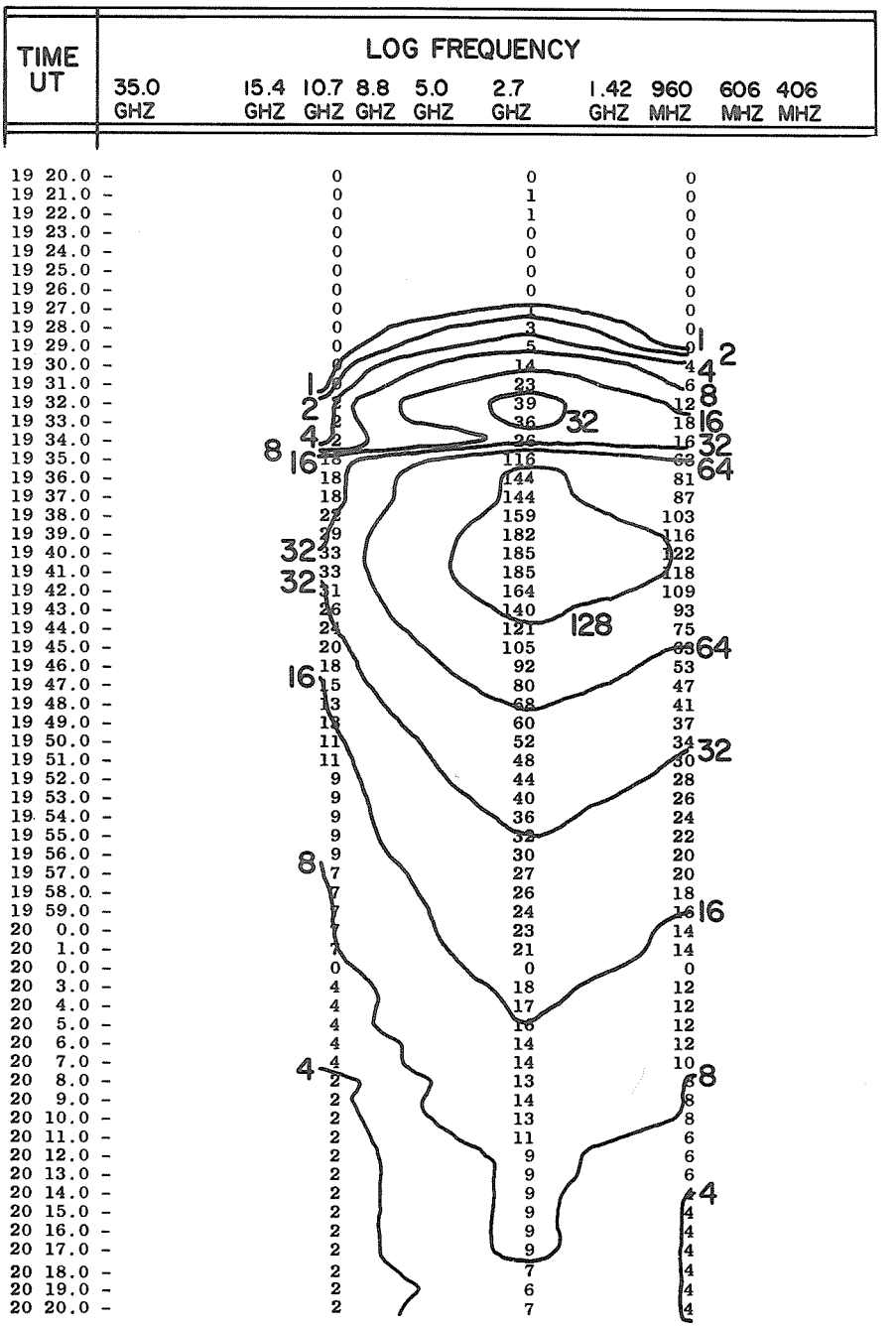

Figure 4. Dynamic spectrum of the 1 September 1971 behind-the-limb microwave flare, constructed from three fixed frequency records.

Solar-Geophysical Data	1972	No. 330 (Supplement), pp. 47-49, February 1972, U.S. Department of Commerce, (Boulder, Colorado).
Solar-Geophysical Data	1971a	No. 325-Part I, p. 7, September 1971.
Solar-Geophysical Data	1971b	No. 326-Part I, pp. 27-28, October 1971.
	1971c	_____ p. 7.
	1971d	_____ pp. 30-71 and p. 78.
	1971e	_____ p. 19.
Solar-Geophysical Data	1971f	No. 327-Part I, pp. 28-67, November 1971.
Hagen, J. P. and Wefer, F. L.	1972	Radio Observations of the Behind the Limb Flare of 1 September 1971 and Theory of Origin, paper given at American Astronomical Society meeting, April 1972.

On the S-Component and Noise Storms in September, 1971

by

A. Böhme and A. Krüger
German Academy of Sciences
Central Institute for Solar-Terrestrial Physics
(Heinrich-Hertz-Institute)
Berlin-Adlershof, GDR

[Editor's Note: See contribution by these authors on pages 61 to 63 for the January 1971 event.]

This report is restricted to a representation of radio flux and polarization data referring to the development of the active regions before the occurrence of the proton event on September 1, 1971. The observed data are shown in Table 1, and are condensed in form of synthetic spectral diagrams of the S-component and the noise storm emission (Figure 1).

It is widely believed that the S-component and noise storm spectra carry some significance about conditions facilitating the outflow of high and medium energetic solar particles, respectively [cf. also Sakurai, 1971]. However, it is indicated by the present examples that the observing conditions by directivity and angular dependence of the emission properties are not always favorable for an exact prediction of energetic events.

The August-September 1971 Period

As demonstrated by Figure 1, during the last decade of August 1971 well-expressed centers of the S-component and the noise storm component were observed, which were closely linked together. The S-component spectrum was evident up to the 3 cm-region as early as August 19, (Figure 2) indicating a proton-dangerous situation, but the event came more than 10 days later when the related active center on the southern hemisphere had passed over the west limb.

The complex of the noise storm was visible between August 20-25. A modulation of the radiation as shown in Figure 1 perhaps could be interpreted by motions of the magnetic structure of the noise storm emitting region or by the passing of different tubes of force through the line of sight. On several days the polarization was varying. The noise storm flux spectrum was broader than that of the former period of January 1971 (cf. Figure 2). After 25 August the noise storm radiation disappeared. The disappearance of the source of the S-component occurred on August 30.

Table 1

Daily Flux and Polarization data
Heinrich-Hertz-Institute

1971 August	9500	3000	1490	510	287	234	113	68	40 MHz
16	271 l	83	86 0	28	7	7	2 0	<	< 0
17	273 l	84	88 0	28	7	7	2 0	<	< 0
18	286 0	91	93 0	28	8	11	3 0	<	< 0
19	300 r	-	101 l	33	11	11	20 r-l	<	< 0
20	293 -	115	110 l	48	28	57	73 L	120	197 l
21	- -	126	112 0	53	41	89	14 l	<	< l
22	- -	-	111 0	35	52	124	170 L	166	306 l
23	- r	130	112 0	35	37	120	98 l	<	< -
24	274:r	130	108 0	39	83	183	586 R-l	741	316 r
25	276:0	125	109 r:	28	16	36	137 l-r	164	331 0
26	270:l	118	105 r:	28	10	9	11 l	<	< 0
27	269:0	115	102 r:	28	11	16	4 l	<	< 0
28	270:r	128	97 r:	32	5	9	2 0	<	< 0
29	262:0	96	87 -	28	5	8	2 0	<	< 0
30	256:0	88	85 r:	35	7	8	2 0	<	< 0
31	253 0	79	80 r:	35	9	7	2 0	<	< 0

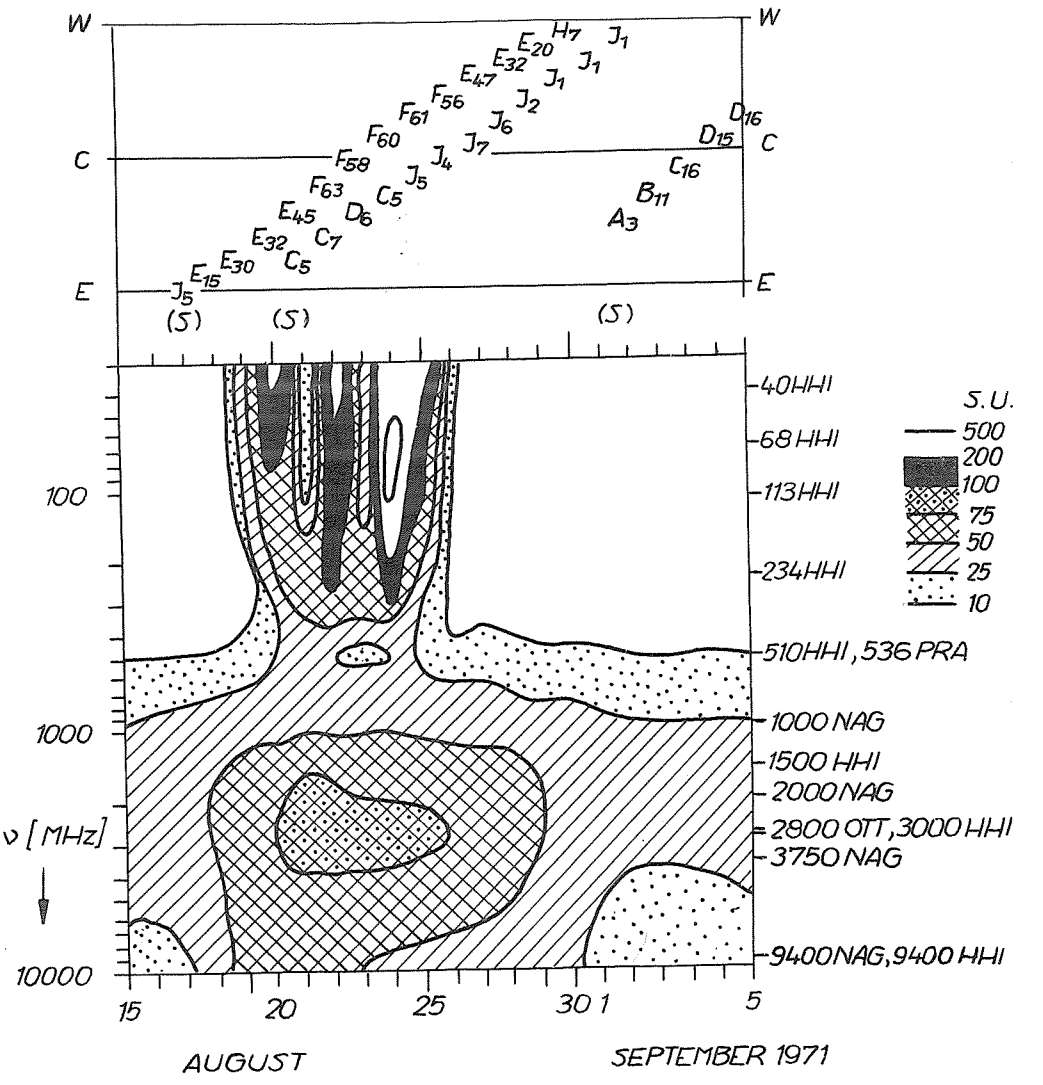

Fig. 1 Spectral diagrams of S- and noisestorm components and major spot groups (top).

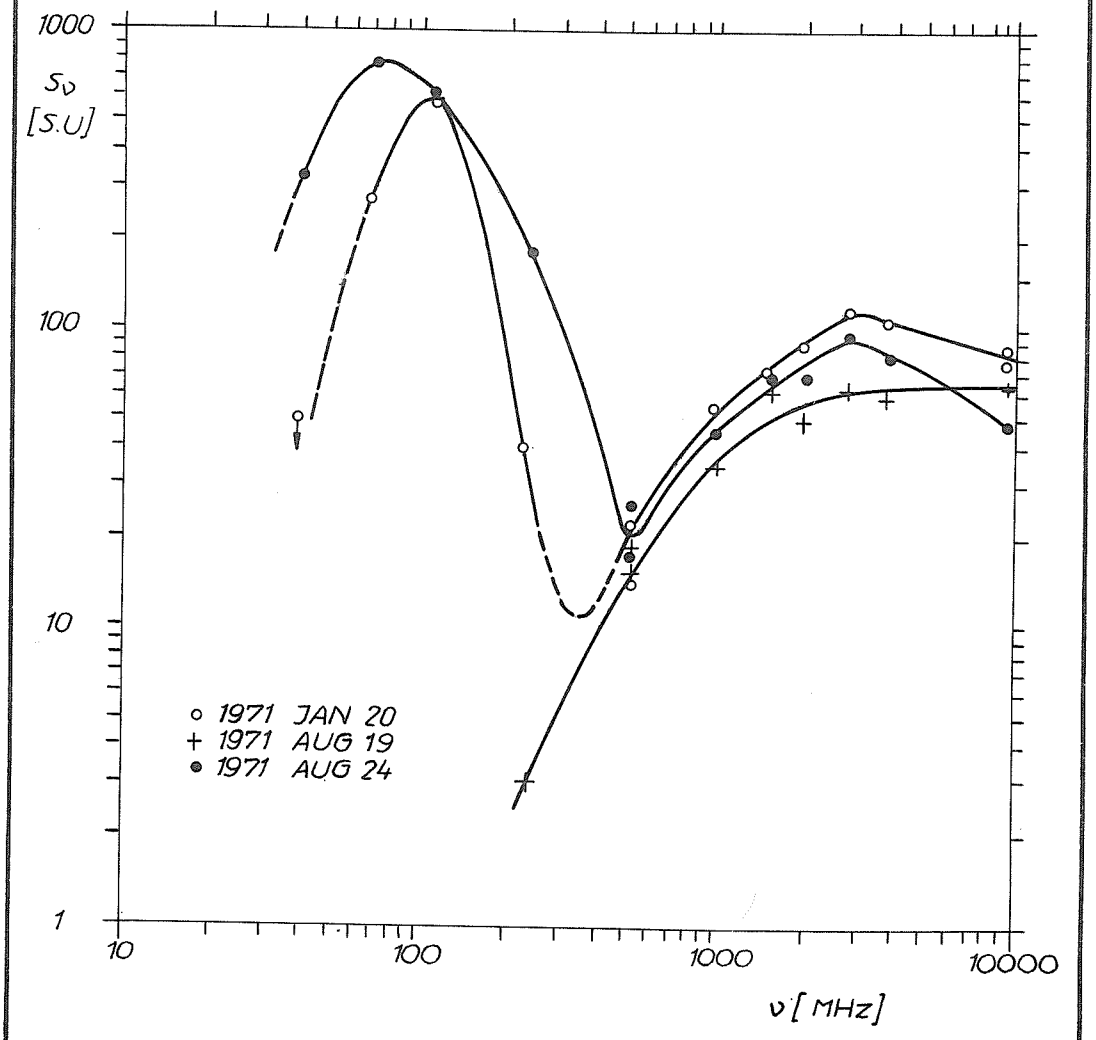

Fig. 2 Spectra of daily mean fluxes of noisestorms and the S-component for selected cases

REFERENCES

BOHME, A. and A. KRUGER 1971 Characteristics of Noise Storms and the S-Component of Solar Radio Emission in March, 1970. World Data Center A - Upper Atmosphere Geophysics Report UAG-12, 71.

SAKURAI, K. 1971 Type I Noise Active Regions and Energetic Electrons from 1 to 10 March 1970. World Data Center A - Upper Atmosphere Geophysics Report UAG-12, 52.

Millimeter Wave Spectroheliograms Associated with the September 1, 1971 Solar Terrestrial Event

by

Larry E. Telford
Air Force Cambridge Research Laboratories
L. G. Hanscom Field, Bedford, Massachusetts 01730

8.6 mm spectroheliograms have been taken on a daily basis (weather and equipment permitting) since the Summer, 1968. In March, 1971, 20 mm spectroheliograms were added to the daily routine. The 8.6 mm and 20 mm spectroheliograms are taken concurrently using a dual frequency feed system on the AFCRL 29-Foot Millimeter Wave Antenna. This submission represents a collection of 8.6 mm spectroheliograms and 20 mm spectroheliograms covering two weeks prior to the September 1 event. Equipment problems prevented the generation of an 8.6 mm spectroheliogram on August 18 and the generation of 20 mm spectroheliograms on August 20, 21, and 24 and September 1.

The following comments apply to the spectroheliograms presented in Figures 1 through 5:

1. All spectroheliogram radio brightness temperatures are to be multiplied by ten, i.e., 520° = 5200°K.
2. All spectroheliogram radio brightness temperatures are antenna temperatures corrected for atmospheric attenuation but not corrected for antenna pattern effects.
3. The 8.6 mm antenna pattern and radiometer parameters are given in the latest "Solar-Geophysical Data Descriptive Text".
4. The antenna half power beamwidth at 20 mm is 8 minutes of arc with first side lobe levels at approximately -18 dB. The 20 mm radiometer is a standard Dicke type with a sensitivity of 2°K for a one second time constant.
5. The difference between the average antenna temperatures in the January (p. 64) and the September sets of 8.6 mm spectroheliograms is due to a change in the calibrate noise tube in the intervening period.
6. The contour levels for the plotted spectroheliograms are:
   Figures 1, 2, and 3 - 3000°K, 5200°K and up in 200°K increments.
   Figures 4 and 5 - 3000°K, 5000°K and up in 100°K increments.
7. The times associated with each spectroheliogram is the time the center grid point was observed. The spectroheliogram observation sequence starts at the upper left corner of the plotted grid and ten seconds are spent at each grid point. The sequence moves from left to right for each line. Using this sequence, the exact observation time for each grid point can be calculated.

In addition to the plotted spectroheliograms, Tables 1 and 2 represent the output of a data reduction computer program which interpolates the original radio brightness temperature grid and searches for maxima with a fixed set of searching constraints. The tables represent the heliographic location and enhancement, or temperature above the average surface background temperature, for each maxima found for each spectroheliogram. In reproducing the table, all maxima with enhancements less than 100°K were ignored. Since the input grid data are not corrected for antenna effects, the maxima locations are not accurate when the region is greater than ±45° from Central Meridian at 8.6 mm or ±25° from Central Meridian at 20 mm. Within these limits, the locations are accurate to ±2° in heliographic coordinates.

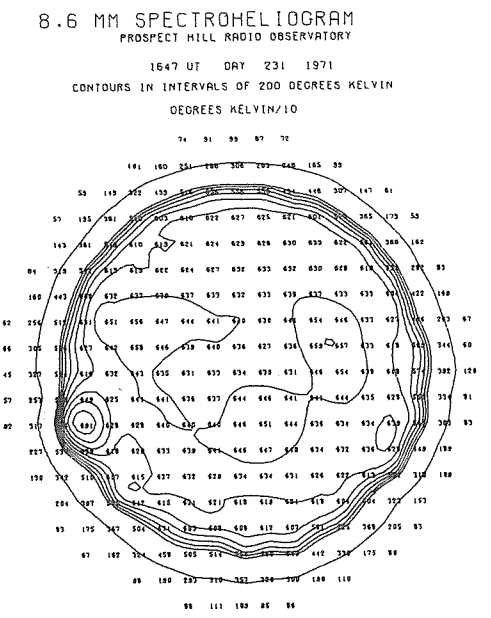
8.6 MM SPECTROHELIOGRAM
PROSPECT HILL RADIO OBSERVATORY
1647 UT DAY 231 1971
CONTOURS IN INTERVALS OF 200 DEGREES KELVIN
DEGREES KELVIN/10

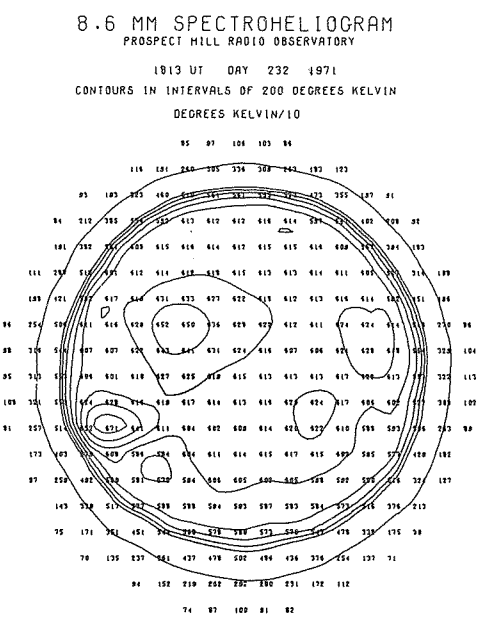
8.6 MM SPECTROHELIOGRAM
PROSPECT HILL RADIO OBSERVATORY
1813 UT DAY 232 1971
CONTOURS IN INTERVALS OF 200 DEGREES KELVIN
DEGREES KELVIN/10

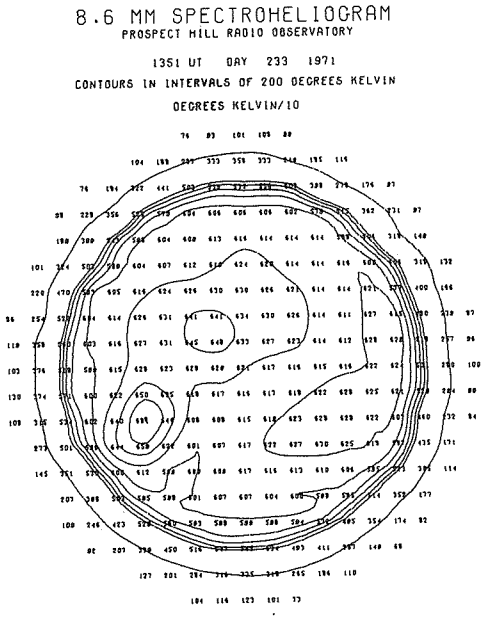
8.6 MM SPECTROHELIOGRAM
PROSPECT HILL RADIO OBSERVATORY
1351 UT DAY 233 1971
CONTOURS IN INTERVALS OF 200 DEGREES KELVIN
DEGREES KELVIN/10

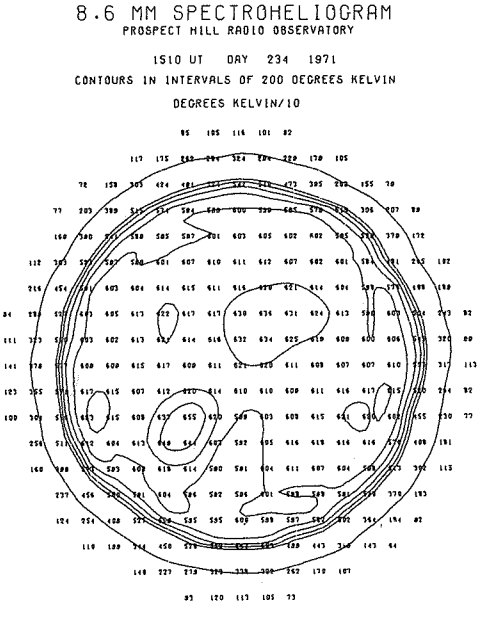
8.6 MM SPECTROHELIOGRAM
PROSPECT HILL RADIO OBSERVATORY
1510 UT DAY 234 1971
CONTOURS IN INTERVALS OF 200 DEGREES KELVIN
DEGREES KELVIN/10

Fig. 1.

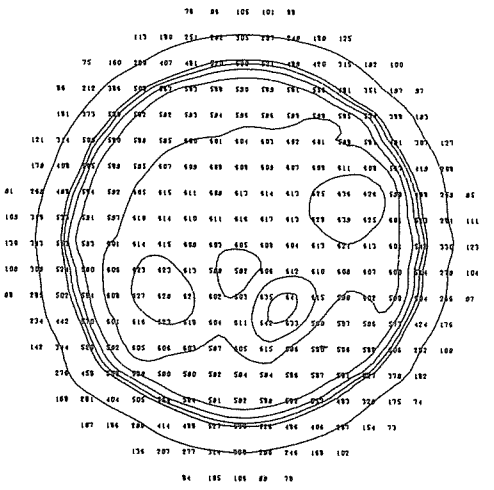
8.6 MM SPECTROHELIOGRAM
PROSPECT HILL RADIO OBSERVATORY
1415 UT DAY 236 1971
CONTOURS IN INTERVALS OF 200 DEGREES KELVIN
DEGREES KELVIN/10

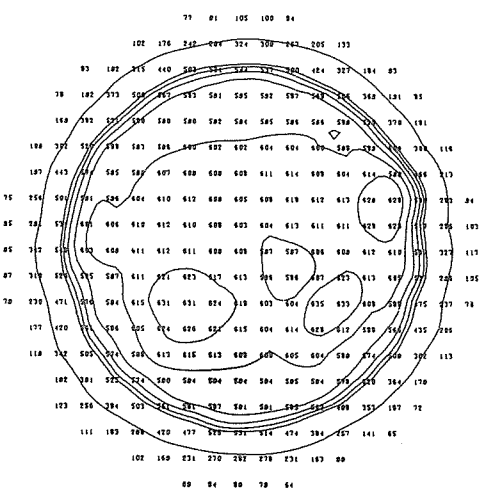
8.6 MM SPECTROHELIOGRAM
PROSPECT HILL RADIO OBSERVATORY
1454 UT DAY 237 1971
CONTOURS IN INTERVALS OF 200 DEGREES KELVIN
DEGREES KELVIN/10

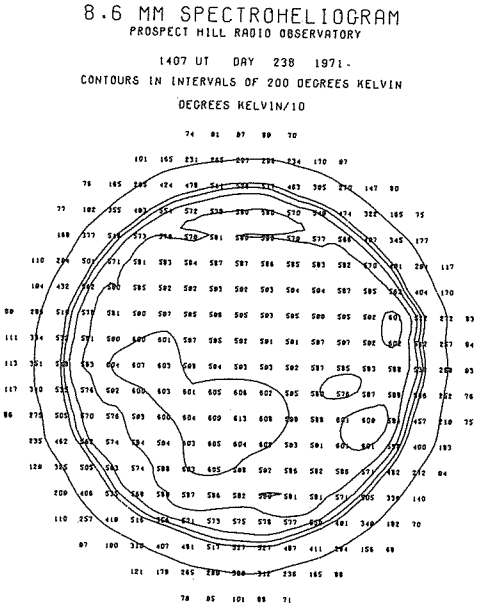
8.6 MM SPECTROHELIOGRAM
PROSPECT HILL RADIO OBSERVATORY
1407 UT DAY 238 1971
CONTOURS IN INTERVALS OF 200 DEGREES KELVIN
DEGREES KELVIN/10

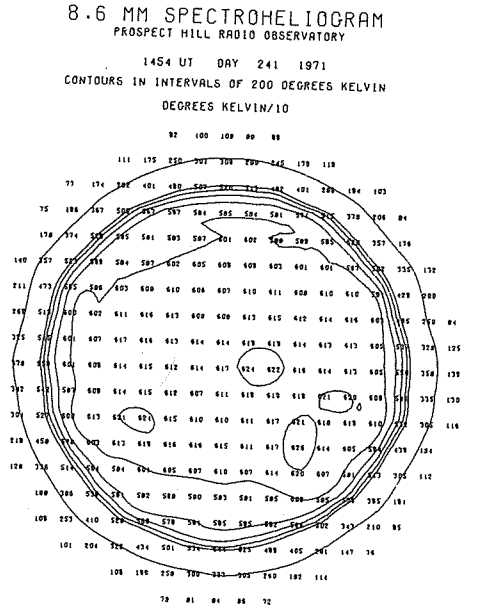
8.6 MM SPECTROHELIOGRAM
PROSPECT HILL RADIO OBSERVATORY
1454 UT DAY 241 1971
CONTOURS IN INTERVALS OF 200 DEGREES KELVIN
DEGREES KELVIN/10

Fig. 2.

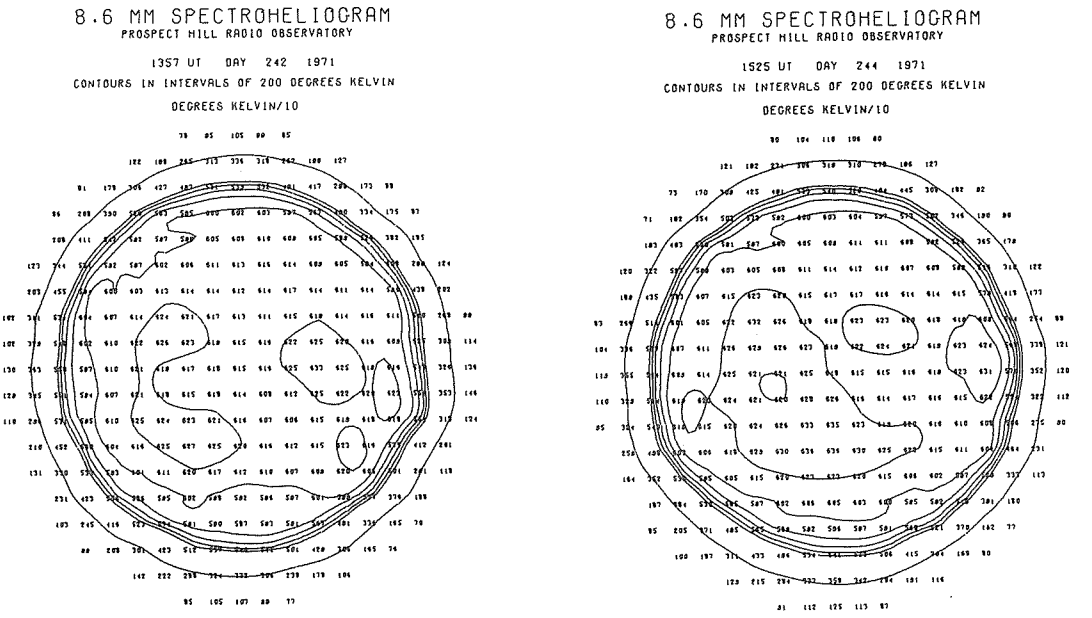
8.6 MM SPECTROHELIOGRAM
PROSPECT HILL RADIO OBSERVATORY
1357 UT DAY 242 1971
CONTOURS IN INTERVALS OF 200 DEGREES KELVIN
DEGREES KELVIN/10
8.6 MM SPECTROHELIOGRAM
PROSPECT HILL RADIO OBSERVATORY
1525 UT DAY 244 1971
CONTOURS IN INTERVALS OF 200 DEGREES KELVIN
DEGREES KELVIN/10

Fig. 3.

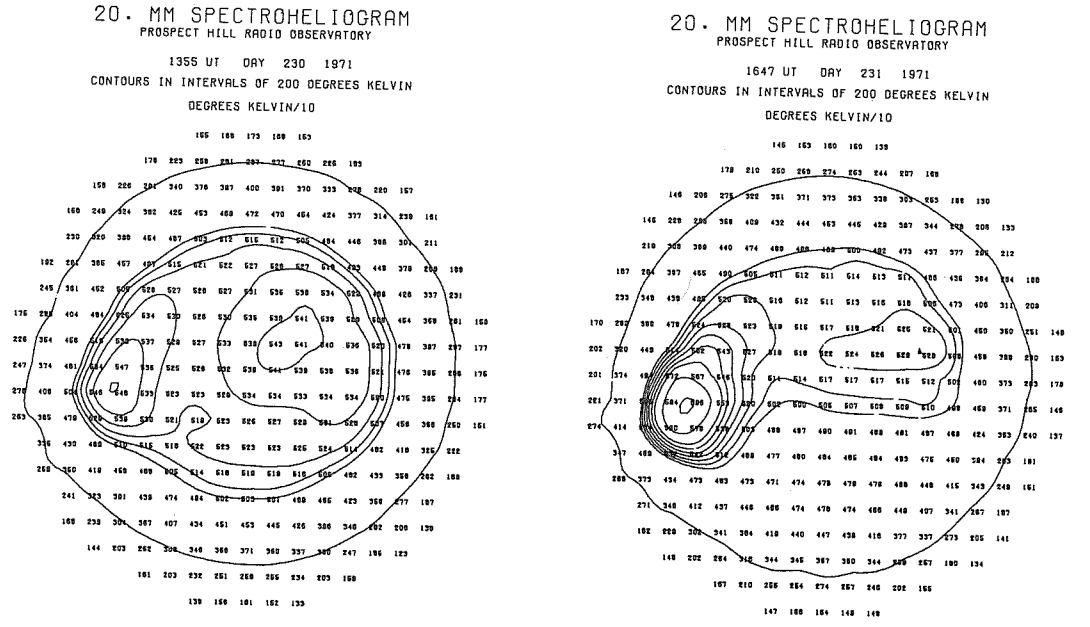
20. MM SPECTROHELIOGRAM
PROSPECT HILL RADIO OBSERVATORY
1355 UT DAY 230 1971
CONTOURS IN INTERVALS OF 200 DEGREES KELVIN
DEGREES KELVIN/10
20. MM SPECTROHELIOGRAM
PROSPECT HILL RADIO OBSERVATORY
1647 UT DAY 231 1971
CONTOURS IN INTERVALS OF 200 DEGREES KELVIN
DEGREES KELVIN/10

Fig. 4.

20. MM SPECTROHELIOGRAM
PROSPECT HILL RADIO OBSERVATORY

1510 UT DAY 234 1971
CONTOURS IN INTERVALS OF 200 DEGREES KELVIN
DEGREES KELVIN/10

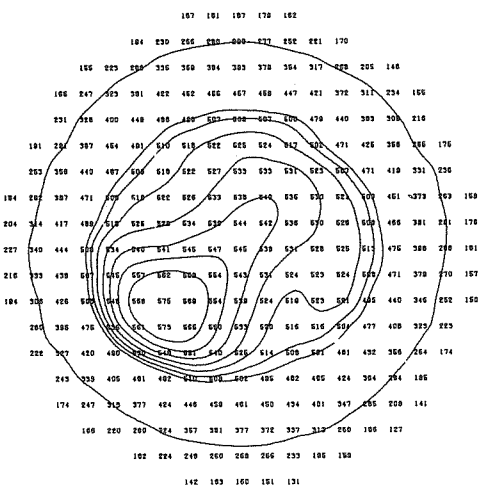

20. MM SPECTROHELIOGRAM
PROSPECT HILL RADIO OBSERVATORY

1454 UT DAY 237 1971
CONTOURS IN INTERVALS OF 200 DEGREES KELVIN
DEGREES KELVIN/10

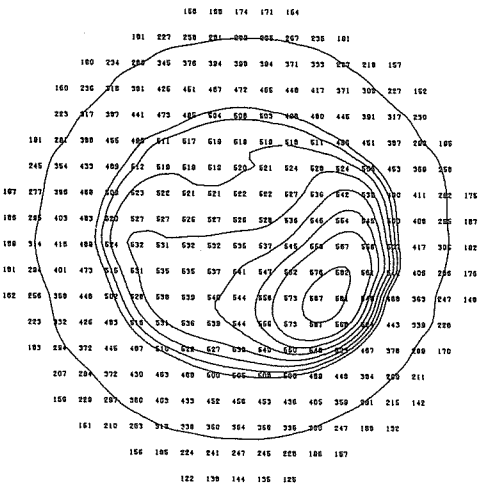

20. MM SPECTROHELIOGRAM
PROSPECT HILL RADIO OBSERVATORY

1407 UT DAY 238 1971
CONTOURS IN INTERVALS OF 200 DEGREES KELVIN
DEGREES KELVIN/10

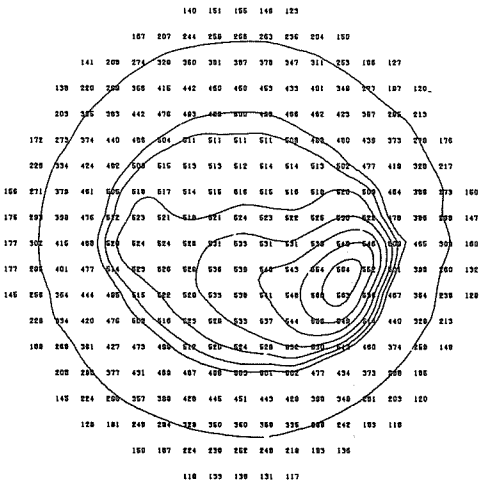

20. MM SPECTROHELIOGRAM
PROSPECT HILL RADIO OBSERVATORY

1454 UT DAY 241 1971
CONTOURS IN INTERVALS OF 200 DEGREES KELVIN
DEGREES KELVIN/10

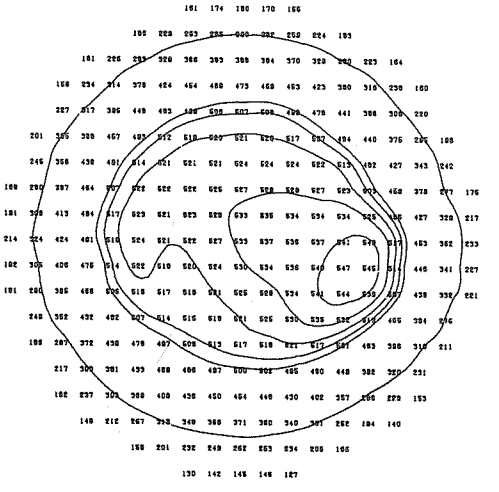

20. MM SPECTROHELIOGRAM
PROSPECT HILL RADIO OBSERVATORY

1357 UT DAY 242 1971
CONTOURS IN INTERVALS OF 200 DEGREES KELVIN
DEGREES KELVIN/10

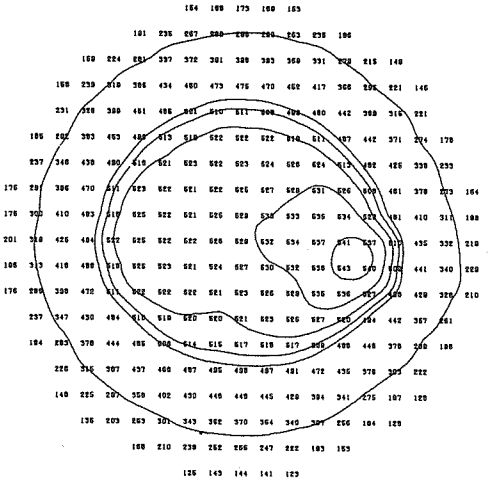

Fig. 5.

TABLE 1

Day 231
AUGUST 19, 1971 1647 UT
$L_o = 326^o$, $B_o = +7^o$

L	LAT	CMD	8 mm
282	09N	44E	220 K
294	07N	32E	295 K
350	04N	24W	320 K
300	07S	26E	140 K
332	10S	06W	210 K
271	14S	55E	835 K

Day 232
AUGUST 20, 1971 1813 UT
$L_o = 311^o$, $B_o = +7^o$

L	LAT	CMD	8 mm
266	12N	45E	160 K
292	09N	19E	455 K
349	05N	38W	185 K
353	03N	42W	180 K
334	08S	23W	150 K
269	13S	42W	655 K

Day 233
AUGUST 21, 1971 1351 UT
$L_o = 299^o$, $B_o = +7^o$

L	LAT	CMD	8 mm
288	05N	11E	340 K
344	03N	45W	200 K
341	07S	42W	110 K
328	09S	29W	150 K
268	13S	31E	665 K
321	16S	22W	155 K

Day 234
AUGUST 22, 1971 1510 UT
$L_o = 286^o$, $B_o = +7^o$

L	LAT	CMD	8 mm
262	09N	24E	130 K
291	08N	05W	290 K
234	12S	52E	180 K
269	14S	17E	495 K

TABLE 1 Continued

Day 236
AUGUST 24, 1971 1415 UT
$L_o = 260^o$, $B_o = +7^o$

L	LAT	CMD	8 mm
237	09N	23E	150 K
290	07N	30W	405 K
263	05N	03W	165 K
234	12S	26E	295 K
270	14S	10W	485 K

Day 237
AUGUST 25, 1971 1454 UT
$L_o = 247^o$, $B_o = +7^o$

L	LAT	CMD	8 mm
262	11N	15W	160 K
289	06N	42W	330 K
227	13S	20E	320 K
271	13S	24W	390 K

Day 238
AUGUST 26, 1971 1407 UT
$L_o = 233^o$, $B_o = +7^o$

L	LAT	CMD	8 mm
257	08N	22W	130 K
283	06N	50W	190 K
200	02S	33E	210 K
232	11S	01E	260 K
270	14S	37W	250 K

Day 241
AUGUST 29, 1971 1454 UT
$L_o = 194^o$, $B_o = +7^o$

L	LAT	CMD	8 mm
235	09N	41W	120 K
166	05N	28E	135 K
203	00	09W	200 K
226	08S	32W	175 K
168	13S	26E	175 K
187	17S	07E	115 K
215	17S	21W	215 K

Day 242
AUGUST 30, 1971 1357 UT
$L_o = 181^o$, $B_o = +7^o$

L	LAT	CMD	8 mm
158	06N	23E	180 K
202	01S	21W	240 K
226	09S	45W	150 K
153	12S	28E	180 K
163	17S	18E	185 K
212	19S	31W	155 K

Day 244
SEPTEMBER 1, 1971 1525 UT
$L_o = 154^o$, $B_o = +7^o$

L	LAT	CMD	8 mm
131	09N	23E	200 K
166	08N	12W	125 K
202	03S	48W	195 K
103	09S	51E	120 K
109	13S	45E	115 K
150	15S	04E	250 K
136	17S	18E	180 K

TABLE 2

Day 230
AUGUST 18, 1971 1355 UT
$L_o = 339^\circ$, $B_o = +7^\circ$

	L	LAT	CMD	20 mm
	346	04N	07W	175 K
*	296	07S	44E	250 K

Day 231
AUGUST 19, 1971 1647 UT
$L_o = 326^\circ$, $B_o = +7^\circ$

	L	LAT	CMD	20 mm
	352	04N	26W	160 K
*	281	09S	45E	870 K

Day 234
AUGUST 22, 1971 1510 UT
$L_o = 286^\circ$, $B_o = +7^\circ$

L	LAT	CMD	20 mm
263	14S	23E	540 K

Day 237
AUGUST 25, 1971 1454 UT
$L_o = 247^\circ$, $B_o = +7^\circ$

L	LAT	CMD	20 mm
269	13S	22W	610 K

Day 238
AUGUST 26, 1971 1407 UT
$L_o = 233^\circ$, $B_o = +7^\circ$

	L	LAT	CMD	20 mm
	199	03S	34W	045 K
*	262	09S	29W	460 K

Day 241
AUGUST 29, 1971 1454 UT
$L_o = 194^\circ$, $B_o = +7^\circ$

	L	LAT	CMD	20 mm
	163	09N	31E	060 K
	161	01S	33E	070 K
*	226	08S	32W	310 K

Day 242
AUGUST 30, 1971 1357 UT
$L_o = 181^\circ$, $B_o = +7^\circ$

	L	LAT	CMD	20 mm
	146	01S	35E	080 K
*	213	08S	32W	260 K

* Heliographic longitude given for reference only and is in error due to large beamwidth at 20 mm. Region corresponds to L269,S13.

REFERENCE

1972 Solar-Geophysical Data, Descriptive Text, Number 330 (Supplement), February, 1972, U.S. Department of Commerce, (Boulder, Colorado U.S.A. 80302), 21.

Dynamic Radio Spectra of the Solar Flare of 1971 September 1 1930 UT

by

A. Maxwell
Harvard Radio Astronomy Station, Fort Davis, Texas 79734

During 1971, the solar dynamic radio-spectrum analyzer at the Harvard Radio Astronomy Station, Fort Davis, Texas, operated over the complete band 10-2000 MHz. Descriptions of the equipment will be found elsewhere [Thompson, 1961; Maxwell, 1971]. The receivers in the band 500-2000 MHz were put into operation in 1970 and are connected to a steerable 85-ft antenna, whose large collecting area permits solar bursts in this band to be recorded at high sensitivity.

The radio burst recorded on 1971 September 1 at Fort Davis was of much shorter duration than that of January 24 (see p. 69). Figure 1 shows a type II burst commenced in the meter band at 19hr 33min 40sec and continued until about 1948 UT. Type IV radiation was recorded in the decimeter band from 19hr 34min 30sec until approximately 1950 UT. In the optical band, the Lockheed, Boulder, and Palehua Observatories, although making observations at the time, did not report sighting any flare. However, Dr. Helen Dodson-Prince (private communication) reports that at the McMath-Hulburt Observatory, although observing conditions were poor, prominence activity was observed off the West limb of the sun at latitude S10 when the clouds cleared at 1953 UT. Further prominence activity was observed at the same location during the following hour. Dr. Dodson-Prince also reports that one of the biggest active areas of the present solar cycle had just passed over the solar limb, and suggests that the whole solar event fits the pattern of proton storm events that have originated from flares that have occurred just beyond the West limb.

REFERENCES

MAXWELL, A. 1971 Solar Phys., 16, 224.

THOMPSON, A. R. 1961 Astrophys. J., 133, 643.

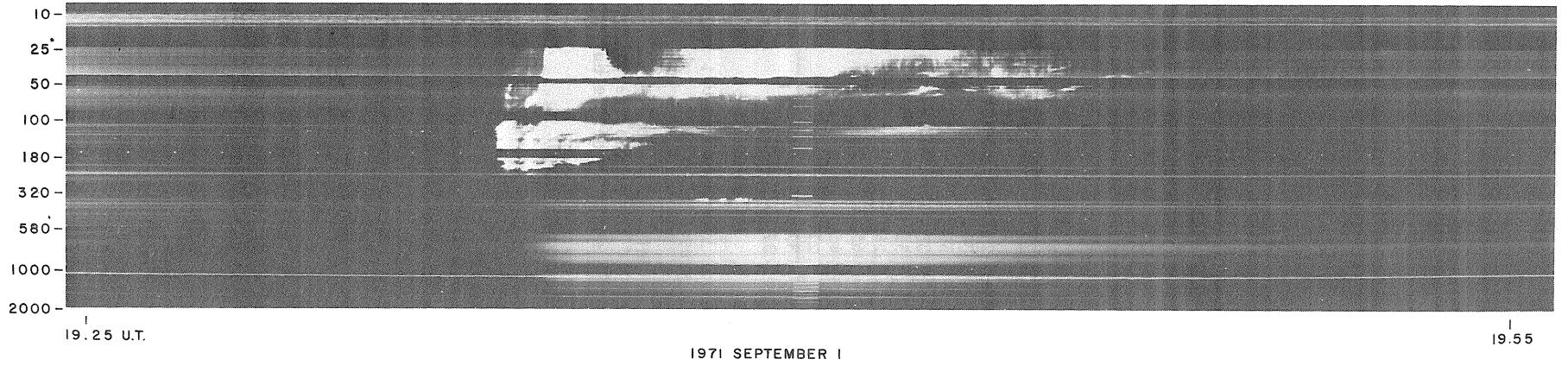

Fig. 1. Dynamic spectra of the solar radio burst recorded at the Harvard Radio Astronomy Station, Fort Davis, Texas.

September 1, 1971, Solar Radio Burst Observation

by

W. R. Barron
Air Force Cambridge Research Laboratories
Bedford, Massachusetts

A proton and ground-level event started this date which was associated with a solar radio burst beginning about 1926 UT. The PCA at 30 MHz, which started September 1 at about 2030 UT, ultimately reached 5.6 dB absorption at 1800 UT on September 2 at Thule Air Base, Greenland. The ground level event reached a maximum of 12% above normal near 2250 UT on September 1. Satellite sensors of greater than 25 Mev particles reached a maximum September 2 near 0400 UT with an enhancement of greater than 50 times normal. Only small X-ray increases were observed.

The solar radio burst was the best indicator of the parent event which apparently took place in McMath Region 11482 at S11, L = 269° which was then estimated to be 30° beyond the west limb. No flare was observed. The only optical evidence was an active prominence seen starting on September 1 at 1944 UT on the west limb near S11.

The Sagamore Hill solar radio data are as follows:

Frequency (MHz)	Time (UT) Start	Time (UT) Max	Duration Min	Flux Density 10^{-22}W m^{-2}(Hz)$^{-1}$ Peak	Flux Density 10^{-22}W m^{-2}(Hz)$^{-1}$ Mean	Type of Event (SGD Classification)
15400	1934.3	1941.2	21.7	21.6	10.1	20
8800	1930.7	1940.9	34.0	36.1	18.0	22
4995	1929.1	1940.5	50.1	68.0	26.2	22
2695	1926.9	1940.5	35.3	120.0	40.0	04
1415	1926.9	1939.6	33.8	160.0	45.0	04
606	1931.1	1940.4	28.9	150.0	45.0	04
410	1932.1	1940.3	65.0	88.0	40.0	06
245	1931.3	1934.4	65.7	810.0	320.0	47
2695	2002.2	2002.2	27.8U	13.0	5.5	29
1415	2000.7	2000.7	32.7	15.4	7.7	29
606	2000.0	2000.0	37.0	14.7	7.3	29

24-48 MHz Group of type III's: 1934.2-1936.3 UT; intensity 2; type IV: 1937.0-1946.9 UT; intensity 2; 30 MHz burst increase.

One of the important uses of these data is in studies of the solar radio burst heights and probable electron densities from knowledge of the probable angular burst position beyond the solar limb, the observed burst spectrum, and probable spectrum of the burst if it had occurred on the visible disk.

Analysis of the Polarization of the Solar Radio Emission at 237 MHz, during the Period 17-31 August 1971, Coming from the McMath Region 11482, Responsible for the Event of September 1, 1971

by

Paolo Santin
Astronomical Observatory
Trieste, Italy

The event that determined the ground level cosmic ray increase of September 1, 1971 originated in the McMath Region 11482, which on that day was not visible on the solar disk since it crossed the West limb on August 31, 1971.

In this paper the solar radio emission at 237 MHz coming from that active zone will be analyzed with particular emphasis on the circular polarization of the background radiation. The period considered is August 17-31, 1971, viz. the whole passage on the visible disk of McMath Region 11482. It was possible to make this analysis, even with an instrument with low resolution power, since during that period McMath Region 11482 was the only active solar region from a radio point of view.

Our receiver, fed by a ten meter parabolic antenna, is a radiopolarimeter functioning at 237 MHz with a bandwidth of 0.5 MHz [Sedmak, 1970]. Its output gives the sum and the difference of the two circularly polarized components, L + R and L - R, with a low time resolution (20 cm/h) and also the details of the two separate components L and R with high time resolution ($\geq$ 2 mm/sec). We thus have the total flux and the degree of circular polarization m = (L-R)/(L+R), whose accuracy can generally be considered better than 10%.

Figure 1 shows the behavior of the daily mean emission during the whole passage of the active region on the visible disk. A noise storm developed with its characteristic directivity in a rather large frequency range, at least from 30 to 540 MHz (see Spectral Data from Weissenau Bulletin). The maximum emission occurred on August 24 at 1330.36 UT, with a flux density of 546 solar flux units (10^{-22} $Wm^{-2}Hz^{-1}$).

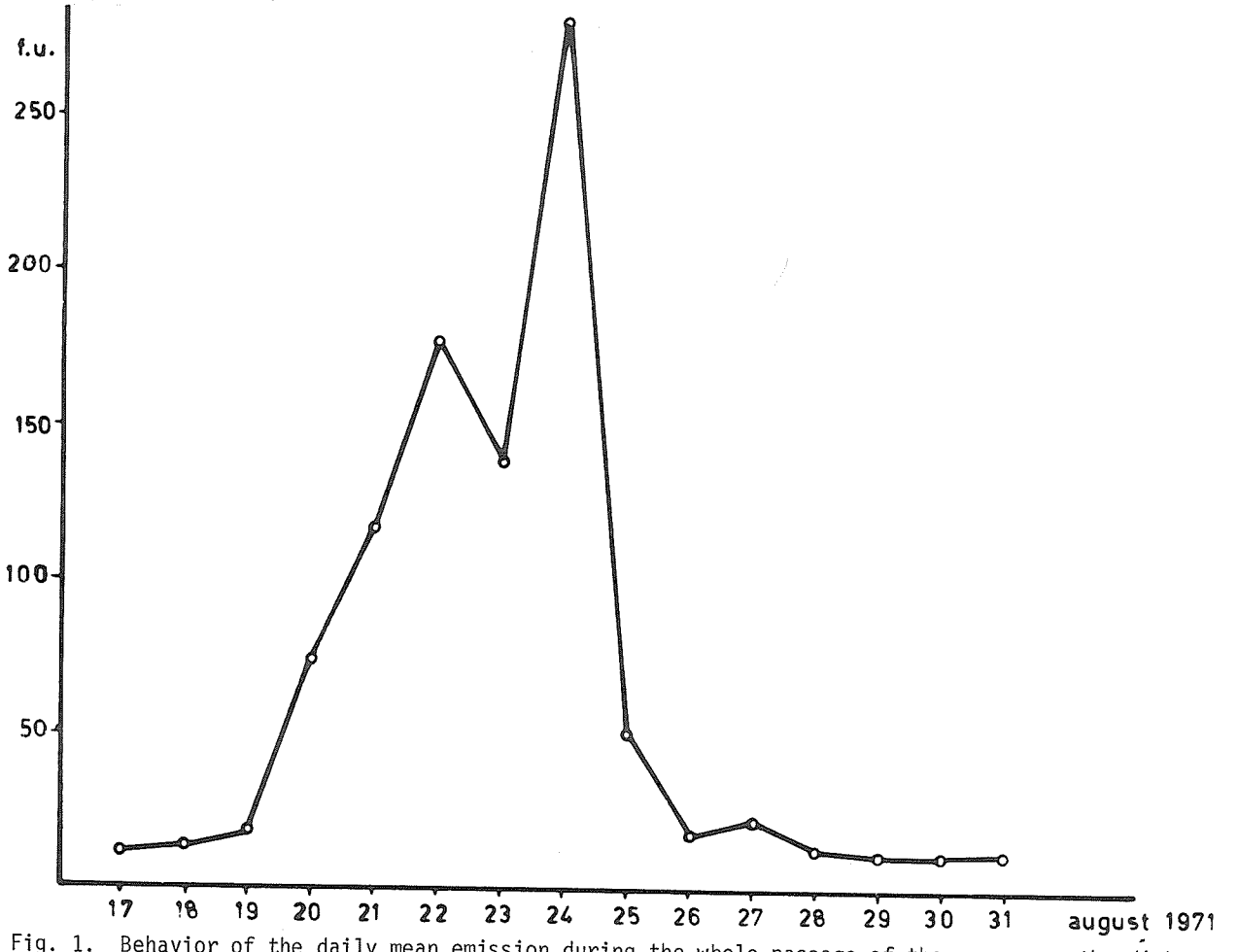

Fig. 1. Behavior of the daily mean emission during the whole passage of the source on the disk.

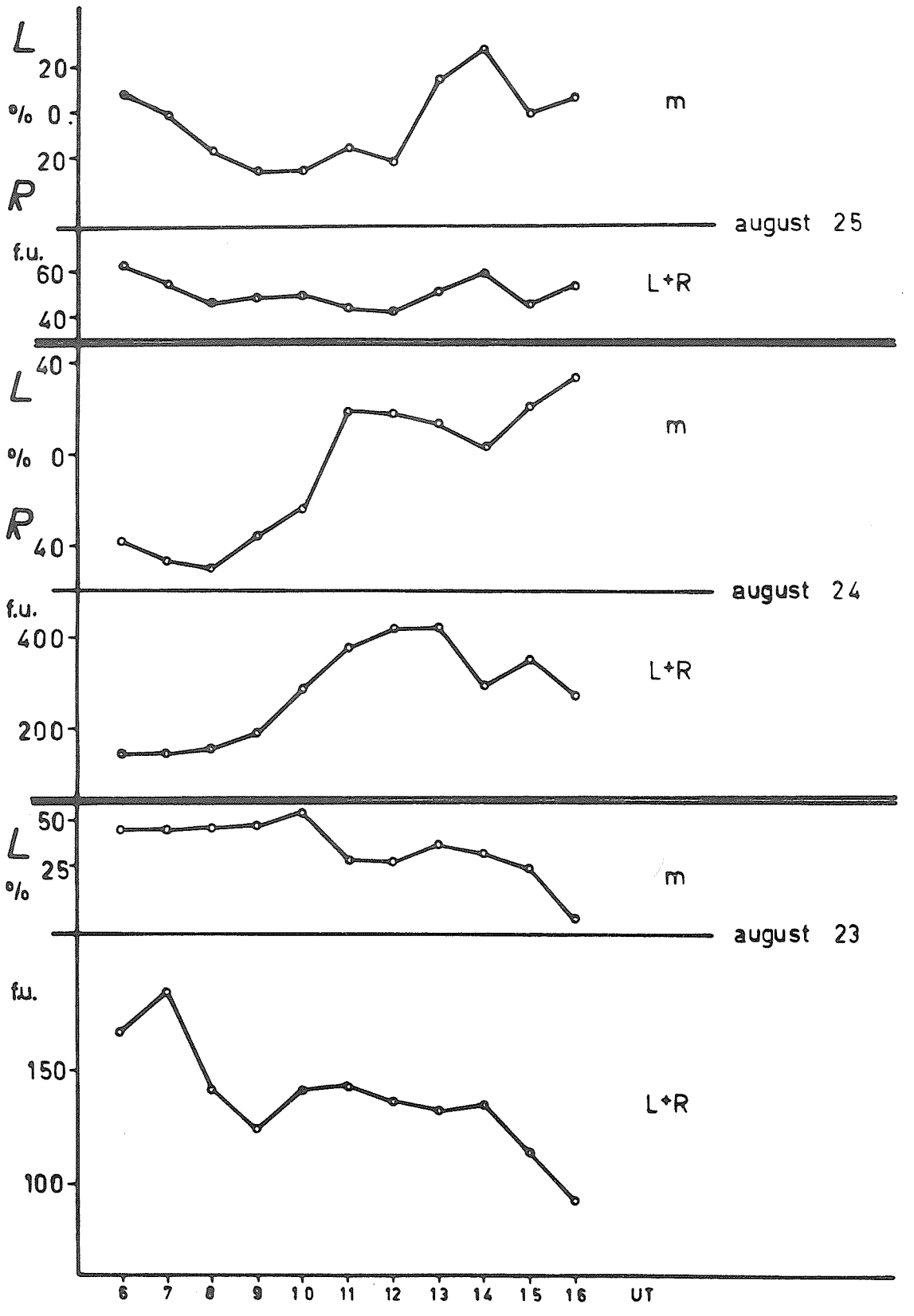

Fig. 2. Total flux and degree of circular polarization during the days of August 23, 24 and 25. The means are referred to the hour following that marked.

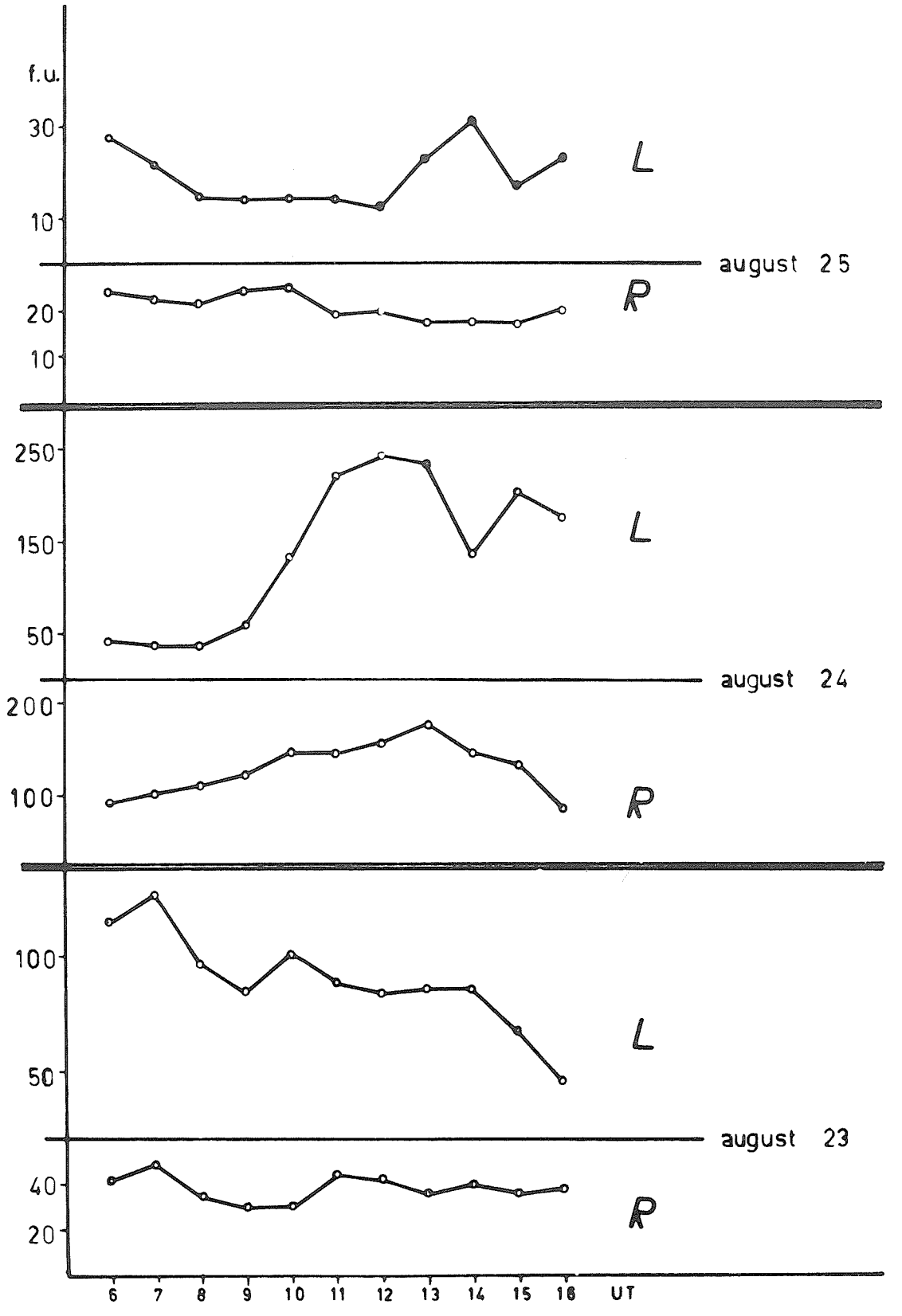

Fig. 3. Behavior of the two separate components, oppositely polarized, during the days of August 23, 24 and 25. The means are referred to the hour following that marked.

Figures 2 and 3 show the behavior of the total flux and of the degree of polarization on the days of August 23, 24 and 25, the most peculiar days of the whole passage. During the other days the polarization percentage was rather stable, at about 50% left polarization.

From a general analysis of the diagrams, and also of the recordings on the other days, one can draw two conclusions: (1) generally the left-handed polarized radiation prevails. This causes the variability of the degree of circular polarization. (2) Since the general trend of the two components is often similar, it is probable that unpolarized radiation is present which in our case splits up equally in the two channels, thus determining the parallel behavior of the two components.

As far as August 24 is concerned, enhancement of the background is present in both channels, but with a delay between them. This delay seems to exclude the presence of unpolarized radiation, and, therefore, we probably have a quasi-contemporary enhancement of the two different sources caused by a unique agent. Moreover, the behavior of type I activity on the same day is rather interesting, although they are not directly considered in this paper: type I bursts are present with a prevalent left-handed polarization until 1000 UT. They disappear almost completely from 1000 until 1400 UT, reappear again, practically unpolarized, from 1400 until 1500 UT, and finally disappear from 1500 UT until the end of the recording. It is interesting to note that the periods during which type I disappear correspond to the two enhancements of the background and to the two periods during which the radiation is left-handed polarized. This behavior of type I activity is perhaps understood by supposing that the two enhancements are due to a type IV event not perfectly recognized. In fact, spectral data published in "Solar-Geophysical Data", 326 Part I, show a type IV event from 1000 UT only in the dekametric band, while in the metric band there is a type IV only from 1400 UT. This is also supported by the fact that the continuum is very similar to the continuum of a type IV burst when observed at a single frequency.

On September 1, 1971, after the sources crossed the West limb, the emisssion decreased to a minimum level (12 flux units) and stayed absolutely quiet all day.

REFERENCES

SEDMAK, G. 1970 Osservazioni Solari, 18 suppl., Trieste.

Radio Bursts Associated with Solar Proton Flare on September 1, 1971

by

Kunitomo Sakurai
Radio Astronomy Branch
Laboratory for Extraterrestrial Physics
NASA/Goddard Space Flight Center
Greenbelt, Maryland 20771

1. Introduction

Solar flares which produce high-energy particles, so-called solar cosmic rays, generally accompany radio bursts of spectral type IV. It is known that the microwave component of these bursts is a good indicator of the generation of high-energy particles in solar flares [e.g., Kundu and Haddock, 1960; Sakurai and Maeda, 1961].

In this paper, we will consider some characteristics of solar radio bursts as obtained by satellite and ground-based observations on September 1, 1971. Since the IMP-I satellite has been recording solar radio emissions after launch on March 13, 1971, we are able to show the observed results on hectometric radio emissions as observed by this satellite in the case of the September 1, 1971 event along with the Clark Lake Observatory data. In this case, we can analyze frequency-onset time relationship for the initial stage of the development of radio bursts of wide frequency band.

2. Radio Bursts on September 1, 1972

Decametric and hectometric radio bursts were associated with the solar flare which seemed to have occurred at about 1925 UT on September 1, 1971. This flare was not directly observed since it occurred about 40 degrees beyond the west limb of the solar disk, but it accompanied the generation of solar cosmic rays and extensive solar radio bursts, both of which were observed on the earth. The record on decametric radio bursts as observed at the Clark Lake Observatory is shown in Figure 1. This shows that weak continuum emission, which seems to be classified as decametric type IV burst, was only observed in addition to intense type II and IV radio bursts. Radio emissions at hectometric frequencies were detected by the IMP-I satellite.

As has been mentioned above, we do not know the exact position of the flare because the sunspot group which produced this flare had already disappeared behind the west limb on August 29, 1971. For this reason, we have no optical data on this flare. By making use of radio data from microwave to hectometric frequencies, we have estimated the starting time of the explosive phase for this flare. Relation between frequency and the onset time of radio emissions is shown in Figure 2.

The result indicates that the start of microwave emissions was delayed more than 7 minutes in comparison with decametric emission around 2000 MHz. However, we do not know as yet whether this delay was produced in connection with the development of the flare, though it seems that this delay was related to some screening effect by the solar disk itself on microwave emissions. If this effect can really explain such a delay, we may estimate a possible relation of the starting times of microwave emissions to frequency by extrapolating the observed relation between onset time and frequency in metric and decimetric frequencies. In doing this, we need to consider the result as obtained in the case of the solar flare on July 7, 1966 [Sakurai, 1971]. Thus we have obtained a possible trend for starting times on microwave frequency range as indicated by the dot-dash line in Figure 2. This trend suggests that the explosive phase started around 1925 UT.

About 15 minutes later after the onset of the explosive phase, the peak flux for each frequency of type IV burst was reached at about 1940 UT as indicated in Figure 2. The spectrum of peak fluxes for microwave and decimetric frequencies is not similar to that which has been deduced by Castelli et al. [1967, 1968] in regard to solar proton flares. The result is shown in Figure 3.

In this event, several trends of drifting radio bursts were detected in low frequency range. Evidence of such radio bursts suggests that several radio sources were consecutively ejected from the flare region.

The relation of observed frequency to angular-distance from the sun-earth line has been obtained for the path of the radio source of type III bursts at hectometric frequencies. Though the result thus obtained is very tentative, two trends for the path of such source have been detected as shown in Figure 4.

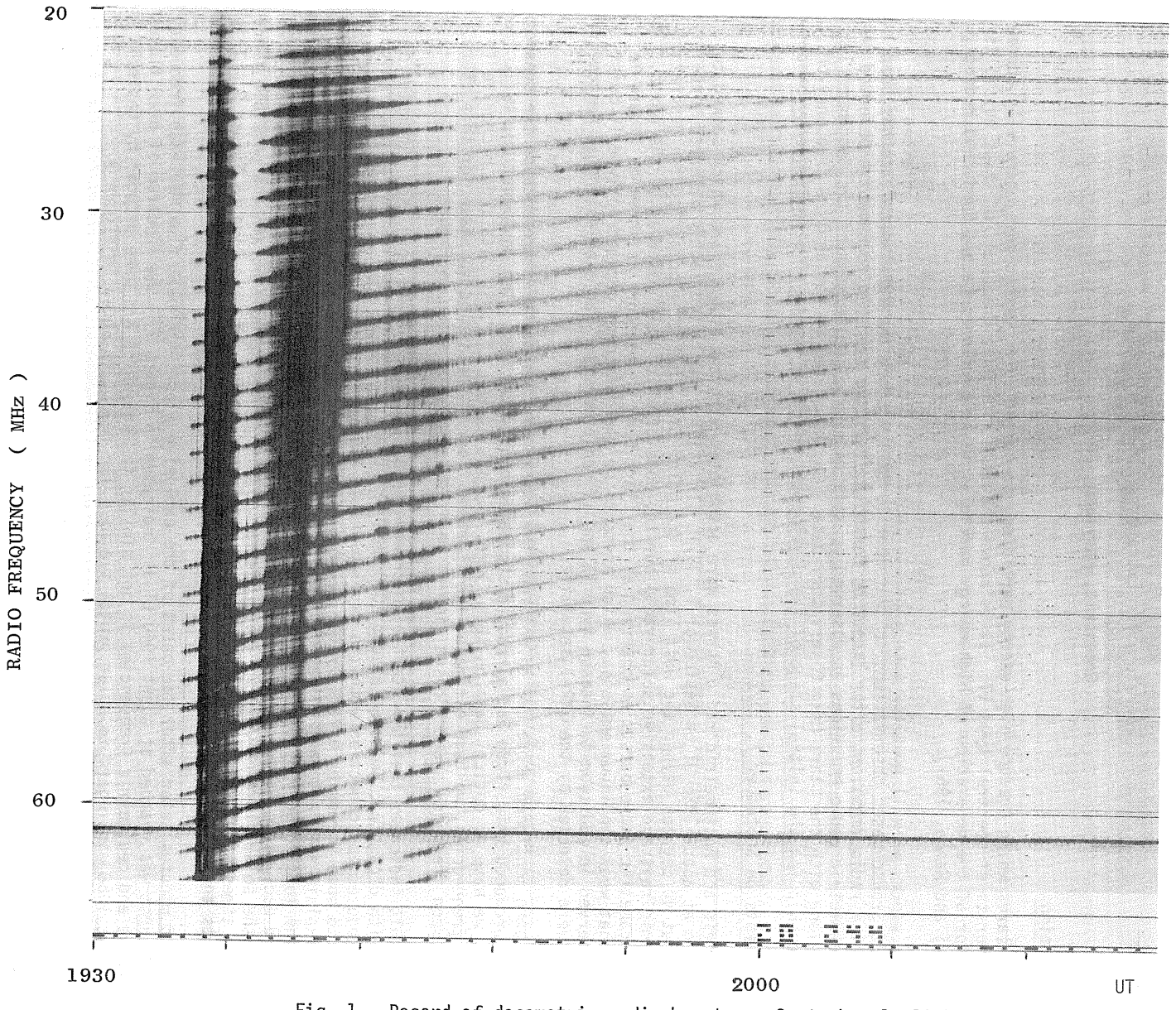

Fig. 1. Record of decametric radio bursts on September 1, 1971.

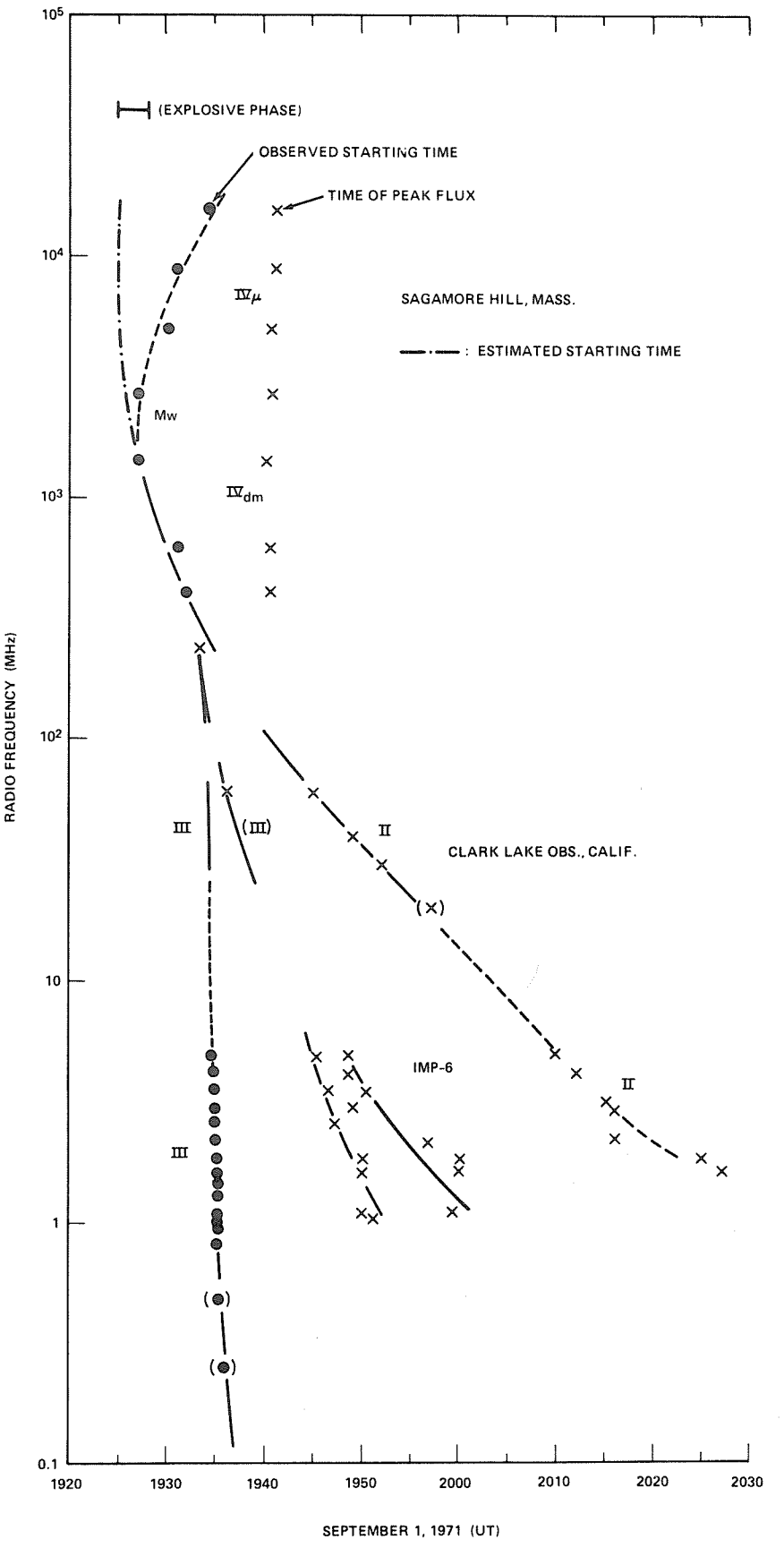

Fig. 2. The time sequence of the occurrence of radio burst of spectral type MW, IV, II and III. Hectometric type II and III radio bursts are seen.

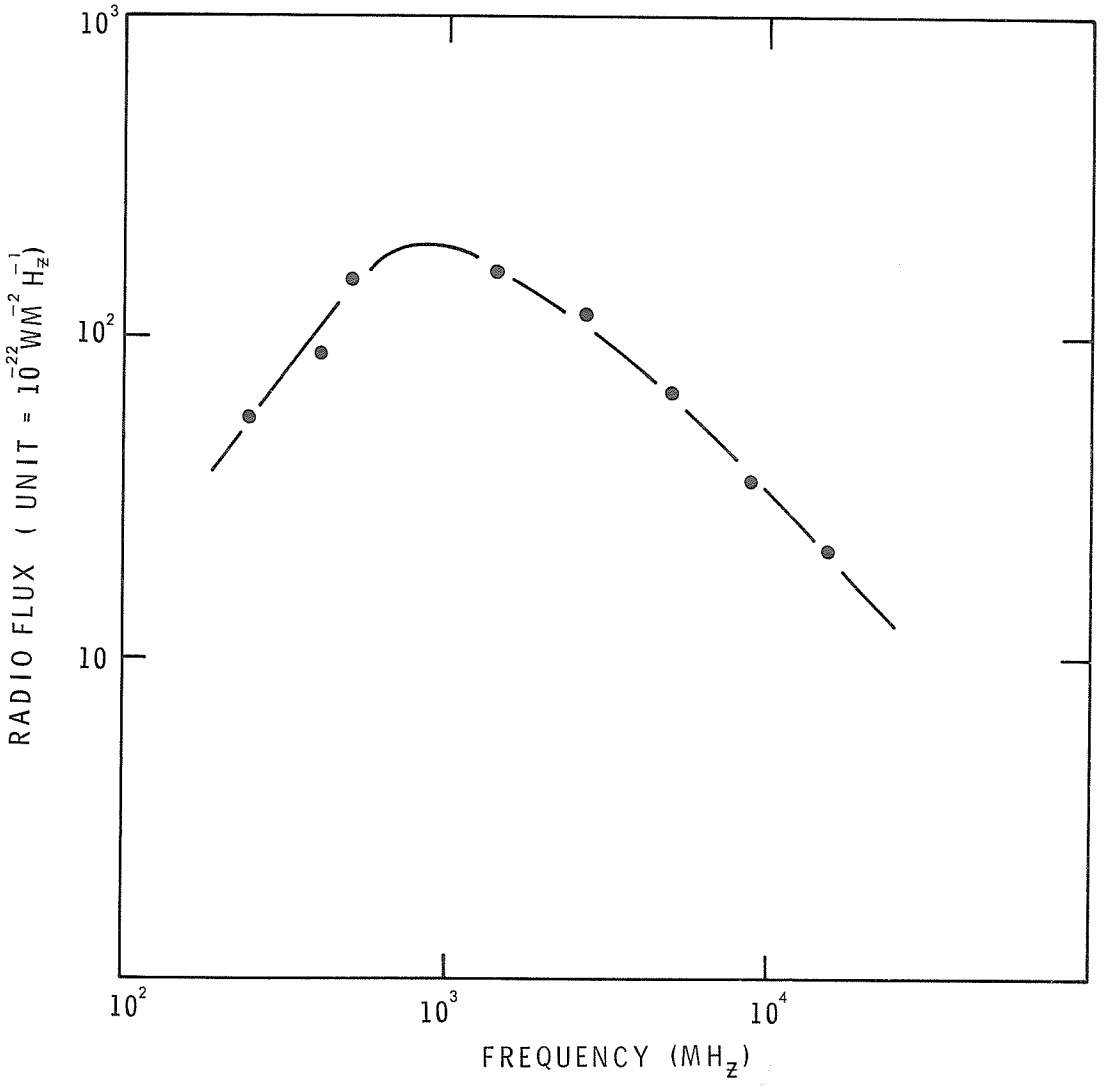

Fig. 3. The peak flux spectrum of type IV radio burst on September 1, 1971.

3. Discussion

In the case of the solar flare on September 1, 1971, the sources for type II and III radio bursts were ejected from the flare site during the explosive phase. During this phase, both microwave impulsive and type IV radio bursts at microwave frequencies must have been emitted, although we have not observed them at all, as is evident from Figure 2. We do not know as yet what mechanism produced such depression of the intensity of these bursts, but we may consider two alternative interpretations for such results. The first takes into account that the source for these bursts was too low to be seen from the earth, because the flare site was beyond the west limb of the solar disk. This is a reason why the onset of both bursts was so much delayed in comparison with that of decimetric radio emissions, a component of microwave impulsive bursts on the lower frequency side. The second one assumes that the position of the source for microwave emissions was high enough in order to be seen from the earth, but the emission directivity at microwave frequencies was so narrow that the emission did not directly reach the earth's observers.

Acknowledgement

I would like to thank Dr. R. G. Stone and Dr. J. Fainberg for their supply of the valuable data on solar radio emission for this event. Comments by Dr. J. Fainberg are appreciated.

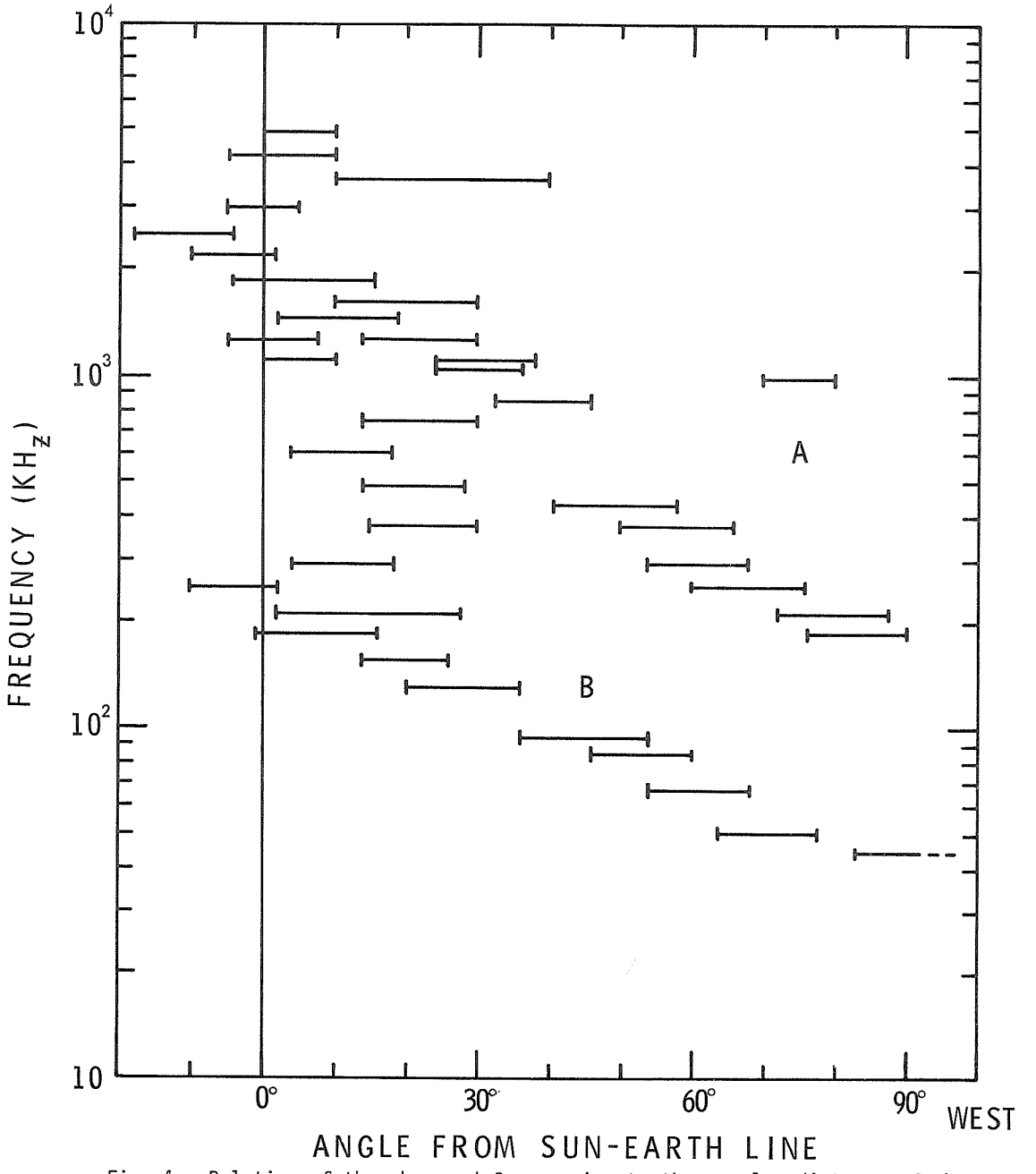

Fig. 4. Relation of the observed frequencies to the angular distance of the radio source with respect to the sun-earth line.

REFERENCES

CASTELLI, J. P., J. AARON, and G. A. MICHAEL	1967	J. Geophys. Res., 72, 5491.
CASTELLI, J. P., J. AARON, and G. A. MICHAEL	1967	Ap. J., 153, 26.
KUNDU, M. R. and F. T. HADDOCK	1960	Nature, 186, 610.
SAKURAI, K.	1971	Solar Physics, 20, 147.
SAKURAI, K. and H. MAEDA	1961	J. Geophys. Res., 66, 1966.

VLF and Solar Observations during the Event of September 1, 1971

by

S. Ananthakrishnan, D. Basu, L. R. Piazza and M. E. Z. Mellone
Centro de Rádio Astronomia e Astrofísica
Universidade Mackenzie
São Paulo, Brazil

VLF Observations

The phase of VLF signals from transmitters NAA (17.8 kHz), Cutler, Maine, U.S.A. and NLK (18.6 kHz), Seattle, Washington, U.S.A., was recorded at São Paulo, Brazil during September 1971. No noticeable effect was present on the phase of either trajectory during the daytime, in the period August 29 to September 5. However the nighttime phase on NAA showed a deviation of $\simeq$ 7 μsec from normal on the 3rd and 5th of September (see Figure 1). In this Figure the quiet days are August 29 and September 8. Values of σ (the standard deviation) are $\pm$ 2 μsec at night on the NAA-São Paulo path. Hence both on September 3 and September 5 there were significant deviations from normal. Possible reasons for this have been discussed in a recent paper [Ananthakrishnan, S. and B. Hackradt, 1972].

The trajectory NLK-São Paulo exhibited marked deviations from normal on the 3rd and 5th of September (between 0400 and 0700 UT), shown in Figure 2. Maximum deviations were of the order of 7 μsec ($\sigma = \pm$ 4 μsec).

Solar Radio Observations

The sun was observed by the 7 GHz polarization-radio telescope [Kaufmann, P., 1971] at the Itapetinga Radio Observatory (22° 11' S, 46° 33' W), São Paulo, Brazil between the hours 1040-2015 UT (with interruption 1520-1537 UT). The daily mean flux value of the day was 201×10^{-22} $Wm^{-2}Hz^{-1}$ with no appreciable polarization. The bursts observed during the patrol period are summarized in Table 1 and the unpolarized burst (Simple 2F with PBI), the largest event of the day, is reproduced in Figure 3.

Table 1

Type*	Class	Start UT	Max UT	Duration Min.	Peak Flux $\times 10^{-22} Wm^{-2}Hz^{-1}$	Peak Polarization Percent
23	Simple 3AF	1717.6	1723.1	50.9	8.2	70.7 L
8	Spike	1722.6	1723.1	0.6	6.5	88.4 L
1	Simple 1	1931.0	1933.0	3.0	4.6	0.0
4	Simple 2F	1934.0	1941.0	19.0	53.3	0.0
29	PBI	1953.0	-	12.0	-	-

* As given in "Solar-Geophysical Data".

REFERENCES

ANANTHAKRISHNAN, S. and B. HACKRADT 1972 Forbush Decrease in the Flux of Galactic Cosmic Rays and Associated VLF Nighttime Propagation Phenomenon, Planetary and Space Science, 20, 81-87.

KAUFMANN, P. 1971 Report from Solar Institute, Pierre Kaufmann/The New Intapetinga Radio Observatory, from Mackenzie University, São Paulo, Brazil, Solar Physics, 18, 336.

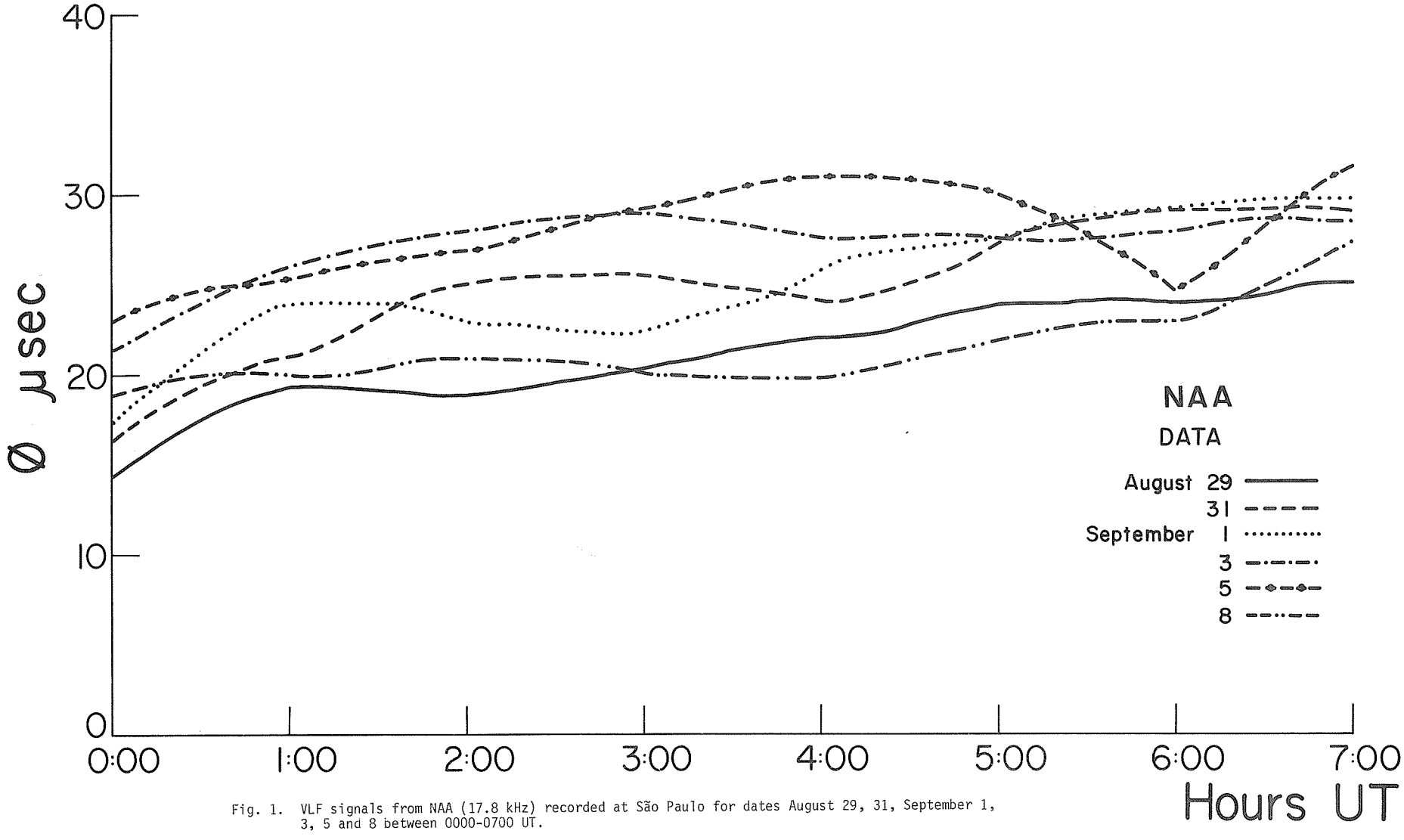

Fig. 1. VLF signals from NAA (17.8 kHz) recorded at São Paulo for dates August 29, 31, September 1, 3, 5 and 8 between 0000-0700 UT.

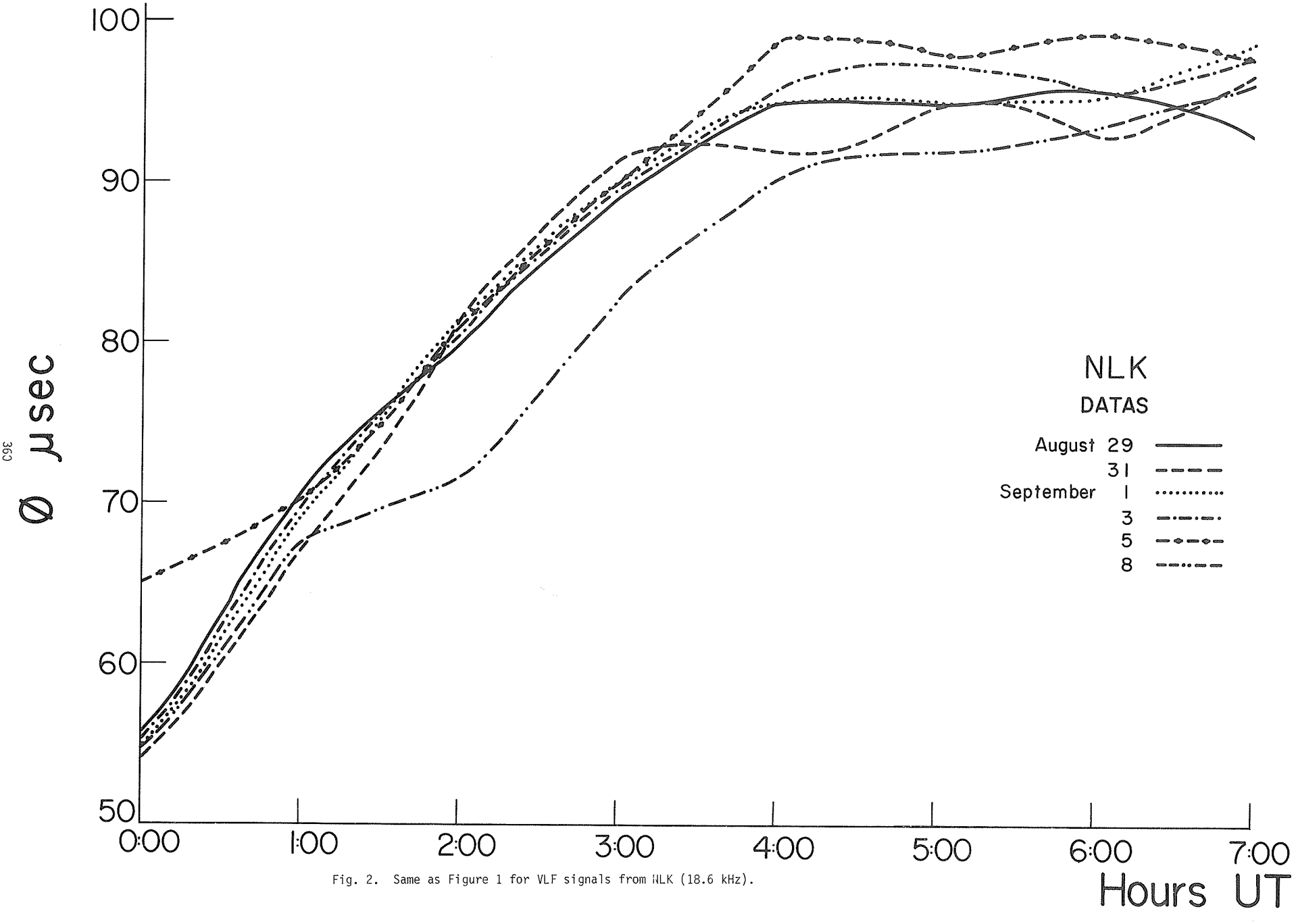

Fig. 2. Same as Figure 1 for VLF signals from NLK (18.6 kHz).

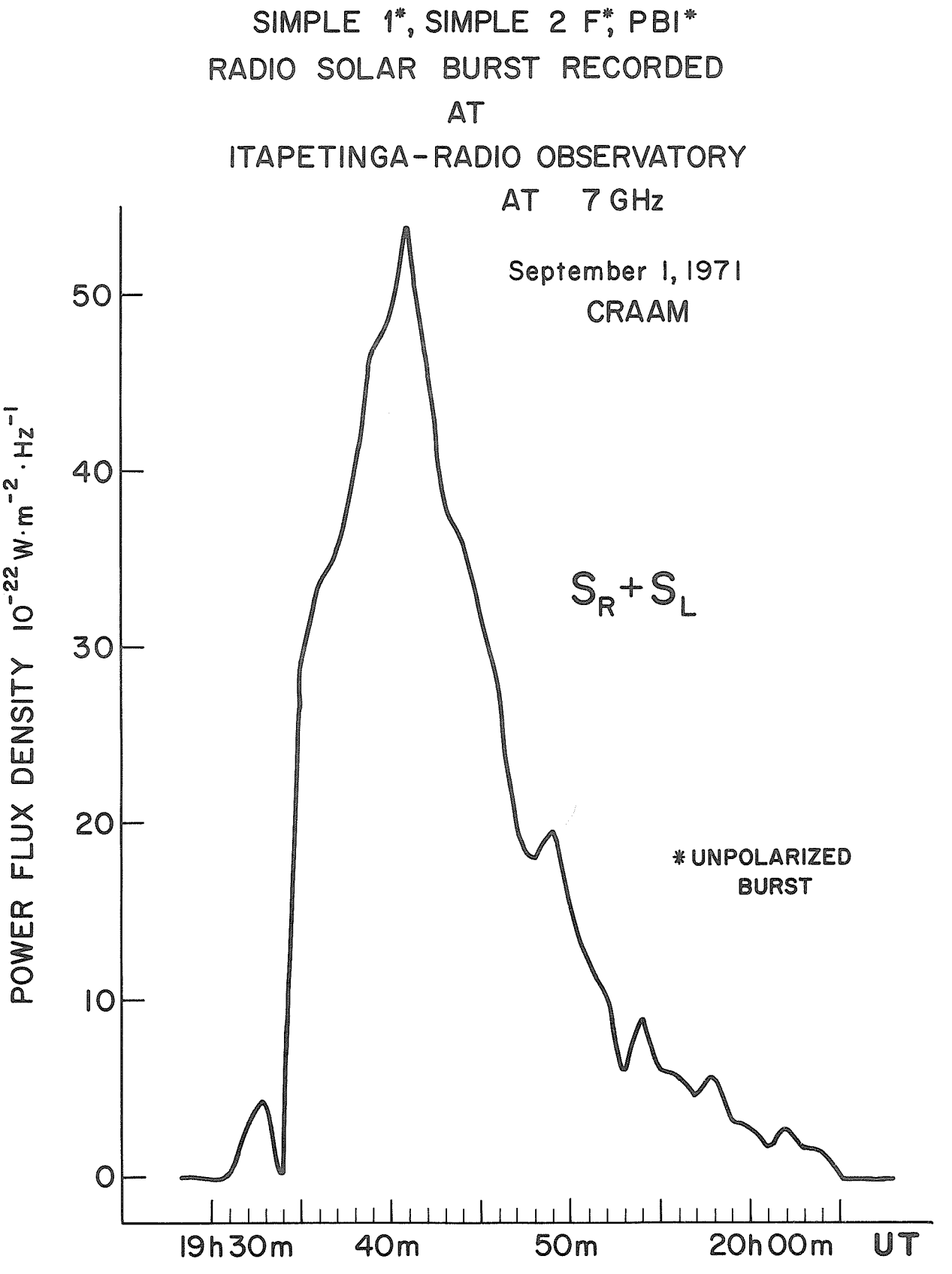
SIMPLE 1*, SIMPLE 2 F*, PBI*
RADIO SOLAR BURST RECORDED
AT
ITAPETINGA-RADIO OBSERVATORY
AT 7 GHz
September 1, 1971
CRAAM
$S_R + S_L$
* UNPOLARIZED BURST
POWER FLUX DENSITY 10^{-22} W·m^{-2}·Hz^{-1}
50
40
30
20
10
0
19h30m
40m
50m
20h00m
UT

Fig. 3.

4. SPACE OBSERVATIONS

Solar X-Ray and Ultraviolet Emission on September 1, 1971

by

D. M. Horan, R. W. Kreplin, and R. G. Taylor
E. O. Hulburt Center for Space Research
Naval Research Laboratory
Washington, D. C. 20390

The records of solar X-ray emission obtained by the Naval Research Laboratory's SOLRAD 9 satellite (Explorer 37, 1968-17A) on September 1, 1971 are shown as Figure 1. The top curve on each plot represents the solar X-ray energy flux in the 8 to 20 Å band. In both cases, a gray-body solar emission spectrum [Kreplin, 1961] with a 2 x 10^6°K color temperature was assumed in converting from ionization chamber current levels to energy flux units. The third curve from the top represents solar energy flux in the 0.5 to 3 Å band based on a gray-body emission spectrum with a 10 x 10^6°K color temperature for the emitting solar region. The curve is quite intermittent because the 0.5 to 3 Å solar energy flux is usually below the threshold level of the detector.

The X-ray emission is plotted in units of ergs/cm^2 sec on a logarithmic scale. The abscissa is linear with the integers denoting hours in Universal Time (UT). Charged particle interference with the X-ray sensors, which can cause the plotted flux values to be higher or lower than the actual flux, is indicated by the lowest data curve. The ionization chamber current caused by the charged particle background is digitized and recorded as a "count". The number of "counts" plotted is linearly related to the current generated in the 0.5 to 3 Å ionization chamber by penetrating charged particles when the detector is facing away from the sun. Counts of 10 to 15 indicate negligible particle interference. Counts of 20 to the maximum value of 127 indicate significant particle interference. The data processing computer program inhibits the plotting of data obviously contaminated by particle interference, and this feature causes randomly spaced data gaps of 30 minutes duration or less.

The record of solar X-ray emission obtained by SOLRAD 9 on September 1, 1971 is shown as Figure 1. The solar X-ray emission in the 1 to 8 and 8 to 20 Å bands was at a very low level at the beginning of the day, and decreased steadily until the satellite passed behind the Earth at 1920 UT. For several hours after 1500 UT, the 1 to 8 Å band emission was so low that the solar signals were at the experiment amplifier's noise level. When the satellite emerged from the Earth's shadow at 1959 UT, a small X-ray flare was in progress. Data from NRL's SOLRAD 10 satellite (1971-058A) were used to verify that the X-ray enhancement began prior to 1928 UT and that peak emission of 1.9 x 10^{-3} ergs/cm^2 sec in the 1 to 8 Å band occurred at 2004 UT. By 2400 UT, the emission in the 1 to 8 Å band had decayed to approximately 3 x 10^{-4} ergs/cm^2 sec with no additional flare activity. X-ray emission in the 1 to 8 Å and 8 to 20 Å bands decreased steadily throughout the day on September 2 with no flare activity. Therefore, the X-ray activity on September 1 was insignificant as viewed from Earth. This does not eliminate the possibility that the X-ray emission seen at Earth was a small portion of the X-ray emission from a large event extending high into the corona and centered over an active region 20° or 30° around the west limb.

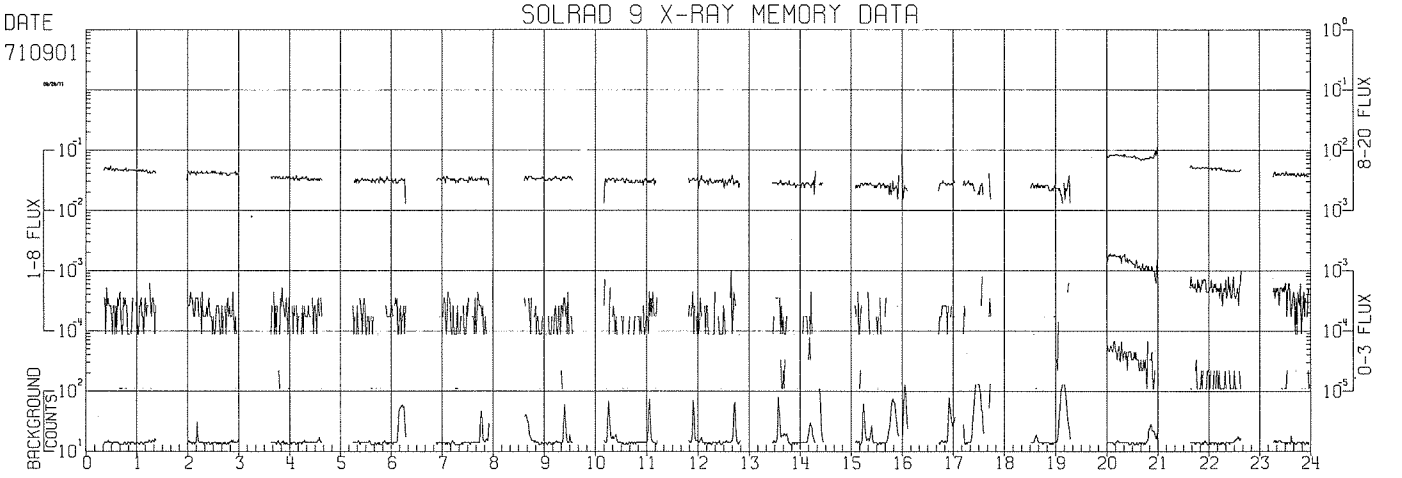

Fig. 1. Solar X-ray flux on September 1, 1971.

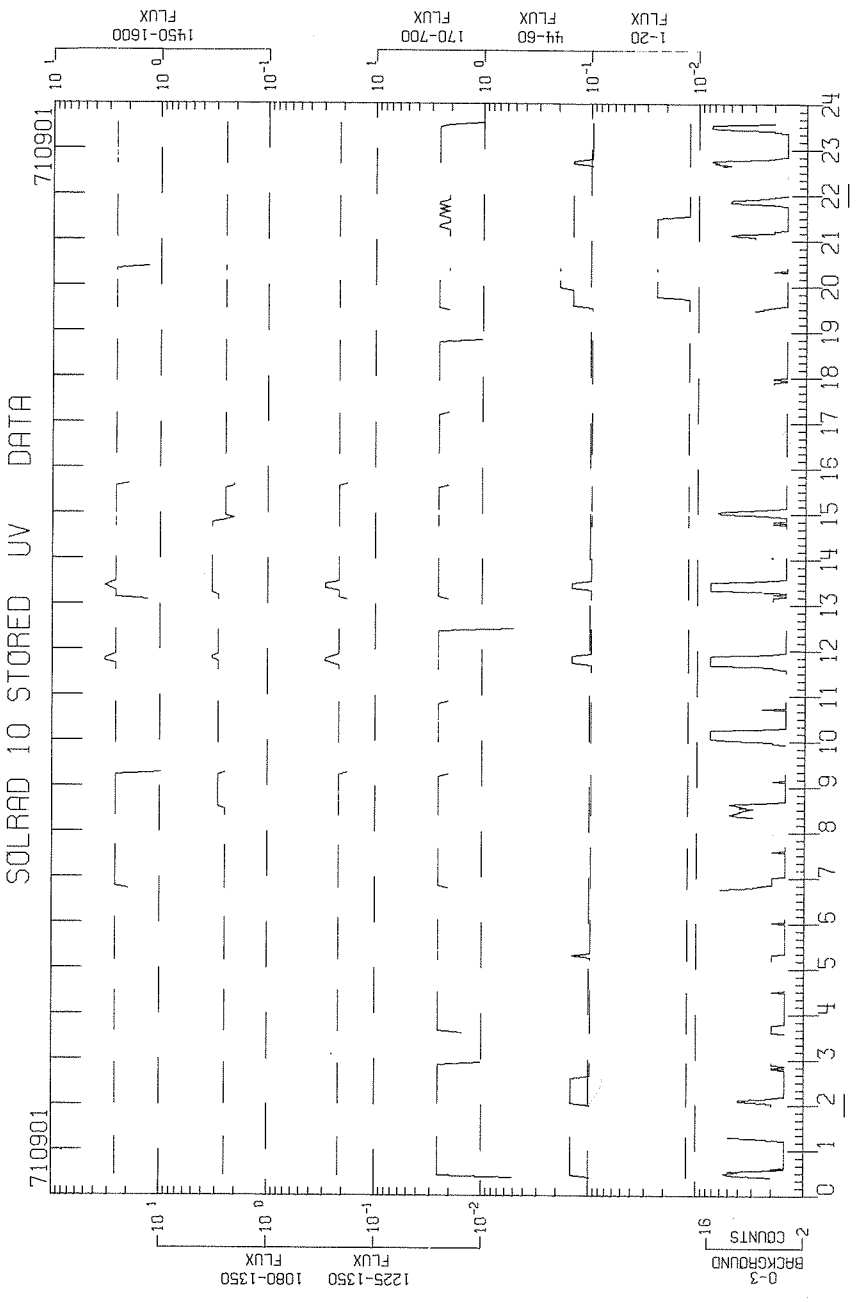

Fig. 2. Solar ultraviolet flux on September 1, 1971.

The record of solar ultraviolet emission on September 1, 1971 is shown as Figure 2. The data were obtained from sensors aboard NRL's SOLRAD 10 satellite (Explorer 44, 1971-058A). The general structure of the plot is identical to the SOLRAD 9 X-ray plots in that the abscissa is linearly scaled in hours of Universal Time, and the ordinate is logarithmically scaled in units of energy flux, ergs/cm^2 sec. Charged particle interference, which can cause the plotted flux values to be higher than the actual flux, is indicated by the lowest data curve. The number of "counts" plotted is linearly related to the current generated by penetrating charged particles in an ionization chamber collimated to prevent it from viewing the sun. On the plot shown in Figure 2, a count of 3 indicates negligible particle interference, and counts of 4 to the maximum value of 15 indicate increasing particle interference. A complete description of the SOLRAD 10 experiments and the assumptions used in converting the data from telemetered numbers to flux units is given in NRL Report No. 7408 [Horan and Kreplin, 1972].

The data curve shown at the top of Figure 2 displays the ultraviolet flux in the 1450 to 1600 Å band. Within the limits of very coarse digitization of the experiment, solar emission was constant throughout the day at a value of 2.56 ± 0.32 ergs/cm^2 sec. The sharp changes which appear several times at the beginning or end of a darkness period are caused by attenuation of the solar emission as it passes through the Earth's atmosphere. The increases at approximately 1150 and 1325 UT are due to interference by trapped charged particles.

The second data curve from the top displays solar emission in the 1080 to 1350 Å band which is dominated by the Lyman-alpha line at 1216 Å. Until 0830 UT the flux was constant within the limits of digitization of the experiment at 2.46 ± 0.41 ergs/cm^2 sec. The absolute flux values presented for the 1080 to 1350 Å band should not be accepted with great confidence because the sensor continuously degraded in sensitivity since launch, and finally became inoperative in February 1972. The absolute values presented are low, probably by a factor of 2 or 3. However, relative changes should still be valid. Between 0830 and 1315 UT the flux level was constant at 2.87 ± 0.41 ergs/cm^2 sec, and then it decreased over six minutes to 2.05 ± 0.41 ergs/cm^2 sec at 1454 UT. The flux value at 1457 UT was 2.46 ± 0.41 ergs/cm^2 sec and it remained at that level for the remainder of the day. The real-time data, which are not subjected to the coarse digitization of the stored data, show a value of 2.00 ± 0.10 ergs/cm^2 sec at 1831 and 2010 UT.

The third data curve from the top displays coarsely digitized stored data for the solar emission in the 1225 to 1350 Å band. Except for deviations caused by atmospheric attenuation or trapped particle interference, the flux level was constant throughout the day at 0.216 ± 0.036 ergs/cm^2 sec.

The fourth data curve from the top displays the solar emission in the 170 to 700 Å band. Again, the stored data are coarsely digitized. The emission in this band was constant throughout the day at 2.55 ± 0.51 ergs/cm^2 sec except for several drops to a level of 2.04 ± 0.51 ergs/cm^2 sec between 2100 and 2220 UT. However, if this represents any actual change in solar emission, it could have been as small as a few hundredths of an erg/cm^2 sec. The real-time data are not subjected to coarse digitization and show a value of 2.15 ± 0.15 ergs/cm^2 sec at 1831 and 2010 UT.

Clearly, within the stored data digitization limits of the ultraviolet experiments, there are no flux changes which occur in conjunction with the X-ray flare at 2004 UT. However, if the X-ray flare observed is centered over a photospheric region well around the west limb, it would be impossible for any lower attitude ultraviolet emission associated with the flare to be visible from Earth. There is evidence of at least a 17 percent change in the 1080 to 1350 Å emission between 0830 and 1457 UT. We believe that the change is real, but we also believe that additional data should be studied in order to rule out possible cumulative particle effects in the sensor response function.

The fifth and sixth data curves from the top show the measured solar emission in the 44 to 60 Å and 1 to 20 Å X-ray bands, respectively. These curves agree with those of Figure 1 in displaying a low X-ray emission level throughout the day with a small X-ray flare around 2000 UT.

REFERENCES

HORAN, D. M. and R. W. KREPLIN	1972	The SOLRAD 10 Satellite, Explorer 44, 1971-058A, NRL Report # 7408.
KREPLIN, R. W.	1961	Solar X-Rays, Annales de Geophysique, 17, 151-161.

Proton and Alpha Particle Fluxes Measured Aboard OV5-6

by
G. K. Yates and J. G. Kelley
Air Force Cambridge Research Laboratories
L. G. Hanscom Field, Bedford, Massachusetts

and

B. Sellers and F. A. Hanser
Panametrics, Inc., Waltham, Massachusetts

Satellite OV5-6 (International designation 1969-046B) measures solar fluxes of protons and alpha particles. The perigee is 16,341 km and the apogee is 112,196 km. Thus, for most of the time the instuments are outside the earth's magnetosphere. The data presented here do not include fluxes within this region. The orbit was described in greater detail in an earlier report in this series [Yates et al., 1971].

The proton-alpha particle detector on OV5-6 consists of two totally depleted silicon surface barrier detectors in a telescope configuration. The detectors each have a 2 cm^2 area and are separated by 2.54 cm. The outer one is 200 microns thick and the inner one 750 microns. The outer detector is shielded from light by 0.6 mil of aluminum foil. In the coincidence mode of operation, the telescope has a geometric factor of 0.52 cm^2-sr, with a detection cone of 30° half angle. The average angle of detection is 17°. A coincidence is set by an energy loss window on the first detector and a threshold on the second detector. The resulting coincidences detect protons and alpha particles (principally) in the following ranges: protons 5.3 to 8 Mev, 8 to 17 Mev, 17 to 40 Mev, and 40 to 100 Mev; alpha-particles 20 to 32 Mev, 32 to 68 Mev, and 68 to 100 Mev. The telescope cycles sequentially through these seven ranges, each range is counted and then read out. The complete cycle is completed in approximately two minutes. The telescope looks in the equatorial plane of the satellite.

The satellite spin axis is stable and is directed toward 0^h and 40^m RA and 32° declination in celestial coordinates. In September 1971 the sun appeared fifty degrees below (-50°) the satellite's equator. Since the spin period at this time was approximately 4.7 seconds, the telescope accumulated counts in a given particle energy range for approximately two satellite rotations.

The Figure shows 30 minute averages of the data from the four coincidence proton channels and the lowest energy alpha particle channel. Fluxes are given in particles/cm^2-sec-sr-Mev; most gaps correspond to periods of no telemetry; points when the satellite was within the trapped radiation belt are omitted.

Armstrong and Krimigis [1971] have shown that there is an inverse correlation between the proton/alpha-particle flux ratio and the hardness of the proton energy spectrum. These data agree with their results. A comparison of the two lower proton energy intervals in the Figure with those of the January event (see p. 120) shows that the January event was the harder of the two. At 0730 hours UT, September 2, the proton/alpha particle flux ratio in the 5 to 8 Mev/nucleon interval was 23.

REFERENCES

ARMSTRONG, T. P. and S. M. KRIMIGIS — 1971 — Statistical study of solar protons, alpha particles, and $Z \geq 3$ nuclei in 1967-1968, J. Geophys. Res., 76, 4230-4244.

YATES, G. K., J. G. KELLEY, B. SELLERS, F. A. HANSER, and P. R. MOREL — 1971 — Proton, alpha and bremsstrahlung fluxes measured aboard OV5-6, World Data Center A, Upper Atmosphere Geophysics Report UAG-12, Part I, 139-146.

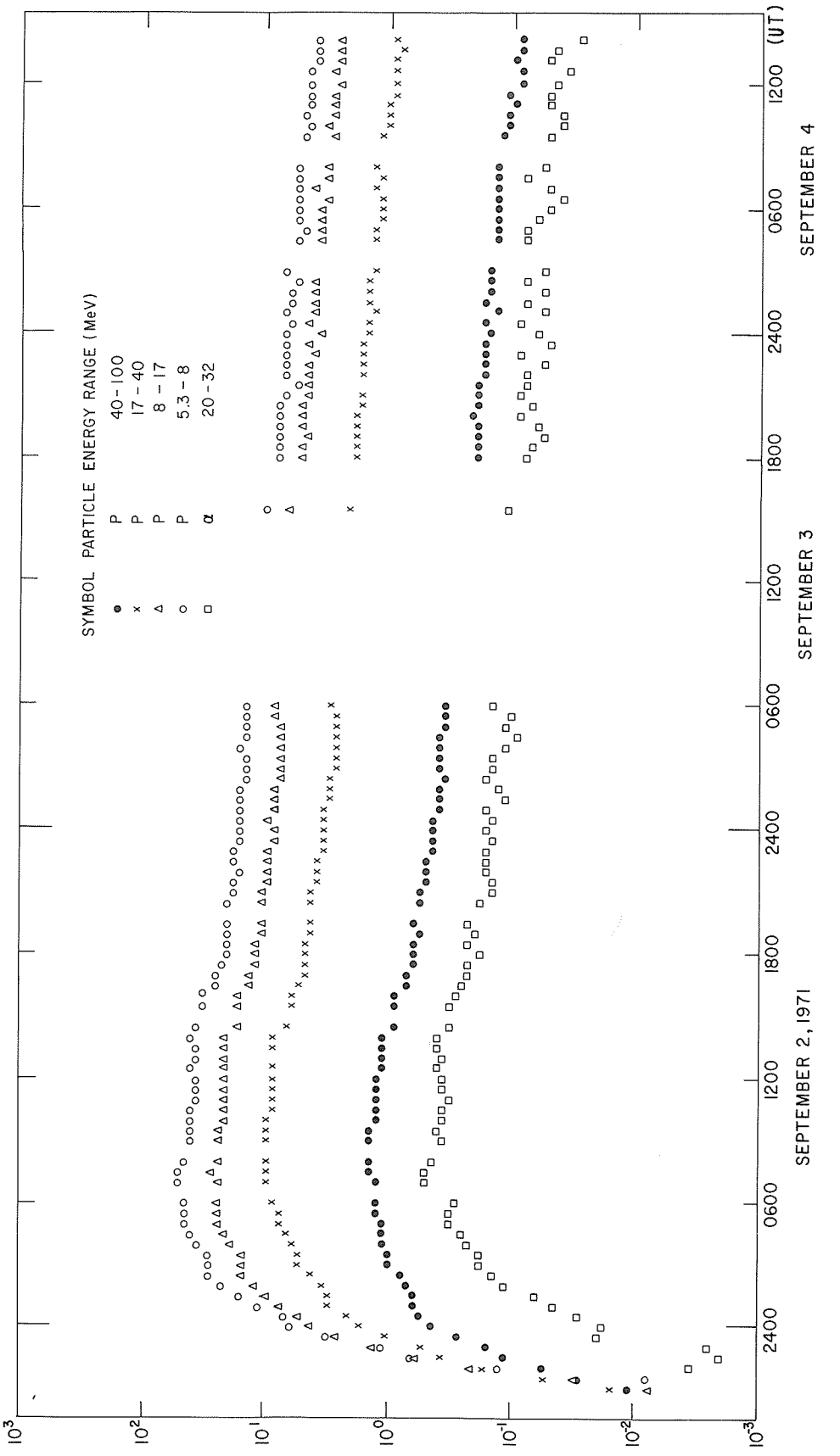

FIGURE 1. TIME VARIATION OF PARTICLE FLUXES (30 minute AVERAGES)

"Solar Wind Plasma Observations Subsequent to the Solar Proton Event of September 1, 1971"

by

H.C. Howe, J.H. Binsack and H.S. Bridge
Center for Space Research
MIT, Cambridge, Massachusetts

At the time of the solar proton event on September 1, 1971, Explorer 33 was in the geomagnetic tail downstream of the earth; therefore, no data for the time of the event are available from the MIT plasma experiment onboard this satellite. Solar wind plasma data were collected starting at 0225 UT, September 3, 1971, when the plasma data indicate Explorer 33 crossed the bow shock into the solar wind. The solar wind was extremely steady from then until 1645 UT, September 4, 1971, when a small but sudden increase in the density and velocity, in the presence of a constant thermal speed, were observed (see Figure 1). A small sudden commencement was observed simultaneously on the earth. It is our opinion that the event observed on Explorer 33 is a tangential discontinuity convected by the solar wind and not a travelling shock, as might have been expected from the flare which caused the proton event of September 1 [Hirshberg et al., 1970]. Therefore, the magnetic unrest observed on the ground on September 4 and 5 is probably unrelated to the solar proton event. Burlaga [1971] gives a general review of shocks and discontinuities.

REFERENCES

Burlaga, L.F. 1971 Hydromagnetic waves and discontinuities in the solar wind, G.S.F.C. Preprint X-692-71-95, to appear in Space Science Reviews.

Hirshberg, J., A. Alksne, D.S. Colburn, S.J. Bame, and A.J. Hundhausen 1970 Observations of a solar flare induced interplanetary shock and helium-enriched driver gas, J. Geophys. Rev., 75, 1.

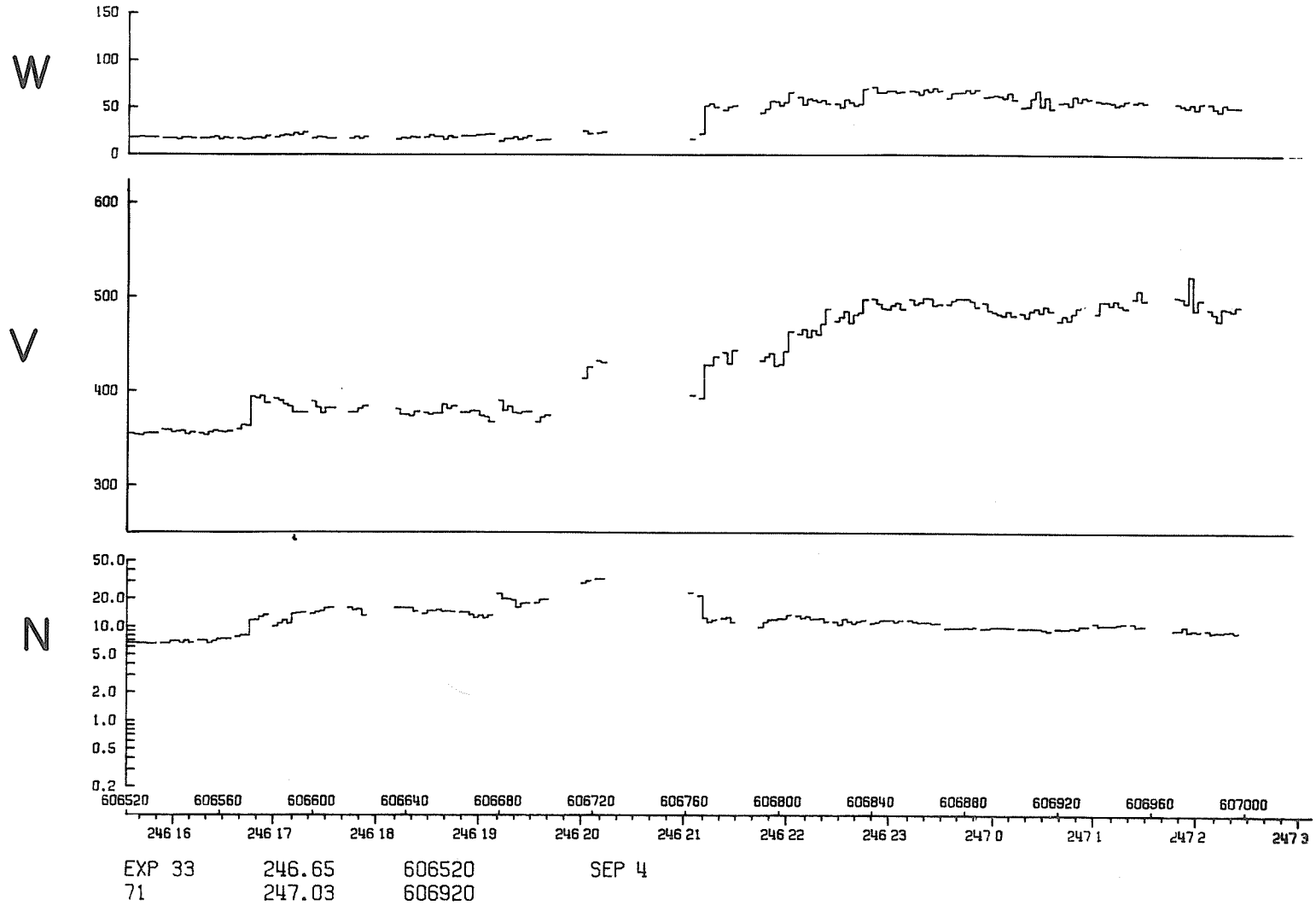

Fig. 1. Solar wind thermal speed (W, km/sec), bulk velocity (V, km/sec) and number density (N, cm^{-3}) between 1545 UT, September 4 and 0230 UT, September 5, 1971. The decimal day and hour UT are given for each hour below the horizontal axis. The thermal speed and temperature (T) are related by the expression $\frac{1}{2} m_p W^2 = kT$, where m_p and k are the proton mass and Boltzmann constant.

5. COSMIC RAYS

Tables of Neutron Monitor Data and Selected Graphs for the September 1, 1971 Event

by

Helen E. Coffey
World Data Center A for
Solar-Terrestrial Physics
NOAA, Boulder, Colorado 80302

Cosmic ray neutron monitor data for the September 1, 1971 event are presented both in tabulated form and graphical displays. In many cases the data for this period were forwarded to us upon special request. We thank all reporting observatories for their cooperation.

Table 1 lists the stations, their equipment, geographical coordinates, cutoff rigidities, scaling factors, pressure coefficients, mean station pressure in mm Hg and multiplication factors, if any. Following is Table 2 which presents hourly values for September 1-2, 1971 from the 28 stations, listed in cutoff rigidity order. Again, the incompleteness of data is due to the lag in compiling cosmic ray data. The data does however cluster around the period we are most interested in, i.e., 2200-0200 UT.

Graphical displays of selected stations show both the variation of data with cutoff rigidity and a quick graphical look at the event. These include: a.) Alert, Deep River, General Belgrano and Inuvik five-minute data given in percentage deviations for 1900 UT September 1 - 1800 UT September 2 (Figure 1); b.) Syowa Base, Mt. Norikura and Tokyo Itabashi five-, fifteen- and ten-minute data, respectively, given in percentage deviations for 1900 UT September 1 - 0900 UT September 2 (Figure 2).

Finally, 24 individual stations data in 5-, 10- and 15-minute hourly rates are presented in Table 3. Information pertinent to each station is given in the headings. All data is pressure corrected except for Tixie Bay and Leeds. Pressure values for Tixie Bay are listed. No pressure data for Leeds was available.

The 24 stations listed in cutoff rigidity order are:

Station	Cutoff rigidity	Hourly rate
Alert	0.00	Five-minute
Dumont d'Urville	0.01	Fifteen-minute
Inuvik	0.18	Five-minute
Fort Churchill	0.21	" "
Syowa Base	0.42	" "
Goose Bay	0.52	" "
Tixie Bay	0.53	" "
Kiruna	0.54	" "
General Belgrano	0.75	" "
Oulu	0.81	" "
Deep River	1.02	" "
Sanae	1.02	Ten-minute
Port aux Francais	1.19	Five-minute
Mt. Washington	1.24	" "
Durham	1.41	" "
Leeds	2.20	" "
Lomnicky Stit	4.00	Ten-minute
Dallas	4.35	Five-minute
Jungfraujoch	4.48	Six-minute
Ushuaia	5.68	Fifteen-minute
Mexico City	9.53	Five-minute
Buenos Aires	10.63	" "
Mt. Norikura	11.39	Fifteen-minute
Tokyo/Itabashi	11.61	Ten-minute

Table 1

Abb-rev.	Station	Equip	Geographic Coordinates Lat	East	Cutoff Rigidity	Scaling Factors	Pressure Coefficient	Mean Station Pressure mm HG	Real Counts
ALE	Alert	SNM	82.5 N	297.6	0.0	--	0.987%/mm Hg	725	100x tabulated
DUM	Dumont d'Urville	SNM	66.4 S	140.0	0.01	--	.99 %/mm Hg	---	200x "
INU	Inuvik	SNM	68.35N	226.2	0.18	--	.987%/mm Hg	758	100x "
CHU	Fort Churchill	NM	58.75N	265.9	0.21	--	--	1010mb	40x "
	Syowa Base	SNM	69.03S	39.6	0.42	--	-.74 %/mb	965mb	100x "
GOO	Goose Bay	SNM	53.33N	299.5	0.52	--	.987%/mm Hg	758	100x "
	Tixie Bay	SNM	71.55N	128.9	0.53	--	-.96 %/mm Hg	758	100x "
	Kiruna	SNM	67.83N	20.4	0.54	--	-.99 %/mm Hg	720	100x "
OUL	Oulu	SNM	65.0 N	25.4	0.81	--	.735%/mb	1000mb	100x "
DEE	Deep River	SNM	46.1 N	282.5	1.02	--	.987%/mm Hg	747	300x "
OTT	Ottawa	NM	45.4 N	284.4	1.08	6.4	--	---	---
BEG	Bergen	NM	60.4 N	5.3	1.13	16	.74 %/mb	990mb	---
SUL	Sulphur Mountain	SNM	51.2 N	244.39	1.14	--	.7665%/mb	---	100x "
POR	Port aux Francais	SNM	49.35S	70.2	1.19	--	1.01 %/mm Hg	---	400x "
MTW	Mt. Washington	NM	44.3 N	288.7	1.24	--	Pressure Corrected		
DUR	Durham	SNM	43.1 N	289.1	1.41	--	Pressure Corrected		
LEE	Leeds	NM	53.82N	358.4	2.20	--	--	---	100x "
KIE	Kiel	SNM	54.33N	10.1	2.29	--	.961%/mm Hg	755	100x "
	Utrecht	SNM	52.08N	5.13	2.76	--	.99 %/mm Hg	760	100x "
LOM	Lomnicky Stit	NM	49.2 N	20.22	4.00	--	-1.024%/mm Hg	550	8x "
PRE	Predigstuhl	SNM	47.7 N	12.88	4.30	--	-.9 %/mm Hg	625	100x "
DAL	Dallas	NM	32.78N	263.2	4.35	--	--	995mb	120x "
JUN	Jungfraujoch	NM	46.55N	7.9	4.48	100	--	---	---
USH	Ushuaia	NM	54.8 S	291.7	5.68	8	--	750	-3000x "
	Mexico City	SNM	19.33N	260.8	9.53	--	-.72 %/mb	778.6mb	100x "
BUE	Buenos Aires	SNM	34.58S	301.5	10.63	--	--	---	32x "
MTN	Mt. Norikura	SNM	36.12N	137.5	11.39	128	-.7 %/mb	720mb	---
	Tokyo/Itabashi	SNM	35.67N	139.75	11.61	128	.666%/mb	1013.3mb	---

Table 2

September 1, 1971

HOUR	13	14	15	16	17	18	19	20	21	22	23	24
ALERT								7180	7653	8151	8127	8007
TERRE ADELIE					2053	2059	2064	2066	2224	2354	2373	2323
INUVIK								82227	86792	91644	91437	90813
CHURCHILL				18944	18966	19105	19154	19075	19927	21186	21259	20934
SYOWA BASE								6517	6766	7114	7159	7114
GOOSE BAY								7038	7208	7602	7660	7606
TIXIE BAY							6681	7114	7486	7511	7464	7373
KIRUNA									7064	7428	7916	8035
OULU	3790	3804	3808	3800	3792	3797	3804	3788	3937	4187	4260	4170
DEEP RIVER								6970	7208	7570	7677	7622
OTTAWA	2980	3003	2981	3012	2973	2977	3014	3085	3125	3319	3322	3311
BERGEN	531	535	531	528	532	520	525	520	560	575	592	575
SULPHUR MT	8603	8633	8687	8660	8684	8724	8757	8763	9260	9998	10233	10129
KERGUELEN						19574	19434	19502	20907	21912	21903	21519
MT WASHINGTON							2309	2309	2444	2637	2649	2584
DURHAM							2277	2282	2369	2455	2458	2416
LEEDS	7122	7050	7039	7003	6954	6883	6890	6803	6915	6986	6865	6788
KIEL	6324	6296	6307	6312	6304	6301	6299	6256	6401	6445	6412	6350
UTRECHT	6325	6348	6335	6313	6336	6327	6342	6293	6394	6380	6335	6334
LOMNICKY STIT								10754	10788	10799	10803	10853
PREDIGTSTUHL	3778	3788	3780	3800	3755	3759	3758	3750	3761	3743	3763	3750
DALLAS	6236	6254	6255	6270	6272	6277	6318	6325	6319	6323	6328	6325
JUNGFRAUJOCH						6085	6064	6065	6086	6054	6062	6049
USHUAIA	410	455	486	439	423	398	447	427	371	426	334	353
MEXICO CITY							654	655	655	656	656	654
BUENOS AIRES						13265	13258	13197	13212	13246	13304	13239
MT NORIKURA				5249	5248	5255	5258	5272	5274	5270	5293	5288
TOKYO/ITABASHI				3552	3554	3546	3550	3547	3562	3576	3571	3583

Table 2 (continued)

September 2, 1971

01	02	03	04	05	06	07	08	09	10	11	12	AVERAGE
7845	7726	7637	7549	7514	7450	7409	7352	7347	7333	7307	7292	7581.1
2269	2254	2216	2193	2173	2162	2146	2129	2122	2125	2105	2101	2175.5
89848	88748	87526	86463	86003	85233	84495	84371	84062	83310	83115	83153	86425.9
20713	20519	20173	20034	19884	19683	19484	19480	19454	19332	19311		19830.9
6996	6896	6829	6743	6725	6707	6713	6689	6713	6739	6798	6765	6822.5
7522	7467	7324	7286	7197	7137	7129	7094	7088	7070	7040	7031	7264.6
7250	7238	7197	7139	7068	7072	7003	7020	6977	6950	6961	6945	7136.1
7888	7734	7614	7499	7432	7387	7319	7302	7275	7304	7277	7256	7490.0
4111	4035	4004	3961	3929	3904	3895	3898	3901	3925	3899	3885	3928.5
7511	7423	7282	7207	7148	7103	7066	7054	7022	7004	6996		7241.4
3295	3236	3152	3067	3041	3117	3056	3117	3035	3038	3068	3009	3097.2
570	547	545	538	546	539	535	535	535	543	536	539	543.8
9981	9777	9596	9456	9286	9138	9099	9057	8996	8966	8896	8866	9176.8
21191	20929	20726	20477	20448	20322	20283	20271	20232	20092	20080	20161	20524.3
2554	2482	2429	2381	2384	2379	2350						2607.0
2383	2363	2329	2309	2308	2292							2353.4
6775	6683	6660	6653	6607	6578	6613	6632	6613	6623	6619	6633	6791.1
6335	6316	6281	6289	6281	6264	6279	6315	6328	6346	6356	6357	6323.1
6306	6314	6295	6298	6293	6301	6304	6330	6346	6371	6339	6361	6329.9
10840	10711	10705	10698	10795	10787	10763	10751	10816	10805	10815		10780.1
3760	3747	3737	3736	3741	3749	3757	3769	3773	3775	3771	3771	3761.3
6312	6272	6267	6245	6253	6236	6255	6259	6255	6263	6253	6261	6276.4
												6066.5
486	401	383	425	394	435	380	426	422	434	424	434	417.2
653	655	653	652	651	652	653	652	655	652			653.8
13172	13162	13179	13143	13171	13227	13252	13223	13216	13230	13316	13259	13224.7
5262	5278	5246	5245	5250	5251	5250	5244					5260.8
3593	3573	3594	3571	3580	3569	3566	3562	3545				3566.3

Table 3

ALERT 82.5N 62.20W CANADA

NEUTRON MONITOR 18-NM-64

REAL COUNTS 100 TIMES TABULATED COUNTS

FIVE-MINUTE BAROMETER CORRECTED HOURLY RATES

SEPTEMBER 1-2, 1971

TIME U.T.	MINUTES AT END OF INTERVAL 05	10	15	20	25	30	35	40	45	50	55	60	AVERAGE
1900-2000	7206	7185	7195	7153	7195	7217	7121	7142	7206	7163	7174	7206	7180
2000-2100	7259	7280	7326	7454	7485	7613	7730	7836	7857	7977	8019	7998	7653
2100-2200	8008	8104	8136	8083	8168	8231	8231	8221	8178	8093	8199	8157	8151
2200-2300	8093	8125	8242	8199	8189	8136	8051	8146	8168	7998	8072	8104	8127
2300-2400	8149	8011	8001	8043	8054	7990	8064	8054	7937	7905	7916	7961	8007
2400-0100	7940	7823	7866	7876	7813	7813	7844	7855	7866	7802	7834	7802	7845
0100-0200	7749	7749	7763	7752	7784	7742	7742	7699	7731	7692	7649	7660	7726
0200-0300	7649	7755	7660	7639	7607	7607	7639	7649	7652	7578	7578	7631	7637
0300-0400	7529	7571	7571	7603	7603	7595	7448	7521	7574	7595	7521	7458	7549
0400-0500	7521	7564	7606	7458	7469	7535	7535	7482	7451	7493	7524	7524	7514
0500-0600	7472	7514	7493	7430	7496	7517	7370	7443	7391	7380	7454	7443	7450
0600-0700	7380	7436	7457	7373	7415	7405	7418	7418	7450	7366	7408	7376	7409
0700-0800	7334	7338	7296	7401	7372	7372	7362	7372	7341	7299	7362	7372	7352
0800-0900	7375	7313	7281	7355	7396	7365	7355	7292	7355	7365	7334	7375	7347
0900-1000	7292	7334	7334	7344	7368	7316	7400	7368	7316	7222	7337	7361	7333
1000-1100	7350	7288	7256	7267	7260	7249	7395	7333	7291	7281	7406	7305	7307
1100-1200	7305	7294	7284	7305	7287	7308	7256	7277	7297	7287	7308	7301	7292
1200-1300	7301	7290	7301	7335	7293	7262	7283	7297	7369	7362	7269	7269	7303
1300-1400	7165	7331	7289	7248	7297	7276	7248	7372	7258	7248	7230	7303	7272
1400-1500	7303	7282	7262	7285	7327	7285	7306	7265	7316	7247	7237	7247	7280
1500-1600	7144	7278	7309	7340	7268	7302	7219	7343	7292	7264	7233	7264	7271
1600-1700	7154	7257	7298	7205	7246	7185	7288	7280	7250	7280	7222	7222	7241
1700-1800	7284	7273	7253	7263	7242	7253	7246	7338	7246	7228	7269	7276	7264

DUMONT DURVILLE 66.4S 140.02E ANTARCTICA

NEUTRON MONITOR 9-NM-64

CORRECTED FOR BAROMETRIC PRESSURE

COEFFICIENT 9.9 PER CENT PER CM HG

MULTIPLY INDICATED NUMBERS BY 200

FIFTEEN-MINUTE HOURLY RATES

SEPTEMBER 1-2, 1971

TIME U.T.	MINUTES AT END OF INTERVAL 15	30	45	60
1600-1700	513	510	516	514
1700-1800	512	515	516	516
1800-1900	518	514	515	517
1900-2000	515	517	514	520
2000-2100	531	568	574	551
2100-2200	578	594	591	591
2200-2300	596	595	598	584
2300-2400	585	579	581	578
2400-0100	573	569	566	561
0100-0200	568	566	557	563
0200-0300	558	556	551	551
0300-0400	548	551	548	546
0400-0500	544	545	543	541
0500-0600	542	543	541	536
0600-0700	538	536	537	535
0700-0800	536	529	535	529
0800-0900	528	530	532	532
0900-1000	534	533	531	527
1000-1100	527	526	527	525
1100-1200	527	523	524	527

Table 3 (continued)

INUVIK 68.21N 133.43W CANADA

NEUTRON MONITOR 18-NM-64

REAL COUNTS 100 TIMES TABULATED COUNTS

FIVE-MINUTE BAROMETER CORRECTED HOURLY RATES

SEPTEMBER 1-2, 1971

TIME	MINUTES AT END OF INTERVAL												
U.T.	05	10	15	20	25	30	35	40	45	50	55	60	AVERAGE
1900-2000	6802	6849	6837	6868	6915	6880	6832	6856	6832	6844	6880	6832	6852
2000-2100	6939	6934	7041	7124	7160	7339	7339	7260	7367	7410	7469	7410	7233
2100-2200	7457	7457	7612	7605	7616	7712	7747	7640	7628	7735	7747	7688	7637
2200-2300	7557	7688	7652	7593	7680	7728	7633	7605	7550	7640	7656	7455	7620
2300-2400	7478	7514	7526	7692	7633	7502	7538	7597	7609	7514	7585	7625	7568
2400-0100	7578	7566	7483	7518	7447	7447	7495	7495	7381	7511	7475	7452	7487
0100-0200	7499	7416	7440	7428	7475	7393	7345	7373	7373	7397	7326	7283	7396
0200-0300	7331	7331	7272	7295	7319	7319	7331	7307	7272	7248	7260	7241	7294
0300-0400	7205	7229	7276	7182	7170	7193	7182	7229	7229	7158	7276	7134	7205
0400-0500	7193	7205	7163	7198	7234	7116	7245	7127	7139	7175	7057	7151	7167
0500-0600	7151	7080	7097	7050	7132	7132	7137	7090	7078	7054	7090	7142	7103
0600-0700	7083	7048	7052	7041	7012	6977	7024	7118	7088	7029	6994	7029	7041
0700-0800	7005	7076	7045	6963	7069	7003	7062	7008	7031	6978	7071	7060	7031
0800-0900	6989	7060	7071	7071	7041	6989	6978	6982	6994	6924	6964	6999	7005
0900-1000	6976	7022	6999	6859	6987	6999	6957	6957	6915	6857	6850	6932	6943
1000-1100	6955	6908	6955	6920	6932	6827	7025	6955	6978	6838	6920	6902	6926
1100-1200	6948	6913	6872	6918	6988	6976	6941	6941	6941	6923	6876	6916	6929
1200-1300	6928	6898	6898	6898	6960	6914	6838	6919	6896	6884	6981	6900	6910
1300-1400	6970	6912	6947	6889	6889	6842	6870	6829	6887	6910	6972	6880	6900
1400-1500	6919	6827	6878	6901	6848	6791	6860	6825	6830	6853	6922	6841	6858
1500-1600	6818	6880	6938	6857	6857	6862	6874	6855	6833	6936	6883	6883	6873
1600-1700	6894	6860	6945	6910	6949	6954	6908	6890	6940	6895	6854	6940	6912
1700-1800	6826	6910	6865	6881	6881	6806	6954	6851	6874	6931	6935	6895	6884

FORT CHURCHILL 58.75N 265.90E CANADA

IGY NEUTRON MONITOR

BAROMETER REFERENCE 1010 MILLIBARS

ATTENUATION LENGTH 137.2 MILLIBARS

REAL COUNTS 40 TIMES TABULATED COUNTS

FIVE-MINUTE BAROMETER CORRECTED HOURLY RATES

SEPTEMBER 1-2, 1971

TIME	MINUTES AT END OF INTERVAL											
U.T.	05	10	15	20	25	30	35	40	45	50	55	60
1500	1567	1578	1584	1581	1574	1579	1575	1586	1580	1579	1588	1572
1600	1578	1565	1597	1580	1577	1577	1594	1581	1572	1581	1566	1598
1700	1614	1576	1593	1588	1596	1586	1582	1606	1576	1602	1593	1591
1800	1589	1596	1601	1600	1595	1604	1594	1591	1604	1592	1603	1584
1900	1586	1590	1590	1592	1602	1587	1591	1593	1593	1589	1583	1580
2000	1600	1622	1621	1647	1631	1655	1662	1661	1684	1701	1719	1725
2100	1733	1732	1755	1750	1736	1765	1768	1782	1782	1787	1804	1792
2200	1809	1807	1790	1769	1760	1774	1773	1756	1746	1752	1747	1776
2300	1752	1749	1770	1764	1733	1761	1732	1745	1729	1733	1734	1732
2400	1710	1725	1732	1740	1734	1724	1717	1715	1714	1728	1737	1734
0100	1709	1715	1718	1717	1720	1709	1730	1702	1696	1693	1708	1702
0200	1695	1674	1689	1686	1696	1694	1681	1690	1665	1668	1666	0
0300	0	1677	1669	1681	1674	1678	1674	1669	1659	1655	1666	1659
0400	1672	1650	1661	1666	1644	1641	1661	1667	1668	1658	1648	1648
0500	1622	1644	0	1646	1631	1636	1636	1662	1644	1657	1620	1638
0600	1617	1642	1609	1630	1642	1627	1625	1604	1621	1622	1622	1622
0700	1627	1636	1618	1629	1624	1615	1644	1626	1614	1599	1612	1634
0800	1612	1624	1630	1623	1632	1611	1617	1619	1617	1624	1630	1617
0900	1610	1607	1616	1613	1615	1602	1600	1619	1622	1607	1602	1616
1000	1602	1628	1618	1597	1601	1603	1603	1622	1606	1609	1616	1605
1100	1617	1614	1600	1602	1615	1618	1625	1605	1607			

Table 3 (continued)

SYOWA BASE 69.0S 39.58E ANTARCTICA

NEUTRON MONITOR 12-NM-64

PRESSURE CORRECTED TO 965 MILLIBARS

COEFFICIENT -0.74 PER CENT PER MILLIBAR

SCALING FACTOR 100

FIVE-MINUTE COUNTING RATES

SEPTEMBER 1-2, 1971

TIME U.T.	MINUTES AT END OF INTERVAL 05	10	15	20	25	30	35	40	45	50	55	60
1900-2000	547	544	543	540	539	536	544	546	547	542	550	539
2000-2100	554	545	547	555	566	566	567	572	572	571	574	577
2100-2200	586	584	593	592	592	596	592	593	598	598	595	595
2200-2300	589	589	589	596	601	601	594	598	597	601	605	599
2300-2400	602	602	597	601	592	591	588	592	583	595	591	580
2400-0100	586	583	580	585	586	580	585	578	581	578	583	591
0100-0200	576	580	578	581	576	578	571	569	571	575	570	571
0200-0300	574	578	568	567	574	567	570	568	568	564	566	565
0300-0400	563	556	564	568	559	560	566	561	566	561	562	557
0400-0500	559	561	565	557	566	556	561	558	556	560	560	556
0500-0600	554	558	555	555	564	555	562	561	557	561	558	567
0600-0700	562	557	556	567	556	554	558	559	558	563	561	562
0700-0800	558	553	557	557	557	558	566	558	558	559	550	558
0800-0900	557	554	561	558	558	559	562	558	570	555	558	563
0900-1000	566	562	562	552	562	566	564	558	563	564	559	561
1000-1100	568	566	573	563	561	571	569	566	562	564	567	568
1100-1200	566	566	574	560	560	562	566	561	561	561	563	565

GOOSE BAY 53.16N 60.24W CANADA

NEUTRON MONITOR 18-NM-64

REAL COUNTS 100 TIMES TABULATED COUNTS

FIVE-MINUTE BAROMETER CORRECTED HOURLY RATES

SEPTEMBER 1-2, 1971

TIME U.T.	MINUTES AT END OF INTERVAL 05	10	15	20	25	30	35	40	45	50	55	60	AVERAGE
1900-2000	7093	6996	7063	7000	7030	7007	7075	7045	7030	7045	6989	7079	7038
2000-2100	7144	6982	7166	7065	7069	7166	7245	7207	7346	7391	7323	7391	7208
2100-2200	7507	7428	7507	7484	7686	7623	7578	7634	7671	7772	7660	7668	7602
2200-2300	7757	7600	7698	7653	7619	7683	7615	7728	7615	7702	7552	7698	7660
2300-2400	7701	7619	7511	7600	7638	7567	7623	7612	7645	7649	7574	7529	7606
2400-0100	7544	7541	7529	7589	7444	7533	7511	7533	7477	7544	7567	7448	7522
0100-0200	7492	7526	7492	7459	7518	7474	7489	7481	7422	7444	7455	7348	7467
0200-0300	7392	7381	7348	7385	7337	7274	7333	7318	7289	7278	7229	7322	7324
0300-0400	7366	7326	7259	7404	7304	7304	7274	7285	7263	7274	7274	7097	7286
0400-0500	7186	7186	7212	7152	7230	7241	7208	7175	7245	7186	7186	7159	7197
0500-0600	7071	7111	7104	7159	7126	7171	7189	7171	7111	7137	7144	7148	7137
0600-0700	7119	7230	7138	7057	7167	7141	7108	7130	7163	7086	7130	7075	7129
0700-0800	7053	7019	7064	7152	7130	7008	7141	7104	7111	7122	7111	7118	7094
0800-0900	7118	7096	7107	7140	7151	7107	7029	7047	7092	7121	7058	6991	7088
0900-1000	7032	7047	7080	7058	7014	7114	7136	7151	6989	7085	7036	7092	7070
1000-1100	7092	6976	7087	6976	7087	6987	7076	7094	7039	6994	7016	7061	7040
1100-1200	7009	7043	7016	7128	7032	7050	6994	6998	7021	7009	7039	7032	7031
1200-1300	7039	7087	7087	7043	7009	7025	7062	7085	7062	7073	7033	7044	7054
1300-1400	7044	7122	6955	6993	6960	7068	7079	7112	7119	7134	7079	7083	7062
1400-1500	7017	7120	7113	7073	7088	7019	7092	7089	7078	7045	7159	7086	7082
1500-1600	7064	7090	7068	7017	7021	7131	7146	7135	7012	7005	7157	7157	7084
1600-1700	7085	7049	7016	7082	7027	7082	7125	7154	7096	7169	7104	7097	7091
1700-1800	7040	7072	7022	7062	7101	7073	7023	7058	7073	7073	7030	7055	7057

Table 3 (continued)

TIXIE BAY 71.58N 128.9E USSR

NEUTRON MONITOR 18-NM-64

UNCORRECTED FOR PRESSURE

RECALCULATING COEFFICIENT 100

FIVE-MINUTE HOURLY RATES

SEPTEMBER 1-2, 1971

TIME	MINUTES AT END OF INTERVAL											
U.T.	05	10	15	20	25	30	35	40	45	50	55	60
1900	555	555	553	562	556	556	547	559	550	564	563	561
2000	561	573	578	582	589	595	591	601	613	615	602	614
2100	613	617	618	626	627	626	631	624	629	626	627	622
2200	624	624	627	636	624	628	619	627	629	626	617	630
2300	626	621	625	623	628	628	615	622	616	622	618	
2400	622	622	615	616	612	616	618	616	610	608	612	606
0100	611	609	611	610	588	600	595	604	609	603	606	604
0200	604	609	605	606	600	606	602	600	605	597	600	604
0300	606	600	598	595	599	601	606	598	600	603	597	594
0400	610	597	597	596	598	591	593	590	595	597	587	588
0500	588	591	586	590	588	582	598	587	592	588	588	590
0600	597	587	593	590	592	596	591	583	581	587	583	592
0700	587	588	580	589	580	584	586	586	584	580	584	575
0800	589	582	590	590	586	587	586	591	577	580	580	582
0900	577	580	579	574	584	594	579	583	578	584	583	582
1000	579	577	573	581	576	577	580	585	579	581	580	582
1100	587	582	578	579	577	573	582	579	578	582	584	580
1200	582	574	579	578	584	575	579	575	578	582	577	582
1300	574	573	583	577	577	572	572	576	578	571	570	570
1400	574	574	573	574	580	572	568	585	576	574	570	572
1500	574	580	576	575	571	578	578	575	577	578	577	571
1600	572	573	579	576	576	564	572	575	573	571	571	570
1700	579	575	574	573	569	575	569	577	573	574	573	570
1800	571	571	574	580	577	576	568	578	575	570	575	571

PRESSURE IN MM HG X 1/10

1900	7579	7579	7579	7573	7573	7578	7578	7578	7578	7573	7573	7578
2000	7578	7578	7578	7578	7578	7577	7577	7577	7577	7577	7577	7577
2100	7577	7577	7577	7577	7577	7573	7576	7576	7576	7576	7576	7576
2200	7576	7576	7576	7576	7576	7576	7576	7573	7576	5576	7576	7575
2300	7575	7575	7575	7575	7575	7574	7573	7574	7574	7574	7574	7574
2400	7574	7574	7573	7573	7573	7572	7572	7572	7573	7573	7573	7573
0100	7573	7573	7573	7573	7573	7573	7572	7572	7572	7572	7572	7572
0200	7572	7572	7572	7572	7572	7572	7571	7571	7571	7571	7571	7571
0300	7571	7571	7571	7573	7570	7570	7570	7570	7570	7570	7569	7569
0400	7569	7569	7569	7569	7569	7569	7569	7568	7568	7568	7568	7568
0500	7568	7568	7568	7568	7568	7568	7568	7567	7567	7567	7567	7567
0600	7563	7566	7566	7566	7566	7566	7566	7566	7566	7566	7566	7566
0700	7563	7566	7566	7566	7566	7566	7566	7566	7566	7566	7563	7566
0800	7563	7565	7565	7565	7565	7565	7563	7565	7563	7564	7564	7564
0900	7564	7564	7564	7564	7564	7564	7564	7564	7564	7564	7564	7564
1000	7564	7564	7564	7564	7564	7564	7564	7564	7564	7564	7564	7564
1100	7563	7562	7563	7563	7563	7562	7562	7562	7562	7561	7561	7561
1200	7560	7560	7560	7560	7560	7560	7533	7559	7559	7559	7559	7559
1300	7558	7558	7559	7559	7559	7533	7559	7559	7560	7560	7560	7560
1400	7560	7563	7560	7560	7560	7560	7530	7559	7559	7559	7559	7559
1500	7553	7558	7558	7558	7558	7558	7553	7559	7559	7559	7559	7559
1600	7559	7559	7559	7558	7558	7558	7558	7558	7558	7558	7558	7558
1700	7558	7558	7558	7558	7558	7558	7558	7558	7558	7558	7558	7558
1800	7558	7558	7558	7558	7558	7558	7557	7557	7557	7557	7557	7557

Table 3 (continued)

KIRUNA 67.83N 20.43E SWEDEN

NEUTRON MONITOR 12-NM-64

CORRECTED TO 720 MM HG

COEFFICIENT -0.99 PER CENT PER MM HG

REAL COUNTS 10 TIMES TABULATED COUNTS

FIVE-MINUTE HOURLY RATES

SEPTEMBER 1-2, 1971

TIME U.T.	MINUTES AT END OF INTERVAL											
	05	10	15	20	25	30	35	40	45	50	55	60
2000	5887	5915	5929	5841	5897	5903	5901	5888	5843	5861	5876	5902
2100	6001	5948	6085	6110	6195	6121	6172	6298	6263	6342	6361	6388
2200	6390	6424	6489	6567	6518	6568	6636	6648	6792	6702	6722	6707
2300	6736	6645	6638	6679	6730	6728	6715	6812	6663	6681	6684	6644
2400	6636	6613	6634	6601	6551	6499	6585	6632	6554	6538	6514	6523
0100	6494	6546	6554	6512	6478	6401	6392	6451	6414	6414	6365	6317
0200	6375	6354	6358	6340	6415	6299	6353	6335	6352	6325	6360	6277
0300	6288	6313	6271	6264	6282	6236	6190	6211	6227	6213	6249	6247
0400	6215	6241	6204	6150	6196	6218	6269	6144	6153	6175	6127	6222
0500	6199	6191	6105	6169	6167	6140	6178	6114	6163	6150	6162	6129
0600	6086	6112	6114	6075	6062	6076	6042	6122	6101	6134	6141	6122
0700	6051	6104	6084	6130	6020	6017	6046	6111	6059	6164	6125	6110
0800	6056	6033	6083	5964	6101	6084	6088	6084	6058	6051	6088	6065
0900	6117	6041	6111	6128	6093	6038	6109	6151	6073	6031	6072	6078
1000	6036	6044	6097	6072	6056	6100	6082	5992	6085	6079	6078	6054
1100	6004	6126	6080	6039	6045	6002	6048	6074	6057	6002	6063	6022
1200	6051	6086	6034	6005	6055	6058	6066	6042	6052	6055	6038	5992
1300	6001	6073	6059	6038	6015	6013	6003	6013	6060	6035	6031	6002
1400	6030	5989	6016	5975	6039	6009	5885	6049	6047	6009	6020	5955
1500	5905	6011	5962	5935	6036	6014	6008	5984	5907	5923	5993	5929
1600	5939	5966	6017	5999	6018	5981	6016	5978	6054	5981	5922	5969
1700	6000	5976	5880	5953	5896	5972	5997	5956	5953	5932	5989	5946
1800	5930	5976	5978	5937	5972	5918	5952	5901	5971	5933	5968	5877
1900	5944	5957	5975	5959	5885	5889	5885	5929	5907	5964	5881	5925

BELGRANO 77.96S 38.8W ANTARCTIC

NEUTRON MONITOR 6-NM-64

REAL COUNTS 16 TIMES TABULATED COUNTS

FIVE-MINUTE BAROMETER CORRECTED HOURLY RATES

SEPTEMBER 1-2, 1971

TIME U.T.	MINUTES AT END OF INTERVAL											
	05	10	15	20	25	30	35	40	45	50	55	60
1700-1800	1345	1375	1352	1343	1364	1369	1373	1353	1372	1370	1373	1356
1800-1900	1376	1376	1365	1368	1385	1388	1363	1384	1367	1379	1358	1351
1900-2000	1390	1364	1371	1375	1388	1387	1371	1399	1388	1363	1352	1367
2000-2100	1383	1364	1385	1402	1410	1406	1380	1424	1429	1431	1460	1464
2100-2200	1454	1482	1506	1489	1507	1506	1515	1517	1525	1522	1524	1504
2200-2300	1512	1474	1506	1488	1510	1494	1464	1462	1500	1496	1509	1485
2300-2400	1517	1493	1495	1502	1522	1495	1523	1501	1494	1485	1490	1484
2400-0100	1511	1470	1462	1505	1506	1473	1486	1502	1501	1461	1464	1476
0100-0200	1469	1483	1488	1474	1484	1485	1462	1445	1472	1479	1468	1453
0200-0300	1455	1459	1413	1453	1456	1451	1442	1447	1430	1421	1430	1426
0300-0400	1423	1470	1440	1423	1398	1448	1452	1441	1475	1448	1424	1431
0400-0500	1426	1431	1410	1408	1415	1417	1445	1422	1453	1444	1424	1416
0500-0600	1393	1418	1405	1394	1410	1397	1404	1388	1398	1424	1394	1407

OULU 65.1N 25.3E FINLAND

NEUTRON MONITOR 9-NM-64

CORRECTED FOR PRESSURE

SCALING FACTOR 64

FIVE-MINUTE HOURLY RATES

SEPTEMBER 1-2, 1971

TIME U.T.	MINUTES AT END OF INTERVAL 05	10	15	20	25	30	35	40	45	50	55	60	AVERAGE
1800	496	498	496	486	497	493	490	503	494	500	488	500	495.0
1900	489	495	487	488	487	495	494	493	497	497	496	497	493.1
2000	506	504	508	510	513	519	522	524	519	526	523	537	517.6
2100	543	549	552	545	547	548	547	553	544	550	556	553	548.9
2200	566	563	559	556	545	556	551	548	550	552	550	544	553.4
2300	548	545	544	544	541	543	540	531	546	538	535	535	540.5
2400	535	541	537	524	539	539	531	530	537	536	526	528	533.5
0100	525	521	533	529	523	526	526	521	522	524	526	525	525.4
0200	526	523	526	523	519	518	518	520	517	516	519	517	520.4
0300	507	521	518	519	513	517	514	520	511	516	511	511	514.6
0400	505	522	514	512	517	515	503	511	507	513	514	509	511.5
0500	515	507	513	506	507	505	506	511	505	502	506	509	507.9
0600	508	507	500	510	505	503	511	513	509	505	511	513	507.8
0700	503	501	509	511	505	506	514	509	504	503	510	506	506.8
0800	514	511	506	503	511	500	508	510	508	507	507	499	507.1

DEEP RIVER 46.1N 77.3W CANADA

NEUTRON MONITOR 48-NM-64

REAL COUNTS 300 TIMES TABULATED COUNTS

FIVE-MINUTE BAROMETER CORRECTED HOURLY RATES

SEPTEMBER 1-2, 1971

TIME U.T.	MINUTES AT END OF INTERVAL 05	10	15	20	25	30	35	40	45	50	55	60	AVERAGE
1900-2000	6947	6986	6973	6960	6927	6998	6959	6991	6965	6991	6971	6971	6970
2000-2100	6964	7010	7029	7067	7099	7222	7261	7299	7331	7395	7408	7414	7208
2100-2200	7427	7504	7504	7581	7535	7612	7638	7599	7586	7612	7612	7625	7570
2200-2300	7669	7669	7695	7656	7643	7695	7725	7636	7700	7713	7679	7648	7677
2300-2400	7648	7648	7641	7692	7667	7628	7602	7602	7590	7590	7602	7551	7622
2400-0100	7533	7559	7559	7507	7489	7491	7568	7473	7473	7506	7467	7506	7511
0100-0200	7467	7487	7462	7454	7416	7454	7467	7397	7403	7364	7377	7332	7423
0200-0300	7345	7332	7320	7255	7268	7307	7332	7216	7242	7242	7255	7268	7282
0300-0400	7242	7229	7203	7235	7196	7216	7165	7210	7198	7203	7203	7183	7207
0400-0500	7196	7183	7145	7139	7113	7203	7152	7165	7087	7087	7178	7126	7148
0500-0600	7126	7126	7087	7120	7094	7107	7146	7094	7120	7068	7113	7029	7103
0600-0700	7093	7106	7042	7054	7061	7074	7042	7093	7080	7003	7100	7048	7066
0700-0800	7042	7094	7074	7036	7029	7099	7060	7060	7086	7073	6996	6996	7054
0800-0900	7022	7060	7022	7015	7028	7021	6988	7027	7039	7039	7007	6994	7022
0900-1000	6994	7020	7020	7000	6987	7000	6949	7020	7058	7033	6961	7000	7004
1000-1100	7026	7064	6993	6967	6993	6987	7026	6974	6974	6981	6968	6994	6996

Table 3 (continued)

SANAE 70.46S 357.51E ANTARCTICA

3-NM-64 NEUTRON MONITOR

REAL COUNTS 10 TIMES TABULATED VALUES

CORRECTED TO 980 MB

COEFFICIENT 0.73 PER CENT PER MILLIBAR

TEN-MINUTE HOURLY COUNTING RATES

SEPTEMBER 1-2, 1971

TIME U.T.	MINUTES AT END OF INTERVAL 10	20	30	40	50	60
1700-1800	2582	2536	2524	2556	2532	2564
1800-1900	2537	2560	2526	2526	2534	2534
1900-2000	2605	2542	2534	2554	2552	2548
2000-2100	2566	2596	2602	2690	2730	2728
2100-2200	2748	2800	2778	2812	2812	2798
2200-2300	2898	2897	2853	2875	2859	2875
2300-2400	2839	2847	2827	2851	2837	2821
2400-0100	2828	2772	2766	2744	2778	2736
0100-0200	2765	2744	2734	2730	2692	2740
0200-0300	2716	2700	2692	2704	2684	2677
0300-0400	2683	2706	2665	2623	2649	2683
0400-0500	2659	2616	2649	2683	2657	2632
0500-0600	2666	2563	2626	2618	2624	2667
0600-0700	2593	2561	2616	2628	2624	2640
0700-0800	2601	2620	2622	2552	2595	2616
0800-0900	2634	2612	2583	2614	2597	2589
0900-1000	2646	2620	2606	2583	2620	2604
1000-1100	2605	2600	2591	2571	2597	2628
1100-1200	2658	2573	2585	2626	2520	2602

PORT AUX FRANCAIS 49.35S 70.25E KERGUELEN ISLAND

NEUTRON MONITOR 18-NM-64

CORRECTED FOR BAROMETRIC PRESSURE

COEFFICIENT 10.1 PER CENT PER CM HG

MULTIPLY INDICATED NUMBERS BY 400

FIVE-MINUTE HOURLY RATES

TIME U.T.	MINUTES AT END OF INTERVAL 05	10	15	20	25	30	35	40	45	50	55	60
1800	1624	1624	1623	1627	1626	1624	1644	1632	1631	1634	1649	1636
1900	1608	1619	1617	1640	1615	1595	1607	1630	1618	1630	1624	1631
2000	1625	1628	1642	1621	1619	1620	1632	1627	1617	1626	1620	1625
2100	1638	1661	1684	1702	1718	1760	1766	1767	1775	1806	1795	1835
2200	1811	1806	1845	1817	1820	1839	1849	1822	1824	1832	1833	1814
2300	1831	1845	1842	1842	1829	1821	1814	1815	1839	1816	1799	1810
2400	1781	1806	1807	1808	1803	1792	1795	1782	1782	1795	1784	1784
0100	1769	1773	1772	1775	1761	1759	1769	1778	1767	1759	1747	1762
0200	1765	1758	1756	1752	1746	1747	1733	1737	1744	1750	1705	1736
0300	1726	1742	1727	1719	1730	1737	1720	1726	1733	1737	1723	1706
0400	1710	1703	1707	1717	1707	1711	1699	1714	1694	1707	1702	1706
0500	1696	1705	1695	1710	1682	1723	1705	1702	1706	1715	1702	1707
0600	1699	1693	1686	1693	1692	1696	1695	1689	1692	1688	1702	1697
0700	1694	1693	1703	1697	1677	1679	1688	1690	1688	1698	1694	1682
0800	1705	1689	1704	1679	1688	1700	1685	1688	1688	1682	1674	1689
0900	1690	1687	1697	1682	1687	1676	1688	1691	1675	1682	1697	1680
1000	1690	1667	1673	1679	1675	1692	1664	1688	1671	1664	1648	1681
1100	1672	1674	1686	1681	1673	1679	1667	1664	1676	1678	1671	1659
1200	1695	1685	1683	1685	1673	1691	1669	1671	1681	1695	1668	1665

MT WASHINGTON 44.3N 288.7E NEW HAMPSHIRE

IGY NEUTRON MONITOR

CORRECTED FOR BAROMETRIC PRESSURE

FIVE-MINUTE HOURLY RATES

SEPTEMBER 1-2, 1971

TIME U.T.	MINUTES AT END OF INTERVAL 05	10	15	20	25	30	35	40	45	50	55	60
1800-1900	190	194	196	192	188	191	197	189	194	187	196	194
1900-2000	193	189	194	193	190	190	196	194	193	191	198	189
2000-2100	192	197	197	201	197	199	204	211	206	214	214	211
2100-2200	219	221	215	224	219	220	220	218	222	219	222	220
2200-2300	219	225	222	230	222	218	222	217	216	220	222	216
2300-2400	216	219	212	215	216	216	212	213	220	212	215	216
2400-0100	211	218	212	215	211	214	214	212	212	213	214	207
0100-0200	208	207	209	210	206	208	206	205	207	207	202	205
0200-0300	0	200	202	203	200	204	199	202	207	203	203	207
0300-0400	201	198	204	198	199	198	198	197	193	198	196	201
0400-0500	199	198	198	200	197	197	200	198	197	205	195	199
0500-0600	200	195	200	195	204	197	194	199	199	203	196	197
0600-0700	197	196	195	196	190	198	200	198	196	192	195	197

DURHAM 43.1N 289.1E NEW HAMPSHIRE

NEUTRON MONITOR 12-NM-64

CORRECTED FOR BAROMETRIC PRESSURE

FIVE-MINUTE HOURLY RATES

SEPTEMBER 1-2, 1971

TIME U.T.	MINUTES AT END OF INTERVAL 05	10	15	20	25	30	35	40	45	50	55	60
1800-1900	191	190	190	189	187	189	189	190	191	189	190	192
1900-2000	190	191	192	190	190	188	189	192	188	188	192	191
2000-2100	193	193	192	194	197	198	197	199	203	200	201	202
2100-2200	201	204	205	205	204	207	202	207	204	205	205	205
2200-2300	207	204	204	209	206	206	205	204	205	205	203	199
2300-2400	202	202	203	202	203	202	198	202	202	202	198	200
2400-0100	202	199	202	197	199	198	196	197	200	197	198	198
0100-0200	198	199	194	198	198	196	198	198	196	199	194	195
0200-0300	195	197	193	194	192	195	193	192	197	195	193	194
0300-0400	191	190	192	193	193	194	194	193	193	193	194	191
0400-0500	197	191	192	192	192	196	192	193	191	190	190	193
0500-0600	193	194	191	192	189	192	190	188	190	192	190	191

Table 3 (continued)

LEEDS 53.8N 01.5W ENGLAND

IGY NEUTRON MONITOR

REAL COUNTS 100 TIMES TABULATED COUNTS

FIVE-MINUTE UNCORRECTED RATES

SEPTEMBER 1-2, 1971

TIME U.T.	MINUTES AT END OF INTERVAL 05	10	15	20	25	30	35	40	45	50	55	60
2400-0100	583	584	581	587	584	590	592	585	589	589	589	592
0100-0200	592	590	596	590	591	590	592	587	588	588	589	588
0200-0300	591	579	587	593	591	583	591	597	586	594	591	601
0300-0400	594	592	593	598	598	600	589	592	595	597	597	588
0400-0500	590	595	601	599	596	592	592	597	599	594	603	597
0500-0600	595	598	591	598	595	595	596	600	589	597	595	589
0600-0700	593	590	597	598	587	596	586	605	599	599	599	597
0700-0800	597	596	598	593	592	593	593	604	596	596	587	591
0800-0900	591	595	595	597	598	595	593	590	599	595	593	596
0900-1000	602	592	596	601	583	602	589	596	598	590	595	589
1000-1100	597	596	597	595	600	591	597	594	589	596	593	590
1100-1200	596	594	595	598	592	601	597	599	600	597	593	588
1200-1300	599	593	593	596	590	595	595	597	595	591	590	588
1300-1400	583	589	591	587	595	590	590	584	588	589	587	577
1400-1500	585	585	586	582	580	585	587	587	591	595	589	587
1500-1600	583	579	584	586	585	586	577	588	583	583	585	584
1600-1700	577	586	586	578	573	577	583	584	577	579	578	576
1700-1800	573	574	573	579	577	567	579	575	574	566	580	566
1800-1900	573	574	577	583	572	569	577	575	574	572	569	575
1900-2000	571	567	567	570	569	563	568	568	564	563	568	565
2000-2100	572	568	573	571	576	576	572	579	573	579	588	588
2100-2200	594	583	581	583	588	577	582	579	583	581	577	578
2200-2300	574	579	579	578	572	572	572	565	571	568	564	571
2300-2400	565	561	573	560	569	566	568	566	566	564	568	562
2400-0100	570	567	565	563	567	563	566	564	566	563	559	562
0100-0200	567	555	554	557	559	552	556	560	555	558	557	553
0200-0300	560	553	558	555	555	561	549	559	553	555	551	551
0300-0400	556	554	557	561	554	560	547	551	552	554	557	550
0400-0500	546	551	551	548	548	552	553	555	550	545	551	557
0500-0600	547	545	543	549	550	550	547	551	549	548	549	550
0600-0700	557	554	546	550	548	555	547	549	552	548	552	555
0700-0800	556	550	549	564	547	550	554	552	555	554	547	554
0800-0900	553	549	554	550	550	549	549	549	554	550	554	552
0900-1000	554	551	555	547	553	554	557	551	555	553	543	550
1000-1100	551	552	551	548	553	548	552	552	550	553	553	556
1100-1200	555	551	554	552	552	553	550	557	555	549	554	551
1200-1300	554	554	550	553	556	550	554	555	553	558	551	557
1300-1400	554	553	561	553	554	556	554	558	555	561	554	552
1400-1500	552	557	557	559	552	551	553	552	559	559	553	551
1500-1600	551	555	555	552	553	554	545	550	559	556	549	551
1600-1700	549	553	551	547	558	548	554	553	550	549	544	556
1700-1800	546	551	554	545	557	549	545	553	554	552	545	550
1800-1900	551	551	543	546	549	549	553	545	550	546	539	543
1900-2000	545	548	552	551	542	545	549	550	548	545	548	545
2000-2100	551	541	540	546	545	545	546	541	546	542	544	547
2100-2200	549	553	543	550	541	542	539	544	543	543	545	543
2200-2300	538	545	544	543	546	543	549	545	542	549	544	538
2300-2400	542	545	540	548	540	543	549	544	545	544	548	544

Table 3 (continued)

LOMNICKY STIT 49.2N 20.22E CZECHOSLOVAKIA

IGY NEUTRON MONITOR

CORRECTED TO 550.0 MM HG

COEFFICIENT -1.024 PER CENT PER MM HG

REAL COUNTS 8 TIMES TABULATED COUNTS

TEN-MINUTE HOURLY RATES

SEPTEMBER 1-2, 1971

TIME U.T.	MINUTES AT END OF INTERVAL 10	20	30	40	50	60
1900-2000	1818.3	1781.3	1774.5	1801.2	1798.0	1781.7
2000-2100	1790.3	1801.7	1793.1	1782.2	1815.9	1804.4
2100-2200	1802.2	1853.7	1768.9	1784.0	1774.3	1816.1
2200-2300	1820.4	1815.1	1788.6	1820.4	1800.1	1758.3
2300-2400	1827.9	1797.1	1821.8	1791.3	1812.4	1801.7
2400-0100	1802.8	1795.6	1802.0	1839.4	1781.7	1808.7
0100-0200	1792.7	1787.4	1757.5	1782.3	1809.0	1781.8
0200-0300	1790.9	1811.4	1781.6	1805.0	1790.4	1725.5
0300-0400	1785.4	1796.8	1798.9	1796.8	1737.5	1782.9
0400-0500	1801.0	1800.3	1791.7	1809.6	1799.2	1793.1
0500-0600	1787.0	1786.7	1796.0	0.0	0.0	1817.5
0600-0700	1813.0	1825.0	1792.0	1738.1	1770.8	1823.9
0700-0800	1770.8	1800.5	1805.1	1802.4	1809.0	1763.4
0800-0900	1767.1	1815.4	1805.8	1815.9	1817.3	1794.9
0900-1000	1776.3	1803.9	1818.6	1781.3	1822.6	1802.3
1000-1100	1801.3	1786.0	1793.5	1813.8	1815.6	1804.9

DALLAS 32.78N 96.80W TEXAS

NEUTRON MONITOR NM-64

REAL COUNTS 40 TIMES TABULATED COUNTS

FIVE-MINUTE BAROMETER CORRECTED HOURLY RATES

SEPTEMBER 1-2, 1971

TIME U.T.	MINUTES AT END OF INTERVAL 05	10	15	20	25	30	35	40	45	50	55	60	AVERAGE
1700	1572	1565	1572	1555	1569	1584	1578	1542	1577	1549	1569	1598	1569.2
1800	1567	1577	1582	1568	1566	1559	1596	1591	1602	1588	1581	1574	1579.5
1900	1573	1579	1585	1600	1568	1576	1581	1572	1600	1580	1595	1565	1581.2
2000	1557	1580	1603	1573	1576	1569	1583	1579	1588	1595	1572	1582	1579.8
2100	1582	1579	1585	1577	1585	1569	1582	1586	1594	1576	1572	1579	1580.7
2200	1565	1592	1585	1592	1593	1589	1571	1565	1575	1589	1583	1586	1582.1
2300	1590	1580	1579	1586	1567	1597	1573	1567	1576	1580	1596	1583	1581.2
2400	1586	1575	1577	1595	1575	1567	1562	1592	1580	1560	1579	1587	1577.9
0100	1565	1560	1553	1565	1573	1596	1570	1566	1557	1586	1559	1565	1568.0
0200	1565	1576	1567	1570	1544	1582	1544	1572	1572	1556	1574	1578	1566.6
0300	1551	1551	1581	1549	1534	1561	1574	1570	1560	1564	1571	1569	1561.3
0400	1555	1586	1571	1547	1561	1571	1585	1559	1551	1543	1567	1569	1563.8
0500	1571	1562	1543	1561	1569	1558	1570	1556	1561	1538	1559	1558	1558.9
0600	1587	1553	1551	1589	1560	1568	1577	1564	1547	1550	1551	1565	1563.7
0700	1572	1557	1574	1565	1537	1575	1565	1556	1560	1577	1580	1557	1564.7
0800	1566	1584	1550	1584	1568	1549	1553	1542	1582	1564	1553	1570	1563.7
0900	1554	1558	1566	1570	1557	1585	1585	1560	1569	1559	1562	1574	1565.8
1000	1561	1560	1556	1580	1574	1575	1580	1559	1539	1556	1542	1576	1563.3
1100	1569	1575	1538	1573	1557	1554	1570	1575	1569	1561	1574	1566	1565.2
1200	1567	1552	1564	1562	1570	1565	1592	1571	1568	1586	1554	1572	1568.7
1300	1565	1551	1559	1566	1572	1577							

JUNGFRAUJOCH 46.6N 8.0E SWITZERLAND

IGY NEUTRON MONITOR

SCALING FACTOR 10

SIX-MINUTES BAROMETER CORRECTED HOURLY RATES

SEPTEMBER 1-2, 1971

TIME U.T.	MINUTES AT END OF INTERVAL 6	12	18	24	30	36	42	48	54	60	AVERAGE
1700	5983	6071	6113	6112	6081	6105	6073	6119	6104	6090	6085.1
1800	6083	6052	6101	6035	6067	6076	6073	6103	6034	6021	6064.5
1900	6090	6067	6049	6071	6026	6074	6028	6111	6078	6054	6064.8
2000	6056	6118	6079	6115	6083	6053	6098	6120	6072	6063	6085.7
2100	6045	6105	6065	6131	6053	6026	6114	6026	5978	6002	6054.5
2200	6075	5966	6130	6030	6129	6006	6101	6026	6033	6129	6062.5
2300	6073	6048	6055	6048	6026	6050	6119	6052	5985	6032	6048.8

USHUAIA 54.8S 68.3W ARGENTINA

IGY NEUTRON MONITOR

REAL COUNTS 8 TIMES TABULATED COUNTS

FIFTEEN-MINUTE BAROMETER CORRECTED RATES

SEPTEMBER 1-2, 1971

TIME U.T.	MINUTES AT END OF INTERVAL 15	30	45	60
1700-1800	848	851	866	863
1800-1900	875	844	873	873
1900-2000	832	860	852	853
2000-2100	842	861	839	831
2100-2200	873	863	868	845
2200-2300	858	0	842	845
2300-2400	835	844	870	885
2400-0100	854	873	836	860
0100-0200	851	847	830	836
0200-0300	851	849	845	839
0300-0400	847	882	856	840
0400-0500	842	873	851	828
0500-0600	829	856	851	856

Table 3 (continued)

MEXICO CITY 19.33N 99.18W MEXICO

NEUTRON MONITOR 6-NM-64

CORRECTED TO 778.9 MILLIBARS

COEFFICIENT -0.72 PER CENT PER MILLIBAR

REAL COUNTS 100 TIMES TABULATED COUNTS

FIVE-MINUTE HOURLY RATES

SEPTEMBER 1-2, 1971

TIME U.T.	MINUTES AT END OF INTERVAL 05	10	15	20	25	30	35	40	45	50	55	60	AVERAGE
1800-1900	650	653	654	658	662	655	657	652	644	651	658	655	654.1
1900-2000	653	651	654	652	658	663	656	647	662	659	657	653	654.7
2000-2100	649	656	650	650	657	662	651	658	662	656	661	651	655.3
2100-2200	653	654	655	649	656	655	663	659	657	658	659	652	655.8
2200-2300	657	653	654	656	655	662	656	654	653	658	657	660	656.2
2300-2400	650	655	654	655	659	652	651	658	658	655	656	650	654.4
2400-0100	652	653	654	653	654	658	656	654	648	658	658	640	653.2
0100-0200	651	662	657	652	653	651	659	650	663	653	652	657	655.0
0200-0300	659	649	644	652	655	650	653	653	657	652	652	655	653.3
0300-0400	656	649	650	656	655	651	650	646	653	659	649	645	652.5
0400-0500	655	654	650	657	656	643	661	654	652	653	654	653	651.4
0500-0600	654	655	644	648	660	645	657	650	653	654	658	650	652.3
0600-0700	649	660	657	648	649	653	649	658	648	654	652	657	652.8
0700-0800	648	647	646	661	651	651	652	658	655	656	646	650	651.8
0800-0900	662	654	647	656	658	656	660	654	662	650	645	654	654.9
0900-1000	648	656	654	654	653	654	653	643	643	654	650	666	652.3

BUENOS AIRES 34.6S 58.49W ARGENTINA

NEUTRON MONITOR 18-NM-64

REAL COUNTS 32 TIMES TABULATED COUNTS

FIVE-MINUTE BAROMETER CORRECTED RATES

SEPTEMBER 1-2, 1971

TIME U.T.	MINUTES AT END OF INTERVAL 05	10	15	20	25	30	35	40	45	50	55	60	AVERAGE
1700-1800	1126	1095	1093	1103	1118	1115	1103	1065	1129	1101	1108	1109	1105.4
1800-1900	1123	1111	1092	1088	1098	1099	1104	1104	1121	1092	1110	1116	1104.8
1900-2000	1076	1124	1087	1096	1109	1096	1086	1124	1100	1105	1090	1104	1099.7
2000-2100	1104	1095	1090	1103	1100	1119	1094	1106	1125	1086	1098	1092	1101.0
2100-2200	1102	1098	1096	1111	1105	1102	1107	1099	1095	1111	1123	1097	1103.8
2200-2300	1107	1109	1118	1117	1099	1090	1107	1106	1119	1118	1129	1085	1108.6
2300-2400	1101	1098	1115	1102	1099	1101	1110	1084	1113	1106	1109	1101	1103.2
2400-0100	1107	1081	1099	1091	1097	1112	1086	1115	1099	1080	1109	1096	1097.6
0100-0200	1091	1099	1105	1088	1100	1097	1099	1105	1099	1090	1091	1098	1096.8
0200-0300	1088	1092	1093	1122	1093	1103	1102	1100	1105	1095	1105	1081	1098.2
0300-0400	1103	1097	1075	1115	1088	1094	1077	1094	1097	1110	1095	1098	1095.2
0400-0500	1078	1092	1118	1096	1083	1095	1095	1091	1124	1103	1103	1093	1097.5
0500-0600	1091	1105	1102	1100	1108	1110	1105	1099	1106	1102	1092	1107	1102.2
0600-0700	1102	1086	1098	1097	1108	1109	1122	1093	1108	1111	1116	1102	1104.3
0700-0800	1097	1100	1101	1113	1113	1105	1098	1109	1108	1094	1085	1105	1101.9
0800-0900	1107	1106	1096	1082	1098	1107	1123	1097	1096	1098	1124	1082	1101.3
0900-1000	1101	1096	1097	1085	1107	1096	1105	1110	1106	1113	1108	1106	1102.5
1000-1100	1101	1112	1104	1107	1108	1128	1108	1117	1092	1092	1122	1125	1109.6
1100-1200	1103	1106	1111	1122	1105	1103	1091	1096	1104	1102	1117	1099	1104.9

Table 3 (continued)

MT NORIKURA 36.11N 137.55E JAPAN

NEUTRON MONITOR 4-NM-64

SCALING FACTOR 128

PRESSURE CORRECTED TO 720 MILLIBARS

COEFFICIENT -0.70 PER CENT PER MILLIBAR

FIFTEEN-MINUTE HOURLY RATES

SEPTEMBER 1-2, 1971

TIME U.T.	MINUTES AT END OF INTERVAL 15	30	45	60	AVERAGE
1600	1315	1315	1309	1310	1312.2
1700	1316	1319	1310	1303	1312.0
1800	1322	1301	1316	1316	1313.7
1900	1314	1319	1310	1315	1314.5
2000	1329	1312	1312	1319	1318.0
2100	1331	1314	1307	1322	1318.5
2200	1319	1330	1311	1310	1317.5
2300	1322	1319	1322	1330	1323.2
2400	1324	1322	1322	1320	1322.0
0100	1322	1310	1316	1314	1315.5
0200	1319	1319	1324	1316	1319.5
0300	1316	1303	1315	1312	1311.5
0400	1322	1301	1311	1311	1311.2
0500	1307	1322	1309	1312	1312.5
0600	1312	1311	1310	1318	1312.7
0700	1314	1315	1314	1307	1312.5
0800	1316	1310	1306	1312	1311.0

ITABASHI 35.75N 139.71E JAPAN

NEUTRON MONITOR 18-NM-64

PRESSURE CORRECTED TO 1013.3 MILLIBARS

COEFFICIENT -0.666 PER CENT PER MILLIBAR

SCALING FACTOR 128

TEN-MINUTE HOURLY RATES

SEPTEMBER 1-2, 1971

TIME U.T.	MINUTES AT END OF INTERVAL 10	20	30	40	50	60	AVERAGE
1600	591	586	598	593	591	593	592.0
1700	593	590	598	591	592	590	592.3
1800	593	592	590	589	593	589	591.0
1900	591	596	594	594	587	588	591.6
2000	587	592	594	598	586	590	591.1
2100	593	593	592	595	593	596	593.6
2200	605	593	595	594	594	595	596.0
2300	594	593	597	594	597	596	595.1
2400	593	604	589	592	603	602	597.1
0100	598	597	598	599	602	599	598.8
0200	591	598	596	600	586	602	595.5
0300	598	594	605	596	608	593	599.0
0400	593	591	594	599	602	592	595.1
0500	597	596	600	599	594	594	596.6
0600	594	592	594	594	600	595	594.8
0700	597	597	588	598	597	589	594.3
0800	589	602	591	589	597	594	593.6
0900	593	593	589	589	592	589	590.8

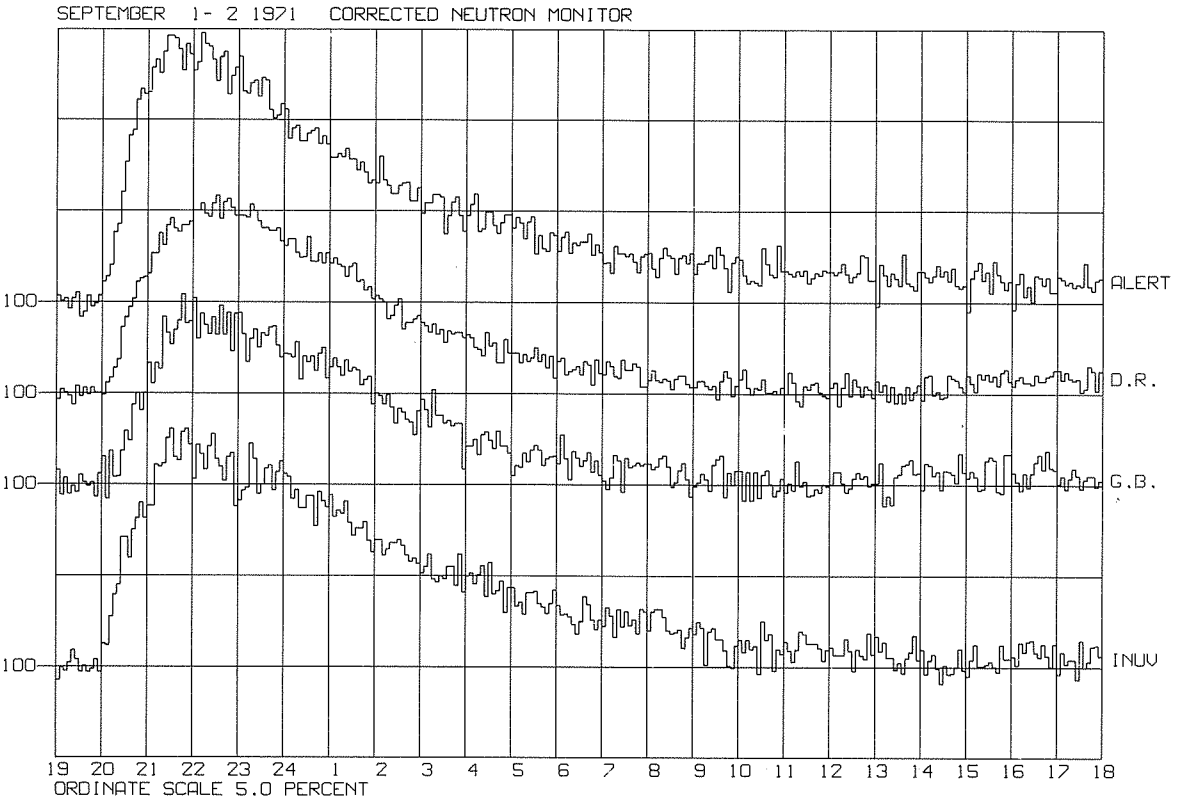

Fig. 1. 5-minute data from Alert, Deep River, General Belgrano and Inuvik, 1900 UT September 1 - 1800 UT September 2, 1971.
(Cutoff rigidities are 0.0, 1.02, 0.75 and 0.18, respectively.)

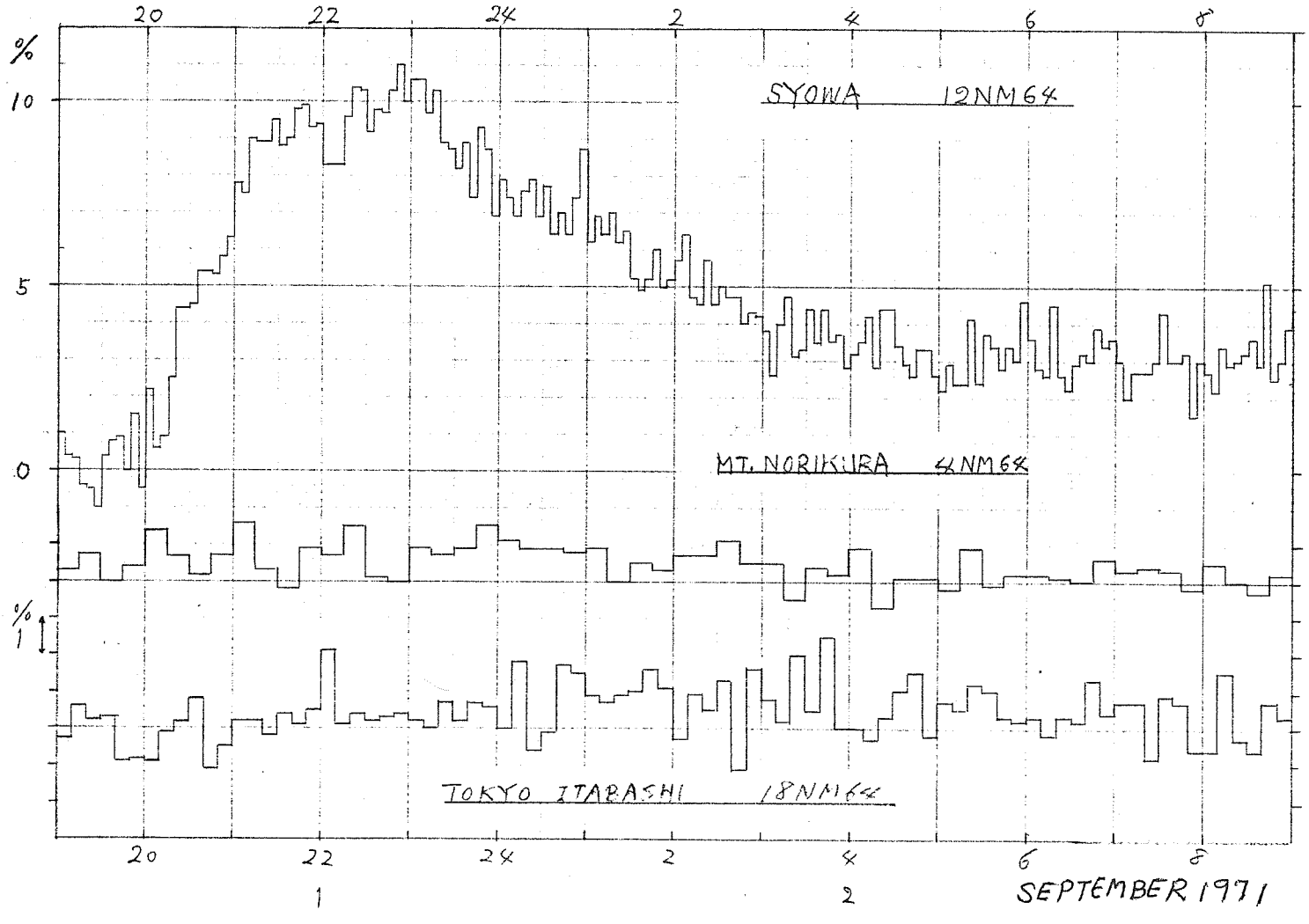

Fig. 2. 5-minute Syowa Base data, 15-minute Mt. Norikura data, and 10-minute Tokyo Itabashi data, 1800 UT August 31 - 1000 UT September 2, 1971. (Cutoff rigidities are 0.42, 11.39 and 11.61, respectively.)

Relativistic Solar Cosmic Rays from the Invisible Disk on September 1-2, 1971

by

S. P. Duggal and M. A. Pomerantz
Bartol Research Foundation
of
The Franklin Institute

1. Introduction

The event of September, 1971, is the most recent of only three occasions on which relativistic solar cosmic rays originating on the invisible disk of the sun were observed to reach the earth. It is certainly the most unusual of this exceedingly rare class of occurrences, in that it displayed an unexpected and marked anisotropy for several hours following onset, despite the fact that the intensity profile bespoke a back-side source. This was confirmed by the absence of a candidate parent flare on the visible disk for at least 15 hours before the initial arrival of the energetic solar particles.

2. Observations

The extreme variability in the nucleonic intensity, as recorded by the Bartol network of polar neutron monitors prior to and following the event of September 1-2, 1971, is shown in Figure 1. Immediately after cessation of the relativistic solar particle precipitation, the galactic cosmic ray intensity appears to have recovered completely from the Forbush decrease that had been in progress since August 27.

The solar cosmic ray intensity, in hourly intervals, at four neutron monitor stations is plotted in Figure 2. The maximum nucleonic intensity increase, about 20%, was recorded at South Pole station and relativistic solar particles were observed there for about 16 hours. In contrast, the integral flux of particles with rigidities exceeding 1.9 GV, recorded at Swarthmore, reached a maximum level only 4% above the pre-event intensity, and the total duration of the event in this case was less than eight hours.

In Figure 3, the data from Bartol stations with asymptotic directions of arrival nearest the north and south poles are plotted on an expanded time scale (6 minute intervals). The data were corrected for pressure fluctuations by the application of two atmospheric coefficients, α and β, appropriate for solar and galactic particles respectively. For solar particles an absorption length of 104 gm/cm^2, derived earlier by Baird et al. [1967] was assumed. The Figure reveals a distinct north-south asymmetry of the relativistic solar cosmic rays.

3. Results of Analysis

A. North-South Asymmetry

A quantitative evaluation of the north-south asymmetry was made by normalizing the data from Thule, Alert, McMurdo and South Pole to a standard pressure level of 760 mm Hg. The asymmetry $A = (N - S)100/N$, where N and S represent the average flux at the northern and the southern stations respectively, is plotted in Figure 4, which shows that A exceeded 44% during the first hour of the GLE, and decreased thereafter. By September 2, the solar flux became essentially isotropic.

B. Spectrum

Figure 5 shows the nucleonic intensity enhancement at a number of stations during the period 0000-0100 UT on September 2, 1971, normalized to a standard pressure of 760 mm Hg and plotted as a function of threshold rigidity. Since the anisotropy was negligible during this period (cf. Figure 4) the primary differential rigidity spectrum can be determined from the data. The considerable scatter among the data points for various stations presumably arises from atmospheric effects, since the data available from only half of the stations included in Figure 5 could be corrected by the application of two pressure coefficients. Furthermore, appreciable fluctuations are attributable to pre-event variations in the galactic flux (see Figure 1) which affect the base level from which intensity increases were reckoned. In view of these uncertainties, the data plotted in Figure 5 are consistent with a knee location near 1.1 GV. The spectral index in the power-law representation of the spectrum determined from the observations at stations characterized by threshold rigidity > 1.4 GV and particle intensity > 1% is $\gamma = 5.7 \pm 0.6$.

4. Conclusion

Since this is the first back-side event which is characterized by an appreciable anisotropy persisting for more than 3 hours, further intensive study of the propagation mechanism is required. It has recently been shown that during anisotropic events ascribed to a source on the visible disk, the arrival of solar particles is not simultaneous on a global scale [Duggal and Pomerantz, 1971; Duggal et al., 1971]. However, during the September, 1971 event, in spite of the anisotropy, there was no difference in the times of the onset of particle arrival in the northern and southern hemispheres.

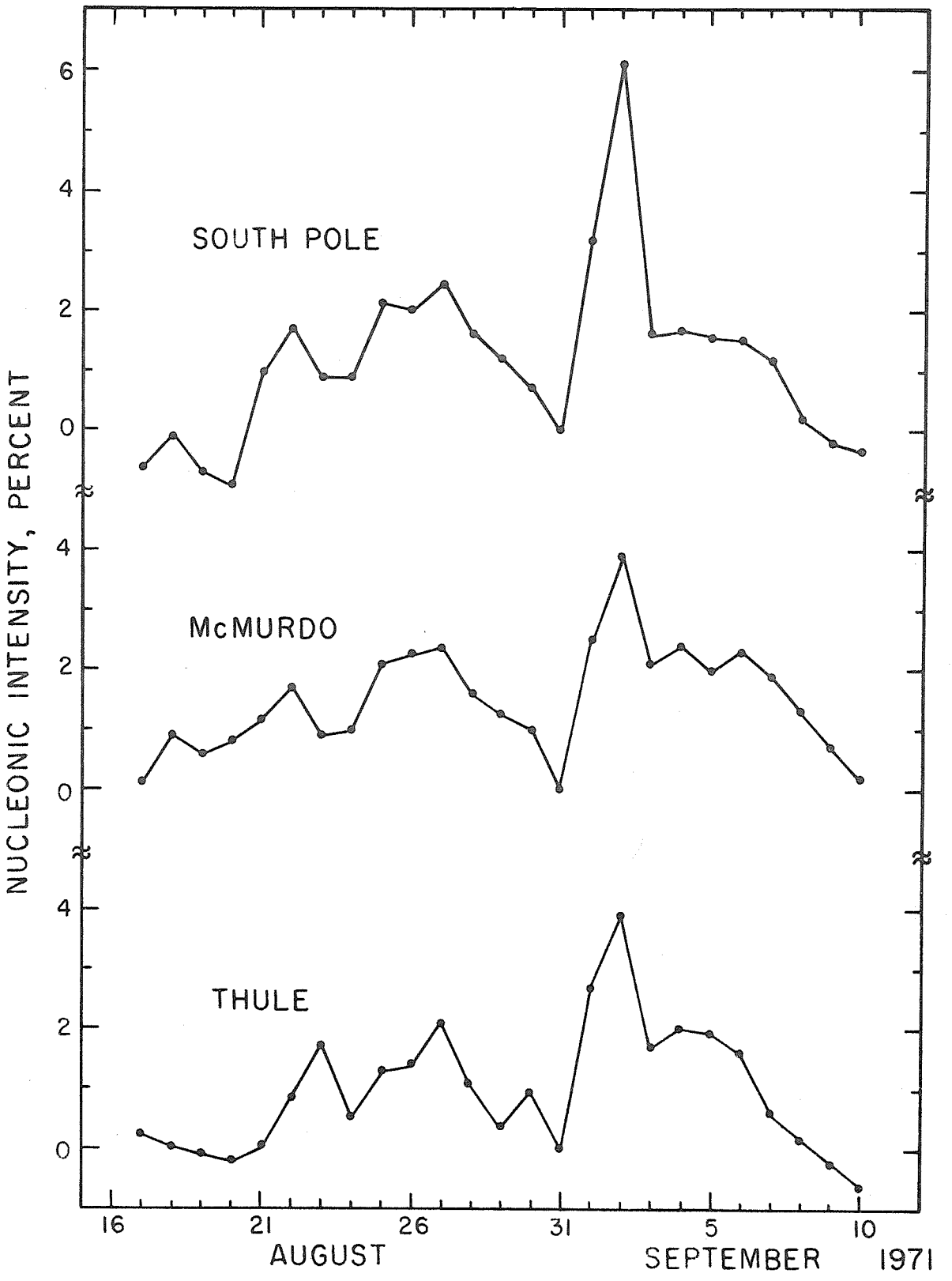

Fig. 1. Nucleonic intensity, expressed as percent of the pre-event level, at polar stations around the epoch of the September, 1971 ground level event (GLE).

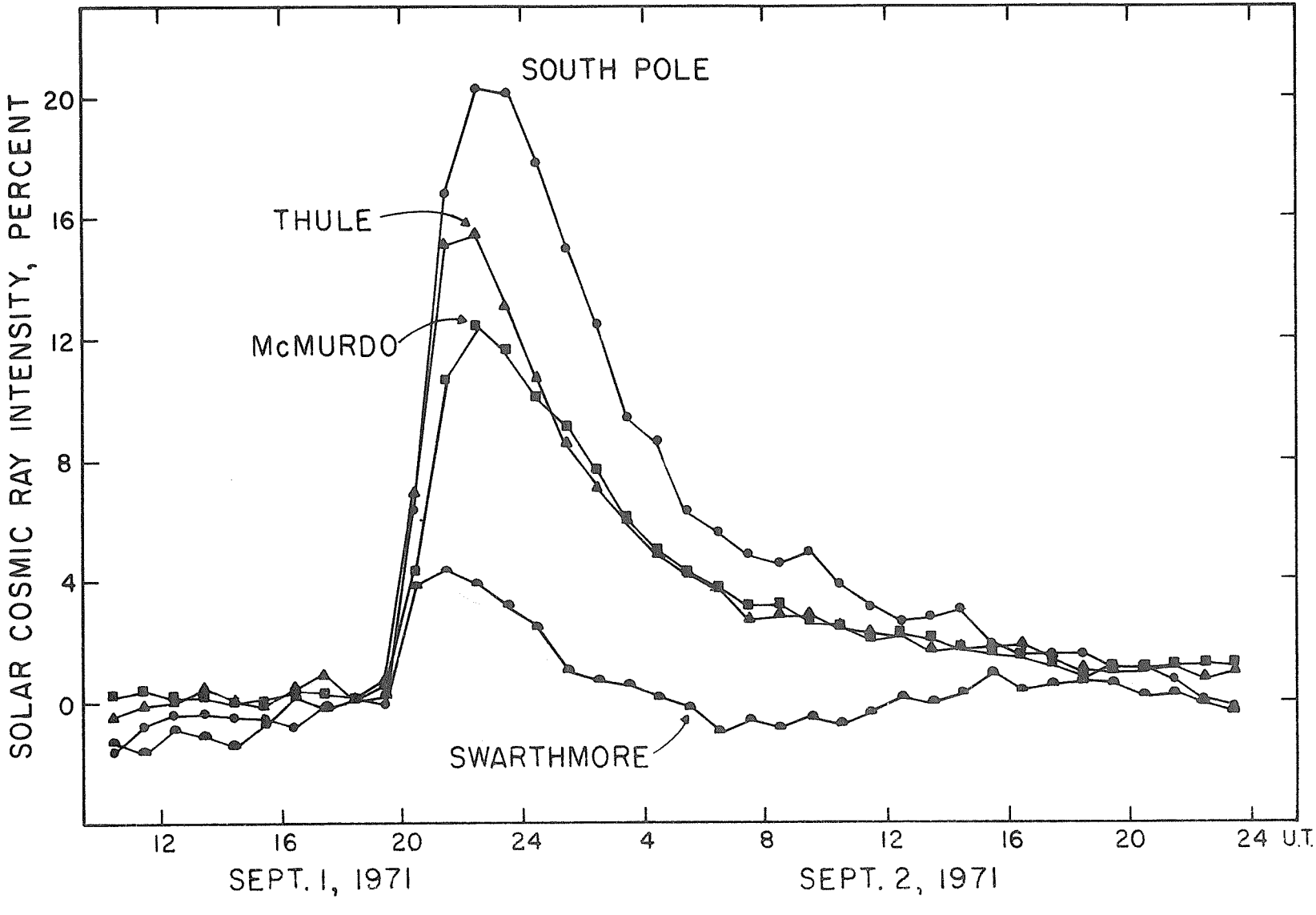

Fig. 2. The September 1-2, 1971 GLE neutron monitor observations at Bartol stations.

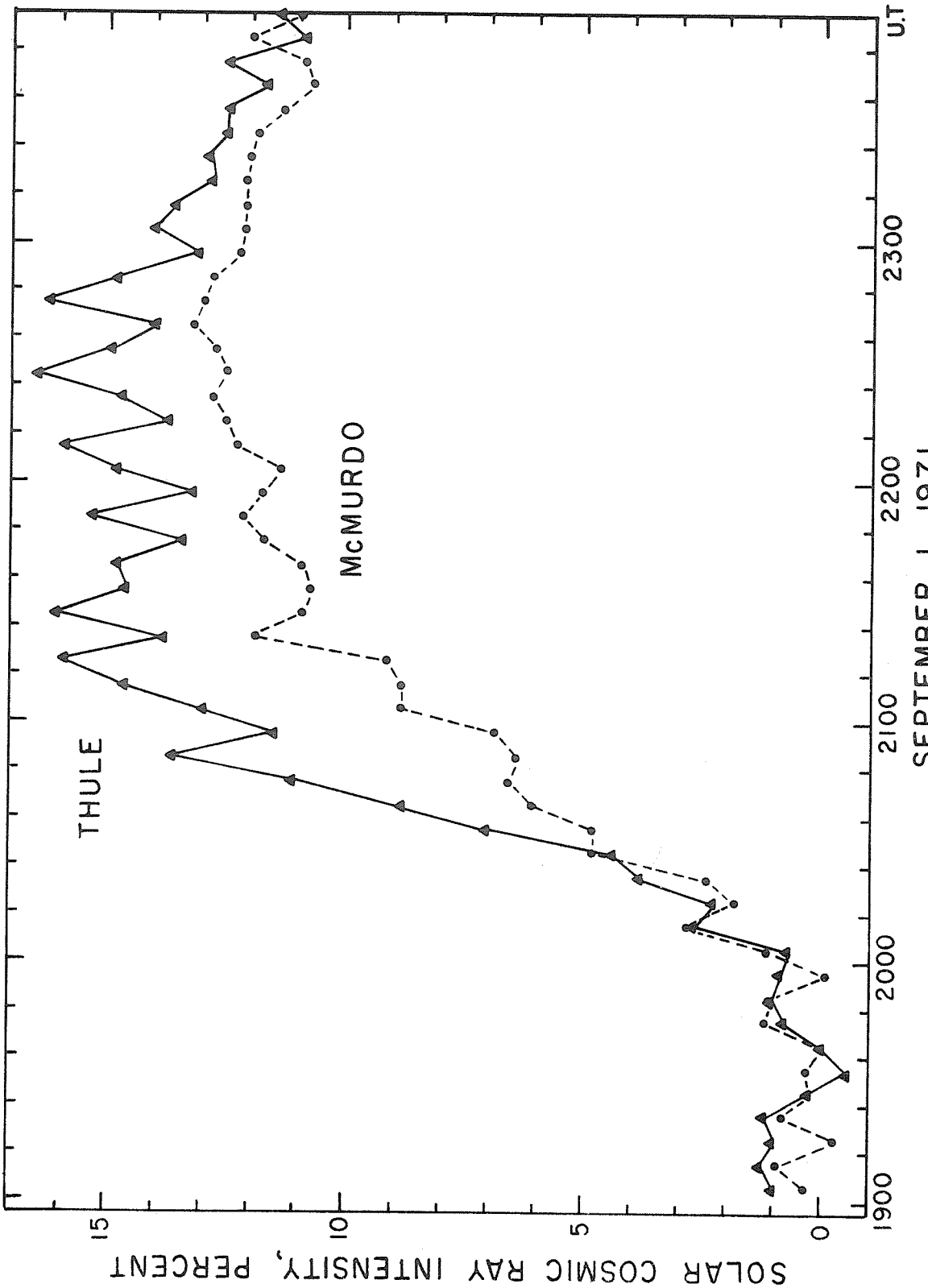

Fig. 3. Plot on an expanded time scale of the solar cosmic ray intensity at north (Thule) and south (McMurdo) polar stations.

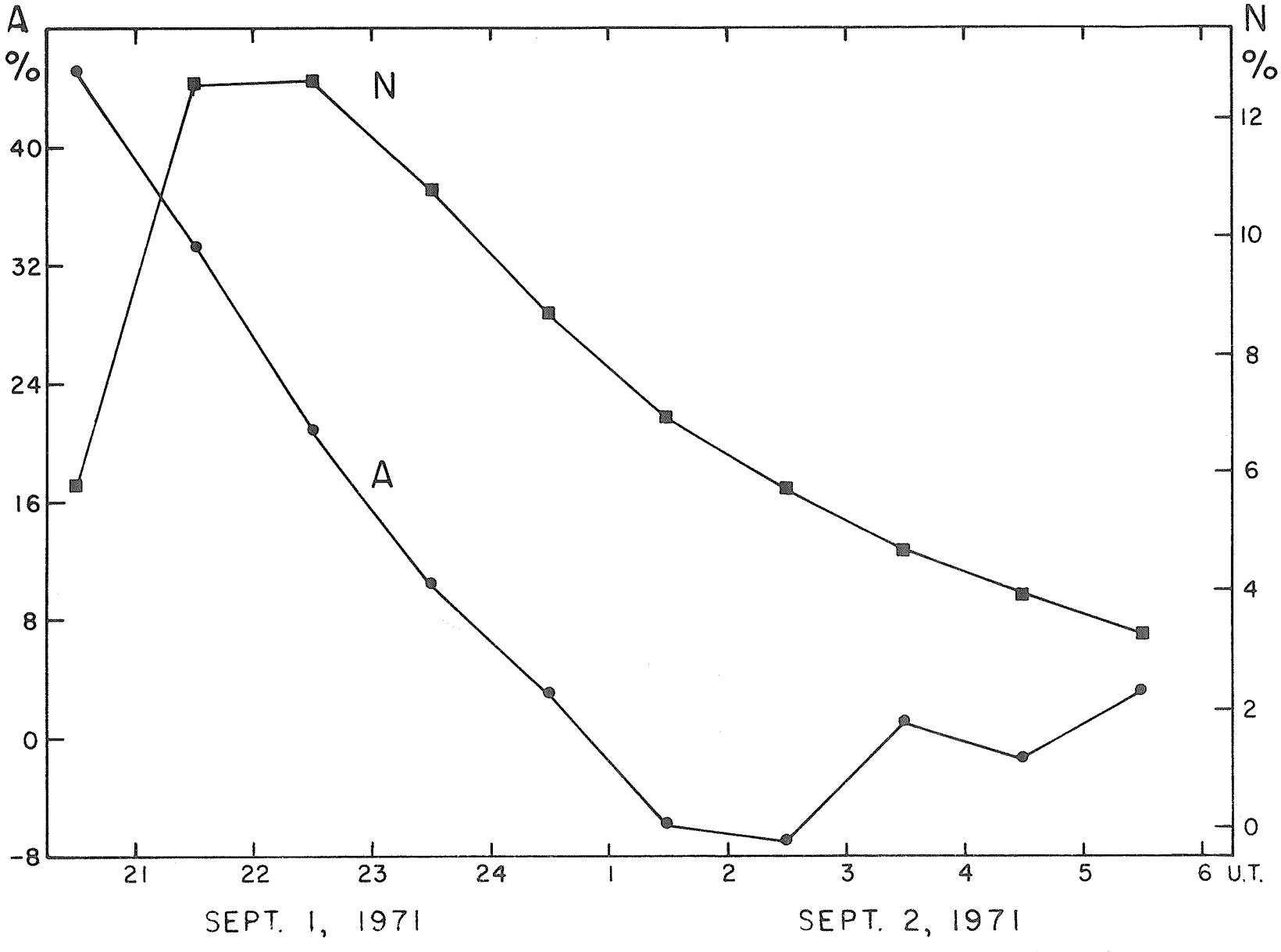

Fig. 4. The asymmetry, A, and the nucleonic intensity enhancement, N, in the northern polar region during the September, 1971 GLE.

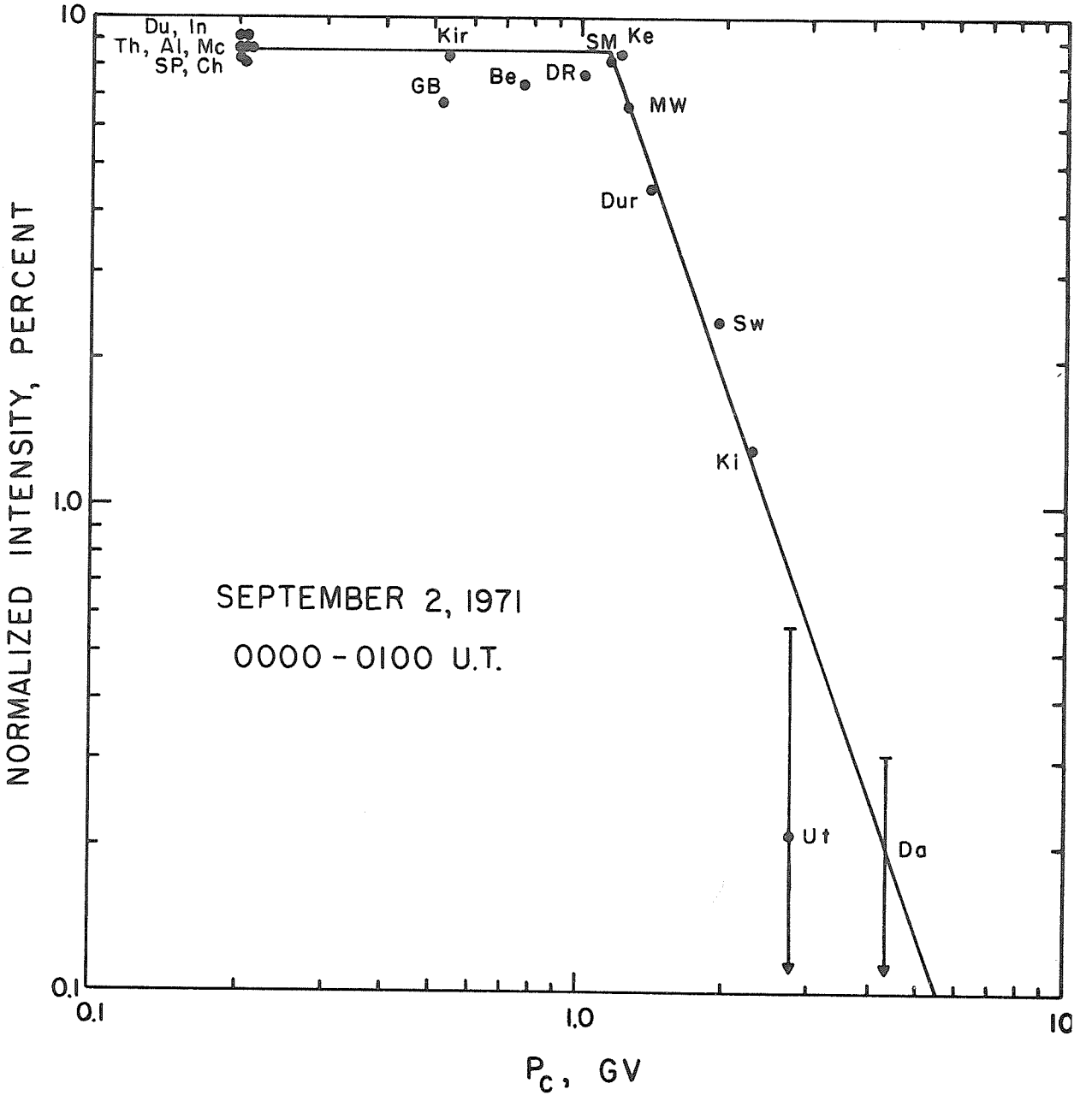

Fig. 5. Log-log plot of neutron monitor data recorded at a number of stations, and normalized to a standard atmospheric pressure, during the isotropic phase on September 2, 1971.

REFERENCES

BAIRD, G. A., G. G. BELL, S. P. DUGGAL, and M. A. POMERANTZ, 1967, Solar Phys., 2, 491.

DUGGAL, S. P., I. GUIDI, and M. A. POMERANTZ, 1971, Solar Phys., 19, 234.

DUGGAL, S. P., and M. A. POMERANTZ, 1971, Proc. Int. Conf. Cosmic Rays, 12th, 2, 533.

The Flare of Cosmic Rays on September 1, 1971

by

N. P. Chirkov, A. M. Novikov, G. V. Skripin, G. G. Todikov, A. T. Filippov
Institute of Cosmophysical Research and Aeronomy, Yakutsk Branch,
Siberian Department of the Academy of Sciences of the USSR, Yakutsk, USSR

Late on September 1, 1971 the Siberian net of stations observed the flare of solar cosmic rays. In the Table below geographical coordinates, threshold rigidities of stations [Shea et al., 1968], and amplitudes of the flare are listed. Stations were equipped with Superneutron Monitors.

Table 1

Number	Station	P(GV)	Geographical		Amplitude (per cent)	
			Latitude	Longitude		
1	Tixie Bay	0.52	71.5°N	128.9°E	12.1	12.3
2	Norilsk	0.60	69.3	88.1	-	11.4
3	Yakutsk	1.85	62.0	129.7	6.6	6.3
4	Magadan	2.16	60.1	151.0	4.0	3.7
5	Irkutsk	3.74	52.4	104.0	1.1	0.7
6	Habarovsk	5.55	48.5	135.2	-	0.4

5-, 15-minute, and hourly values of cosmic ray intensity during the flare are given in Figure 1. The statistical errors are indicated. From Figure 1 it is seen that the flare of cosmic rays started at 2010 UT, September 1, and reached its maximum at 2140-2200 UT, i.e., in 90-110 minutes.

In Figure 2 experimental and estimated according to Krymsky [1969] intensity values at various values of α in the equation

$$n(t) = B\tau^{\frac{3}{2-\alpha}} e^{-(1/\tau)}$$

are presented, where τ is a non-dimensional time. From Figure 2 it is evident that one can observe the best agreement between the theory and the experiment if $\alpha = 0$, and if we assume that particle emission on the Sun began at 1915 UT, i.e. 55 minutes earlier than the commencement of cosmic ray intensity increase observed on the Earth.

Knowledge of the emission commencement enables us to determine a path length L and a diffusion coefficient D for the present flare:

$$L = \frac{R_{\odot}^2}{(2-\alpha)ct_{max}} = 4\cdot10^{11} \text{ cm}; \quad D = \frac{Lc}{3} = 4\cdot10^{21} \text{ cm}^2/\text{sec}$$

where $R_{\odot}$ is a distance from the Sun to the Earth.

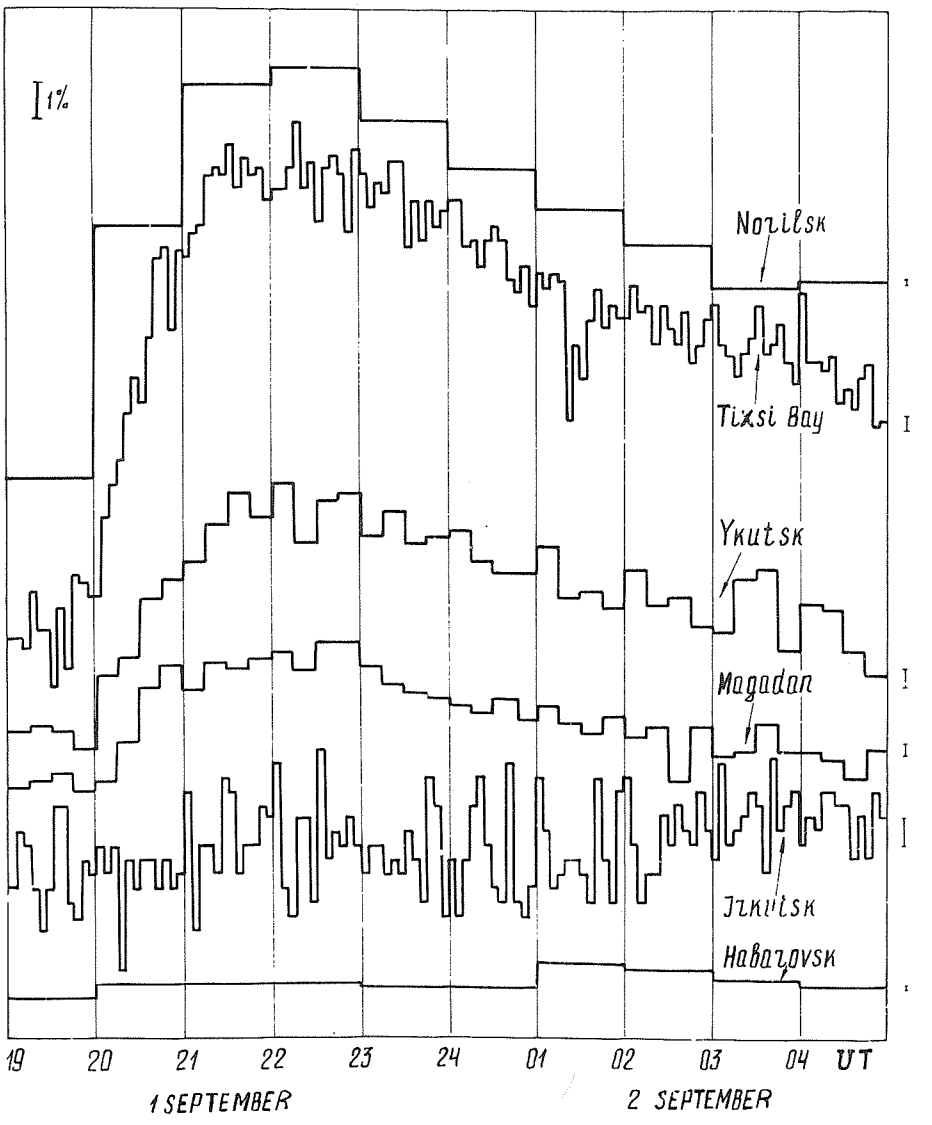

Fig. 1. Variations of cosmic ray intensity for the period 1900 UT September 1 - 0500 UT September 2, 1971 at stations Norilsk, Tixie Bay, Yakutsk, Irkutsk, Magadan and Habarovsk.

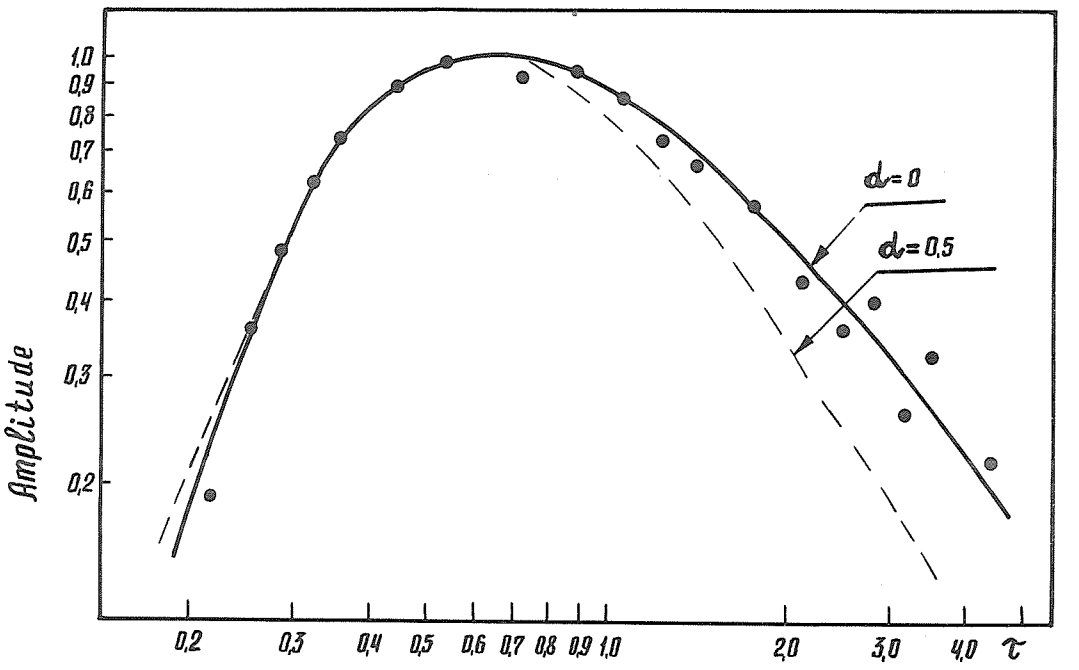

Fig. 2. Estimated values of cosmic ray intensities (curves) for α = 0 and 0.5, and experimental values (points) depending on time. Maximum amplitudes are normalized to 1.0.

In Figure 3 a latitudinal dependence of the flare amplitude is given. Points are amplitudes based on 15-minute values for 2245 - 2300 UT (amplitudes are presented in the Table in the next to the last column). Circles are amplitudes based on hourly values for 2300 UT September 1 (tne last column in the Table).

It is evident from Figure 3 that a latitudinal dependence of amplitudes is very well described by the expression

$$A(P) \sim P^{-\gamma}, \text{ where } \gamma = 2.6 \pm 0.1.$$

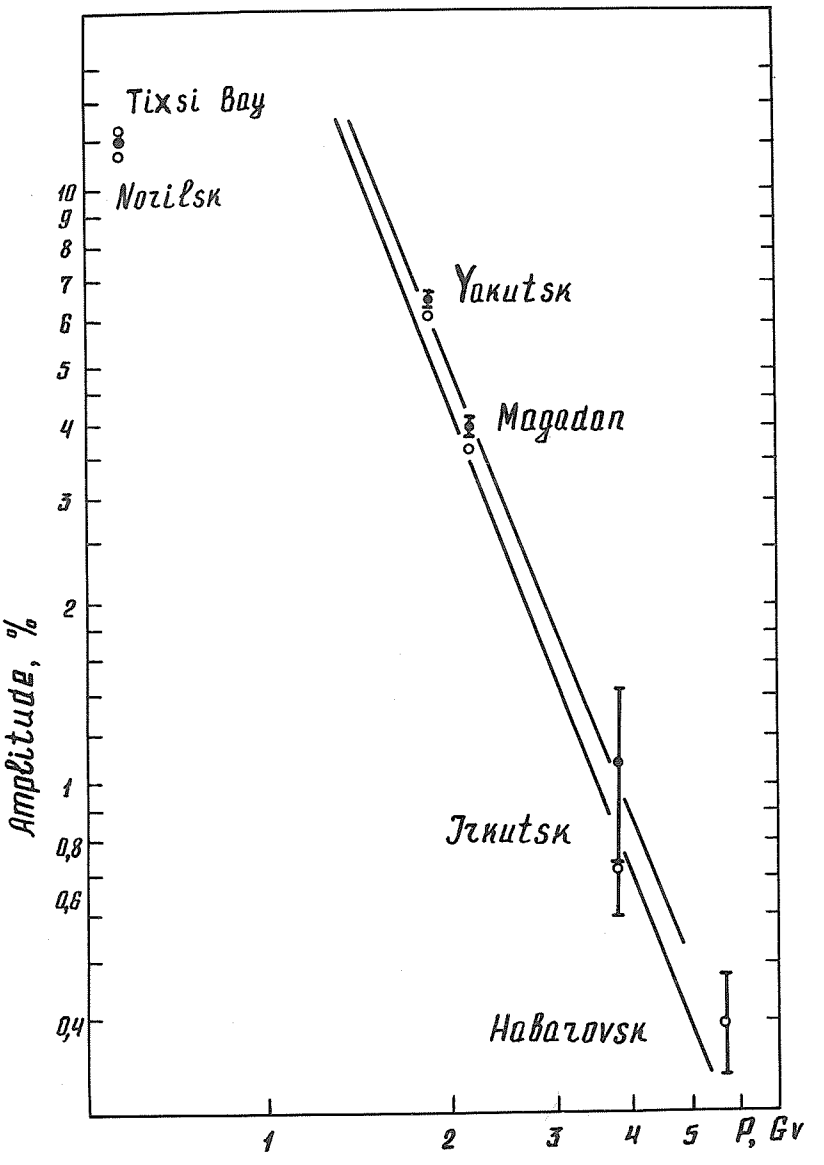

Fig. 3. Dependence of the flare amplitude on threshold rigidity. Points are amplitudes based on 15-minute data, circles are amplitudes based on hourly data.

REFERENCES

KRYMSKY, G. F. 1969 Modulyatsia kosmicheskikh luchei v mezhplanetnom prostranstve, Izd. "Nauka", Moscow.

SHEA, M. A., D. F. SMART, and J. R. MC CALL 1968 A Five Degree by Fifteen Degree World Grid of Trajectory-Determined Vertical Cutoff Rigidities, Canadian J. of Physics, 46, 10, 4, S1098-1103.

The Ground Level Cosmic Ray Increase of September 1, 1971 Recorded by the Neutron Monitor in Bergen, Norway

by

R. Amundsen and H. Trefall
Department of Physics
University of Bergen, Norway

The Bergen neutron monitor data for the September 1, 1971 event is presented in Figure 1. The graph presents hourly values and is plotted as a percentage of the pre-event average count-rate. The data are pressure corrected to 990 mb (coefficient 0.74%/mb) and represent the mean of two sections. The 100% level is at 8370 counts per hour for the September event. The standard deviation is shown on the graph.

The neutron monitor station in Bergen is at sea level, and the geographical position is 60°24'N latitude and 5°24'E longitude. The cut-off rigidity is 1.2 GV.

For the September event, the maximum count-rate occurs in the interval 2200-2300 UT September 1, and the increase amounts to 13.2%. The September event has a markedly slower increase and decay rate than the January event.

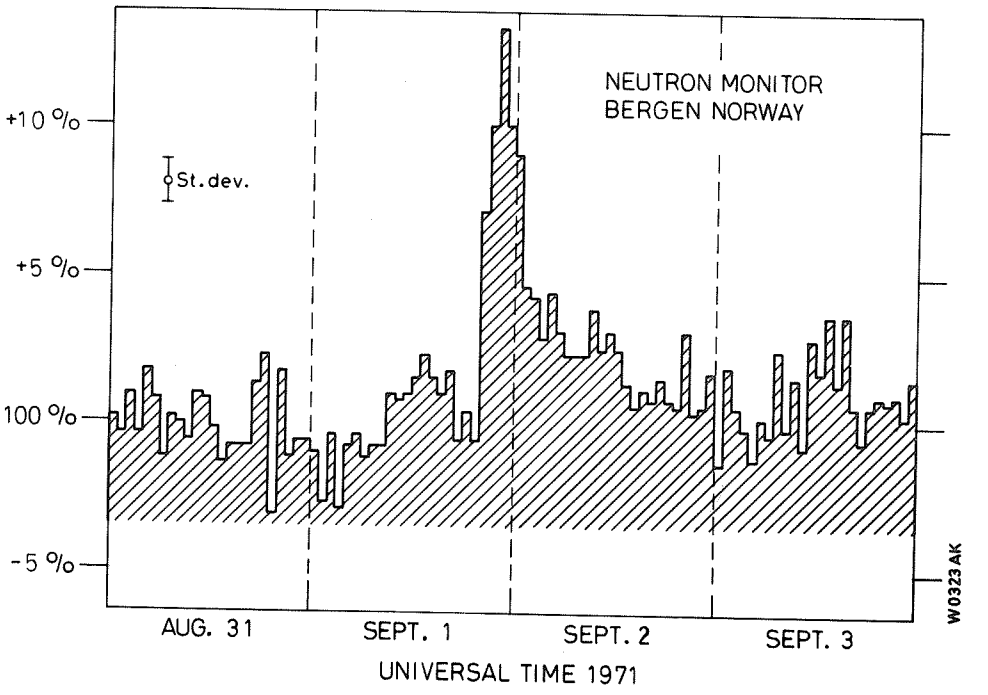

Fig. 1. Bergen neutron monitor data for the September 1, 1971 event.

"Scintillation Monitor, Bologna, Italy. 15-Minute Observations"

by

M. Galli, L. Fiandri
Istituto di Fisica "A. Righi"
Università degli Studi di Bologna

M.R. Attolini
Laboratori T.E.S.R.E.
Consiglio Nazionale delle Ricerche, Bologna

Figure 1 presents for August 28 to September 4, 1971 the total ionization (T), the atmospheric pressure at ground level (P), and the hard components: 45° inclined towards West (W), 45° inclined towards East (E) and vertical cubical coincidences (V).

Table 1 presents the data from the scintillation monitor at Bologna. The tabulated data should be read with a decimal point after the second figure of each number. The numbers are deviations in % units from a fixed value of pressure corrected data at the end of each 15-minute interval.

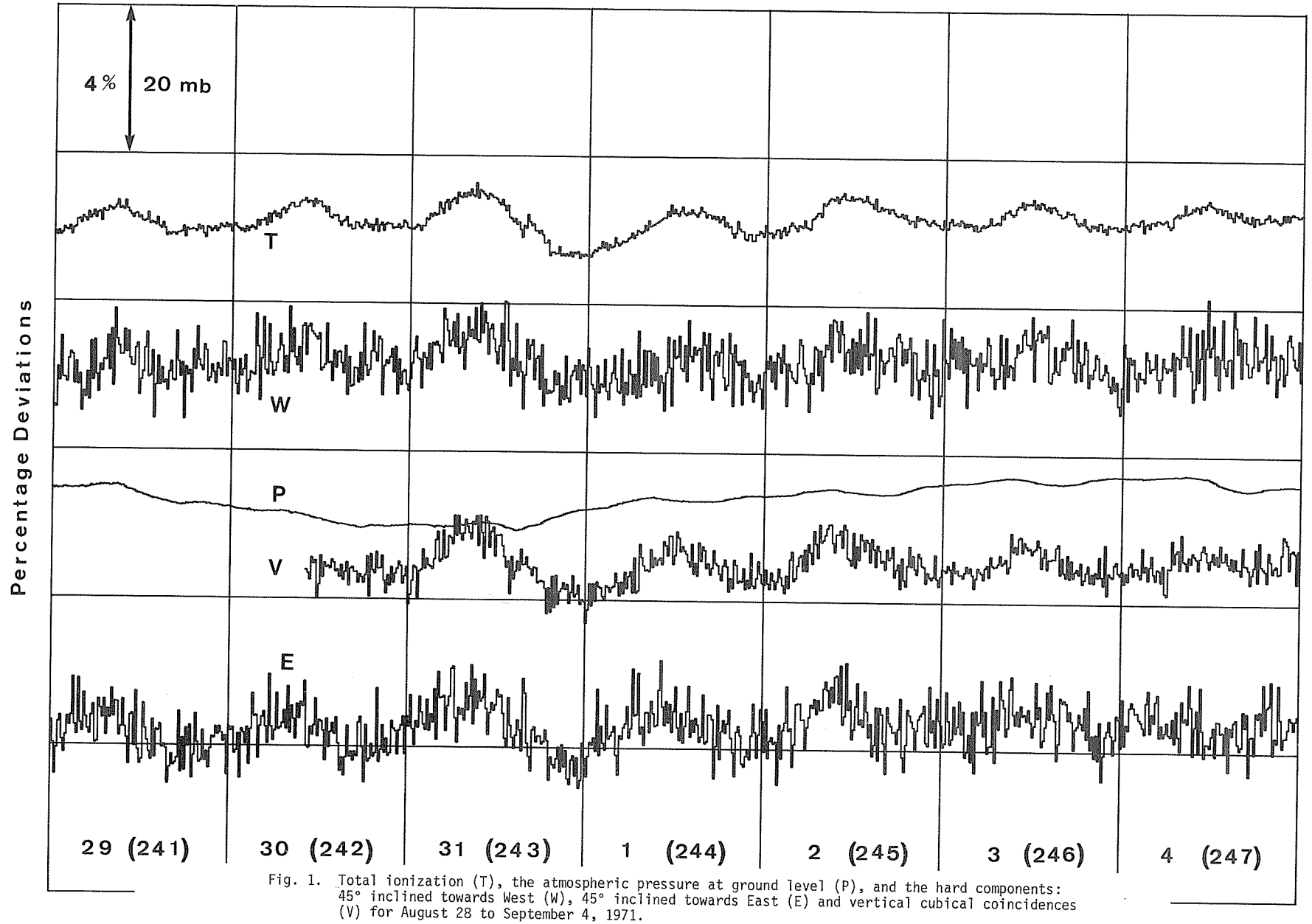

Fig. 1. Total ionization (T), the atmospheric pressure at ground level (P), and the hard components: 45° inclined towards West (W), 45° inclined towards East (E) and vertical cubical coincidences (V) for August 28 to September 4, 1971.

Table 1.

15-MINUTE COSMIC RAY DATA AT BOLOGNA DURING SEPTEMBER 1,2 1971

Scintillation Meniter for Cosmic Rays
Location Bologna 44.5 N 11.35 E 50 m a.s.l.
Tabulated Deviations in percent units from a fixed value of pressure corrected totals, at the end of each interval

* Total Ionizing Component counts under 5 gr/sqcm * S.D. 0.08%

* Coincidence counts 45 degrees inclined towards West filtered by 10 cm of lead * S.D. 0.54%

* Vertical Cubical coincidence counts filtered by 10 cm of lead * S.D. 0.30%

* Coincidence counts 45 degrees inclined towards East filtered by 10 cm of lead * S.D. 0.54%

Bar. coeff. 0.20 percent/mb
September 1,2 1971

	Minutes at End of Interval																			
U.T. hours	15	30	45	60	Mean	15	30	45	60	Mean	15	30	45	60	Mean	15	30	45	60	Mean
1200-1300	4.43	4.55	4.67	4.49	4.54	4.63	5.18	4.31	4.24	4.59	4.25	4.89	4.72	4.35	4.55	4.03	4.70	3.59	3.25	3.89
1300-1400	4.45	4.53	4.48	4.60	4.51	4.93	3.96	5.61	4.64	4.79	4.49	4.37	4.29	4.08	4.31	3.98	3.18	3.63	4.03	3.71
1400-1500	4.51	4.47	4.40	4.51	4.47	4.50	4.89	4.68	4.81	4.72	3.95	4.56	3.75	4.04	4.07	4.72	3.34	3.80	3.48	3.83
1500-1600	4.67	4.56	4.54	4.39	4.54	4.86	3.73	5.29	4.95	4.71	3.70	4.60	4.10	4.49	4.22	3.85	3.67	3.21	3.35	3.52
1600-1700	4.47	4.46	4.37	4.43	4.43	4.25	5.26	4.04	3.47	4.25	4.39	3.90	4.03	3.73	4.01	4.49	3.17	3.22	3.95	3.71
1700-1800	4.34	4.42	4.26	4.34	4.34	4.68	4.78	4.39	4.75	4.65	3.91	4.39	4.04	3.99	4.08	3.94	3.82	2.22	3.10	3.27
1800-1900	4.42	4.15	4.26	4.13	4.24	5.11	4.07	3.74	3.86	4.19	3.76	3.58	3.97	4.14	3.86	4.21	2.75	3.50	3.80	3.56
1900-2000	4.15	3.96	3.85	3.97	3.98	5.27	4.72	3.30	4.96	4.56	3.95	3.28	3.63	3.37	3.56	3.46	3.71	4.08	3.32	3.64
2000-2100	4.29	4.08	4.02	4.02	4.10	4.50	4.42	4.52	3.35	4.20	4.14	4.00	3.52	3.57	3.81	2.93	2.29	3.49	3.64	3.09
2100-2200	3.81	3.78	3.94	3.94	3.87	4.55	4.09	4.20	3.72	4.14	3.55	3.91	3.35	3.60	3.60	3.39	2.63	2.55	2.83	2.85
2200-2300	3.76	3.76	3.93	3.93	3.85	3.99	3.43	3.69	3.94	3.76	3.38	4.33	3.44	3.38	3.63	3.02	2.75	3.39	4.25	3.35
2300-2400	4.03	3.98	3.88	4.19	4.02	4.16	3.78	3.24	4.23	3.85	3.64	4.10	3.76	3.52	3.75	3.48	2.80	3.42	4.11	3.45
0000-0100	4.00	3.97	3.99	3.85	3.95	4.53	4.32	4.67	3.98	4.38	3.46	3.38	3.50	3.36	3.55	3.78	2.96	4.11	2.79	3.41
0100-0200	3.95	4.07	4.08	3.85	3.99	4.51	3.78	4.75	4.63	4.42	3.80	3.59	3.36	3.56	3.58	3.25	3.35	3.18	3.23	3.25
0200-0300	4.04	4.14	3.93	4.03	4.04	4.22	4.97	4.46	4.32	4.24	3.91	3.67	3.46	3.25	3.57	2.07	3.69	2.78	3.55	3.02
0300-0400	4.18	4.27	4.19	4.13	4.19	4.46	4.26	4.08	4.01	4.20	3.72	3.39	4.16	4.37	3.91	3.75	4.73	3.53	3.60	3.90
0400-0500	4.04	4.20	4.17	4.13	4.14	3.94	4.48	5.12	4.96	4.63	3.58	3.65	3.99	4.23	3.86	2.56	3.17	4.25	4.27	3.56
0500-0600	4.33	4.14	4.12	4.08	4.17	4.35	4.15	3.94	3.17	3.90	4.28	3.86	4.43	3.85	4.10	4.27	3.83	3.84	3.02	3.74
0600-0700	4.36	4.39	4.45	4.53	4.43	4.22	3.92	4.93	4.86	4.48	4.58	4.35	4.05	4.94	4.48	3.63	3.90	4.24	4.16	3.98
0700-0800	4.54	4.43	4.80	4.73	4.63	4.16	4.82	3.75	4.67	4.35	4.59	4.21	5.11	4.63	4.63	4.39	3.99	4.37	4.10	4.21
0800-0900	4.79	4.88	4.94	4.92	4.88	4.98	4.87	5.53	4.53	4.98	4.69	4.83	5.01	5.11	4.91	4.10	4.68	4.87	4.64	4.57
0900-1000	4.88	4.98	4.91	4.93	4.90	5.66	5.61	5.35	4.79	5.35	5.12	4.62	4.37	4.85	4.74	4.18	4.73	4.32	5.00	4.56
1000-1100	5.00	5.08	4.91	4.90	4.97	5.63	5.27	4.29	4.79	5.00	4.85	4.96	4.50	5.12	4.86	5.03	4.28	5.31	3.72	4.58
1100-1200	4.89	5.00	4.88	4.94	4.93	4.87	4.22	5.16	4.24	4.62	4.99	4.21	4.17	4.02	4.35	3.94	5.38	4.12	4.38	4.46

6. IONOSPHERE

The September 1971 Solar Cosmic Ray Event

by

A. J. Masley
Space Sciences Department
McDonnell Douglas Astronautics Company
Huntington Beach, California

Introduction

The McDonnell Douglas Polar Observatories are located at McMurdo Sound, Antarctica (77°51'S, 166°43'E) and at magnetically conjugate Shepherd Bay, N. W. T., Canada (68°49'N, 93°26'W). These stations, at a geomagnetic latitude of 80°, are located inside the polar cap regions, removed poleward from the auroral zones to minimize auroral interference.

Radio techniques are used which allow effects taking place at altitudes from 30 to 90 kilometers to be observed with ground-based equipment. Riometers are operated which measure the signal strength of galactic radio noise at 30 and 50 MHz. The ionization produced by the interaction of the charged particles with the atmosphere increases the electron density so that radio waves passing through the ionosphere are significantly absorbed. The absorption of the radio waves at a given frequency is proportional to the square root of the intensity of charged particles. This technique is sensitive to protons from about 5 to 100 Mev. Other equipment operating at the stations includes magnetometers and photometers at 3914 Å and 5577 Å.

1 September 1971 Event

At 1935 UT September 1 a 10 minute radio noise burst was seen on the riometers in both polar regions. Absorption began on the McMurdo 30 MHz riometer at 2040 UT September 1, during sunlight hours (see Figure 1). The arrows in Figure 1 show the 30 km sunrise and sunset for each station. Maximum 30 MHz absorption at McMurdo was 3.4 dB at 0300 UT September 2 during daylight. The maximum at Shepherd Bay was 4.2 dB at 1400 UT September 2 during daylight. The actual peak intensity of the event may have occurred between these times while both stations were in darkness. The absorption level decreased to about 2 dB at 1500 UT September 4 at Shepherd Bay. There was a small decrease in absorption at both stations after the sudden commencement at 1646 UT September 4. The absorption remained near 1.5 dB for several days at Shepherd Bay until September 7. The absorption at Shepherd Bay was about 1 dB larger than at McMurdo Sound during most of the event, the difference increasing in the final days. If this difference is not due to ionospheric effects it suggests a 200% to 400% North-South asymmetry. During the 2 September 1966 event under similar sunlight conditions the absorption was nearly identical over both polar regions [Masley and Goedeke, 1968].

Acknowledgement

This work was supported by the Polar Programs Office of the National Science Foundation under Contract NSF-C393 and the McDonnell Douglas Independent Research and Development Program.

REFERENCE

MASLEY, A. J. and A. D. GOEDEKE — 1968 — The 1966-1967 Increase in Solar Cosmic Ray Activity, Canadian Journal of Physics, 46, S766-S771.

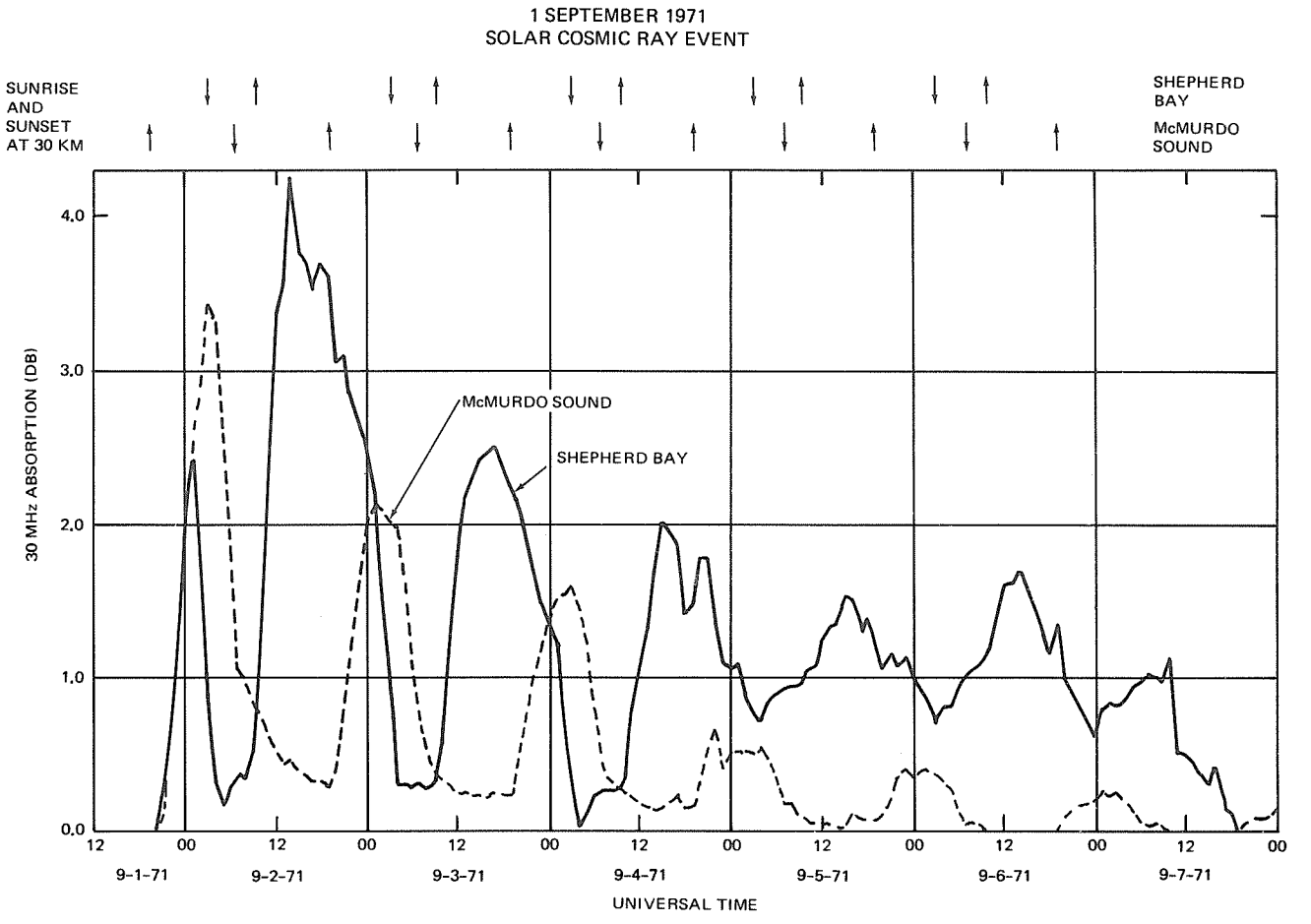

Fig. 1. 30 MHz riometer absorption data for Shepherd Bay and McMurdo Sound, September 1-7, 1971.

30 MHz RIOMETER DATA FOR SEPTEMBER 1971 SOLAR PARTICLE EVENT

RAYMOND J. CORMIER
IONOSPHERIC RADIO PHYSICS BRANCH
IONOSPHERIC PHYSICS LABORATORY
AIR FORCE CAMBRIDGE RESEARCH LABORATORIES
BEDFORD, MASS. 01730

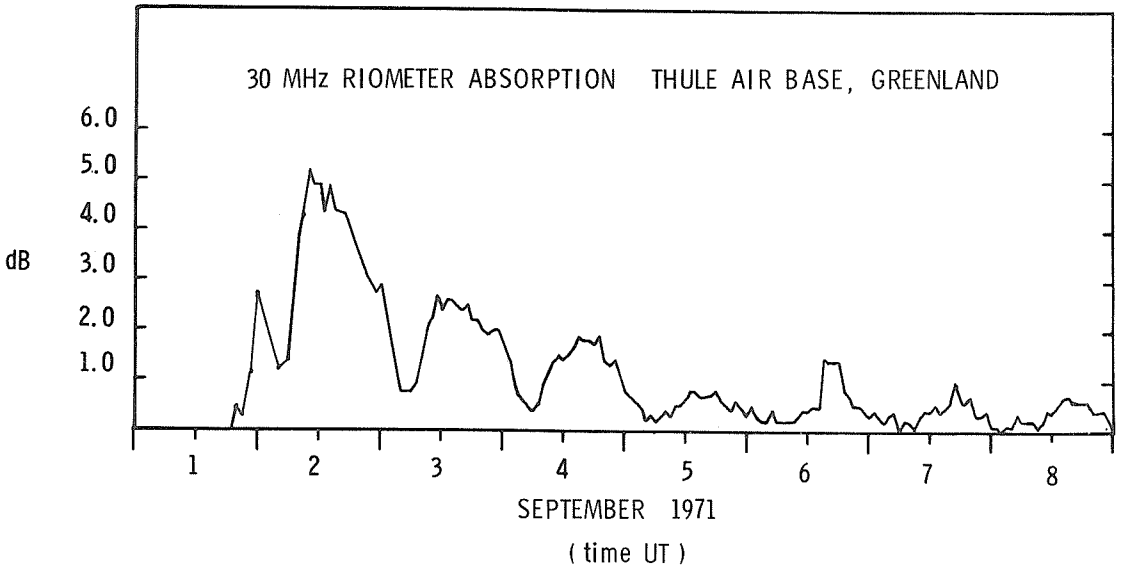

AFCRL Geopole Observatory 30 MHz Riometer Data
for September 1971 Solar Particle Event

Cormier, R. J. 1971 Geophysics & Space Data Bulletin
Vol. VIII; No. 4
AFCRL Bedford, Mass. 01730

Polar Cap Absorption of September 1, 1971 by Riometer Data in the Arctic and Antarctic

by

V. M. Driatsky and V. A. Ulyev
The Arctic and Antarctic Research Institute, Leningrad
USSR

The present study is concerned with one of the two strongest Polar Cap Absorption events recorded in 1971. PCA data were obtained by riometers installed at the Soviet Arctic and Antarctic stations. Table 1 presents the station list, their geographical positions, invariant latitudes and the Sun's altitudes.

Table 1

STATION LIST

	Station Name	Geographic Positions		Φ'	Sun's Altitude 3 September 1971		Notes
		Latitude	Longitude		Noon	Midnight	
1	North Pole 19	83°17'N	142°48'E	76,0°N	+14°25'	+ 0°59'	Positions for Sept. 3, 1971
2	Dixon Island	73 30	80 14	67,2	+24 12	- 8 48	
3	Salekhard	66 32	66 32	61,0	+31 6	-15 42	
4	Vostok Station	78°27'S	106 52	84.3°S	+ 3 50	-19 14	Data received by radio
5	Mirny	66 33	92 01	76,8	+15 45	-31 9	" "
6	Molodezhnaya	67 10	45 51	67,6	+15 8	-30 32	" "

Notes: Riometer frequencies: Vostok Station - 30 and 50 MHz; Mirny - 31.8 and 40 MHz; other stations had riometers at 32 MHz.

Antennas at Vostok station are co-phasal, directed to zenith; at other stations antennas are of Yagi, directed to North Pole.

PCA Event 1-6 September 1971

This event was not associated with any particular solar flare, since no optical solar flare data were readily available. We can, however, assume that a solar flare occurred at about 2000 UT 1 September on the basis of the data of radio emission bursts [Solar-Geophysical Data, 1971]. Vela Satellite measurements show that the proton flux with energies Ep > 25 Mev reached its maximum value F = 3640 particles/cm^2/sec at 0400 UT on the following day [Solar-Geophysical Data, 1971].

Figure 1 shows PCA intensity variations with data from 6 stations, three being in the Arctic, the other three in the Antarctic. North Pole-19 data show the absorption onset at 2000 UT, reaching its maximum at about 0600-0800 UT 2 September. Almost simultaneously, PCA maxima occurred at all other stations.

This PCA event occurred close to the autumn equinox, thus the night-day effect was well-pronounced at all the stations except NP-19. The evaluation of the ratio of the daytime absorption to the nighttime absorption has shown that it always decreased during PCA, having different values at the various stations, on an average ranging from 4 to 7. At Salekhard the effect of the geomagnetic cutoff was well-pronounced, and the absorption intensity was an order of magnitude less compared to other stations. At NP-19, though at midnight the Sun's altitude was + 0°59', the day-night effect was not observed. The equilibrium conditions at this station occurred because of the polar day during the

Sun's lower altitudes. An sc magnetic disturbance occurred on 4 September at 1646 UT. However, no marked changes related to it were observed in the PCA event. No midday recovery for this PCA event was observed.

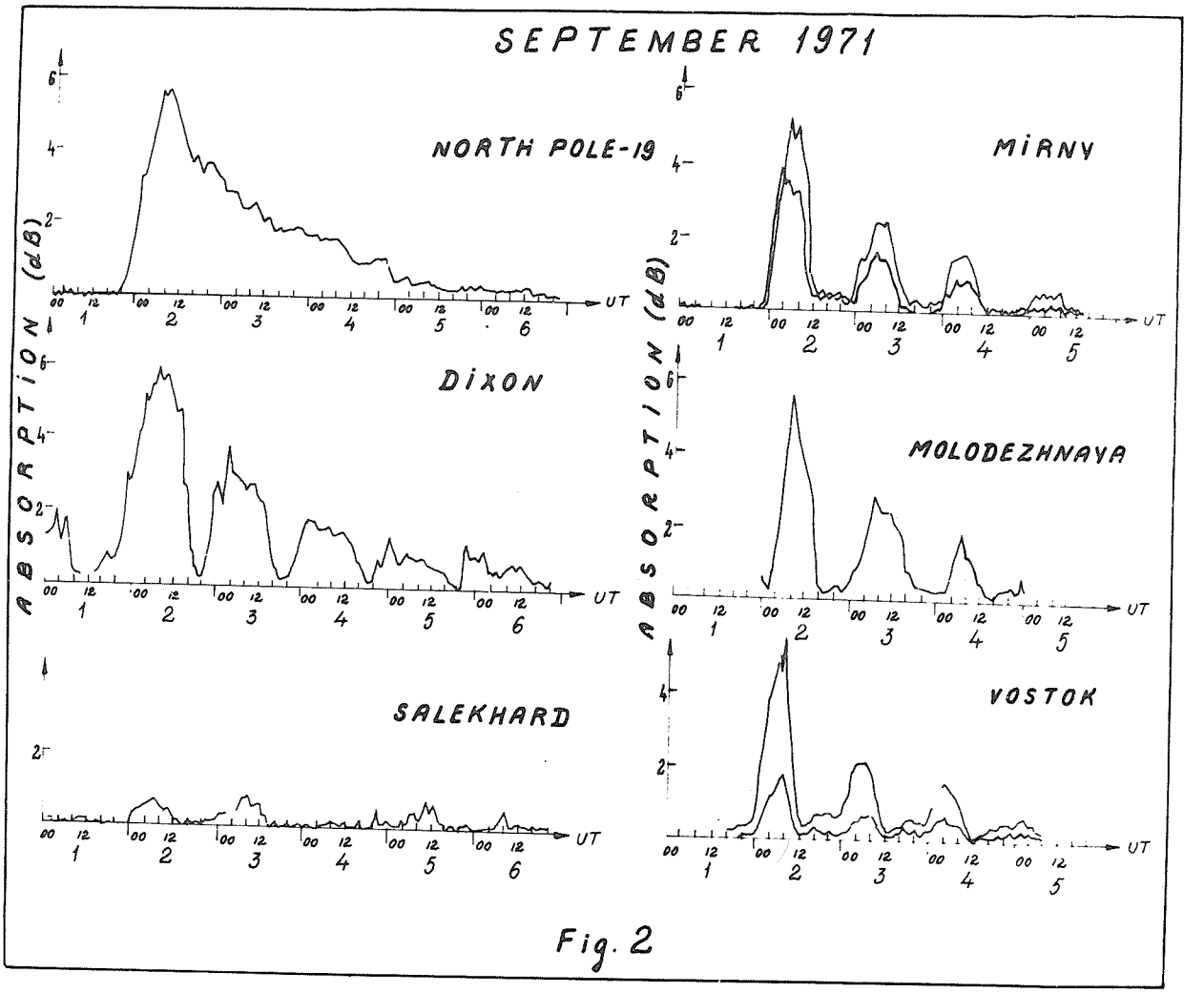

Fig. 1. Variations of PCA intensity over the period 1-6 September 1971.

REFERENCE

1971 Solar-Geophysical Data, 326 Part I, U.S. Department of Commerce, (Boulder, Colorado, U.S.A. 80302).

Ground Based Ionospheric Observations from the Danish Geophysical Observatories in Greenland during the September 1 Event 1971

by

J. Taagholt and V. Neble Jensen
Ionosphere Laboratory
Technical University of Denmark
DK-2800 Lyngby, Denmark

The ionosphere data published below are reduced data based on routine measurements made at the field sites:

Narssarssuaq	(geomagnetic coordinates:	Lat. N 71.4° Long. E 37.1°)
Godhavn	(geomagnetic coordinates:	Lat. N 80.0° Long. E 33.1°)
Thule	(geomagnetic coordinates:	Lat. N 89.1° Long. E 357.5°).

All three observatories, situated on the west coast of Greenland, are run by the Ionosphere Laboratory, a division of the Danish Meteorological Institute. The vertical sounder used at Narssarssuaq is a modified C-3/4, at Godhavn a J-5, and at Thule a C-4.

Additionally, Cosmic Noise Absorption (CNA) data obtained by means of IONLAB-Riometer at 30 MHz are shown from the same observatories as well as from Station Nord (geomagnetic coordinates: Lat. N 80.7° Long. E 134.5°), Sdr. Strømfjord (geomagnetic coordinates: Lat. N 77.6° Long. E 34.8°), and Godthaab (geomagnetic coordinates: N 75.0° Long. E 29.7°).

The three latter stations are operated for the Ionosphere Laboratory by the Greenland Technical Organization, Telesection.

September 1 Event

The riometer observations for September 1 (see Figure 1) at the four southern stations and especially at Narssarssuaq show normal auroral observation events varying between 0 and 3 dB absorption. Only at Thule and Station Nord is another feature seen starting about 2000 UT with a steadily increasing absorption.

The CNA data for September 2 show high absorption at all 6 stations, indicating a real polar cap absorption event. Station Nord due to the extremely high geographic latitude and the time of year shows no diurnal solar effect corresponding to 24 hours of sunlight in the lower ionosphere. From about 5 dB maximum absorption at about 0730 UT on September 2 the absorption decreases slowly during the following 3 days at Station Nord. The diurnal variation is more pronounced farther south. The rapid increase of absorption at the four West Greenlandic stations shows a latitude time dependence, with the earliest occurrence at Thule and a delay of about 3 minutes per degree towards the south.

Some HF propagation data for the period September 1 to September 7 (Figure 2) illustrate the HF communication problems caused by such an absorption event. At Reersø near Copenhagen (N 55.1° E 11.0°) WWV signals from Fort Collins, Colorado (N 40.68° E 254.97°) are recorded every second hour. Figure 2 shows the signal strength received at Reersø with the scale from 1 = barely audible, 2 = poor, 3 = fair, 4 = good, to 5 = excellent, placed according to the different receiving frequencies in the range from 2.5 - 25 MHz. Additionally, information about HF communication from Godthaab, Greenland (N 64.2°E 308.2°) to Reersø is presented as a full line for normal communication, as a thin line for reduced communication, and marked with B for "black out" periods. On Figure 2 the 30 MHz riometer data from Godthaab are also presented, showing pronounced correlation between the CNA data and the HF communication data.

On Fiqure 3 the propagation paths are shown: Fort Collins - Reersø about 7000 km and Godthaab - Reersø about 3500 km. The normal propagation Godthaab - Reersø is usually a one hop propagation via F-layer with the reflecting point situated in the auroral zone over Iceland. The transmitter is situated on a small island on the West Greenland shore and the radiation angle is as small as about 4°.

The riometer data shown, giving information about absorption in D-region vertically above the transmitting station, could thus not be expected to give valuable information about the Godthaab - Reersø communication. However, based upon data from Figure 1 and Figure 4a and b, it can be expected that the PCA covers the total polar cap. The signal from Godthaab (as well as Fort Collins) therefore will be absorbed when crossing the D-region near Greenland's east coast. This is in agreement with Rybner and Ungstrup [1957] as seen on Figure 5 showing the area with high absorption based upon data collected during the 1932-33 international polar year. During the summer the Ionosphere Laboratory will start operation of a 30 MHz riometer at Angmagsalik. This riometer should give information about absorption in the area where the propagation path Godthaab - Reersø crosses the D-region.

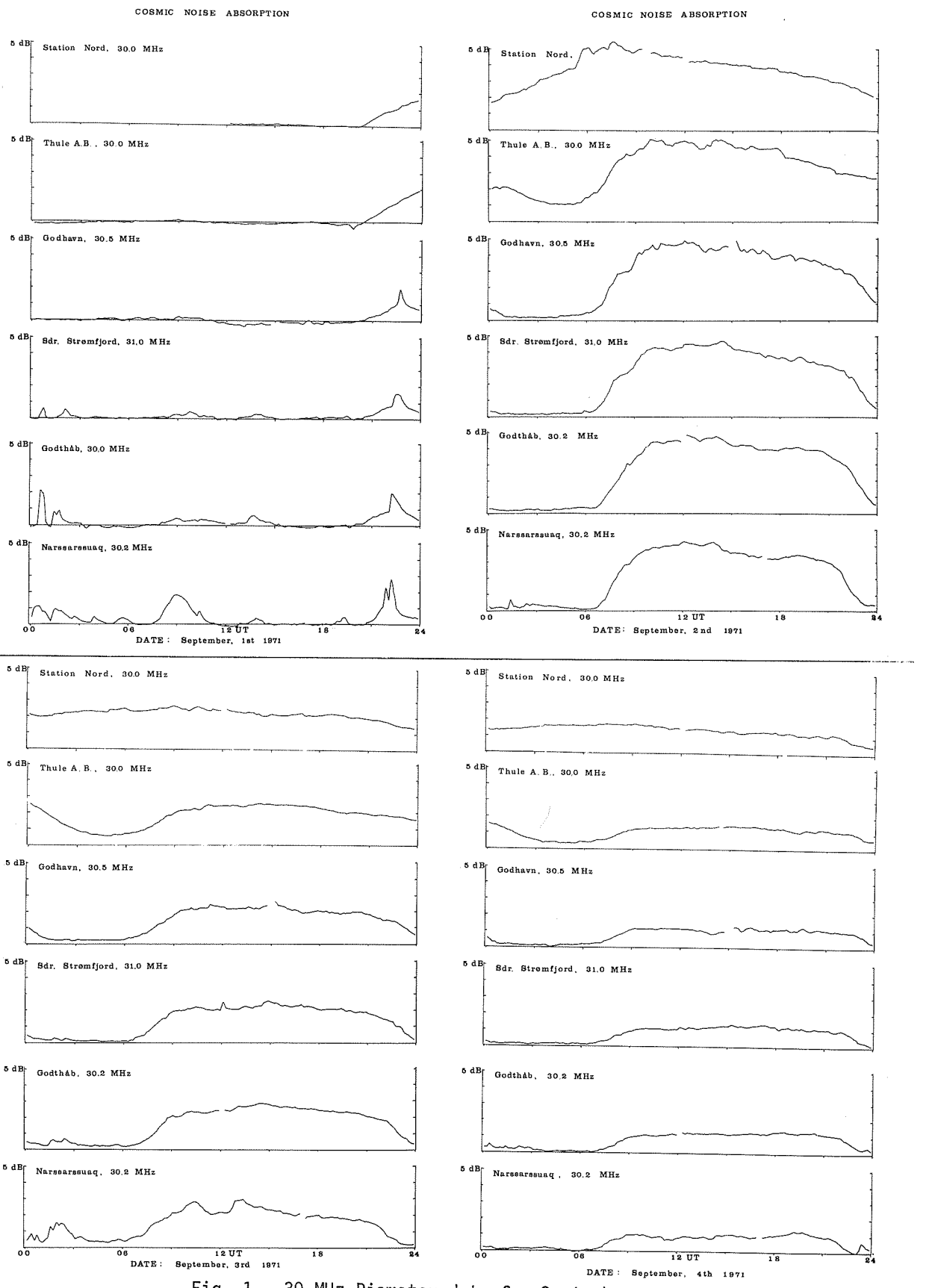

Fig. 1. 30 MHz Riometer data for September event.

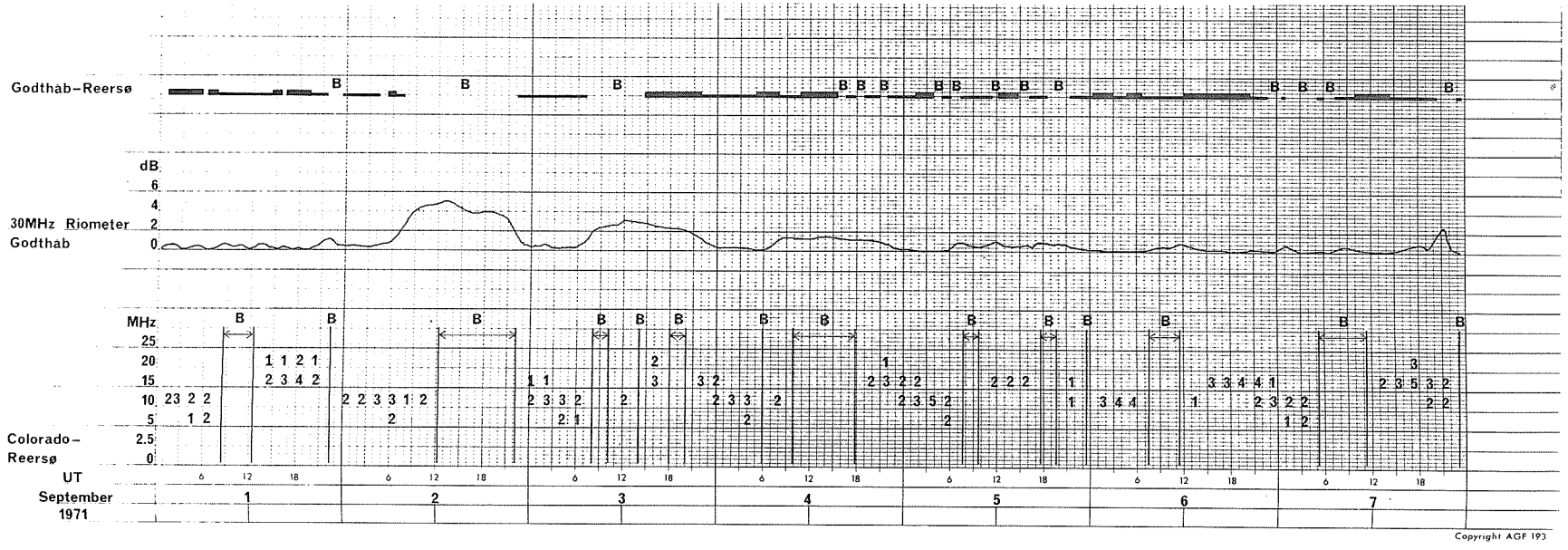

Fig. 2. HF communication data for September event.

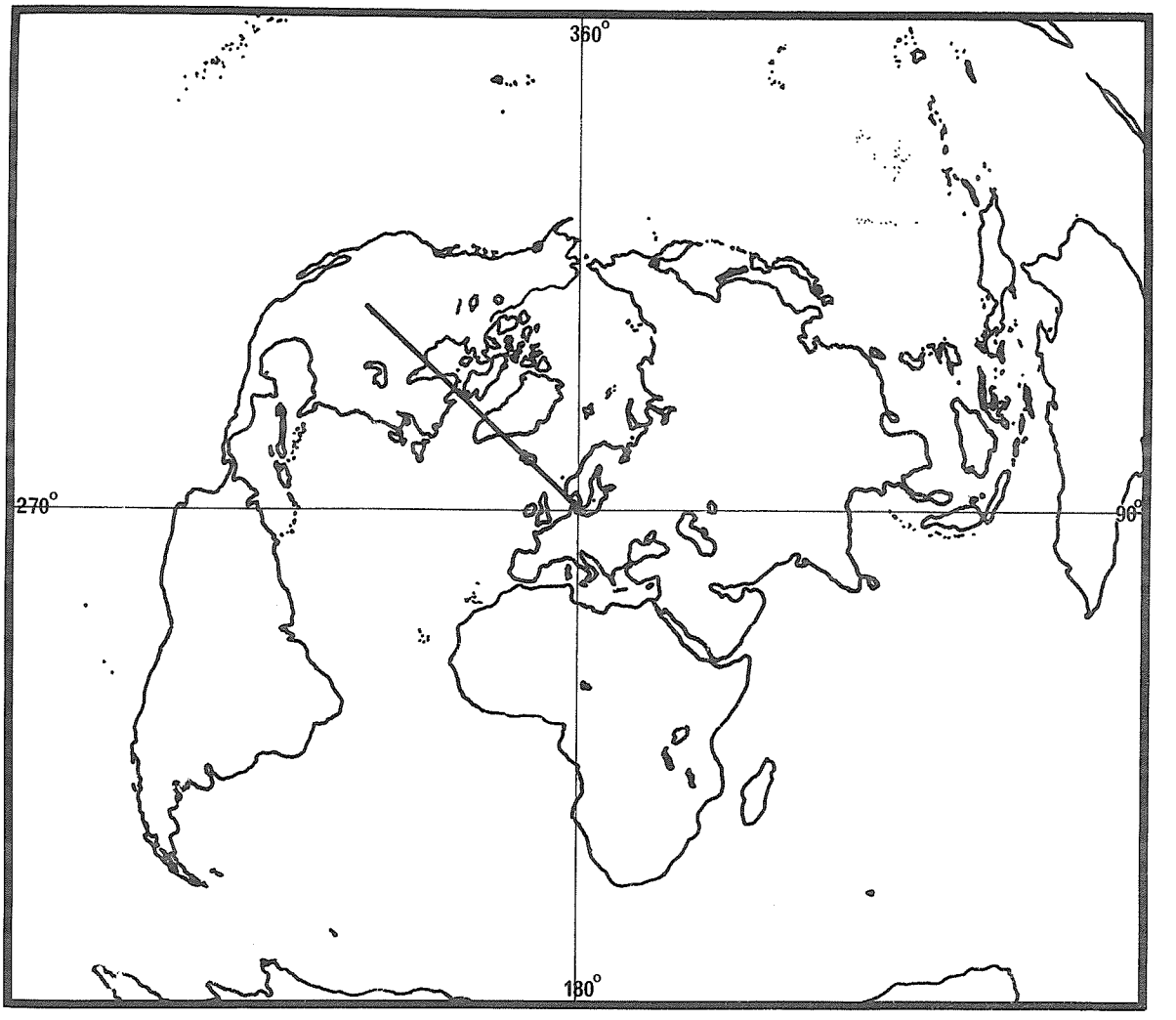

Fig. 3. HF communication path.

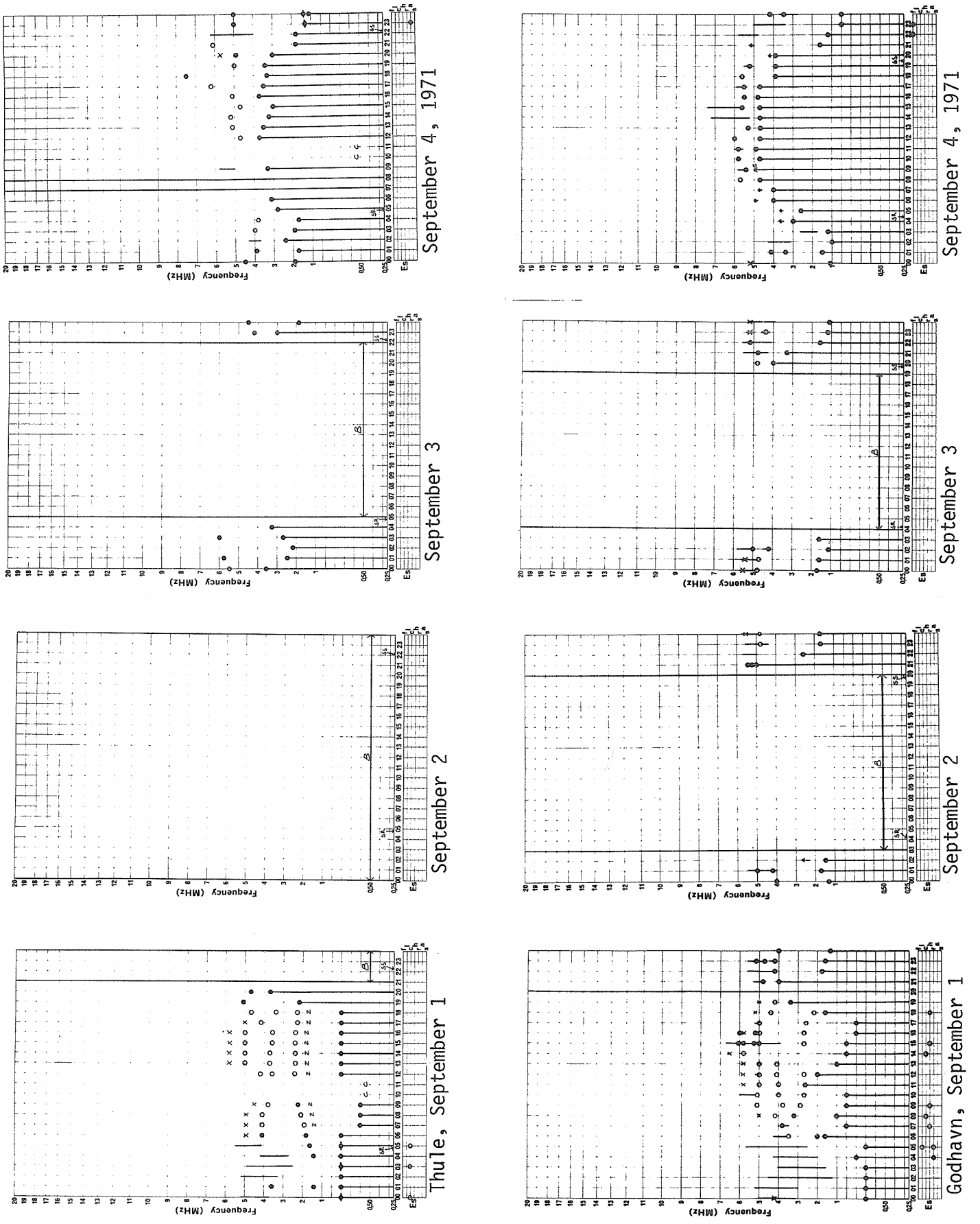

Fig. 4a. f-plots for September from Godhavn and Thule.

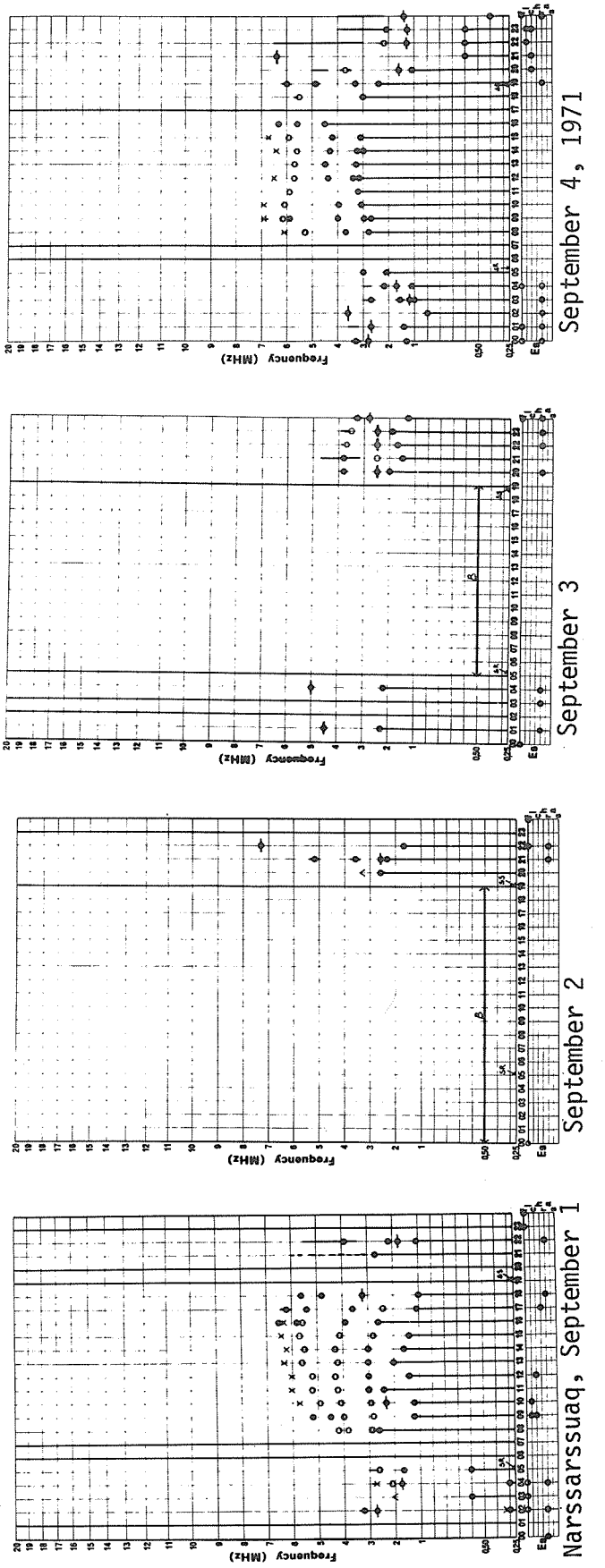

Fig. 4b. f-plots for September event from Narssarsuaq.

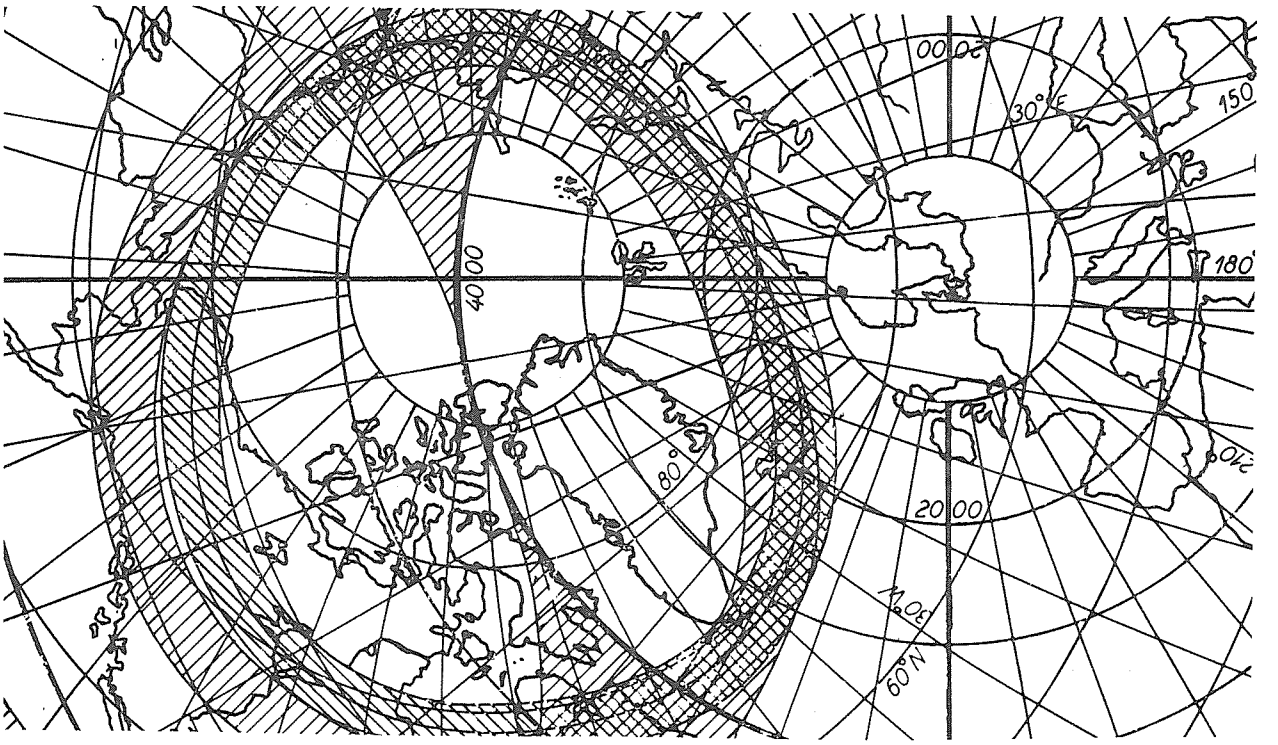

Fig. 5. Rybner and Ungstrup map showing area with max. geomagnetic disturbances during 1932-33 covering area with bad radio communication from Denmark.

REFERENCES

RYBNER, J. and E. UNGSTRUP 1957 L'influence de la zone d'aurores boréales sur les liaisons radioélectriques, Annales des Telecommunications, 12, 172-173.

Ionospheric Observations in Kiruna of the PCA Event of 1 September 1971

by

C. Jurén and J. Svennesson
Kiruna Geophysical Observatory
S-981 01 Kiruna 1, Sweden

Introduction

Ionospheric observations from Kiruna which may be related to the outstanding PCA event of September 1, 1971 and the associated geomagnetic events are collected and presented in synoptic figures. Reproductions of magnetometer and riometer records are given in separate figures. Ionosonde records from observing stations other than Kiruna have been included in the synoptic figures to show the latitudinal variations.

The coordinates of the stations are given in the table below:

	Geographic		Corrected Geomagnetic[+)]	
	Latitude	Longitude	Latitude	Longitude
Kiruna	67.8°N	20.4°E	64.8°N	104.2°E
Lycksele	64.6°N	18.7°E	61.7°N	100.6°E
Uppsala	59.8°N	17.6°E	56.9°N	97.1°E

The riometer records from Kiruna are replaced by records from Down Range Station, ESRANGE, when, for longer periods, the riometer records in Kiruna are highly affected by radio interference. These records are marked with the letters DRS.

The ionosonde data used are from the bulletins published by the Research Institute of National Defence, Stockholm, Sweden.

The geographic coordinates of the transmitters of the VLF signals shown in this data report are as follows: NAA (17.8 kHz) 44.6°N, 67.3°W; NLK (18.6 kHz) 48.2°N, 121.9°W; and HAIKU (13.6 kHz) 21.4°N, 157.8°W.

The PCA Event of 1 September 1971

A ground level cosmic ray increase started around 2015 UT on 1 September. The increase at Deep River was about 27% around 2200 UT.

The PCA onset was observed in Kiruna on the two VLF signals NLK (18.6 kHz) and HAIKU (13.6 kHz) around 2020 UT on 1 September.

No optical flare was observed which could be responsible for the emission of the particles causing the above two events. However, the Sagamore Hill Observatory recorded a complex radio burst with onset 1926 UT, and Type IV solar radio emission of medium intensity (with onset time 1937 UT) was observed in Boulder. It was probably a "behind limb event" with the particle emitting area supposedly (Ursigram) about 3 days behind the West limb of the Sun.

A general view of the event as observed in Kiruna is shown in Figure 1.

VLF Propagation

The onset of the PCA event was observed as a phase advance starting about 2020 UT of both the VLF-signals. The maximum phase advance of the HAIKU signal was about 45 μsec and occurred early in the morning on 2 September (UT).

The amplitude of the NLK signal decreased and the maximum difference from the normal level was greater than 30 dB in the night of 1-2 September. About 6 September the amplitude began to increase slowly reaching normal level on 9 September.

Radio Wave Absorption

The typical proton induced cosmic radio noise abosrption, showing smoothly varying and high absorption during day and low absorption during night, started early on 2 September and remained for 2 days. A moderately severe magnetic storm started with an sc at 1646 UT on 4 September and the absorption observed between 4 and 8 September was more variable.

+) G. Gustafsson, Arkiv för geofysik, 5, 595, 1970.

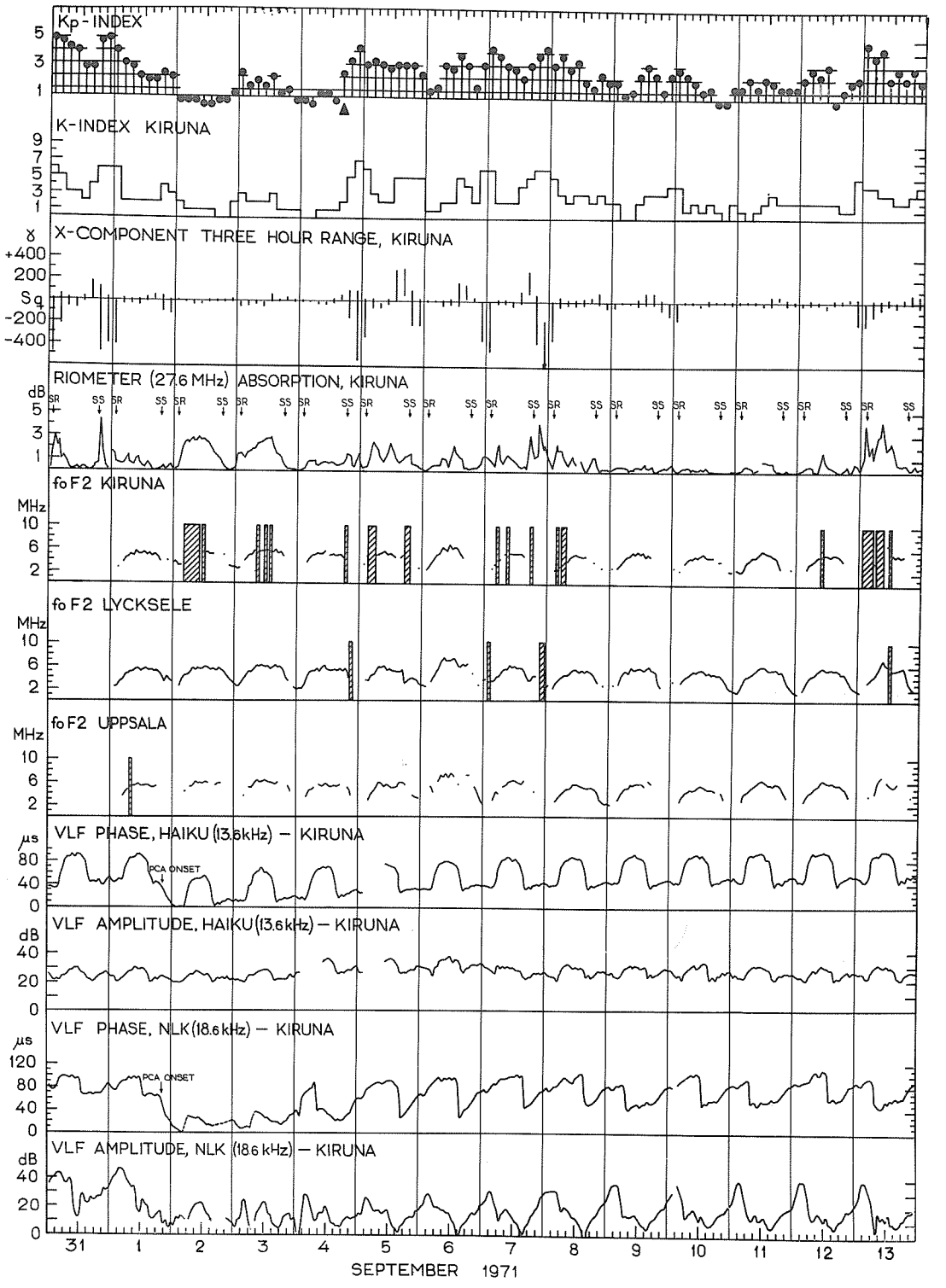

Fig. 1. Survey of ionospheric effects as recorded in Kiruna and nearby observatories. The foF2 plots are presented in the order of decreasing latitude.

The riometer absorption curve shows the maximum absorption during each hour. One-hour values of the critical frequency foF2 have been plotted. The hatched areas indicate periods when the critical frequency was not measured due to black-out, and empty areas correspond to periods when foF2 could not be measured for other reasons. The onset of the PCA is observed on the phase and amplitude records of the VLF signals.

A reproduction of the riometer records is shown in Figure 2.

The diagrams of the critical frequency of the F2-layer show black-out in Kiruna for some time every day between 2 and 8 September and only during very short time periods in Lycksele during the geomagnetic storm on 4 and 7 September. This indicates that the proton precipitation reached somewhat south of Kiruna. No black-out was recorded in Uppsala.

Geomagnetic Activity

The PCA onset occurred during a period with weak geomagnetic activity. The geomagnetic storm with the sc at 1646 UT on 4 September gave a smooth slowly growing X-component for two hours after the sc. At 2100 UT the X-component has a positive maximum. The X-component was negative with a minimum of about -500 γ from the Sq curve at 2330 UT. At the same time there was a maximum in both the Y- and Z-components, 200 γ and 250 γ, respectively. This indicates that the main activity occurred to the south of Kiruna. During the following nights the magnetic activity in Kiruna remained high.

Figure 3 shows the magnetometer records from Kiruna for the period 3 - 11 September 1971.

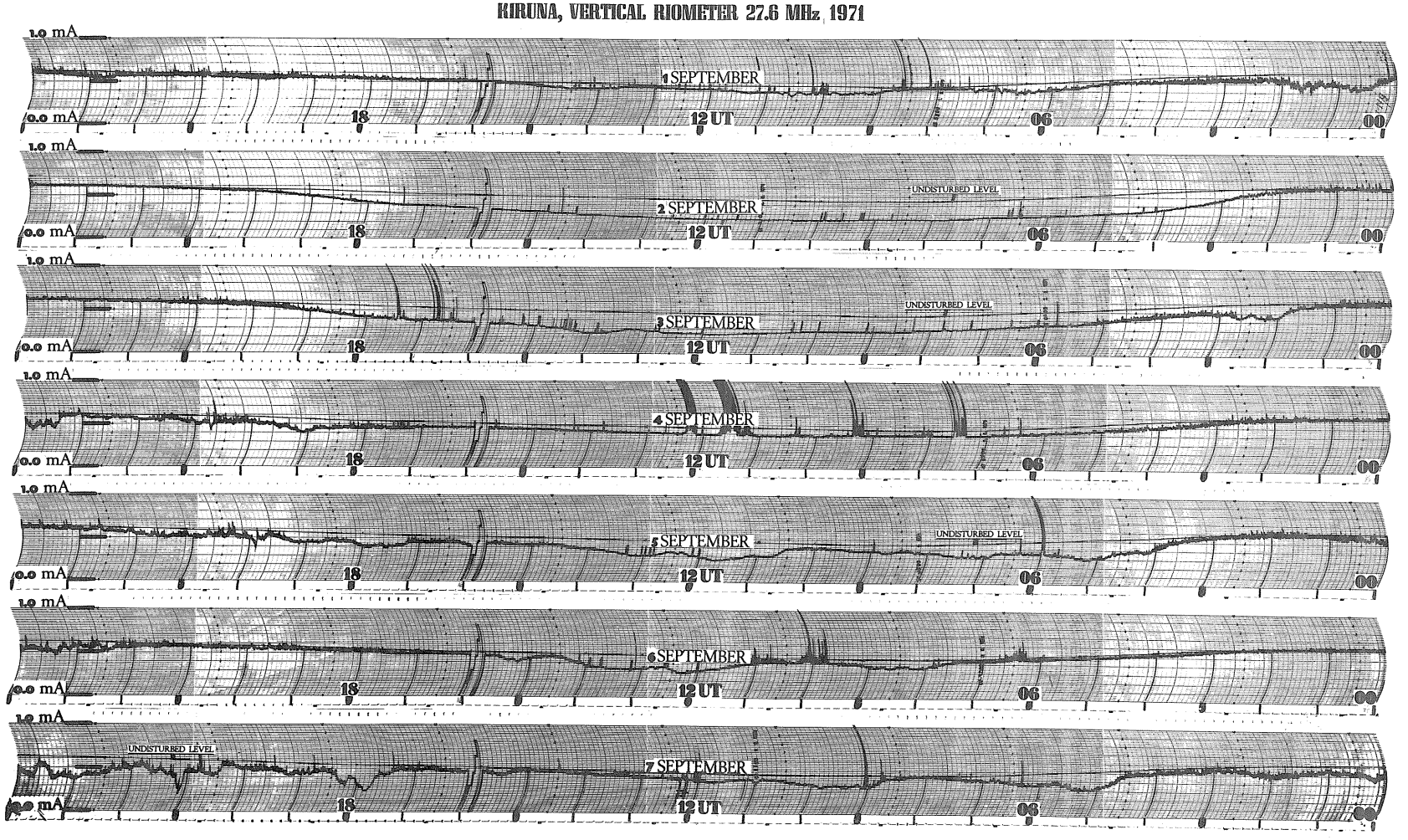
KIRUNA, VERTICAL RIOMETER 27.6 MHz, 1971
1.0 mA
0.0 mA
1 SEPTEMBER
2 SEPTEMBER
3 SEPTEMBER
4 SEPTEMBER
5 SEPTEMBER
6 SEPTEMBER
7 SEPTEMBER
UNDISTURBED LEVEL
18
12 UT
06
00

2a.

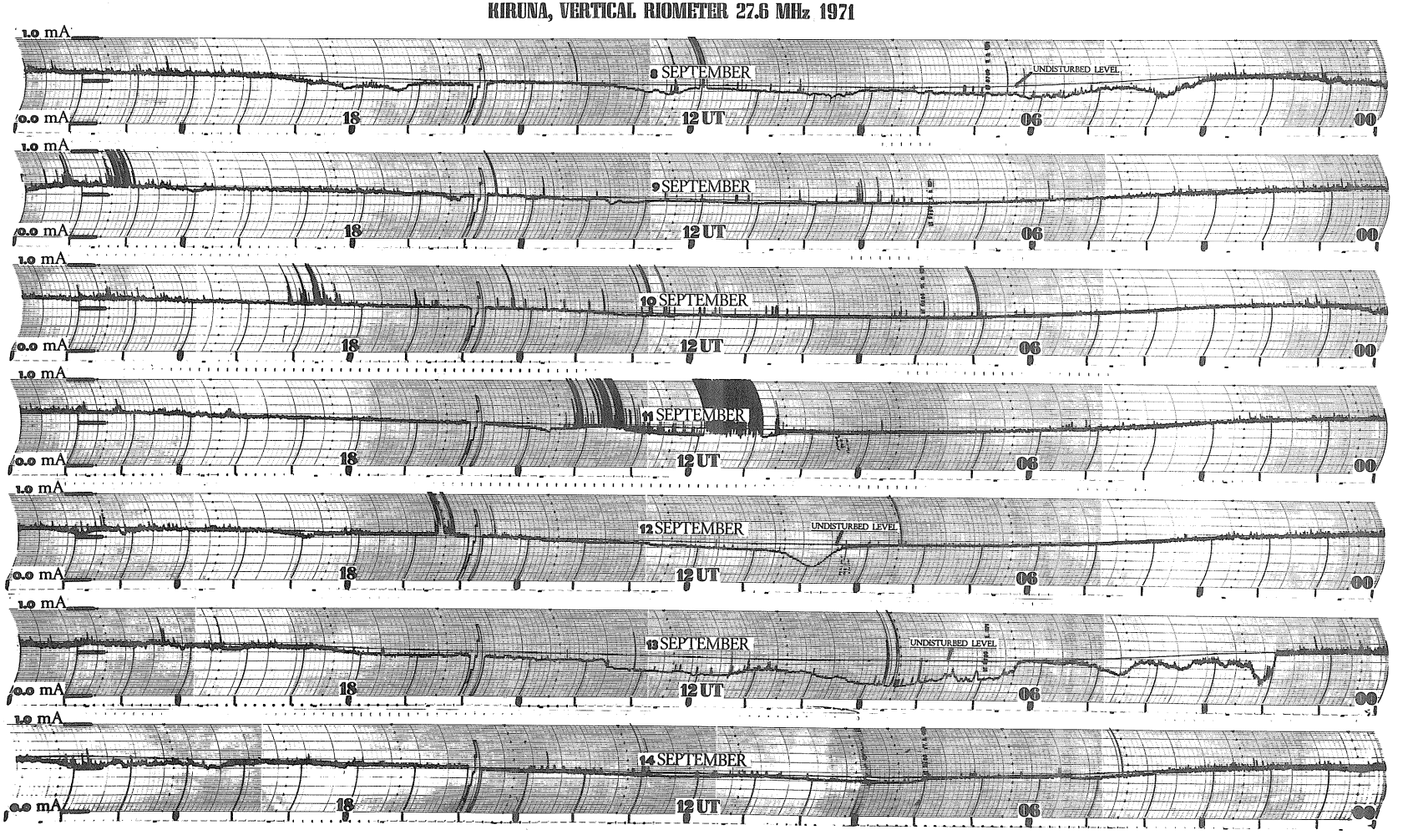

2b.

Fig. 2. Riometer records from Kiruna 27.6 MHz receiver. In case of severe interference in Kiruna, the less disturbed records of the Down Range Station (DRS) at ESRANGE, (27.6 MHz), have replaced the Kiruna records. The reproductions are extracted from "Kiruna Geophysical Data".

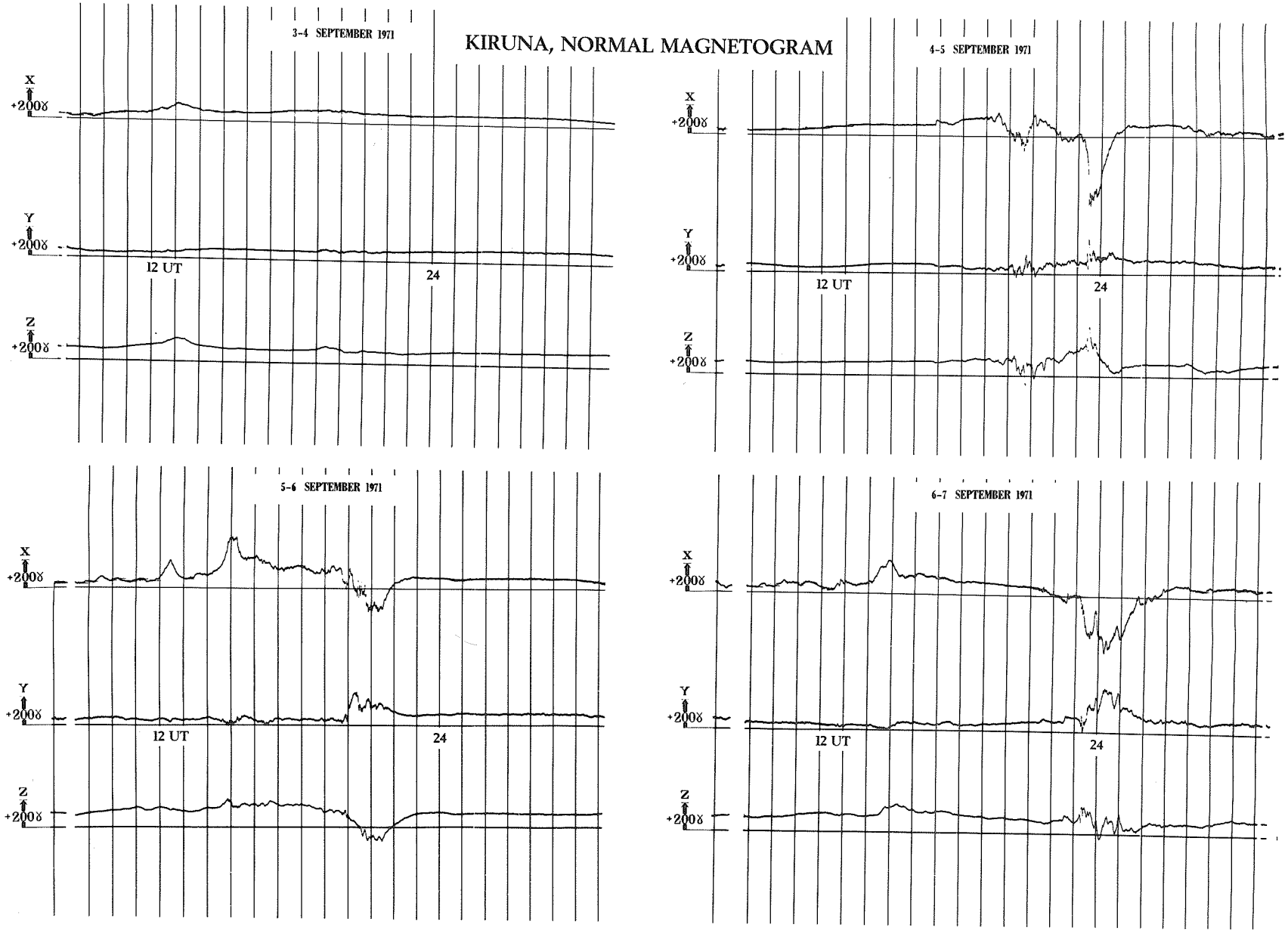
KIRUNA, NORMAL MAGNETOGRAM
3-4 SEPTEMBER 1971
4-5 SEPTEMBER 1971
5-6 SEPTEMBER 1971
6-7 SEPTEMBER 1971
X
Y
Z
+200γ
12 UT
24

3a.

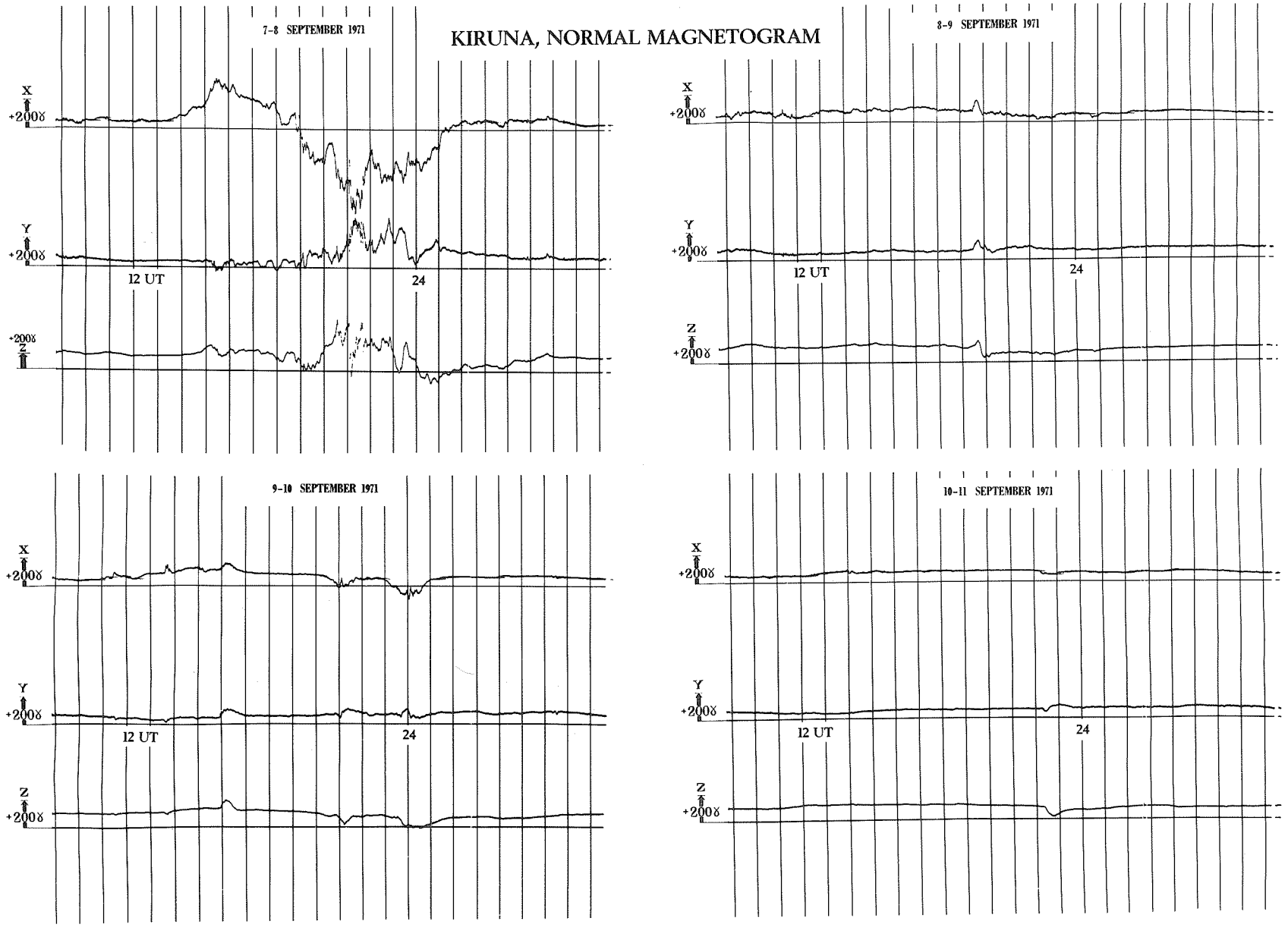

3b.

Fig. 3. Kiruna normal magnetogram. The reproductions are extracted from "Kiruna Geophysical Data".

EFFECTS OF THE SEPTEMBER 1971 SOLAR PARTICLE EVENT ON POLAR VLF PROPAGATION

JOHN P. TURTLE
POLAR ATMOSPHERIC PROCESSES BRANCH
AERONOMY LABORATORY
AIR FORCE CAMBRIDGE RESEARCH LABORATORIES
BEDFORD, MASS. 01730

Measurements of VLF propagation in polar cap regions are made at the AFCRL Geopole Observatory at Thule AB in Greenland as a monitor of D-region particle precipitation disturbances. During the solar particle event on 1 September 1971 two transmitters were being monitored; one was GBR (16.0 kHz) in England and the other was NPG (18.6 kHz) in Washington. These paths are shown in Figure 1.

The effects of the 1 September 1971 solar particle event on the amplitude and phase of the signals from the two transmitters are shown in Figure 2. A rubidium frequency standard was used as the phase reference. Although both propagation paths were solar illuminated at the beginning of the event no definite SPA effects were recorded. The D-region particle disturbance began at about 2010 UT on 1 September. On the NPG-Thule path the maximum attenuation was about 12 dB at 0330 UT on 2 September and a maximum phase advance of 204° occurred at 0915 UT. On the GBR-Thule path the signal was lost during the daylight hours on 2 and 4 September due to the enhanced attenuation effects of the Greenland ice cap. The maximum attenuation on this path was probably more than 25 dB. Recovery to normal signal propagation conditions was not complete until 11 September 1971.

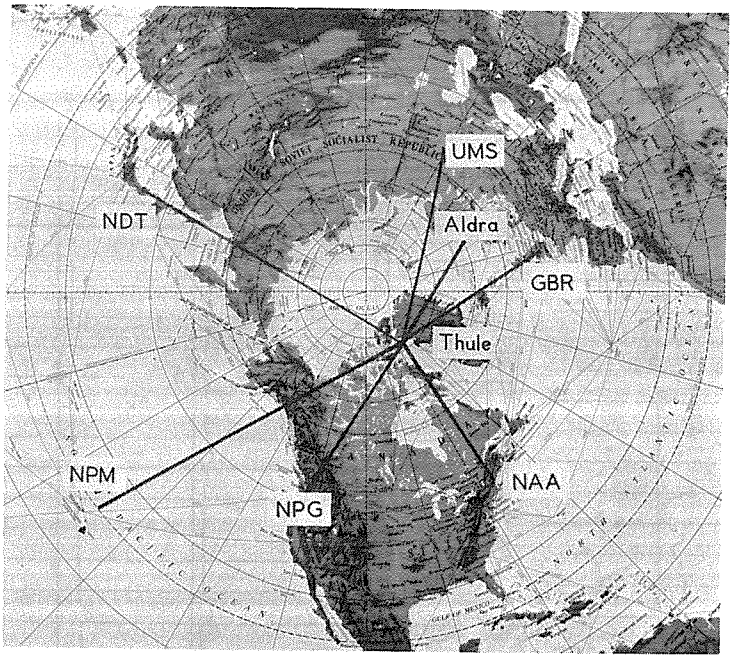

Fig. 1 Polar VLF Propagation Paths to the Geopole Observatory

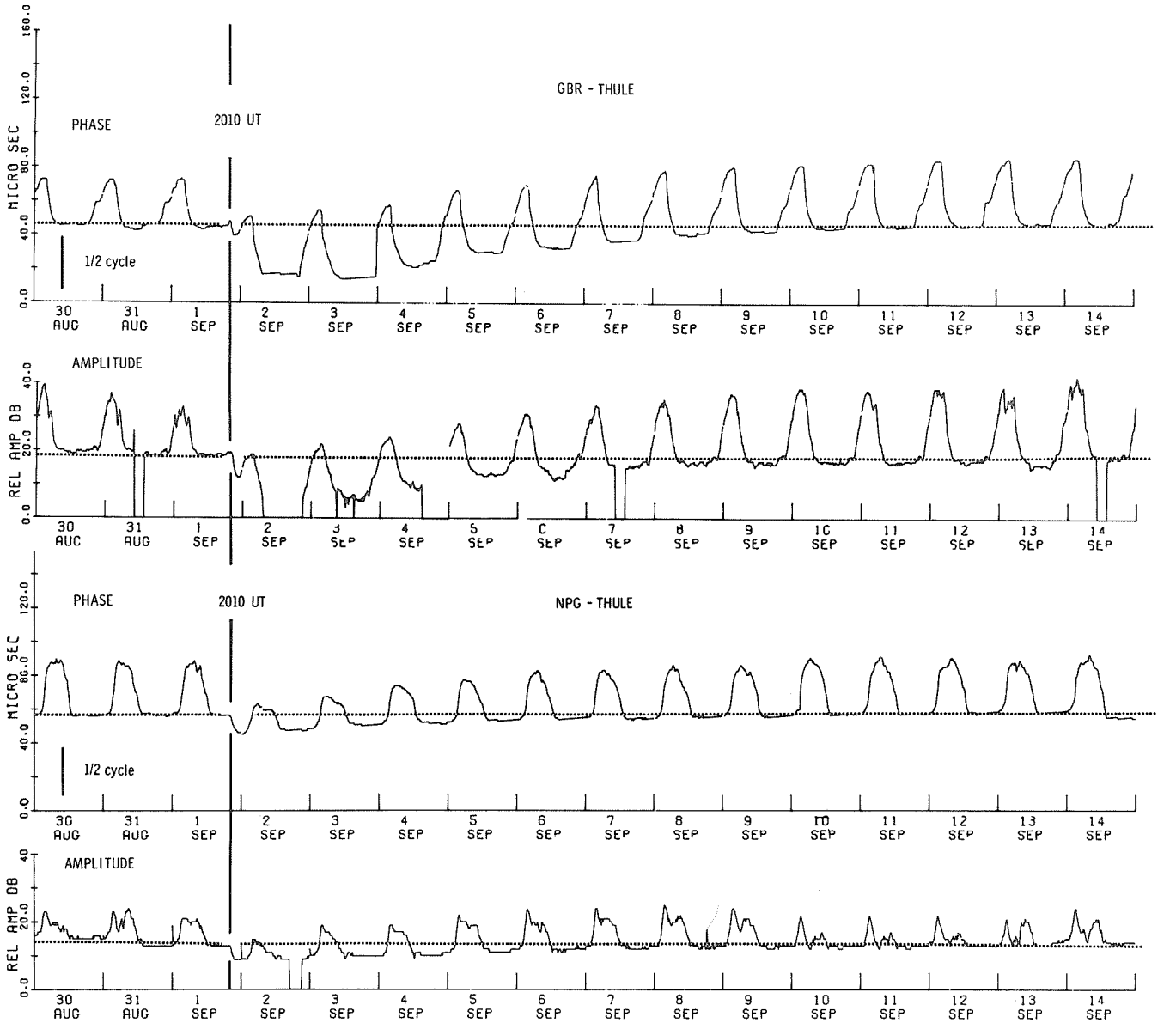

Fig. 2 VLF Amplitude and Phase Data for the September 1971 Solar Particle Event (The dotted line is an arbitrary reference level)

Mid-Latitude Total Electron Content During Cosmic Ray Event September 1-2, 1971

by

J. A. Klobuchar
Air Force Cambridge Research Laboratories
Bedford, Massachusetts

and

M. J. Mendillo
Astronomy Department, Boston University
Boston, Massachusetts

Continuous measurements of the ionospheric total electron content (TEC) using the Faraday rotation technique are routinely made from Sagamore Hill, Hamilton, Massachusetts, by monitoring the VHF signal from the geostationary satellite, ATS-3. The TEC of the mid-latitude ionosphere consists mainly of the integrated electron densities of the F-region; that is, the lower layers contribute a negligible amount to the total. The equivalent vertical TEC values for September 1-2, 1971, are shown in the Figure below. The dashed curves give the monthly median behavior for the month. The small vertical arrow indicates the approximate time of the commencement of ground level cosmic ray increase. The September period was magnetically quiet, as indicated by the Ap values in the Figure. Geomagnetic storms typically cause large scale changes in TEC which last several days while large solar flares produce effects of much smaller magnitude and shorter duration. For this period, however, no changes occurred in TEC which could be directly associated with the cosmic ray increase.

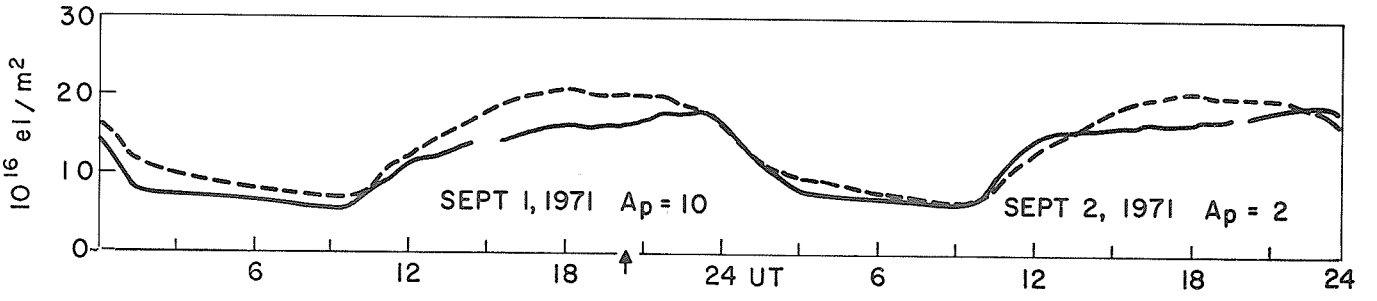

EQUIVALENT VERTICAL TOTAL ELECTRON CONTENT OBSERVED FROM SAGAMORE HILL, HAMILTON, MASS.

Polar Cap Disturbances of September 1, 1971, Observed on the Phase of VLF Waves

by

Y. Hakura
Radio Research Laboratories
Koganei, Tokyo, Japan

and

T. Ishii, T. Asakura, and Y. Terajima
Inubo Radio Wave Observatory
Radio Research Laboratories
Choshi, Chiba, Japan

Phase measurements with a cesium frequency standard of VLF waves propagating over great distances have been made at Inubo Radio Wave Observatory, Choshi, Chiba, Japan (35°42'N, 140°52'E). Among them, transpolar VLF waves provide a very sensitive method of detecting solar proton events at the middle latitude [Nakajima et al., 1970]. The transpolar signal paths for NAA-17.8 kHz, GBR-16.0 kHz, and WWVL-20.0 kHz are shown in Figure 1, in which the corrected geomagnetic latitudes of 60° and 70° are shown by two elliptical lines.

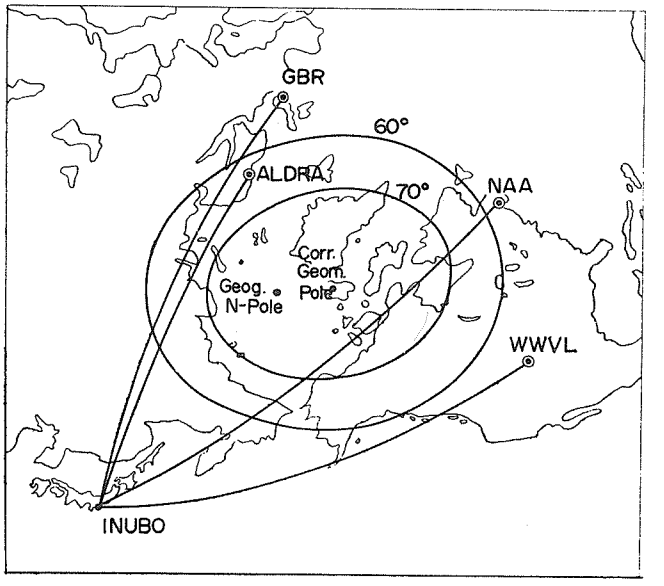

Fig. 1. Transpolar signal propagational paths.

Figure 2 shows solar proton flux with energy 5 - 21 Mev [Solar-Geophysical Data, October, 1971], phase deviations in the NAA and GBR signals and geomagnetic Kp indices on August 29 through September 11, 1971. Occurrence times of polar cap disturbances (PCD) and related solar-terrestrial events are listed in Table 1.

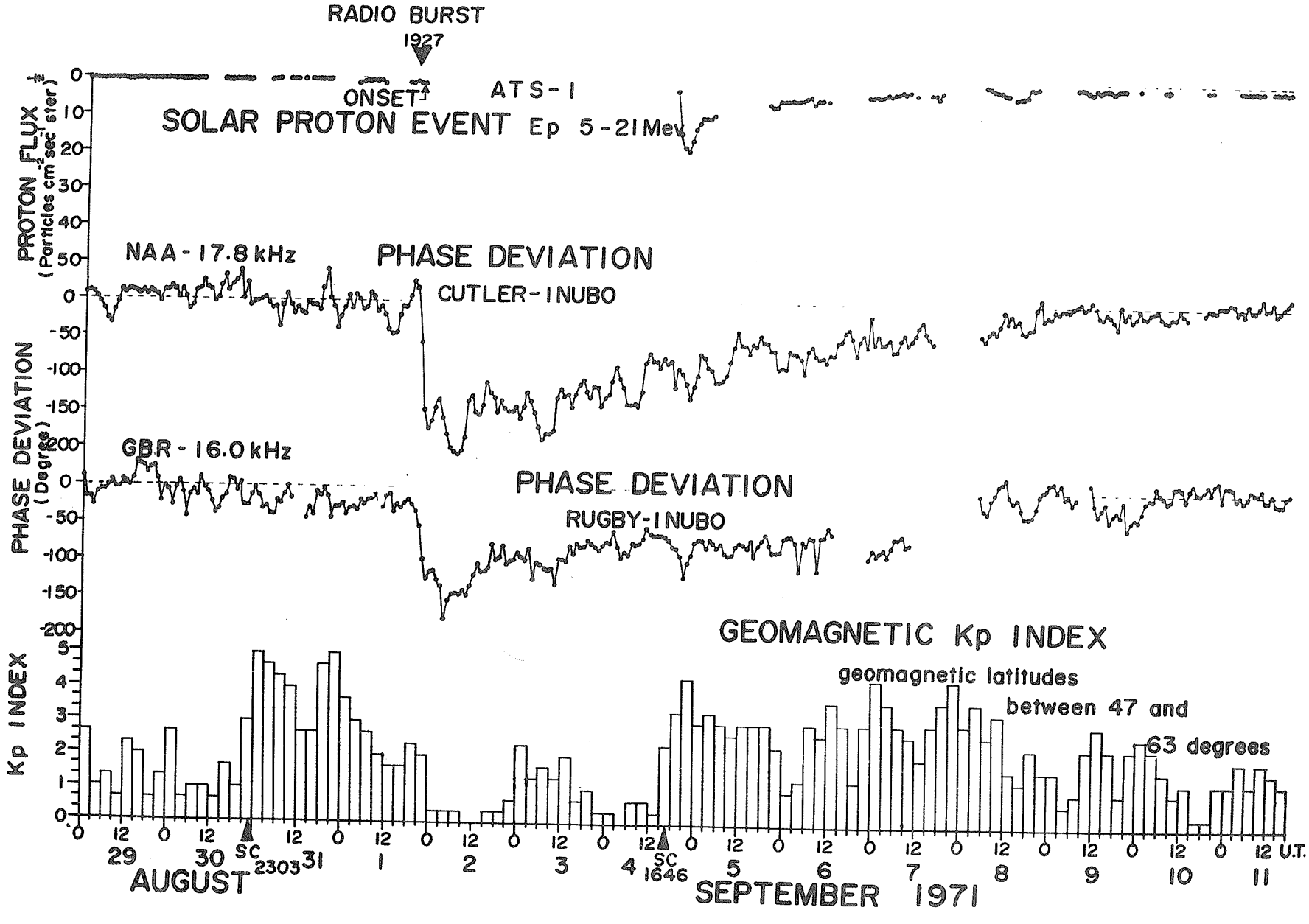

Fig. 2. Polar Cap Disturbance of September 1, 1971.

Table 1

PCD's observed at Inubo and related solar-terrestrial events of September 1, 1971

Event		Start time	Max. time	End	Flux, or Phase deviation
Radio burst at 2695 MHz (Sagamore Hill)		1/ 1926.9 2002.2	1940.5 2002.2	2002.2 2030D	1.2×10^{-20} wm^{-2}Hz^{-1} 1.3×10^{-20}
PCD	NAA-17.8 kHz	1/ 2032	2/0741	9/08	218°
	GBR-16.0 kHz	2045	0352	8/09	150°
Solar proton	ATS 1 (21-70 Mev)	2100E		11/07	
	Neutron monitor (Deep River)	2020	2250	2/1230	11.5 % above background

D = after
E = before

REFERENCES

NAKAJIMA, T., T. ISHII, K. TSUCHIYA, A. SAKURAZAWA, and Y. HAKURA 1970 Results of special observations for the Proton Flare Project 1969: Polar cap disturbance of June 7, 1969, observed on the phase of VLF waves, J. Radio Res. Labs., Japan, 17, 49-54.

1971 Solar-Geophysical Data, 326 Part I, U.S. Department of Commerce, (Boulder, Colorado, U.S.A. 80302), 24-25.

Report on Ionospheric and Whistler Activity at the Panská Ves and Průhonice Observatories on September 1, 1971

by

F. Jiricek, J. Lastovicka and P. Triska
Geophysical Institute
Czechoslovak Academy of Sciences
Prague, Czechoslovakia

The proton flare event on September 1, 1971 was accompanied by nearly no effect in the ionosphere above Central Europe. It is rather difficult to decide precisely what was the ionospheric response to the proton flare in question, because the flare influence was superimposed on the two magnetic storms that started on 30 August at 2303 UT and on 4 September at 1646 UT [NOAA, 1971].

The state of the upper ionosphere is studied using the foF2 data of the ionosonde located at Průhonice (49°59'N, 14°33'E). The foF2 values during the period August 31 - September 4 are close to monthly median values except the daytime values of August 31 and September 1, which are distinctly higher and lower, respectively, than median values. These two days, however, precede the proton flare event. Consequently, this proton flare event caused no observable changes in the upper ionosphere.

The X-ray burst accompanying this proton flare event was too weak to cause any SID-event, which is in agreement with observational SID data [NOAA, 1971]. The daytime lower ionosphere during the period August 30 - September 4 was fairly quiet according to the HF A3-absorption data obtained at Panská Ves (50°32'N, 14°34'E). The nighttime lower ionosphere is studied using the LF A3-measurements of the ionospheric absorption. The nighttime absorption data measured at 272 kHz (reflection point 49°34'N, 16°03'E) are presented in Table 1:

Table 1

Date	Aug. 30-31	Aug.-Sept. 31-1	Sept. 1-2	Sept. 2-3	Sept. 3-4	Sept. 4-5	Sept. 5-6	Median x)
L(dB)	11.7	13.2	15	13.2	12.7	12.4	16.9	13

x) monthly median value

If we compare the results of absorption measurements made at 272 kHz (Table 1) and 185 kHz (reflection point 51°09'N, 14°06'E) with monthly median values and with the absorption values in the vicinity of the studied period, we obtain a general nighttime absorption characteristic of the period under study Table 2):

Table 2

Night	Aug. 30-31	Aug.-Sept. 31-1	Sept. 1-2	Sept. 2-3
272 kHz	low	normal	slightly enhanced	normal
185 kHz	normal	enhanced	enhanced	more enhanced

Night	Sept. 3-4	Sept. 4-5	Sept. 5-6
272 kHz	normal	low	enhanced
185 kHz	B_0 2015 - 2125 UT; slightly enhanced	slightly enhanced	slightly enhanced

The absorption enhancement starting on September 5-6 which continues during at least the next two nights may be attributed to the magnetic storm with ssc at 1646 UT on September 4 [NOAA, 1971]. The bay-like disturbance (B_0) observed at 185 kHz on September 3-4 seems to be of a random origin, because it is neither confirmed by any other absorption data nor supported by geomagnetic data. The time-development of absorption between the nights of August 30-31 - September 4-5 allows us to say that the absorption enhancement at 185 kHz and very probably also at 272 kHz is the absorption after-effect of the magnetic storm started at 2303 UT on August 30, but the possibility of some influence of the proton flare of Septmeber 1, 1971 cannot be excluded. The nighttime absorption

data of the Nagycenk Observatory (272 kHz; A3; reflection point 48.4°N, 17.1°E) indicate no observable influence of the given proton flare either [Bencze, 1972].

If we compare the lower ionosphere response to the solar proton flares of September 1, 1971, January 24, 1971 [Tríska et al., 1972] and November 2, 1969 [Krivský et al., 1972] and to the March 1970 event [Tríska and Lastovicka, 1971; Knuth et al., 1971], we can conclude that the effect of the proton flare itself probably does not occur in the lower ionosphere (except SID due to the EUV-radiation) above Central Europe (∿50°N, ∿15°E) nor somewhat more northerly. The main condition for the occurrence of the lower ionosphere disturbances accompanying the proton flare event seems to be a sufficiently disturbed geomagnetic situation caused by the given proton flare or by another solar event coinciding accidentally with the proton flare interval, e.g. by the mechanism proposed by Bednárová and Halenká [1969].

The whistler activity, as is usual in Czechoslovakia in this part of the year [Jiřícek, 1971], was so weak that it was impossible to obtain any results based on VLF-data. For instance, at the Panská Ves Observatory no whistler was observed during August 30 and only one was observed during September 1 in the routine observational program of 2 minute tape records every hours.

REFERENCES

BENCZE, P. 1972 Private communication.

BEDNAROVA-NOVAKOVA, B. and J. HALENKA 1969 A Universal Interpretation of the Generation of Geomagnetic Storms using Features of the Solar Corona, Planet. Space Sci., 17, 1039-1044.

JIRICEK, F. 1971 Whistler Activity in Central Europe during the Period of Increasing Solar Activity from 1964 to 1968, Trav. Inst. Géophys. Acad. Tchécosl. Sci., 1969, No. 313, 281-289, Academia, Praha.

KNUTH, R., W. LIPPERT and J. WEISS 1971 Midlatitude Ionospheric Effects in March 1970, Upper Atmosphere Geophysics Report UAG-12, Part II, 222-226.

KRIVSKY, L., A. TLAMICHA, J. HALENKA, J. LASTOVICKA, P. TRISKA, S. PINTER and L. ILENCIK 1972 Development and Spatial Structure of Proton Flares near the Limb and Coronal Phenomena. V. Emissions and Effects of the Proton Flare and Active Processes from November 2nd, 1969. Bull. Astron. Inst. Czechosl., 23, No. 2.

TRISKA, P., F. JIRICEK and J. LASTOVICKA 1972 Report on Ionospheric and Whistler Activity at the Panská Ves and Průhonice Observatories on January 24, 1971, this compilation.

TRISKA, P. and J. LASTOVICKA 1971 Ionospheric Disturbance during the Night of March 8-9, 1970, Upper Atmosphere Geophysics Report UAG-12, Part II, 211-212.

1971 Solar-Geophysical Data, 327 Part I, U.S. Department of Commerce, (Boulder, Colorado, U.S.A. 80302).

Solar Particle Events in the Ionosphere during the Period of September 1 - 8, 1971

by

P. Velinov and G. Nestorov
Geophysical Institute
Bulgarian Academy of Sciences
Sofia, Bulgaria

Introduction

The ground-level cosmic ray increase on September 1, 1971 is recorded only by the stations situated in higher latitudes, thereby distinct from the event on January 24, 1971. For instance in Europe on 1 September the event was observed at Kiel, Germany (geomagnetic threshold of rigidity $R_c \simeq 1.9$ BV), at Dourbes, Belgium with $R_c \simeq 3.2$ BV, etc. However, this event was not observed by the Pic-du-Midi ($R_c \simeq 5.6$ BV) neutron monitor.

Thus in our region of observation where $R_c \simeq 5$ BV, ionospheric effects caused directly by relativistic solar cosmic rays on September 1 are absent. However, in this case as well as during the event on January 24, a number of secondary ionospheric effects were observed of the soft as well as of the high energy solar particle fluxes throughout the high atmosphere during the period following September 1. These anomalies are ordinarily connected with geomagnetic field disturbances.

Effects in the Low and Middle Ionosphere during the Period August 28 - September 8

Two days before the event on September 1 there was a strong geomagnetic storm with evident after-effects during the period of investigation September 1 - 8. Thus, it is only proper to begin the study of the case a few days earlier. In order to follow up more clearly the effects in the different ionospheric regions, Figure 1 represents a diagram of the absorption time - variations of the radio waves of different frequency ranges during the period August 28 - September 8. All measurements are performed at the Ionospheric Observatory, Sofia (N42.6, E 23.4) in typical middle latitudes.

In order to assess more objectively the absorption course in the given period it is necessary that we give the equivalent frequencies f_i of the observed path for the A3 method. They are shown in the table below where the path length d is also given as well as the coordinates of the reflection points.

f(kHz)	d(km)	f_i(kHz)	Coordinates North	East
155	380	75	44°13'	24°27'
164	1720	25	45°28'	13°13'
557	180	400	43°30'	23°32'
593	140	480	43°02'	24°03'

In the VLF range (f_i = 25 kHz, L_{164}) on August 29 we observe a considerable absorption decrease which can partially be explained by the small Forbush effect in the cosmic rays on the same day. A similar decrease, but of a smaller amplitude, can be established in the L_{155} curve. From the monthly median absorption values

$$L_{m,\,164} = 4 \text{ dB}; \quad L_{m,\,155} = 17 \text{ dB}$$

and the values on August 29

$$L_{164} = 2 \text{ dB} \quad ; \quad L_{155} = 15 \text{ dB}$$

We can determine the relative variation of electron production rate in the cosmic ray layer by means of the expression [Velinov, 1968 and 1971]:

$$\frac{\Delta q}{q} = \frac{\Delta L}{L}\left(2 + \frac{\Delta L}{L}\right) \qquad (1)$$

Hence the result obtained is

$$(\Delta q/q)_{164} = 125\% \text{ and } (\Delta q/q)_{155} = 25\%.$$

These values, however, cannot be explained only by cosmic ray Forbush decrease (3-hour Kp index reaches maximum 3) which can be easily established by the calculations made by Velinov [1971]. Similar estimations are given by Nestorov and Velinov [1972].

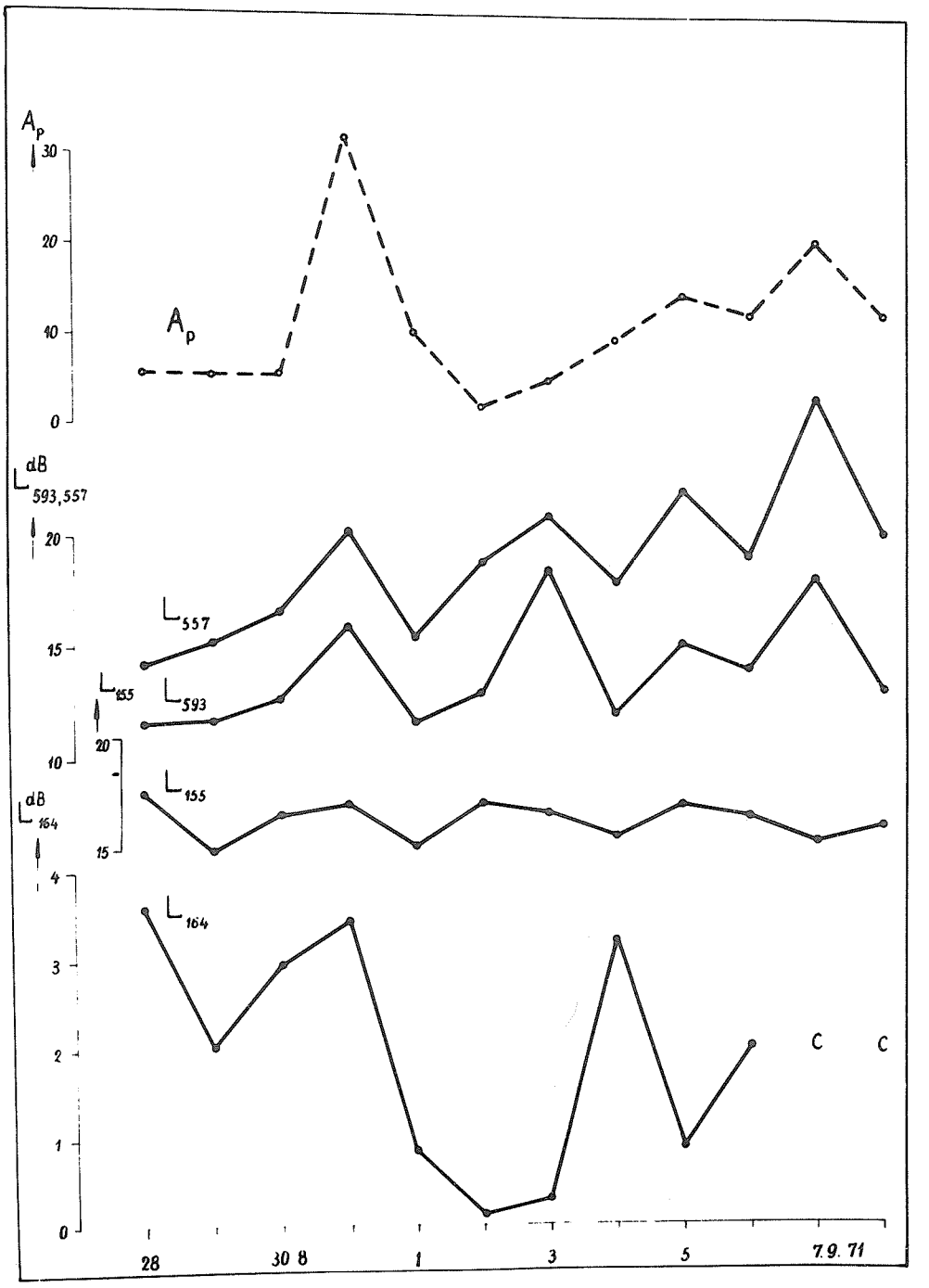

Fig. 1. Absorption in the low and middle ionosphere during the period of August 28 - September 8.

The absorption decrease effect on September 1 - 3 and 5 is much greater. The cause is as follows: since conditions of propagation for L_{164} at night are determined mainly by a deviative component, i.e. according to Nestorov [1962] from the logarithmic gradient of the electron density in the reflection region, it can be expected that around and above this height there acts an excessive ionization course which increases the electron density in the night E-layer. This means that for radio waves crossing the layer the absorption will increase.

Actually from the absorption measurements L_{557} and L_{593} can be seen that they increase on August 31 and September 3, 5 and 7.

Similar to the January 24 - February 3 events [Nestorov and Velinov, 1972] as well as the established behavior of L_{155} in other cases by Nestorov [1969], essential changes cannot be observed here. In the absorption on this path during the research period results confirm the compensation by opposite active factors in the reflection region during anomalies at the base of the thermosphere.

Thus in the studied case it is a confirmed fact that during as well as after the time of geomagnetic disturbances at the base of the thermosphere is formed increased ionization which favors VLF reflections and increases the absorption of the radio waves crossing this region.

The increased absorption L_{557} and L_{593} on August 31 coincides with the day of the geomagnetic storm, while the increase of L on September 3 is a well-known after-effect, taking place three days following the basic disturbance.

On September 5 and 7 there is a new increase in the geomagnetic activity accompanied by an L increase. Actually on September 7 the basic ionospheric effect is superimposed on the after-effect of September 5, thus the L value (especially L_{557}) greatly increases. It is to be regretted that records of L_{164} are missing because of technical reasons.

The monthly median absorption value ($L_{m,\ 593}$ = 12.8 dB) as well as the current L values given in Figure 1 make it possible for us to estimate the intensity of the additional acting ionization source in the region h_1 to $h_2 \simeq 80$ to 120 km by means of the expression [Velinov, 1969]:

$$I = \frac{2Q(h_2 - h_1)}{E_{k,eff}} \Delta q \qquad (2)$$

where Q ≃ 30 ev is the energy required in the formation of 1 electron-ion pair, $E_{k,eff}$ is the effective energy of the particles.

For instance for the main effects on August 31 and September 5 we have

$$\Delta L_{31.8} = 3.2 \text{ dB} \quad \text{and} \quad \Delta L_{5.9} = 2.3 \text{ dB}$$

whence by means of equation (1) is obtained:

$$(\Delta q/q)_{31.8} = 0.55 \quad \text{and} \quad (\Delta q/q)_{5.9} = 0.4$$

From this at q = 0.3 $cm^{-3}sec^{-1}$ [for further details refer to Nestorov and Velinov, 1972] for the necessary flux of protons $E_{k,eff}$ = 300 kev we obtain

$$I \simeq (1 - 1.3)\times 10^2 \text{ particles } cm^{-2}sec^{-1},$$

and in the case of electron precipitation $E_{k,eff} \simeq 40$ kev from equation (2) is obtained:

$$I \simeq (0.7 - 1)\times 10^3 \text{ particles } cm^{-2}sec^{-1}$$

for the number of particles with pitch angle in the cone of losses. The total number of particles can be determined when I is divided by the factor $K \simeq 6\times 10^{-2}$ to 5×10^{-3} depending on the kind of distribution of the particles for the parameter of McIlwain L = 1.8.

High Energy Solar Particle Effect on the Low Ionosphere

Figure 1 indicates that on September 4 there is an unusual increase of L_{164} which indicates the presence of additional ionization in the low ionosphere which is absent in the night E-layer (L_{557} and L_{593} decrease). The calculations made by Velinov [1966, 1968 and 1970] show that for an explanation of the experimentally observed L increase it is necessary to postulate that a very small number of particles - less than 1% of the particles causing the polar cap absorption penetrate the mid-latitude ionosphere. Moreover the main problem is how a part of the PCA particles has been able to penetrate up to the middle latitudes where the geomagnetic threshold is high. Probably the weak geomagnetic disturbance on the night of September 4 - 5 with the 3-hour Kp index 3 to 4 caused an insignificant part (<1%) of PCA particles to precipitate at middle latitudes.

The detailed trend of the increased absorption ΔL_{164} on September 4 - 5 is shown in Figure 2. The base level taken here for the mean absorption includes the period September 1 - 7. In the same Figure the dashed line represents the trend of the 5 - 21 Mev energy level, showing hourly averages from the solar proton monitor ATS-1 (1966 - 110 A) [Solar-Geophysical Data, 1971]. As is well-known, the solar proton flux measured at ATS-1 is representative of the flux in interplanetary space and over the polar caps. Unfortunately, the data from ATS-1 for the energy level 21 - 70 Mev protons are incomplete. Nevertheless on Figure 2 the good correspondence between the trends of ΔL_{164} and 5 - 21 Mev protons to 2200 UT is seen. After that ΔL_{164} increases at 2300 UT, while the 5 - 21 Mev proton flux decreases. However, at the same time the number of 21 - 70 Mev energy protons increases. The Kp index also has its maximum value during the night.

It must be emphasized that the polar cap absorption begins about 1 hour after the ground-level cosmic ray increase on September 1 and effectively terminates in the morning on September 5. During this whole period however, there was no PCA influence because the geomagnetic field was comparatively quiet (Kp = 0 to 2). The geomagnetic storm (ssc) starts as late as September 4 with Kp = 3 to 4. The unsettled geomagnetic conditions that followed are believed to be the result of the passage of an interplanetary sector boundary rather than as a consequence of the behind-the-limb event on September 1. It is at this point that conditions for the middle latitude PCA event appear; it is also observed experimentally by L_{164}.

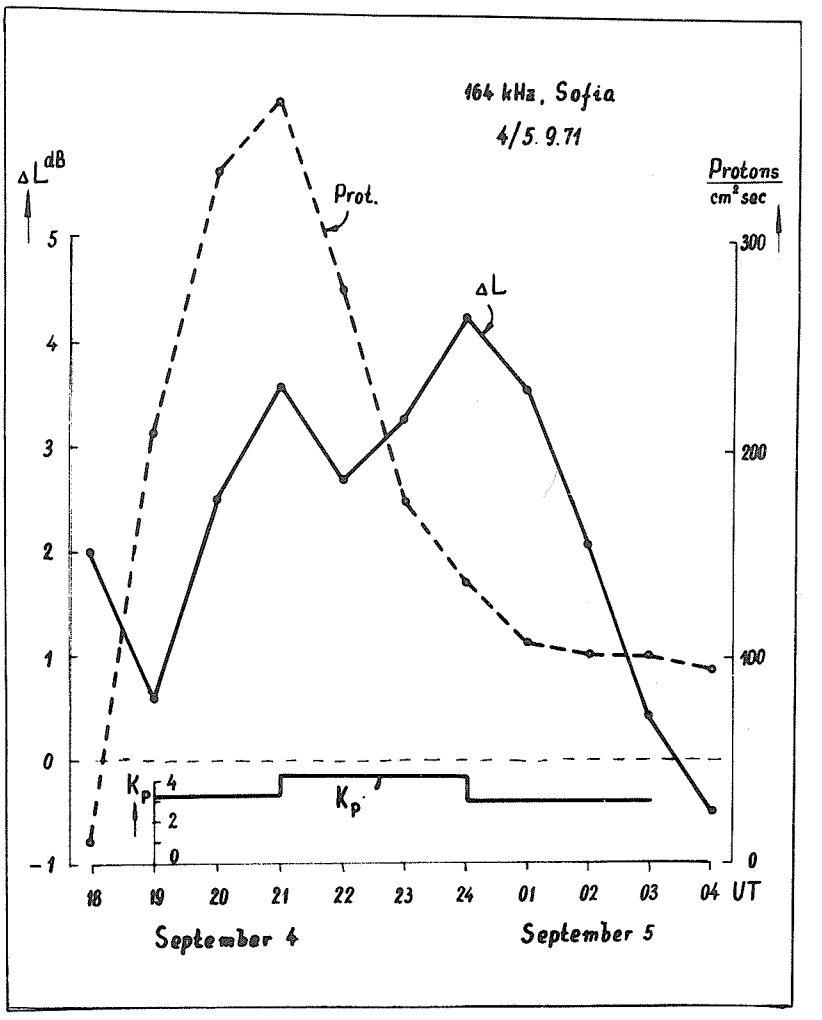

Fig. 2. The hourly trend of the additional absorption in the low ionosphere and 5 - 21 Mev protons during the night of September 4 - 5. The 3-hour Kp index is indicated also.

The behavior of the night E-layer (90 - 120 km) is of special interest. That layer is controlled by L_{593} and L_{557}. As an illustration, in Figure 3 is shown a recording of the night of September 4 for the path 593 kHz. The monthly median absorption value is given by a dashed line. It is clear that a bay effect appeared in the absorption between 2000 and 2200 UT coinciding with the peak of 5 - 21 Mev protons. At the same time a strong polarization disturbance starts, continuing during the whole night (this conclusion is drawn from the observation of other MW paths). The bay effect is quite strong.

This shows that simultaneous with the high energy particles at the base of the thermosphere there is an influx of lower energy particles. This corresponds to our expectations because of the geomagnetic disturbance having taken place.

Effects in the High Ionosphere

Simultaneously with the current phenomena in the low and middle ionosphere were recorded disturbances in the higher level. In Figure 4 is shown the result of the ionogram interpretation obtained at the Sofia Ionospheric Station. In the upper part of the Figures is given the trend of foF2 averaged for 3-hour intervals during the period of August 28 - September 8. The averaging of foF2 for 3-hour intervals was performed in order that the trend of foF2 and of the geomagnetic index Kp((shown in the lower part of the Figures) could be compared more easily. The smooth trend of the monthly median values foF2 for August and September is shown by a dashed line. It can be easily seen that from the afternoon of August 30 to noontime on September 1 are obtained two positive and two negative anomalies of foF2 coinciding with the increased geomagnetic activity (the shaded parts of the diagram with the marks "+" and "-"). The relative amplitude of the anomalies is between 20 and 25% and can be assessed as medium magnetoionic disturbances. With the geomagnetic storm (ssc) on September 4 is connected the weak positive ionospheric disturbance during the pre-sunset period on the same day; on the contrary the ssc on September 7 evoked a negative ionospheric disturbance on the morning of September 8.

The disturbance series begins with the well-known sunset increase anomaly in the ionization of the F2-layer during the pre-sunset period on August 30. This increase of foF2 is not necessarily connected with the directly following geomagnetic storm ssc at 2303 UT. On the contrary the decrease of foF2 between the end of August 30 and the beginning of August 31 in the main phase of the storm is a regular phenomenon, connected most probably with an additional heating of the neutral gas at different heights of the F2-layer. The essential increase of foF2 during the whole day of August 31 is more interesting than the weak effect on September 4. Such positive disturbances are exceptions after a geomagnetic storm. According to a new investigation of Fatkullin [1971], such effects in the daytime ionosphere at medium latitudes during the time of geomagnetic anomalies could be even quantitatively explained by the increase of the concentration n(O) at the turbopause levels, i.e. on the basis of aeronomical processes. The anomaly series ends with a negative daytime disturbance in the F2-layer during the morning hours on September 2. In this way is established that the disturbances in the period of the geomagnetic storm and after it influence the entire ionosphere. Almost simultaneously the disturbances appear in the high and middle ionosphere. Later (by 1 - 3 days) they arise in the low ionosphere. This conclusion coincides with the previous results of Nestorov [1970].

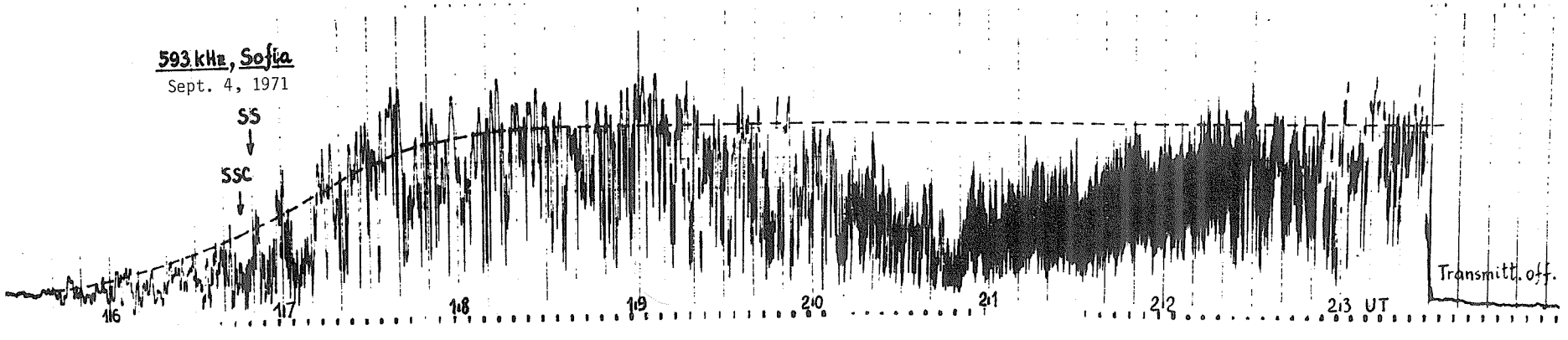

Fig. 3. Recording of the field strength of 164 kHz on September 4, 1971.

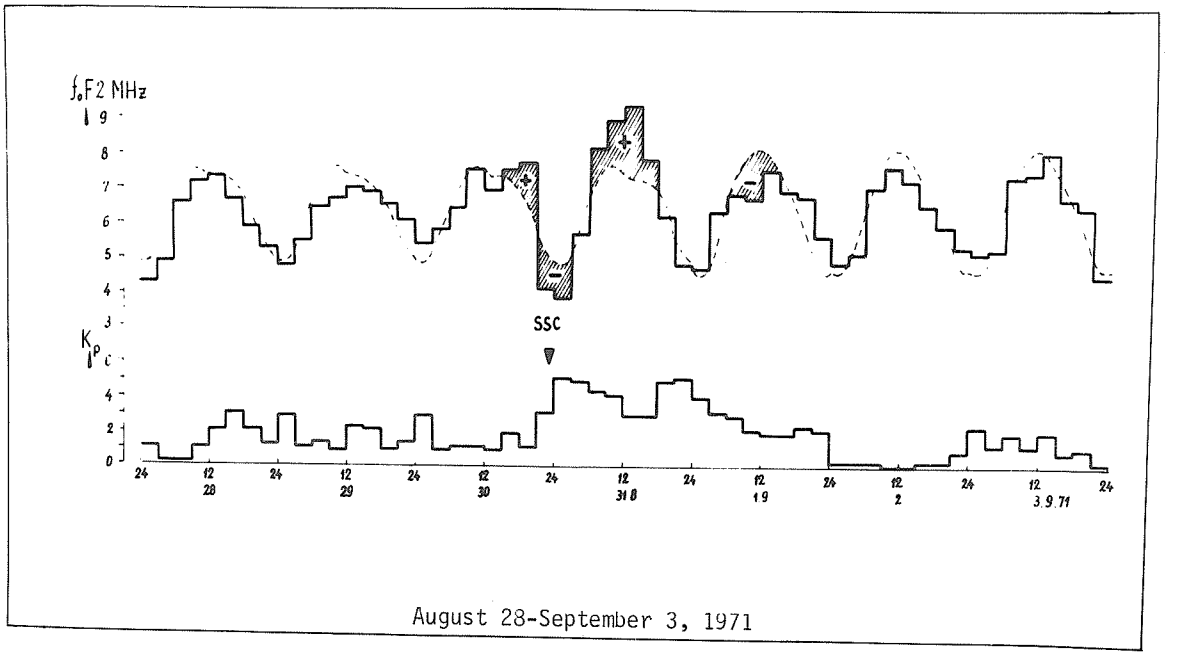

August 28-September 3, 1971

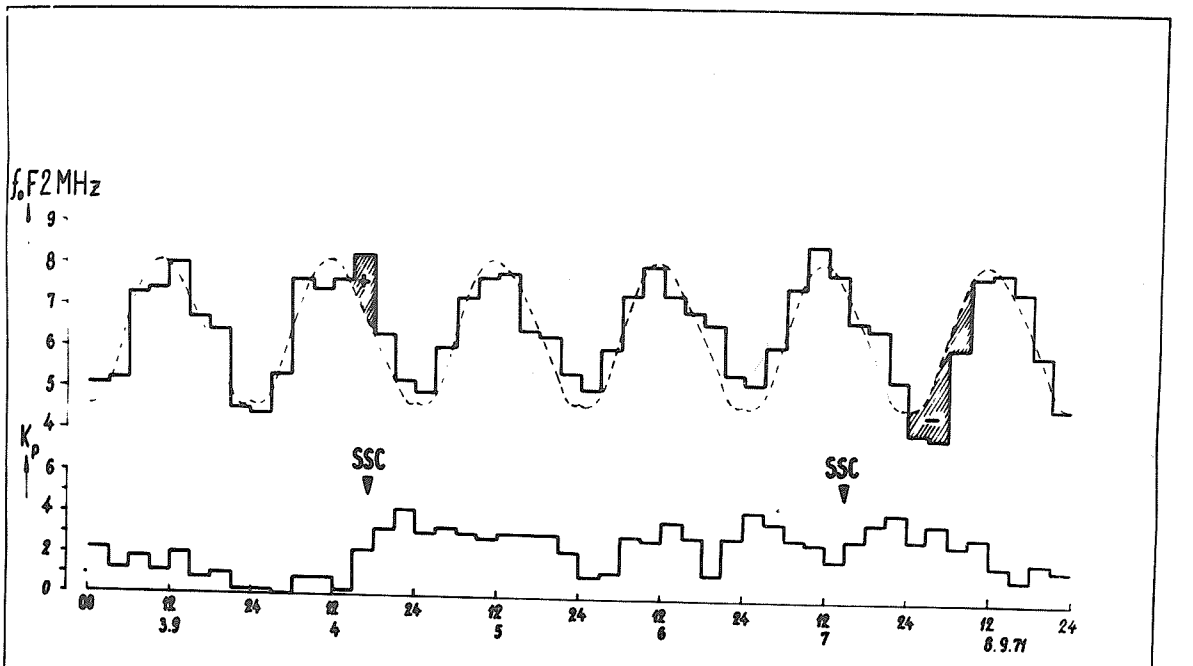

September 3-8, 1971

Fig. 4. 3-Hour values of the F2-layer critical frequency and geomagnetic Kp index during August 28 - September 8.

REFERENCES

FATKULLIN, M. N.	1971	Some Ionospheric Indications for the Disturbances of Neutral Gas in the Turbopause during Geomagnetic Storms, Acad. Sci. USSR-- IZMIRAN, Moscow, Preprint No. 14.
NESTOROV, G.	1969	Effects in the Night Lower Ionosphere at Middle Latitudes Caused by Solar Corpuscular Fluxes, Proc. Geoph. Inst. Bulg., 14, 53.
NESTOROV, G.	1970	Development of Ionization Processes in Night Ionosphere with Geomagnetic Storms, Compt. rend. Acad. bulg. Sci., 23, 149.
NESTOROV, G.	1972	Positive Disturbances in the Night Ionosphere at Mesopause Region during Geomagnetic Anomalies, Compt. rend. Acad. bulg. Sci., 25 (in press).
NESTOROV, G. and P. VELINOV	1969	Effects in the Night Lower Ionosphere as a Result of Particle Precipitation on Middle Latitudes, Solar-Terrestrial Physics, Acad. Sci. USSR, 1, 181.
NESTOROV, G. and P. VELINOV	1972	Ionospheric Effects from Solar Particles during January 24 - February 3, 1971, this compilation p. 240.
VELINOV, P.	1966	An Expression for the Ionization in the Ionosphere, Cosmic Rays, Compt. rend. Acad. bulg. Sci., 19, 109.
VELINOV, P.	1968	On Ionization in the Ionospheric D-Region by Galactic and Solar Cosmic Rays, J. Atmos. Terr. Phys., 30, 1891.
VELINOV, P.	1969	On the Influence of Corpuscular Fluxes in the Magnetosphere on Night Ionosphere, Compt. rend. Acad. bulg. Sci., 22, 33.
VELINOV, P.	1970	Solar Cosmic Ray Ionization in the Low Ionosphere, J. Atmos. Terr. Phys., 32, 139.
VELINOV, P.	1971	On Variations of the Cosmic Ray Layer in the Lower Ionosphere, J. Atmos. Terr. Phys., 33, 429.
	1971	Solar-Geophysical Data, 327 Part I, U.S. Department of Commerce, (Boulder, Colorado, U.S.A. 80302).

The Effects of a Solar Proton Event and Associated Geomagnetic Disturbance on the Phase of VLF Signals Received at Leicester, UK

by

J. W. Chapman and R. E. Evans
Department of Physics
University of Leicester
Leicester, U. K.

Introduction

This paper presents the effects of a period of enhanced solar proton flux and geomagnetic disturbance on the phase, recorded at Leicester, UK, of VLF radio signals propagated over medium and long distance paths. Details of the transmissions are given below.

Transmitter	Frequency (kHz)	Path Length (km)
Trinidad	12.0	7200
Aldra	10.2	1800

Aldra-Leicester is a high latitude path, the transmitter being situated in the northern auroral zone. The geomagnetic latitude (Φ) is less than 40° for about half the Trinidad-Leicester path and hence charged particle effects might be expected to have the least influence on the signals for this circuit.

The Disturbance of September 1971

All the available evidence suggests that this was a less severe disturbance than the January one (see page 237 this report). There is practically no data from ATS-1 during the first 3 days of the proton event (Figures 1d, e), but the maximum proton flux observed by the Vela satellite (3640 particles/cm^2 sec at 0400 UT on 2 September) was considerably less than for the earlier event (5640 particles/cm^2 sec at 0800 UT on 25 January). Comparison of ATS-1 measurements at the same time delay after the onset of the two events confirms that the flux is less for this event. The magnetic storm which began with a sudden commencement at 1646 UT on 4 September was only of relatively minor importance, Kp not exceeding 4^+ at any time (Figure 1c).

Figures 1a and 1b show that the ionospheric effects are small for the 2 paths monitored (dashed lines indicate limits of undisturbed phase variation). There appears to be very little effect on the Trinidad phase immediately following the onset of the proton event, and only a small phase advance for the night-time following the onset of the storm (maximum advance $\sim 0.1\ \lambda$ on 5-6 September). Rather surprisingly the effect on the Aldra-Leicester path is even smaller, night-time phase advance at no time exceeding $\sim 0.05\ \lambda$ and there is also only a small effect on the day-time phase. A possible explanation of this is discussed below. The absence of short period irregular fluctuations at night and lack of distortion of the diurnal variation on the Aldra records is further evidence that the ionospheric disturbance was a relatively minor one.

Discussion

Marked phase fluctuations at night were obtained on the 12.3 kHz Aldra-Leicester transmissions during the March 1970 event [Jones, 1971], and the lack of fluctuations during the September 1971 event suggests that the ionospheric disturbance at that time was not particularly severe. However, there is a small effect on the Trinidad phase, suggesting that a larger phase advance should be expected on a high latitude path. It seems possible that mode effects are involved for the Aldra-Leicester path, similar to the well-known effect on the 16 kHz Rugby-Rome transmission when phase retardation occurs as the reflecting region moves downwards during a solar flare [Burgess and Jones, 1967]. These 2 path lengths and frequencies are similar; there is a relatively small ($< \frac{1}{2}\ \lambda$) phase path change from day to night on both, and the shapes of the diurnal phase path variations are very similar. Further evidence for mode effects on the Aldra-Leicester path is provided by measurements at 13.6 kHz where there is very little change in phase path throughout the day. Calculations are being undertaken to determine which modes are important for the Aldra-Leicester circuits.

REFERENCES

BURGESS, B. and T. B. JONES (1967) Solar Flare Effects and VLF Radio Wave Observations of the Lower Ionosphere, Radio Science, 2, 619.

JONES, T. B. (1971) VLF Radiowave Observations of Ionospheric Disturbances during the Period 4-18th March, 1970, World Data Center A, Upper Atmosphere Geophysics, Report UAG-12, 247.

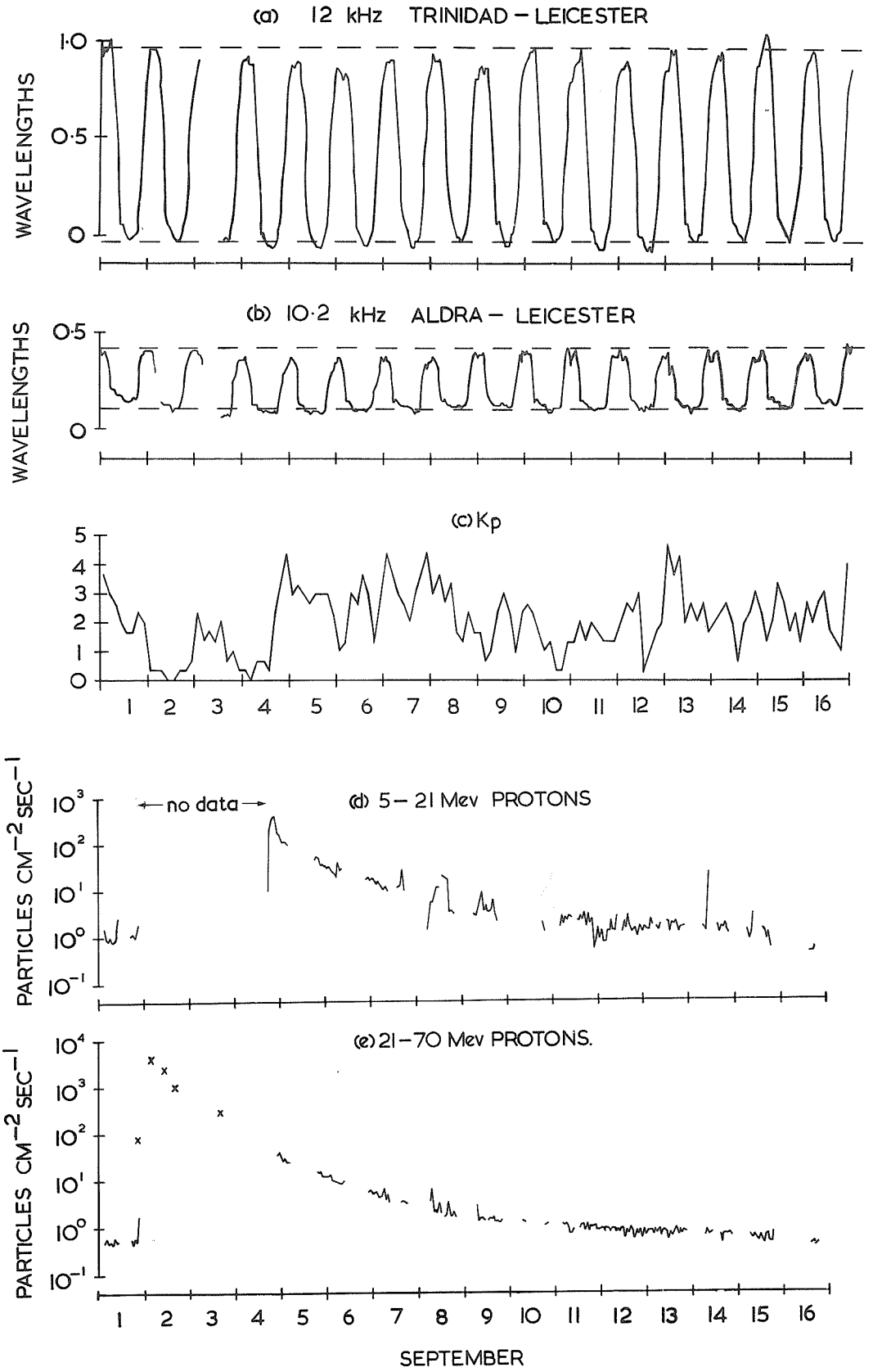

Fig. 1. DATA FOR THE SEPTEMBER 1971 EVENT. (a) and (b) VLF PHASE; (c) Kp; (d) and (e) ATS–1 SOLAR PROTON FLUX (CROSSES INDICATE VELA (>25 Mev) VALUES).

1971 Solar-Geophysical Data, 326 Part 1, October 1971, 327 Part 1, November 1971, U.S. Department of Commerce, (Boulder, Colorado, U.S.A. 80302).

7. AURORA

The Auroral-Zone Effects of the September 1 Event over Cola Peninsula

by

B. E. Brunelli, L.S. Evlashin, S. I. Isaev, L. L. Lazutin,
G. A. Loginov, G. A. Petrova, V. K. Roldugin, N. V. Shulgina,
G. V. Starkov, G. F. Totunova, and E. V. Vasheniuk
Polar Geophysical Institute
Academy of Sciences of U.S.S.R.
Apatity, Murmansk Region, U.S.S.R.

Description of the 1-4 September 1971 event is given here using the same set of stations, observational technique and the manner of presentation as in our previous report [Brunelli et.al., 1971]. Development of the September 1971 event was similar to the January one (see p. 247 of this report) but with less intense solar proton flux and geomagnetic disturbance. Sudden commencement of the storm seen here as two moderate negative bays was delayed from the solar proton burst for 68.5 hours. The data are presented in Figures 1-4.

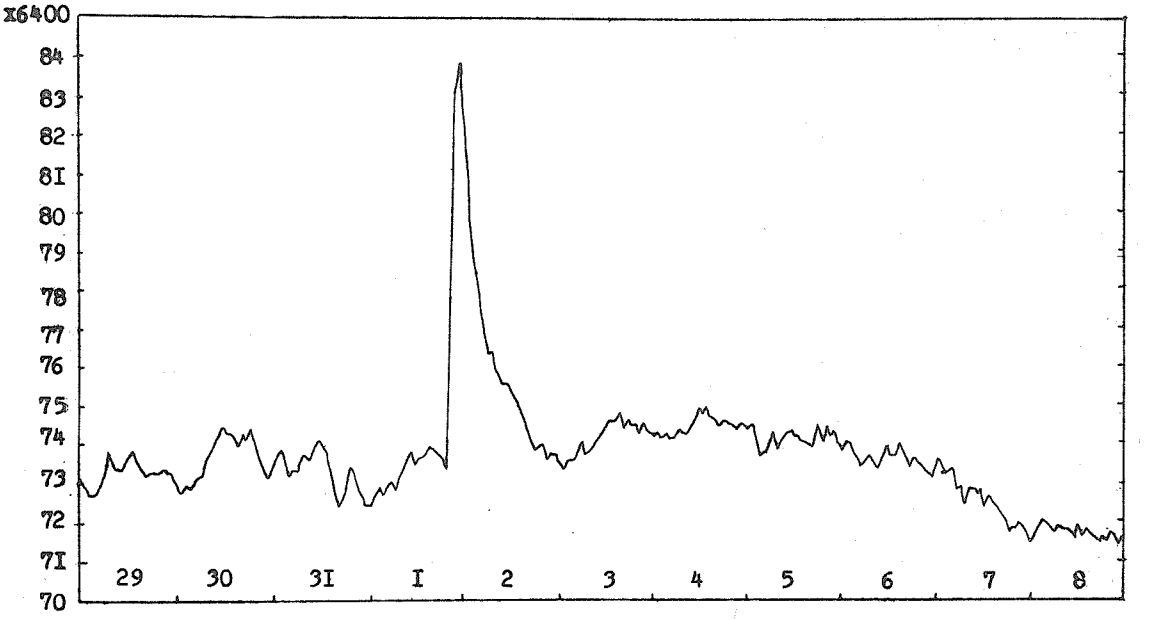

Fig. 1. Corrected hourly values of counting rate NM, Apatity, from August 29 to September 8.

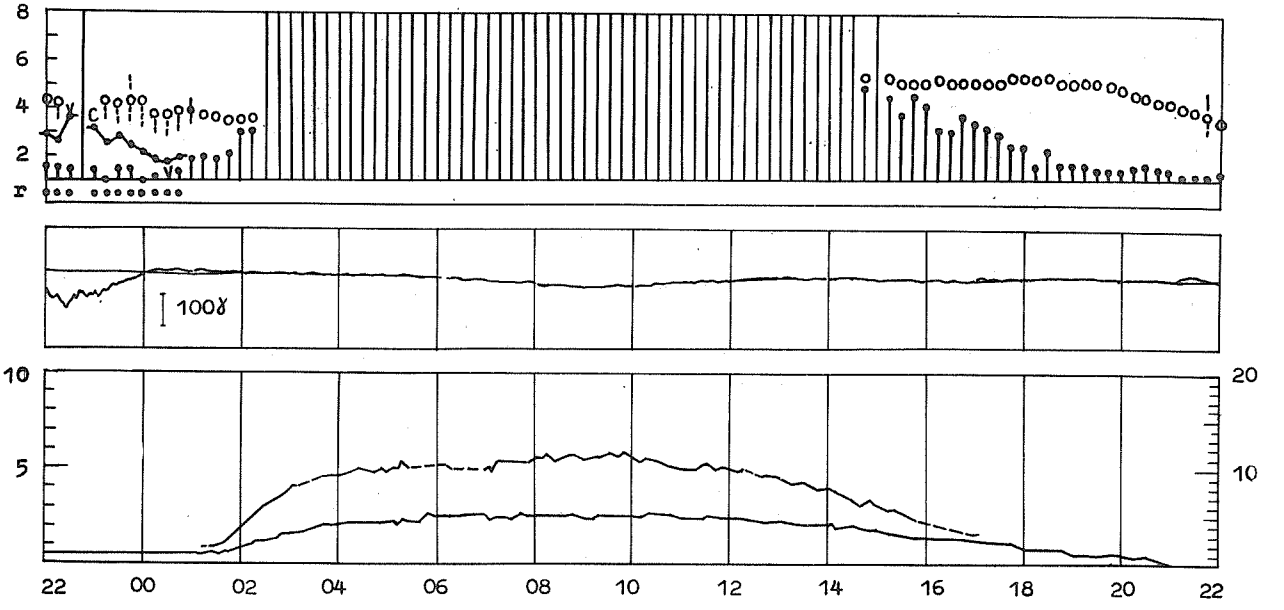

Fig. 2. Ground-based data, September 1-2: f-plot, ionosonde Murmansk; geomagnetic H-component on this day and undisturbed level; riometers 25 and 9 MHz left and right scales, respectively.

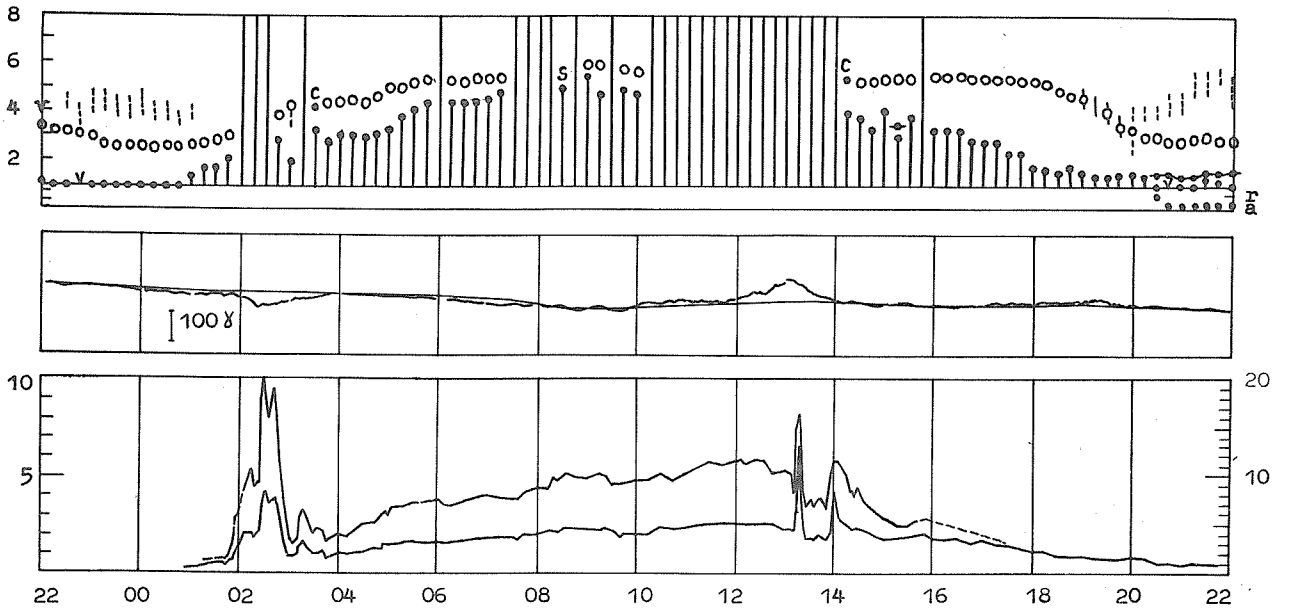

Fig. 3. The same as Figure 2, September 2-3.

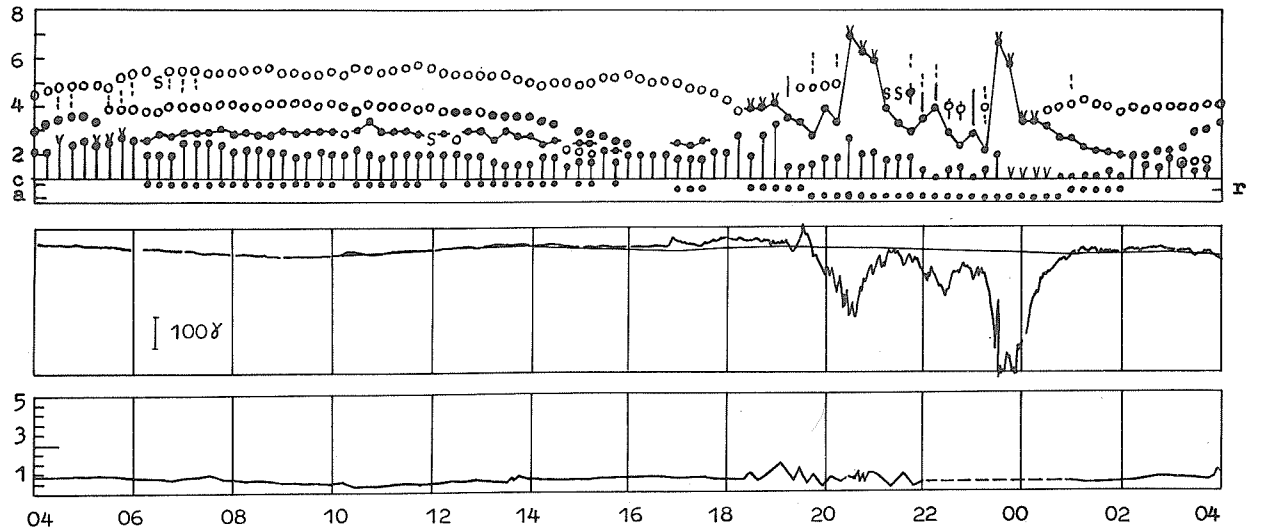

Fig. 4. The same as Figure 2, September 4-5.

Figure 1 presents Apatity neutron monitor data from August 29 to September 8, 1971. During this event the galactic cosmic ray background was fairly stable, no Forbush decrease was seen. The first 15-minute interval of enhanced counting rate at Apatity NM began at 2015 UT September 1. The geomagnetic field was quiet. In the ionosphere only a weak sporadic layer and the absorption near 0.5 dB at the frequency 25 MHz were observed. Gradual increase of cosmic noise absorption began at 0200 UT September 2, while the magnetic field remained undisturbed, Figure 2. This PCA event differs from the January one by showing a broader maximum due to the increase of the sunlit period. During the second day of event, Figure 3, September 3, the PCA value remains fairly large; in the morning hours PCA was mixed with the morning type of auroral absorption (AA), in the evening - with the second sharp increase of absorption, seen on all frequencies and accompanied by the small negative geomagnetic bay. On the third day after cosmic ray burst, Figure 4, September 4, a magnetic storm with sudden commencement at 1646 UT was registered. The main phase of the storm consisted of two negative bays accompanied by the appearance of a sporadic E-layer type "a" with large blanketing frequencies and sporadic structures in the F-region partially screened by the E-layer.

REFERENCES

BRUNELLI, B. E., L. S. EVLASHIN., S. I. ISAEV, L. L. LAZUTIN, G. A. LOGINOV, V. K. ROLDUGIN, G. V. STARKOV, N. S. SHULGINA, G. F. TOTUNOVA, and E. A. VASILKOVA 1971 Auroral-zone events of March 1970 on data of Cola Peninsula stations, World Data Center A, Upper Atmosphere Geophysics Report UAG-12, 325-336.

K-Indices for August 23 - September 11, 1971

by

D. van Sabben
International Service of Geomagnetic Indices
Royal Netherlands Meteorological Institute
DeBilt, Netherlands

The geomagnetic K-indices from the individual observatories for August 23-September 11, 1971 are given below. Please refer to IAGA-Bulletins 12 or IAGA-Bulletin 32 for definition of the symbols.

AUG	23	24	25	26	27	28	29	30	31
BT	5554 4363	4434 4455	5434 3334	4444 4454	3322 2223	3223 3343	4343 3323	4333 2334	6664 3456
CC	6444 4253	3223 3444	3223 2534	4343 4354	3111 1232	2112 2533	3132 3423	4212 2344	5443 2556
DI	6444 4454	3223 4655	3323 3447	6354 6565	3222 2243	2122 3443	3233 4324	4223 3355	6554 3577
TI	4344 4452	3333 4544	3323 3334	3478 8877	2221 1111	1123 7633	2233 3323	3234 3554	5455 3677
PB	1023 3411	1000 1232	3555 5533	3223 2355	5457 4443	3256 5532	2243 3332	2356 6564	---- ----
TR	6323 4333	3212 3334	3212 2336	6233 3455	2111 1123	2000 3422	3011 2214	5011 1234	7533 2366
GO	3224 4322	2223 3432	2124 3443	3224 3433	2111 2323	2123 3532	2033 3323	3124 3333	4344 4555
MM	7233 4242	1121 3223	1112 2206	7133 3465	1111 1122	1011 3421	2011 2212	4111 1123	5433 2476
KI	7223 4232	2111 1223	1112 3217	7113 3454	2212 1122	1112 2421	2122 2303	4212 2223	6533 2466
SO	7223 3242	2112 2223	2112 2226	7122 3353	1000 0123	1001 3311	2011 2202	3011 1223	5433 2465
WE	3332 4122	2222 3133	2212 1323	2255 4432	2010 1112	0101 2421	1111 1112	2111 1213	3355 2333
CO	2333 5220	2113 3222	2213 3222	3266 5521	1010 0100	0000 2411	1111 1100	1112 0112	3466 1233
RY	7532 3344	4422 3434	4322 3336	6344 -354	4221 2235	3112 3432	5121 2324	6121 2235	7653 3587
DO	5333 3222	2333 3323	2323 3324	4233 3242	1122 2222	1023 4422	3122 3322	3122 3213	5543 3355
YA	5422 3132	3324 4324	3431 3424	4355 3454	3322 1123	3112 3533	3222 3234	4212 1245	5444 2465
NU	4333 3231	1112 2333	1112 2213	3122 2242	1122 0111	0012 3321	2122 2212	3111 1122	4444 3355
LE	5322 3121	1101 2222	1112 2214	4221 1132	1000 0112	1001 2321	3010 2201	2001 1212	5432 2254
MG	4342 3232	2222 3223	2222 2224	3245 2343	3331 0123	2222 2422	2122 2222	3322 2233	4343 2354
LN	4334 3231	1122 2233	2212 3324	3122 3243	1122 2222	1122 3422	2123 3312	3122 2223	4444 3355
LO	4233 3221	1111 2233	1112 3324	4122 3243	1112 1112	1011 3422	2022 3312	3012 2213	5444 3355
SI	3331 3221	2222 2211	0000 0022	2155 2210	1010 0100	0000 1221	2110 2110	2112 1212	3465 1233
SV	4323 2231	1111 2323	1212 1213	3122 2232	1100 0112	1001 2321	2121 3211	3011 1223	4334 2244
RS	4333 3221	2212 2233	2222 2313	3233 2242	1110 0112	1011 3322	2111 3322	3111 1223	5444 3355
KN	4433 2131	2232 1323	2322 2213	4222 2241	1321 1112	1331 2321	2211 2211	3232 1123	4434 2254
MO	4333 3232	1222 2333	2223 3324	3233 3342	2222 2222	2222 2322	2222 3312	3122 2223	4434 3355
ES	4222 2221	1111 2223	1212 2213	3111 1132	2010 0212	1002 3322	3111 3312	3011 1223	5433 3345
ME									
HL	4444 4443	2224 4444	3334 4434	4233 4343	2222 2223	2123 4543	3233 4433	4123 3434	5444 4455
MN	4343 3232	1132 3233	2123 2313	3132 3242	1112 2211	1121 2321	2122 3212	2122 2223	4433 3253
WN	5333 2221	2112 2223	2212 2323	3122 2242	2110 1122	1112 2322	3112 3312	3112 1223	5444 3355
WI	5323 2332	2212 2333	2222 2323	4233 2243	2110 0122	1002 2422	3111 3312	3012 1324	5444 4355
IR	3343 3233	2232 3223	3323 3323	4233 2343	3221 1212	3221 2421	---- ----	2222 1133	---- ----
SW	4333 3231	2222 2333	2233 2323	3233 2342	2223 1222	2123 2322	2233 3322	3222 2223	4433 3355
NI	4333 2232	2112 2223	2212 2323	3122 2242	2110 1112	1002 2422	3121 3312	3011 1223	5434 3354
VL	5222 3232	1212 2333	1112 3323	4133 1343	2111 1212	1022 2332	3132 2321	3012 1213	5433 4355
BE	4324 3232	2322 2233	2323 2323	3323 2242	2323 1122	2223 2422	3223 3312	3222 1223	4434 3354
HA	4323 2232	2212 2333	2222 3323	4232 1333	2110 0212	1002 2332	3021 3322	3011 1313	5433 4355
KV	3222 2221	1112 2222	1122 1212	2122 2232	2121 2211	1112 2321	2112 2211	2221 1122	3322 2244
MA	4333 3232	2222 2233	2222 2322	3222 2223	2222 2222	2223 2322	3222 3322	3112 2323	5333 3354
DB	4223 2231	2211 2223	2212 2313	3232 2232	2111 1112	1002 2322	3111 3312	3012 1213	5333 3255
PR	4333 2231	2211 2233	2222 3323	3132 2232	2211 1112	1112 2332	2122 3312	3112 1223	4334 3355
LV	4333 3121	1111 2123	2323 2212	3233 2332	1213 2222	1223 4322	1223 2211	2122 1223	4433 3354
KD	2222 2212	1110 2100	0112 1222	3022 1222	1001 1012	1011 2112	1112 2210	3112 2223	3233 2243
VI	3332 3212	2232 3223	2212 2223	3245 2211	1010 1101	0011 2322	2122 3211	3121 0213	5455 2333
NE	4331 2212	2232 1223	2212 1323	3244 2122	1010 1102	1011 2322	2121 3211	3121 0214	4454 1234
FU	4323 2221	2112 2223	2212 2213	3122 2131	2110 0112	1001 1321	2111 2211	3112 1113	4333 2244
CF	4322 2231	1211 2223	2212 2223	3222 2333	2100 2222	1001 2322	3111 2212	3011 1213	5433 3254
HB	4333 3221	1212 2233	2222 2213	3243 3343	2212 1212	1123 2422	2222 3211	3112 0223	5444 3355
UB	4443 3232	2332 3233	3322 3323	5333 2343	3323 0222	3223 3432	3332 3322	4323 2233	5444 3354
JO	4222 2222	2222 1223	2312 1323	4132 2121	2011 1112	1012 1221	3121 2222	3222 1213	4433 2244

SA	4432	3333	3231	2325	4342	2322	2243	2332	3321	0224	3231	2434	3322	1234	4332	1224	5333	3235
TY	4333	4232	2112	3233	2212	3323	3233	3343	2112	2222	2112	3422	3212	3322	3023	2224	5534	3355
OD	4333	3222	1122	2223	2222	2223	3222	2232	1121	1112	2023	3422	2223	3322	3133	1224	4334	3254
KK	4333	3232	3333	2323	3333	3313	4333	3342	2343	2221	3342	3322	2233	2222	3432	1133	4334	3344
OT	4221	2222	3221	2133	2312	1224	4244	1022	2010	1111	1000	1321	2111	2211	3101	1113	4543	2245
SU	4343	3121	1111	2223	2222	2311	3043	1331	1122	1212	1213	2422	1132	3221	3122	1223	4234	3354
GC																		
MT	3332	3222	2221	2123	2222	2222	2233	2121	1110	0111	1122	2422	2222	2212	2221	1223	3343	2333
VK	3443	3223	3333	3233	3432	3223	3333	2332	3222	1112	4222	3423	3322	3223	3332	1224	5344	3343
AT	4433	3232	2233	2334	3223	3323	4233	2343	1243	2212	2232	3311	3332	3222	3332	2134	43--	3444
LG	5322	2221	2201	2233	2202	1223	3122	2232	2100	0113	2111	2322	3112	2312	4111	1214	5333	2266
AQ	4312	2132	2101	2223	1101	2223	3021	1132	1000	0112	2001	1322	2011	2212	3011	0213	4333	2155
TF	4444	4232	2343	2233	2443	3323	2434	3342	2443	3222	2444	4322	2434	2222	2333	3223	4444	3354
TK	3434	4322	2331	2224	1332	2214	3233	3342	2122	2222	2332	3312	3232	2223	3121	1124	4334	3354
IK	4323	2221	1111	1323	2112	2223	3122	1231	1110	0112	2112	2422	2112	3212	3111	1224	4433	3255
CI	4322	2121	2111	2233	1112	1323	3022	2132	1000	0101	2001	2422	2111	2211	3011	1213	4333	3244
TL	4222	1121	1211	2223	2111	2212	3122	1221	1110	0112	1111	2221	2111	1111	3011	1113	4333	2155
FR	4332	2122	3221	2233	2312	2223	4233	1121	2000	0102	2110	2221	2121	2111	3110	0113	5433	2244
PE	4342	2121	1111	2233	1101	1221	3011	1132	1110	0112	1111	1311	1111	2111	3111	1113	4333	2254
AK	3322	3332	2331	1112	1112	2111	3244	5433	----	----	----	----	----	----	----	----	----	----
SM	4333	2322	2332	2322	2323	2323	4232	2343	2222	2322	2222	3332	3234	4332	2232	3322	4323	2454
AE	4343	3231	2133	3333	2234	3323	3143	1231	2032	2103	2132	4412	2133	2212	3132	2213	4344	3455
SF	4433	3232	3211	3334	2123	3313	3233	2131	2200	1213	2122	3422	3213	3312	4213	1324	5544	4466
KA	3432	3222	1212	2123	1212	2212	2133	1131	1110	0111	1121	2421	2221	2211	1222	1213	4343	2333
KS	5442	1232	2122	2234	2211	1322	3122	2132	1110	0112	2112	2432	3232	3322	4132	2325	4334	3362
AV	4322	2221	1211	1133	1222	1313	3131	1131	2110	0111	1111	4311	2112	2212	3111	1213	3333	2244
DS	4432	3122	2321	3233	3322	3323	4243	2231	2110	1112	2121	2322	3231	2221	3222	2224	5544	3244
TU	4432	1212	1221	2223	2211	3313	4233	2121	2010	1101	2011	2322	2221	2211	3121	1214	5444	3243
KY	3432	3222	1212	2133	1211	1212	2133	1131	0100	0111	1121	3421	1221	2211	1122	1213	4334	3332
QU	3443	3231	1322	2123	1222	2223	2421	1341	1343	1113	2331	3322	3322	3222	2231	1222	4443	3353
ML	5543	4232	2332	3224	2322	2322	3342	2332	1232	2123	2333	3323	2332	3222	3344	3234	4444	4455
SZ	4333	3222	2111	3333	2112	3313	2132	1131	2110	2112	2011	3422	2112	2211	3112	3213	3333	3255
LP	454-	----	3422	2223	3432	2123	3333	2332	1111	1001	3222	3422	3322	3222	2322	2223	5344	3344
TA	4332	2131	2111	2133	1111	1223	2222	1132	2110	1113	2111	2312	---2	2222	3122	1124	4334	3254
HO	2322	1111	1010	1123	1111	1111	1033	1000	0000	0000	2001	1211	1111	2111	1010	0113	4343	2132
TE	5432	2322	2222	2333	3222	3324	4233	3332	2111	2322	2221	2332	3231	2213	3222	3224	5443	3243
AL	3432	3231	1222	2223	2212	2223	2333	2341	1211	1122	2111	3322	2222	2223	3221	2223	5333	3453
SJ	4332	1111	2210	1222	1201	2204	4122	1222	2000	0100	2011	2221	2121	2212	2111	0223	5433	2153
MB	3322	2221	2101	2223	1111	1213	2021	1022	2010	0011	2011	2321	2111	2212	3121	1113	4333	3244
MU	4542	4223	3332	2233	4423	2222	4344	2342	3222	2223	4422	3323	3322	3222	3332	2314	5444	3343
GU	3432	3221	3312	2123	3211	1112	3133	1221	2110	1101	2111	3322	2231	2211	1212	1214	5333	2223
BA	4332	3232	2222	2223	2122	2322	2232	2232	2121	2113	2221	2322	3222	3222	3122	1323	4234	3254
MC	4333	2221	2101	0223	1003	2313	2022	2221	1000	0002	2012	3422	3222	2323	3021	0223	4234	3254
TG	5552	3222	4333	2123	4333	2221	4354	2353	4441	1103	5341	3333	4351	2212	4342	0324	4444	3243
LU																		
PM	3432	3122	2122	2123	1111	1222	2133	2222	2210	1110	1101	2311	2221	2211	2221	1213	3233	2233
HU	3322	4331	1221	3333	2211	4433	3122	2221	1011	2221	1021	2432	1111	3422	1111	3323	5533	4443
PP	3322	0101	1010	01-2	1001	0002	2131	1000	----	----	0000	1221	0011	1000	1000	0002	5242	1032
TN	3231	3120	0111	2122	2113	2211	2022	2121	1021	2012	1122	2311	2021	1111	--22	1222	3123	2342
PI	4432	2222	3321	2323	3311	2314	4233	2243	2210	1112	2212	3322	3222	2323	3211	2223	5543	3354
GN	4321	2221	2122	2234	2111	1313	1133	3241	1110	0111	1011	1411	1121	2211	3111	1223	4343	2363
HR	4332	2121	3111	1223	1111	1112	3121	2031	1010	0002	1011	2311	2111	2101	3022	0113	4334	2354
AC	----	----	----	----	----	----	----	--33	2100	1201	1111	2422	2211	2312	2111	1---	----	----
TO	3322	3121	1223	3123	1212	2212	2044	2130	0110	0000	1000	1410	1111	2200	2111	1112	3343	2344
AM	3333	2110	2121	2112	2102	1101	1144	2220	0100	0000	1010	2311	1111	2100	2110	1102	3444	1333
TW	4332	1222	2221	1222	2210	2224	4123	2232	2000	0121	1122	2421	2212	2222	2111	1223	5432	3343
MI	2333	4120	1114	4112	1112	2---	2266	5533	1110	0001	0000	2501	1111	0001	1111	1102	3355	1333
MY	4554	2243	4433	2233	3443	2234	3442	2243	3331	1133	3332	1332	3342	3223	4443	2334	5565	3676
MW	7433	3244	3322	2255	4332	2336	5453	3364	3221	1124	2211	2332	3222	2225	5222	2245	7563	2377
NL	6332	2122	3211	1124	2212	1115	5332	2132	3101	0102	1001	1211	4111	1113	5222	1112	7742	2265
SB	4232	3222	2221	2223	3212	2232	3233	2233	0011	1111	1011	1312	2111	1102	3111	2223	4432	2344
VO	3323	3122	2222	2222	3222	2222	3232	2233	1221	1112	2111	1322	2222	2112	3222	1213	3433	2245

TABLE 1 THREE-HOUR-RANGE INDICES, K S E P T E M B E R 1971

SEP

	1	2	3	4	5	6	7	8	9	10	11
BT	5543 3554	3322 1223	4444 5253	3323 2445	4544 4543	3344 5545	4553 4645	5445 3433	3433 4633	3433 3332	3344 4332
CC	5323 3435	2111 1223	2233 5142	1112 2444	4334 6645	3335 5524	5343 5546	6334 5534	3333 4633	3233 3432	2133 4323
DI	6333 3556	3222 1223	3234 5252	2222 2466	5435 6676	3235 5545	7344 6666	6444 3565	3223 4734	3223 3333	2233 4444
TI	3444 3444	1111 1212	2235 4232	2222 2565	3436 7665	3345 5554	4454 7674	3353 2222	3444 5734	3334 4422	2334 4433
PB											
TR	7533 2366	5321 0102	3212 3122	0001 1356	5422 5465	2023 5325	5322 4466	5423 3213	3112 3434	4211 1114	2101 2333
GO	3234 3344	1121 2322	3234 4222	1122 1433	3234 5433	2134 5533	4334 4433	3223 4322	2223 4433	3233 3211	1233 4332
MM	5222 1243	1011 0001	2212 3121	0111 1255	5233 5554	1123 5415	6232 4566	6223 2142	1013 3314	3111 1011	1011 3222
KI	6222 2243	2111 1002	3222 3111	0011 1257	6322 5555	1122 5426	6222 4566	5323 3232	2002 3334	4121 2102	1012 3222
SO	5211 2243	1000 0001	2211 3121	0001 0256	5222 5554	1012 4325	6222 3565	5323 2232	1112 3323	3111 1112	1101 3322
WE	3332 3112	0000 0111	1123 4112	0110 0233	2346 6632	1134 6523	3243 5643	3335 3321	1112 2421	1133 2101	1223 3222
CO	3333 3112	1000 0000	1134 4000	0000 0122	2346 6622	1145 5512	3345 5623	2345 3211	2112 3311	1134 3000	1225 4210
RY	6532 3345	2121 1112	5432 2232	2121 2357	6553 4453	3132 4436	6533 4566	5533 2334	4222 3326	5422 2213	3222 2333
DO	3333 3333	1222 2112	2332 2121	1122 2345	3322 3343	1132 4313	5333 3345	3223 3232	2123 4313	3221 2112	1222 3322
YA	5444 4243	1322 0112	3322 3133	2312 1356	3435 6544	3334 5435	4555 5655	4536 4333	3222 4424	3344 4213	2234 4242
NU	3222 2223	1011 0001	2101 2020	0112 1224	2223 3342	1032 4313	4322 2344	3212 2132	1012 3412	3221 1102	1111 1222
LE	4321 2222	1000 0001	2210 1110	0000 0235	4321 2333	0021 3213	4211 2344	3212 1132	1001 3212	3100 1002	1100 1111
MG	4343 3233	3221 1123	2323 3123	3321 1335	4434 4344	4334 3334	4344 3444	3426 3323	3333 3434	3333 2213	2223 3232
LN	4233 2223	1112 2112	2123 2121	0122 2334	2323 3352	1133 3323	4333 3354	3324 2233	1123 4413	3222 2112	1213 2333
LO	3222 2333	0000 1101	2122 2110	0112 2224	3322 3343	1133 3313	5332 2344	3223 2232	1113 3313	3212 1112	2212 3333
SI	2331 1012	0000 0000	1122 2000	1000 0233	2335 4421	1133 3222	2344 3423	2444 1211	1112 2211	1232 2000	1114 3210
SV	3221 2232	0000 0001	1022 2010	0000 0234	3323 4432	1123 3323	3232 3333	2223 2232	1012 3412	2111 1101	0011 2222
RS	3222 2232	0000 0101	2112 2111	0011 0324	3333 3343	1133 3423	4322 2345	3222 2232	1112 3323	3212 2112	2221 2333
KN	4322 2232	1232 1111	1234 2121	0233 2235	2434 3341	1223 3322	3332 2343	1324 1231	1232 3412	3222 1101	1122 2322
MO	4233 2233	2221 2112	2222 2121	1222 2334	2333 3342	1233 3423	4332 2344	3333 2232	2123 3423	3223 2112	1222 3333
ES	3222 2232	1000 0101	2111 2111	0001 1334	3222 3333	0121 4323	4322 2344	3323 2132	2112 3212	3211 2112	2211 2232
ME	3343 2222	1111 1212	2132 3221	1011 1224	3456 3322	2245 4323	4365 3333	3566 2221	2112 2222	2342 2211	1125 2212
HL	4334 3343	2222 2222	3232 3232	0132 2444	4333 4443	2343 4423	4343 2444	3334 3342	2224 4423	4333 3323	2323 3332
MN	3223 3232	1023 2202	2133 3211	1033 3323	2323 3342	1133 3323	5332 3344	3223 2232	1113 3412	3223 2112	2221 3332
WN	4222 2333	1111 0111	2121 2111	1111 1334	3322 3342	1122 3313	5323 2345	3322 2132	2113 3313	3211 2112	1212 2222
WI	4232 2342	0000 0112	2111 2121	0011 1335	4332 3343	1133 4423	5332 3345	3323 2232	2013 4313	3211 2113	1212 2232
IR	---- ----	2232 1112	3342 2122	2222 1344	3334 5443	3343 4323	3344 4443	3334 3322	2323 3422	3223 3322	3223 3232
SW	3233 3233	1122 2112	2222 2221	1123 2334	3233 2342	1132 3323	4333 2344	3333 2232	1123 3323	3222 2222	1232 2232
NI	4222 2233	1010 0112	2111 2121	0011 1334	3233 3343	1132 3323	4322 2345	3323 2132	1113 3313	3111 2112	1212 2222
VL	4222 2232	1011 1101	2112 2111	1012 2234	3223 3343	1123 3313	4332 2345	3322 1131	1112 3223	3223 1112	1213 2222
BE	3323 1333	1222 1212	2222 2221	0123 2334	3333 3342	1232 3323	4323 3344	3323 2232	2224 3423	3222 2112	2222 2233
HA	4322 3232	0000 0101	2111 2111	0002 0334	3232 2343	0122 3413	4322 2345	3322 2132	2013 3223	3211 2002	2212 2222
KV	3222 2122	1112 1211	2123 2110	0122 2223	2223 3332	2122 3322	3222 2233	2222 1222	2222 2312	2212 1101	1222 2222
MA	4322 2232	1000 0011	2222 2121	0000 0334	2223 3342	2222 3423	4332 2335	3333 2232	2103 3322	3221 2112	2222 2222
DB	4332 2232	0000 0101	2121 2111	0011 1334	3233 3343	1123 3413	4332 2345	3333 2231	2123 3323	3212 2112	1222 2222
PR	4222 2233	1022 1111	2122 2111	1122 2334	3333 3332	1132 3323	3322 2344	3322 2232	1112 3312	3112 2212	1222 2222
LV	3324 1232	1212 1111	1222 2111	1223 2234	3233 3332	1222 3323	3233 2233	2323 2131	1123 3212	2111 2111	1331 3322
KD	2222 3232	1021 0000	0221 3010	0112 2234	3323 3434	1103 4313	2221 3343	2322 1222	1221 2403	2122 1000	1222 1212
VI	4432 1112	0000 0000	2112 3000	0010 0234	2444 3322	2244 3213	3353 2323	2455 1111	2122 3302	2332 1000	1224 2110
NE	3332 2123	1000 0001	2122 3111	0010 0334	3444 3222	2234 3223	4442 2323	2445 2211	2112 2312	2232 1101	1224 1111
FU	4212 1232	1010 0101	2111 1010	0011 1223	2222 2232	1122 2213	4222 2234	2212 1131	1112 2312	2111 1102	1112 1122
CF	4222 1232	0011 1101	2121 1111	1022 1234	3222 3343	1122 3313	4321 2245	3323 2131	2012 3313	3112 1112	1112 2332
HB	4323 2233	1112 1201	2222 2111	1133 2335	3333 3343	1232 3423	5333 3345	3322 2132	2103 3413	3121 1101	1212 3332
UB	3343 3232	3333 1112	3333 3123	3332 1345	3335 5444	3343 5434	3344 4544	3335 3332	3223 3523	4232 2222	3223 3332
JO	5322 1122	0011 0111	3221 1121	1111 0234	3332 3332	1132 3223	3323 2334	3332 3221	2012 2222	3221 1111	2222 2121
SA	3332 2122	2330 0012	3232 2011	2321 0234	3434 4433	4333 2433	4333 2433	3334 2223	3222 2322	3232 0122	2232 2233
TY	4333 3232	2233 2211	2333 3221	1233 3335	3334 3343	2233 3423	5343 3453	3333 3332	2223 3313	3333 2112	1323 2332
OD	4223 2232	1111 0101	2122 2011	0122 1335	3334 3342	1233 4423	3233 3333	2223 2232	2123 4423	2222 2212	2222 2232
KK	2222 2221	0221 1101	2223 2011	1233 1223	2322 3331	1122 3312	2222 2222	1222 1121	0222 2311	1222 1101	1222 2221
OT	3333 1123	0000 0001	3222 2001	0010 0244	2443 3232	1143 3313	4434 1234	2534 2121	2011 3223	2231 1001	2233 2010

SU	4322	1232	0101	2111	1213	2110	0121	3235	3334	4331	1223	4323	3232	3233	1312	3232	2112	4212	3113	2112	1323	3322
GC																						
MT	2222	2122	0000	0001	1111	2010	0110	0234	1335	4422	1233	3213	2233	2422	1234	2221	1122	2412	2112	1101	1112	2221
VK	4433	2223	3322	2123	3222	2123	3332	2345	2345	4433	3343	3434	4354	3434	3335	3323	2343	3424	3333	2212	2333	3233
AT	----	----	----	----	-343	3121	1343	3344	3434	5442	2333	4323	3-33	4433	2334	2232	2222	2412	2232	32--	----	3331
LG	--11	----	----	----	----	----	----	----	----	----	----	----	----	---5	3312	2232	2112	3213	3210	1112	1210	1122
AQ	4311	1132	1000	0001	2111	1010	0000	0234	3222	3342	1122	3313	4221	2244	2212	1032	1002	3312	2100	1002	2201	1122
TF	3444	2232	1334	2112	1443	2111	1333	2335	2442	4332	1332	4423	3434	4233	2434	3232	1334	4222	2333	3222	2333	4322
TK	3333	1222	2221	1022	2231	2011	2220	1344	3334	3343	1222	3312	3333	3244	2224	1130	0211	3422	2221	2112	1332	3322
IK	4212	2233	1001	0111	2111	2111	0011	1335	3223	3342	1212	431-	---2	333-	2313	2132	1112	3312	2111	2112	1212	1222
CI	4222	2222	0000	0000	2111	1000	0000	0234	3222	2232	0111	3313	3322	2334	3322	1021	1002	2212	2100	1001	1112	1121
TL	4211	1132	1000	0101	2111	1111	0011	1135	3222	2332	1121	2313	3221	1234	2212	1121	1101	1212	2111	1112	1212	1121
FR	4332	1122	1000	0000	3123	2111	0011	0244	3433	3232	1233	3223	4432	2234	3433	2122	2112	3212	2231	1001	2233	1012
PE	4111	1132	0000	0101	2110	1011	0111	0235	3211	2232	1211	2213	4211	1133	2212	1121	1111	3312	2111	1112	1112	2121
AK	----	----	----	----	-111	1011	1123	2223	1123	3331	----	----	--22	1432	1213	1111	0212	2101	1221	1112	2311	3211
SM	3222	2332	2222	3222	2223	3222	2233	3225	4333	3233	2233	2323	3332	2344	3333	3222	2223	2222	4332	3222	2333	3222
AE	4343	2231	1033	2301	3323	2311	0033	2335	3232	4332	2132	3322	3344	3324	2233	2122	2124	4323	3132	2211	2233	3232
SF																						
KA	2222	2121	1000	0000	1001	1010	0110	0234	2235	3412	1233	3212	2233	2422	1224	2221	1112	2422	2112	1100	1012	2221
KS	4313	2242	0011	1102	2010	2011	0011	1345	1143	4432	1212	3212	3232	2224	2223	2231	1012	4322	1111	2222	2212	2132
AV	3321	1122	1011	0111	2111	1111	0101	1234	2222	3233	1221	2213	3322	2244	2222	1122	2012	2212	2111	2101	1111	1222
DS	4332	1112	1110	0001	2122	2111	0020	0244	4433	2221	2242	3324	4432	2234	2434	2121	2222	3213	3231	2001	2223	2111
TU	4432	1212	1000	0000	2122	3001	0020	0234	3334	3232	2233	3213	4442	2233	3444	3111	1122	3212	2231	1000	2223	1122
KY	2222	2122	0000	0000	1011	1011	0011	1233	2325	3322	1233	3312	2232	2422	1224	2211	1112	2412	2112	1101	1012	3221
QU	2334	2221	1223	0001	2231	3010	2223	1334	2433	3332	1232	3312	3334	3343	1233	1131	1323	3312	2222	1111	1322	3221
ML	4434	3232	1333	3222	2332	3222	2332	2345	4433	4333	2342	4324	3444	4333	2354	3233	2333	4223	3334	2222	2354	3233
SZ	4222	2132	1012	1101	3211	2211	0012	2342	3233	2321	2222	3213	4323	3324	2224	2122	2112	4312	2112	3211	2113	3222
LP	3322	2122	2222	1112	2222	2122	2121	2334	3535	3423	2335	3323	3433	3333	3323	2223	3222	3423	4322	2113	4423	3222
TA	4321	1232	1001	0111	3211	1010	0111	0235	3323	3232	2222	2222	3321	1223	2233	1122	2112	3213	3111	1111	1211	1132
HO	2222	0011	0000	0000	1111	3000	0010	0243	1112	2121	1212	1212	1322	1212	1333	1110	1111	2212	1121	1100	1012	1111
TE	3433	3122	3111	3322	2222	3222	1121	1444	3433	3343	2242	4334	4333	3444	3433	4332	2222	4123	3332	2222	2323	2233
AL																						
SJ	3211	1112	0000	0101	2012	1000	0010	0233	3323	3234	1232	2213	4322	2133	3323	1110	2001	1110	2210	1100	1112	0022
MB	3211	1121	1000	0011	2211	1011	0010	0234	1222	3333	1212	3323	4312	3334	3212	1122	2012	3322	2101	1101	1111	1022
MU	3322	2222	2332	0102	3322	3123	3322	1334	3434	3333	2334	3313	2323	2332	3333	2222	3212	3422	3312	2212	3332	3322
GU	3221	2112	1110	0101	1111	2011	0110	0234	2224	3311	2223	3213	3222	2313	2223	2111	2112	2322	2112	1111	2111	2221
BA	42--	-232	1111	0112	3221	1121	1121	0235	3233	5232	2222	3222	3232	2223	2223	2222	2122	3212	2101	2112	2222	2122
MC	4222	1132	0000	0112	3212	2111	0010	0245	4223	4331	1212	3223	4223	3334	2123	2122	2122	3222	2100	1001	2102	4222
TG	3341	2223	4440	0112	2340	3122	4340	0333	4554	3333	3354	3312	3352	2343	3453	2022	3343	3403	3341	1212	2353	3333
LU																						
PM	4221	2122	1110	0012	2211	2012	1120	1233	3234	3322	1233	3222	3332	2322	2333	2112	2222	2412	2222	1111	2111	2121
HU	3212	2323	1101	2221	21--	-220	0111	2444	3333	4432	1121	4423	4311	3334	3322	2220	1112	4312	1221	2221	1222	2321
PP	3321	0001	0000	0000	1112	2000	0000	0233	2333	1011	0122	1011	2222	1110	2332	0000	1001	2101	1211	0001	2222	1010
TN	2031	2122	2101	1101	1131	3001	0010	1124	2123	2131	2122	2212	2221	3333	2223	2120	1023	2011	1011	2001	1131	1010
PI	3321	1223	1110	1112	3222	2212	0121	1344	4432	3344	2232	3324	4322	3344	3432	2223	211-	4223	2221	2212	2222	2242
GN	3222	2332	1010	0001	1111	3021	1000	0234	2234	4342	1223	3323	2232	4433	1223	3221	1111	2411	1011	1110	1011	2121
HR	4221	0132	0000	0001	2011	1010	0011	0235	3324	3332	1123	3113	3332	2334	2122	1021	1022	2213	2111	1001	1133	1021
AC	----	----	1000	0000	2111	1010	0010	0333	3322	3233	2232	3333	4321	3334	3322	2122	2112	3222	1211	1111	2111	2232
TO	3232	2112	0100	0001	2221	3010	0000	1223	3324	4332	1233	3312	2332	3432	----	----	1112	2311	1122	1100	1222	2111
AM	3332	1111	0100	0000	2122	3010	0000	0123	1234	3211	2233	3202	2333	2321	2334	1112	1111	3202	2122	1000	1122	2000
TW	3221	2212	1000	0001	2210	2110	0021	1234	3432	3243	1232	2324	4321	2334	3322	2121	2112	3222	2220	1110	1212	2221
MI	3232	3011	1000	0001	1135	4001	1101	0122	1346	7722	1135	---2	3344	5633	2345	4311	1112	3411	2124	3012	1224	4110
MY	4454	3464	2333	1233	3343	3243	3333	1244	3454	3343	3455	3334	4454	3334	3454	3244	3343	3322	4345	2222	3343	2222
MW	6543	2365	2221	1124	5434	4244	3211	1366	6554	3566	2243	3336	6434	3465	4543	4345	4223	4334	4532	2225	4433	4334
NL	5422	1133	1111	1111	4221	1111	1111	1245	4542	2233	1133	2214	4422	1346	3422	1122	211-	2213	3212	1002	2222	1111
SB	3332	2322	1221	1222	3322	3221	1010	0223	2323	3322	3133	3323	3333	2322	3333	2222	2112	2222	2211	1111	1223	2222
VO	3332	2233	2222	2112	3232	3222	1122	1223	3333	3333	3333	3313	3333	3323	3333	2222	3222	3312	2222	2111	2222	2222

Provisional Equatorial Dst

by

M. Sugiura
Laboratory for Space Physics
Goddard Space Flight Center, Greenbelt, Maryland 20771

Provisional equatorial Dst is plotted below for the period August 27 to September 7, 1971. The Dst data presented here are provisional. The base line, which is based on extrapolations of the base lines for the four observatories, Kakioka, Hermanus, San Juan, and Honolulu, from the 1957-1970 series [Sugiura and Poros, 1971], will be redetermined later when the final Dst values are calculated.

REFERENCE

SUGIURA, M., and D. J. POROS 1971 Hourly values of equatorial Dst for the years 1957 to 1970, Goddard Space Flight Center, X-645-71-278.

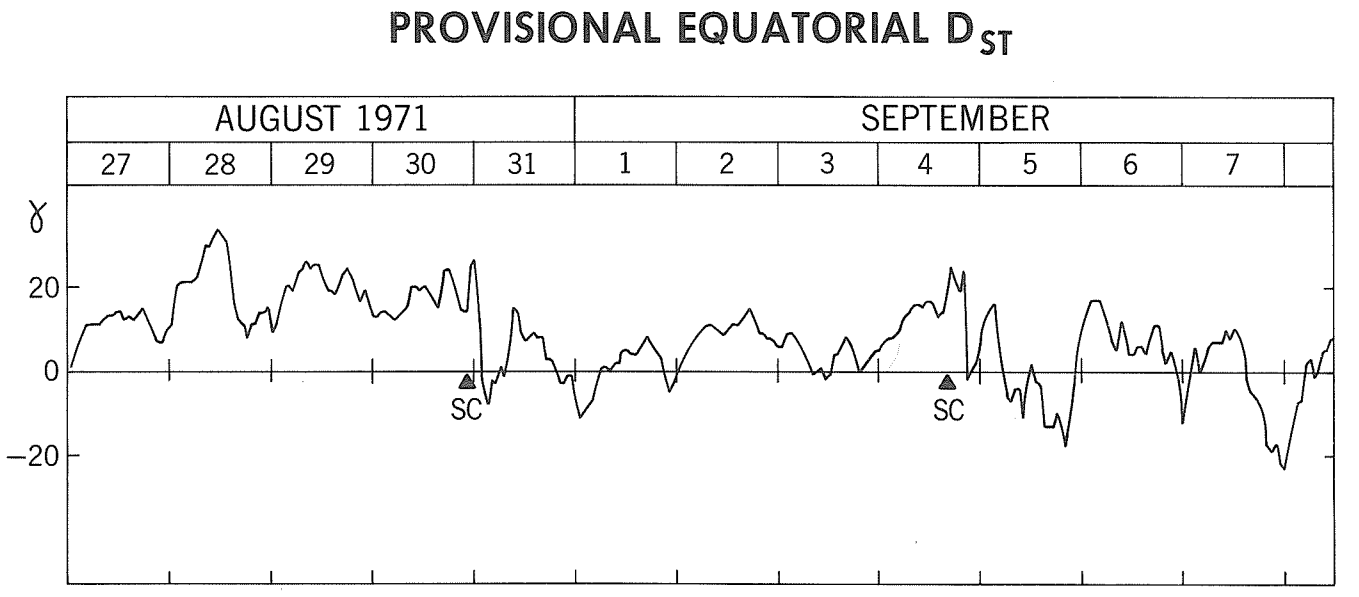

Geomagnetically Active Plages and Flares Observed during the Interval Including September 1, 1971

by

M. C. Ballario
Osservatorio Astrofisico di Arcetri
Florence, Italy

Abstract

The moderate geomagnetic disturbance observed on September 1 (Kp max = 5), 1971, is related to an importance 2 flare recorded on August 30 (Time-lag of about 2 days).

The other geomagnetic storms and disturbances observed during the interval August 14-September 20, including the selected day, are well-correlated either with CMPs of positive plages or with occurrences of "specific flares", namely proton flares (Figure 1).

Introduction

Solar phenomena occurring during the interval August 14-September 20, 1971 are examined.

In Figure 1 are marked:

A. The CMPs of all recurrent and non-recurrent plages as given in the McMath calcuim plage list ("Solar-Geophysical Data", Part I, Boulder, Colorado).

B. The CMPs of recurrent positive plages only.

The positive plages are never associated, before the meridian transit, with spot-groups type C or greater but, at the most, with spot-groups type A or B (spots without penumbra).

The CMPs of positive plages are generally associated with geomagnetic storms or disturbances; the correlation being about 78% [Ballario, 1970a].

On the contrary the negative plages are associated, before the meridian transit and at least for part of their life, with spot-groups type C or greater (spot with penumbra).

The CMPs of negative plages, as well as their CMPs in the subsequent rotations, are generally associated with quiet or slightly disturbed geomagnetic conditions [Ballario, 1970a], unless a resurgence takes place.

It is also seen that the CMPs of non-recurrent plages, whatever the associated spot-group type may be, are geomagnetically inactive.

The subdivision into negative and positive plages, depending on the associated spot-group type, is based on the Fraunhofer Institut Solar Maps.

The plage subdivision into recurrent and non-recurrent is given in the McMath calcium plage list. However, we have to note that, particularly when the active centers show only very small and negligible plages which appear and disappear during their life, some classified non-recurrent plages may be considered as recurrent ones. Thus, in this regard, some changes have been made.

C. The geomagnetic index Kp (Bartels).

D. The geomagnetically active flares.

We are not able, at present, to give the characteristics distinguishing the geomagnetically active flares from the inactive ones. Only "a posteriori" we may correlate geomagnetic storms and disturbances with flare occurrences.

In a previous paper [Ballario, 1970a] we have found that 48% of importance 2 and 3 flares, 53% of importance 1 proton flares and 21% of importance S proton flares were followed by geomagnetic storms or disturbances with Kp maximum value $\geq$ 4+ (time-lag of about 2 days), while the others were followed by quiet or slightly disturbed geomagnetic conditions. On the other hand it is well-known that importance 1 and S flares are geomagnetically inactive.

In some cases the geomagnetic storms or disturbances are related both with CMPs of positive plages and with flare occurrences. Only when there are not CMPs of positive plages associated with the disturbance, can we consider the flare entirely responsible for the disturbance itself.

E. All the flares observed as given in the Quarterly Bulletin on Solar Activity.

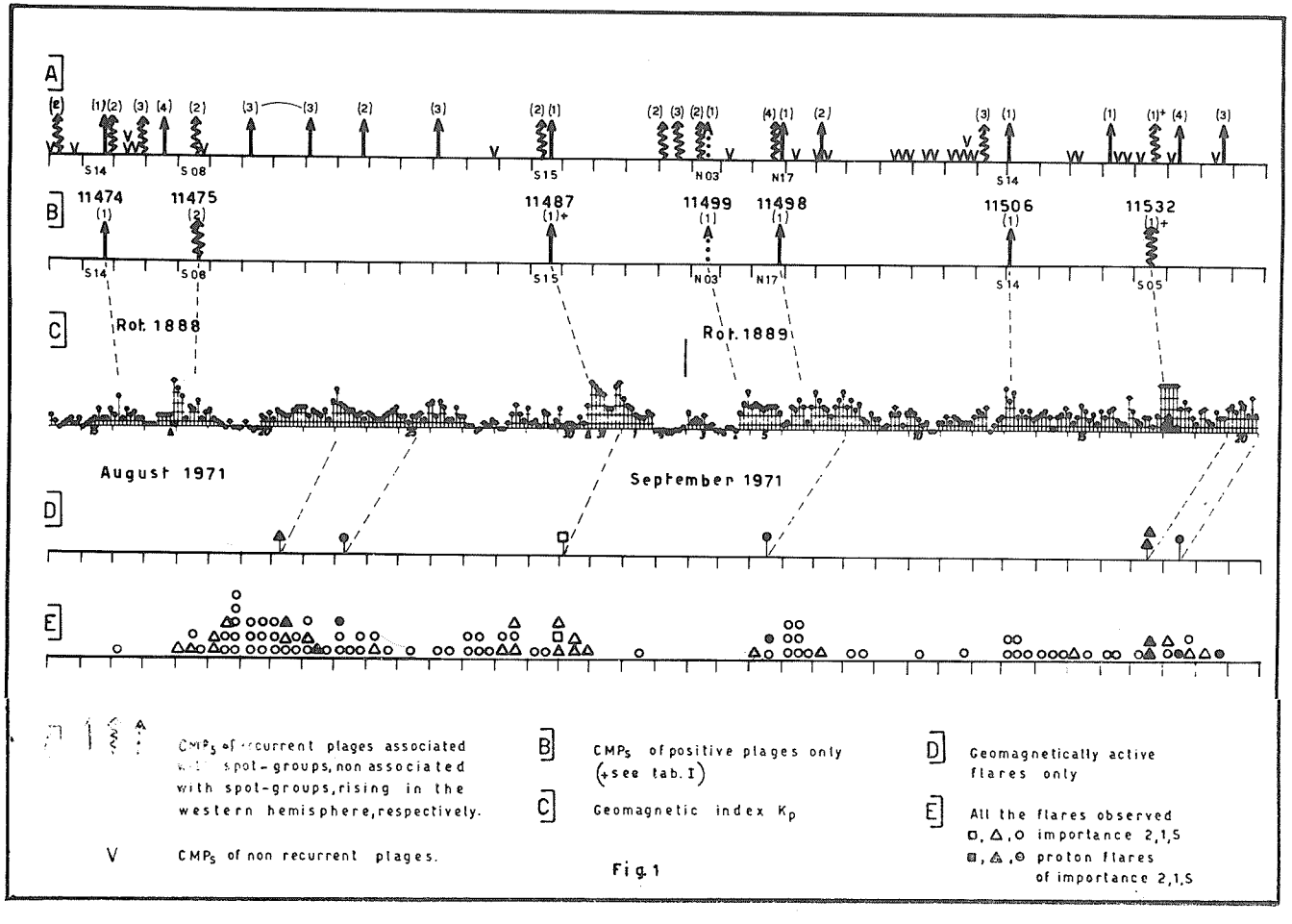
A
B
11474
11475
11487
11499
11498
11506
11532
S14
S08
S15
N03
N17
S14
S05
C
Rot. 1888
Rot. 1889
August 1971
September 1971
D
E
CMPs of recurrent plages associated with spot-groups, non associated with spot-groups, rising in the western hemisphere, respectively.
V CMPs of non recurrent plages.
B CMPs of positive plages only (+see tab. I)
C Geomagnetic index Kp
D Geomagnetically active flares only
E All the flares observed □, △, ○ importance 2,1,S
■, ▲, ● proton flares of importance 2,1,S

Fig. 1

The Events of August 14-September 20

Plages

The CMPs of recurrent and non-recurrent plages observed during this interval and their subdivision into positive and negative plages are presented in Table 1 and marked in Figure 1A.

The positive plages are 7 in number and are marked in Figure 1B.

Broken lines relate the CMPs of positive plages with geomagnetic storms or disturbances (Figures 1B-1C).

Flares

The data referring to importance 2 flares and importance 1 and S proton flares are presented in Table 2. They are 9 in number and seven of them (two of which occurred in the same day) are followed by geomagnetic disturbances.

These geomagnetically active flares are marked in Figure 1D.

Broken lines relate the maxima of the flares with the maxima of the disturbances (Figures 1D-1C).

Conclusion

From Figure 1 it is seen that the geomagnetic storms and disturbances recorded during this interval are related either to CMPs of recurrent positive plages or with flare occurrences.

Particularly we note:

1.) The moderate disturbance of September 1 (Kp max = 5) is entirely due to the importance 2 flare recorded on August 30 (time-lag of about 2 days), since no CMPs of positive plages are correlated with the disturbance itself.

2.) The sc disturbance of August 31 and the storms of August 17 and September 18 are correlated with the CMPs of the recurrent positive plages McMath Nos. 11487, 11475, 11532 respectively.

3.) The geomagnetic disturbance of September 5 (Kp max = 4+) is not preceded by any reported flare for more than 3 days. It is correlated with the CMP of the recurrent positive plage McMath No. 11499 rising in the western hemisphere. During its central meridian transit this center of activity does not show chromospheric-photospheric phenomena, but appears to be geomagnetically active. Thus we think it possible to identify this center as a Bartels "M solar region".

The results here obtained are in good agreement with those found in examining the solar and geomagnetic phenomena recorded during the year 1968 [Ballario, 1970a] and in other selected intervals [Ballario, 1969a, 1969b, 1970b, 1971, 1972].

REFERENCES

BALLARIO, M. C. 1969a On the special events of March 1966, Ann. Geophys., 25, fasc. 1, 135-146.

BALLARIO, M. C. 1969b The IQSY 27-day recurrence sequence for 1964, Mem. SAIt., 40, fasc. 3, 271-294.

BALLARIO, M. C. 1970a Solar and geomagnetic events of the year 1968, Ann. Geophys., 26, 459-473.

BALLARIO, M. C. 1970b On the solar and geomagnetic events of Oct.-Nov., 1968, World Data Center A Upper Atmosphere Geophysics Report UAG-8, 231-238.

BALLARIO, M. C. 1971 March 1970: Solar and geomagnetic events, World Data Center A Upper Atmosphere Geophysics Report UAG-12, Part III, 349-358.

BALLARIO, M. C. 1972 On the geomagnetically active flares of September 1963, Mem. SAIt., in press.

Table 1

CMPs of plages recorded during the interval Aug. 14 - Sept. 20, 1971 and their subdivision into positive and negative plages.

Mc Math Data						Characteristics	Remarks (group types from Fraunhofer Institut solar maps)
CMP 1971	Lat.	Hel. long.	McMath plage number	Return of region	Age		
Aug.							
14.2	N14	36°	11471	New	1	non-rec. negative	- -
14.3	N07	35	11466	11425	2	recurrent "	E groups in the prec.rot.
14.7	N31	29	11476	New	1	non-rec. "	- -
15.8	S14	15	11474	New	1	rec. positive	Eastern A group
15.9	N08	14	11473	11429	2	rec. negative	J groups in the prec.rot.
16.4	N17	7	11483	New	1	non-rec. "	- -
16.4	N04	7	11485	New	1	non-rec. "	- -
16.5	S03	6	11481	New	1	non-rec. "	- -
16.9	S16	0	11472	11432	3	rec. "	C groups in the prec.rot.
17.7	N14	350	11467	11433	4	rec. "	E,J groups in prec.rot.
18.7	S08	336	11475	11434	2	rec. positive	No spots
18.7	N48	336	11477	New	1	non-rec. negative	- -
20.3	N15	315	11478	11438	3	rec. "	D,C groups in the prec.rot
22.1	N17	292	11480	11438	3	rec. "	- -
23.8	S12	269	11482	11445	2	rec. "	Eastern E groups
26.2	S12	237	11484	11442	3	rec. "	Eastern C groups
27.8	N09	216	11493	New	1	non-rec. "	- -
29.4	N06	195	11486	11447	2	rec. "	C groups in the prec.rot.
29.6	S16	193	11487	New	1	rec. positive^{+}(a)	A spots
Sept.							
2.1	N11	146	11489	11465	2	rec. negative	C groups in the prec.rot.
2.5	S11	141	11490	11455	3	rec. "	D groups in the prec.rot.
3.5	N13	128	11491	11456	2	rec. "	D groups in the prec.rot.
3.5	N03	128	11499	New	1	rec. positive	Rising in the W hemisph.
4.2	S06	119	11496	New	1	prob.rec. negative	Eastern C groups
5.8	S11	97	11492	11457	4	rec. "	E groups in the prec.rot.
5.8	N17	97	11498	New	1	rec. positive	Eastern A,B groups
6.2	N03	92	11495	New	1	non-rec. negative	- -
7.0	S14	82	11507	New	1	non-rec. "	- -
7.1	N21	80	11494	11479	2	rec. "	J groups in the prec.rot.
7.2	S19	79	11505	New	1	non-rec. "	- -
9.5	N13	49	11512	New	1	non-rec. "	- -
9.6	N03	47	11500	New	1	non-rec. "	- -
9.9	S09	43	11510	New	1	non-rec. "	- -
10.4	N24	37	11502	New	1	non-rec. "	- -
10.6	N11	34	11520	New	1	non-rec. "	- -
11.2	N25	26	11513	New	1	non-rec. "	- -
11.3	N06	25	11517	New	1	non-rec. "	- -
11.4	N14	23	11508	New	1	non-rec. "	- -
11.6	S29	21	11503	New	1	non-rec. "	- -
11.7	S17	20	11504	11474	2	rec. "	C groups in the prec.rot.
12.1	N16	14	11501	11473	3	rec. "	J groups in the prec.rot.
13.1	S14	1	11506	New	1	rec. positive	Eastern B groups
13.9	N15	350	11509	11467	5	rec. negative	E groups in prec.rot.
15.0	N03	336	11521	New	1	non-rec. "	- -
15.2	S12	333	11529	New	1	non-rec. "	- -
16.2	N13	320	11511	New	1	rec. "	Eastern J groups
16.4	S27	318	11519	New	1	non-rec. "	- -

Table 1 continued

Mc Math Data						Characteristics	Remarks (group types from Fraunhofer Institut solar maps)
CMP 1971	Lat.	Hel. long.	McMath plage number	Return of region	Age		
Sept.							
16.8	S13	312	11522	New	1	non-rec. negative	- -
17.1	S18	308	11526	New	1	non-rec. "	- -
17.7	S05	300	11532	New	1	rec. positive+(b)	Rising in the W hemisph
18.2	N01	294	11518	New	1	non-rec. negative	- -
18.4	N14	291	11514	11480	4	rec. "	Eastern C groups
19.4	N05	278	11515	New	1	prob. rec. "	Eastern J groups
19.6	S13	275	11516	11482	3	rec. "	Eastern E,D groups

+(a) Plage 11487 at L = 193° is recurrent with the negative plage 11531 at S15 and L = 190° (see McMath footnotes in Solar Geophysical Data n° 327) CMP: Sept. 26.1

+(b) Plage 11532 at L = 300° is recurrent with the positive plage 11553 at S05 and L = 305° (see McMath footnotes in Solar Geophysical Data n° 327) CMP: Oct. 14.5

Table 2

Importance 2 flares and importance 1,S proton flares observed during the interval Aug. 14 - Sept. 20, 1971 (from Quarterly Bulletin on Solar Activity)

Date 1971	Time U.T.	Max U.T.	Position	Imp.	App. and corr. aerea	Charac.	McMath Region	Proposed correlation between Kp max. and flare max. (time-lag of about 2 days)
Aug.								
21	0930 0950	0936	09S-25E	1B	2.9 3.2	FHQUVW	11482	Kp max = 4+ on Aug. 23.1
22	0730 0817	0735 0752	09S-11E	1B	2.9 3.0	FHKUWZ	11482	Geomagnetically inactive
23	0719 0743	0727	10S-12E	SN	1.1 1.1	HU	11482	modest Kp fluctuation
30	0303 0410	0332	12S-87W	2F	1.9 -	-	11482	Kp max = 5 on Aug. 31.9
Sept.								
5	1323 1405	1329 1339	17S-05E	SN	1.7 1.7	HU	11492	Kp max = 4+ on Sept. 7.9
17	1400 1525	1415 1429	11S-21E	1B	2.6 2.7	FLU	11516	Modest Kp fluctuation
17	1544 1610	1549	17S-22E	1B	2.1 2.3	HRU	11516	
18	1330 1410	1338	03N-08E	SB	1.6 1.6	EUZ	11545	Kp max = 4 on Sept. 20.7
19	1122 1212	1132	10S-04W	SN	1.4 1.4	KU	11516	Geomagnetically inactive

ACKNOWLEDGEMENTS

This Report would not have been possible without the many contributions from the worldwide scientific community.

ALPHABETICAL INDEX

	Page JAN	SEPT
Airglow		
Thule	253	
Patrol Spectrograph Thule	259	
Aurora		
All Sky Camera		
Thule	253	
Loparskaya	247	
Auroral Absorption (AA)	249	444
Auroral Electrojet	291	
HILDA's (High Latitude Discrete Auroras)	259	
Patrol Spectrograph	247	
Photometer	247	
Calcium Plage Data	1	299
Manila Observatory	38	
Faculae - Catania, Rome	7	
Cosmic Rays	134, 171, 178	370, 396
Cut-offs	182	
Intensity-Time Profile	192	
Neutron Monitor Stations:		
Alert	90, 134, 154, 171, 178, 265	265, 370, 389
Apatity	134, 154, 247	443
Belgrano	17, 134, 154	370
Bergen	134, 171, 188	370, 389, 400
Buenos Aires	17	370
Calgary	134, 171, 192	
Churchill	134, 154, 171, 178, 192	370, 389
Climax	134	
Dallas	134, 171, 178, 182, 240	182, 370, 389
Deep River	134, 154, 171, 178, 182, 192, 200, 236, 240	182, 370, 389, 429
Dourbes		432
Dumont d'Urville	134, 154, 171, 192	370, 389
Durham	134	370, 389
Goose Bay	134, 154, 171, 178	370, 389
Heiss Island	154	
Hermanus	134	
Huancayo	134	
Inuvik	134, 154, 171, 178	370, 389
Irkutsk	134, 178	396
Jungfraujoch		370
Khabarovsk	178	396
Kiel	134, 171, 192	370, 389, 432
Kiruna	134, 154, 171, 192	370, 389
Leeds	134, 171, 182	182, 370
Lindau	134, 182	182
Lomnicky Stit	134,	370
Magadan	134, 178	396
Mawson	154	
McMurdo	154, 171	389
Mexico City	134	370
Mirny	154	
Moscow	134	
Mt. Norikura	134	370
Mt. Washington	134	370, 389
Norilsk	134, 178	396
Novosibirsk	178	
Ottawa	134	370
Oulu	134, 154, 171, 192	370
Pic-du-Midi	134, 171, 240	182, 432
Port aux Francais (Kerguelen)	134, 154, 171, 182, 192	182, 370, 389
Predigstuhl	134	370

	Page JAN	SEPT
Cosmic Rays (continued)		
Neutron Monitor Stations (continued)		
Resolute	154	
Rome	134	
Sanae	134, 154	370
South Pole	154, 171	389
Sulphur Mt.	134, 154, 171, 192	370, 389
Swarthmore	171	389
Syowa Base	134, 154	370
Thule	154, 171	389
Tixie Bay	134, 154, 178	370, 396
Tokyo/Itabashi	134	370
Uppsala	134, 171, 192	
Ushuaia	134	370
Utrecht	134, 192	370, 389
Vostok	154	
Yakutsk	178	396
Rigidity Spectrum	192	
Scintillation Monitor, Bologna	197	401
Trajectories	154	154
Cosmic Noise Absorption (CNA)	210, 249	410, 444
Forbush Decrease	115, 178, 247, 290	432
Geomagnetic		
Fraunhofer Institute Maps	43, 271, 277	277, 311, 451
Göttingen Daily Geomagnetic Character Figures	43	311
Indices:		
Ap	242	432
C9	43	311
Dst	261	450
K	262, 283	446
Kp	122, 208, 223, 224, 234, 238, 242, 264, 268, 271 290	264, 269, 427, 432, 440, 451
Pulsations	252, 283, 287	
Sudden Commencements:		
0430 UT Jan 27	102, 122, 217, 223, 244, 279, 283, 290	
1646 UT Sept 4		102, 283, 302, 367, 408, 417, 430, 440, 444
Variations:		
Abisko	287, 290	
Alert	287, 290	
Baker Lake	287, 290	
Budkov	283	
Churchill	287, 290	
College	6, 287, 290	
Dixon Island	290	
Dõmbas	287	
Fredericksburg	290	
Great Whale River	6, 287, 290	
Godhavn	290	
Hermanus	261	450
Honolulu	6, 261, 287, 290	450
Kakioka	6, 261	450
Kiruna	220, 287	422
Leirvogur	6, 287, 290	
Manila	279	
Meanook	6, 287, 290	
Mould Bay	287, 290	
Murmansk	247	443
Narssarssuaq	290	
Ottawa	287, 290	
Point Barrow	290	
Průhonice	283	
Resolute Bay	287, 290	
San Juan	6, 261, 287, 290	450
Sitka	287, 290	
St. John's	287	
Tangerang	6	

	Page JAN	SEPT
Geomagnetic(continued)		
Variations (continued)		
Tucson	287, 290	
Victoria	287, 290	
Hα Faculae: Catania, Tome	7	
Hα Plage		
Observatories:		
Big Bear	31	
Boulder	19, 26	
Canary Islands		303
Goto Optical Company	34	
Haleakala	28	
Manila	38	
Pasadena	31	
Ramey	19, 26	303
Tokyo Astronomical Obs.	34	
Synoptic Chart	26	303
Interplanetary Magnetic Field	89, 130	
Ionosphere		
Blanketing Frequencies		444
F2-layer Evolution, Sofia	240	
foF2	224	
Kiruna	216	417
Lycksele	216	417
Manila	229	
Maynard	226	
Prøhonice		430
Sofia		436
Uppsala	216	417
f-plots		
Godhavn	210	410
Gothaab	210	410
Murmansk	247	443
Narssarsuaq	210	410
Sdr. Strømfjord	210	410
Station Nord	210	410
Thule	210	410
HF Absorption	222	410, 430
HF Doppler	200	
LF	222, 223	430
Propagation Paths:		
Aldra-Leicester		440
BPV-Kyoto	200	
GBR-Inubo	234	427
GBR-Manila	279	
GBR-Thule	202	424
Godthaab-Reersø		410
HAIKU-Kiruna	215	417
JG2AS-Akita	223	
JJY-Akita	223	
JJY-Kyoto	200	
NAA-Inubo	234	427
NAA-Kiruna	215	417
NAA-Leicester	237	
NAA-São Paulo		358
NDT-Manila	279	
NLK-Kiruna	215	417
NLK-Manila	279	
NLK-São Paulo		358
NPG-Thule	202	424
Trinidad-Leicester	237	440
WWVL-Inubo	234	427
WWV-Reersø		410
Riometer Absorption:		
Anderma	207	
Byrd	205	
Cape Zhelaniya	207	
Dixon Island	207	407
ESRANGE	215	417
Godhavn	72, 210	410

	Page JAN	SEPT
Ionosphere (continued)		
Riometer Absorption (continued)		
Gothaab	210	410
Heiss Island	207	
Kiruna	215	417
McMurdo Sound	204	404
Mirny	207	407
Molodezhnaya	207	407
Murmansk	247	443
Narssarssuaq	210	410
North Pole	207	407
Salekhard	207	407
Sdr. Strømfjord	210	410
Shepherd's Bay	72, 204	404
South Pole	205	
Station Nord	210	410
Thule	203, 210	406, 410
Vostok	205, 207	407
SFD	200	
SPA	202	424
TEC, Sagamore Hill	233	426
TID	223	
VLF	202, 215, 222, 234, 237	358, 417, 424, 427, 432, 440
VHF	233	426
McMath Regions:		
11089	21	
11091	21	
11128	1, 7, 15, 19, 26, 28, 31, 38, 51, 58, 71, 102, 236, 279, 287, 290	
11129	7, 280	
11130	7, 280	
11445		299, 303
11482		102, 299, 303, 318, 329, 348, 349
11496		299
11516		329
Mt. Wilson Magnetograms	2, 43	300, 311
PCA	205, 207, 240, 249	348, 407, 410, 444
PCD		427
Plage -- see Calcium or Hα Plage		
Positive and Negative	270	449
Rocket, Kiruna	189	
Satellite and Space Probe Observations:		
International Designation - Name		
1964-40A Vela 3	242, 265	264, 407
1965-58A Vela 5	242, 265	264, 407
1965-105A Pioneer 6	111, 265	264
1966-58A Explorer 33		367
1966-75A Pioneer 7	111, 265	264
1966-110A ATS-1	205, 238, 242, 259	435, 440
1967-70A IMP V (Explorer 35)	58, 102	
1967-111A ATS-3	233	
1967-123A Pioneer 8	111, 130	
1968-14A OGO-5	113	
1968-17A SOLRAD 9 (Explorer 37)	58, 100	322, 362
1968-100A Pioneer 9	111	
1969-46B OV5-6	120	365
1969-53A IMP-G (Explorer 41)	122, 126, 207, 242, 259	
1971-19A IMP-I (Explorer 43)		353
1971-58A SOLRAD 10 (Explorer 44)		362
Solar		
Alpha Particles	102, 120, 122, 128, 189	365
Corona	43, 58, 89, 93	311, 318
Coronal Holes		323
Electrons	102, 113, 126	
Evolution of Active Region	7, 15, 19, 26, 28, 31, 43	303, 311, 319
Evolution of Flare	34	

	Page JAN	SEPT
Solar (continued)		
Flares		
Jan 24	3, 15, 19, 28, 31, 34, 38, 43, 51, 58, 69, 71, 89, 93, 98, 102, 244, 279, 287, 290	431
Sept 1		299, 303, 311, 348 353, 362, 431
July, 1966	21	
Sept, 1966	17	
May, 1967	21	
Nov, 1969	21	431
March, 1970	21	431
Indices		
Daily Flare Index		322
Long Wavelength Spectral Index		322
Short Wavelength Spectral Index		322
Loop Prominences	28, 34, 51	
Magnetic Field	19, 26, 43, 51	303, 311, 329
Photoheliograph, Tel Aviv	31	
Protons	102, 113, 120, 122, 127, 189, 236, 279	365, 427
Radio		
Bursts	28, 69, 71, 75, 77, 84, 86, 89, 93, 98, 102, 236, 281	327, 346, 348, 349, 353, 358, 429
Emission	4, 61, 64, 75, 200	302, 319, 325, 327, 329, 334, 338, 349
Observatories		
AFCRL		327
Boulder		319
Clark Lake	98	
Culgoora	69, 86, 89, 93	346
Fleurs		319, 329
Harvard Radio Astronomy Station	69, 86	346
Heinrich Hertz Institute	61	334
Itapetinga		358
Kyoto	200	
Manila	71, 84	
Ondrejov	77	
Penn State Univ. Radio Astronomy Observatory (PSURAO)		327
Penticton	71	
Prospect Hill		319
Sagamore Hill	71, 77, 236	348, 353, 429
Stanford	58	319, 329
Thule		348
Toyokawa	75, 89, 200, 236	
Trieste		349
Polarization	61, 75	318, 334, 349
Spectral Events	4, 69, 89, 93, 98, 281	302, 327, 346, 353
S-Component	61	334
Ultraviolet Emission	282	362
Wind	264	264, 367
X-Rays	5, 58, 100, 102, 236, 280	300, 322, 362
Sudden Ionospheric Disturbances	3, 200, 222, 225, 279	
Sunspots	15, 19, 28, 38	303, 316
Data	1, 7, 15, 19, 31	299
Numbers	3	299
Maps	10, 19	
Observatories		
Baguio	38	
Canary Islands		303
Culgoora		303
Manila	38, 200	
Ondrejov		316
Sac Peak	19	303
San Miguel	15	
Whistlers, Panská Ves	222	431

AUTHOR INDEX

	Page
Amundsen, R.	188, 400
Ananthakrishnan, S.	358
Arens, M.	192
Asakura, T.	234, 427
Attolini, M. R.	197, 401
Badillo, V. L.	84
Balboa, D.	38
Ballario, M. C.	271, 451
Barron, W. R.	71, 348
Basu, D.	358
Bednárová-Nováková, B.	277
Bibl, K.	226
Binsack, J. H.	367
Böhme, A.	61, 334
Bracewell, R. N.	325
Bridge, H. S.	367
Brunelli, B. E.	247, 443
Buck, R. M.	113
Bumba, V.	43, 311
Castelli, A.	130
Chapman, J. W.	237, 440
Chirkov, N. P.	178, 396
Coffey, H. E.	1, 134, 299, 370
Cormier, R. J.	203, 406
D'Arcy, R. G., Jr.	113
de Feiter, L. D.	192
Deuter, J. H.	325
Driatsky, V. M.	207, 407
Duggal, S. P.	171, 389
Ecklund, W. L.	205
Énomé, S.	75
Evans, R. E.	237, 440
Evlashin, L. S.	247, 443
Fiandri, L.	197, 401
Filippov, A. T.	178, 396
Galli, M.	197, 401
Godoli, G.	7
Gupta, J. C.	287, 290
Hakura, Y.	234, 427
Halenka, J.	268
Hall, W. N.	259
Hanser, F. A.	120, 365
Hempe, H.	189
Hennessey, J. J.	229
Heristchi, Dj.	182
Heyden, F.	38
Horan, D. M.	100, 362
Howe, H. C.	367
Ipatjev, V. I.	178
Isaev, S. I.	247, 443
Ishii, T.	234, 427
Jensen, V. N.	210, 410
Jiricek, F.	222, 430
Jongen, H. F.	192
Jurén, C.	215, 417
Kelley, J. G.	120, 365
Klobuchar, J. A.	233, 426
Kohl, J. W.	122
Krajcovic, S.	264
Kreplin, R. W.	100, 362
Krüger, A.	61, 334
Lanzerotti, L. J.	126
Lastovicka, J.	222, 430
Lazutin, L. L.	247, 443
Loginov, G. A.	247, 443
Loomer, E. I.	290
Lund, D. S.	318
Machado, M. E.	15
Maclennan, C. G.	126
Mariani, F.	130
Masley, A. J.	204, 404
Maxwell, A.	69, 346
McCabe, M.	28
McDonald, F. B.	102
McIntosh, P. S.	19, 26, 303
Mellone, M. E. Z.	358
Mendillo, M. J.	233, 426
Moore, J. G.	253
Moriyama, F.	34
Ness, N. F.	130
Nestorov, G.	240, 432
Novikov, A. M.	396
Ogawa, T.	200
Olmr, J.	77
Palmer, I. D.	86, 89
Peraza, J. Pérez	182
Petrova, G. A.	247, 443
Piazza, L. R.	358
Pomerantz, M. A.	171, 389
Prikner, K.	283
Rafael, F., Jr.	229
Retallack, W. M.	205
Riddle, A. C.	86, 89, 93
Roldugin, V. K.	247, 443
Rust, D. M.	51
Sakurai, K.	98, 353
Salcedo, J. E.	279
Santin, P.	349
Sauer, H. H.	205
Sciuto, V.	7
Sellers, B.	120, 365
SenGupta, P. R.	58
Shea, M. A.	154
Sheridan, K. V.	93
Shulgina, N. V.	247, 443
Skolnik, J.	192
Skripin, G. V.	178, 396
Smart, D. F.	154
Smerd, S. F.	89
Starkov, G. V.	247, 443
Sturiale, M. L.	7
Sugiura, M.	261, 450
Svennesson, J.	215, 417
Sýkora, J.	43, 311
Taagholt, J.	210, 410
Takenoshita, Y.	223
Tanaka, H.	75
Taylor, R. G.	100, 362
Telford, L. E.	64, 338
Terajima, Y.	234, 427
Tlamicha, A.	77
Todikov, G. G.	178, 396
Totunova, G. F.	247, 443
Trefall, H.	188, 400
Triska, P.	222, 430
Trottet, G.	182
Tsutsui, M.	200
Turtle, J. P.	202, 424
Ulyev, V. A.	207, 407
Van Hollebeke, M.	102
van Sabben, D.	262, 446
Vasheniuk, E. V.	247, 443
Velinov, P.	240, 432
Walton, J. R.	113
Wang, J. R.	102

	Page
Wefer, F. L.	327
West, H. I., Jr.	113
Witte, M.	189
Yates, G. K.	120, 365
Zappala, R. A.	7
Zirin, H.	31

Publication Notice

WORLD DATA CENTER A for SOLAR-TERRESTRIAL PHYSICS REPORT UAG
(Prepared by World Data Center A for Solar-Terrestrial Physics, NOAA, Boulder, Colorado)

These reports are for sale through the National Climatic Center, Federal Building, Asheville, NC 28801, Attn: Publications. Subscription price: $9.00 a year; $2.50 additional for foreign mailing; single copy price varies. These reports are issued on an irregular basis with 6 to 12 reports being issued each year. Therefore, in some years the single copy rate will be less than the subscription price, and in some years the single copy rate will be more than the subscription price. Make checks and money orders payable to: Department of Commerce, NOAA.

Upper Atmosphere Geophysics Report UAG-1, "IQSY Night Airglow Data" by L. L. Smith, F. E. Roach and J. M. McKennan of Aeronomy Laboratory, ESSA Research Laboratories, July 1968, single copy price $1.75.

Upper Atmosphere Geophysics Report UAG-2, "A Reevaluation of Solar Flares, 1964-1966" by Helen W. Dodson and E. Ruth Hedeman of McMath-Hulbert Observatory, The University of Michigan, August 1968, single copy price 30 cents.

Upper Atmosphere Geophysics Report UAG-3, "Observations of Jupiter's Sporadic Radio Emission in the Range 7.6-41 MHz, 6 July 1966 through 8 September 1968" by James W. Warwick and George A. Dulk, Department of Astro-Geophysics, University of Colorado, October 1968, single copy price 30 cents

Upper Atmosphere Geophysics Report UAG-4, "Abbreviated Calendar Record 1966-1967" by J. Virginia Lincoln, Hope I. Leighton and Dorothy K. Kropp, Aeronomy and Space Data Center, Space Disturbances Laboratory, ESSA Research Laboratories, January 1969, single copy price $1.25.

Upper Atmosphere Geophysics Report UAG-5, "Data on Solar Event of May 23, 1967 and its Geophysical Effects" compiled by J. Virginia Lincoln, World Data Center A, Upper Atmosphere Geophysics, ESSA, February 1969, single copy price 65 cents.

Upper Atmosphere Geophysics Report UAG-6, "International Geophysical Calendars 1957-1969" by A. H. Shapley and J. Virginia Lincoln, ESSA Research Laboratories, March 1969, single copy price 30 cents.

Upper Atmosphere Geophysics Report UAG-7, "Observations of the Solar Electron Corona: February 1964-January 1968" by Richard T. Hansen, High Altitude Observatory, Boulder, Colorado and Kamuela, Hawaii, October 1969, single copy price 15 cents.

Upper Atmosphere Geophysics Report UAG-8, "Data on Solar Geophysical Activity October 24-November 6, 1968", Parts 1 and 2, compiled by J. Virginia Lincoln, World Data Center A, Upper Atmosphere Geophysics, ESSA, March 1970, single copy price (includes Parts 1 and 2) $1.75.

Upper Atmosphere Geophysics Report UAG-9, "Data on Cosmic Ray Event of November 18, 1968 and Associated Phenomena" compiled by J. Virginia Lincoln, World Data Center A, Upper Atmosphere Geophysics, ESSA, April 1970, single copy price 55 cents.

Upper Atmosphere Geophysics Report UAG-10, "Atlas of Ionograms" edited by A. H. Shapley, ESSA Research Laboratories, May 1970, single copy price $1.50

Upper Atmosphere Geophysics Report UAG-11, "Catalogue of Data on Solar-Terrestrial Physics", compiled by J. Virginia Lincoln and H. Patricia Smith, World Data Center A, Upper Atmosphere Geophysics, ESSA, June 1970, single copy price $1.50.

Upper Atmosphere Geophysics Report UAG-12, "Solar-Geophysical Activity Associated with the Major Geomagnetic storm of March 8, 1970", Parts 1, 2 and 3, compiled by J. Virginia Lincoln and Dale B. Bucknam, World Data Center A, Upper Atmosphere Geophysics, NOAA, April 1971, single copy price (includes Parts 1-3) $3.00.

Upper Atmosphere Geophysics Report UAG-13, "Data on the Solar Proton Event of November 2, 1969 through the Geomagnetic Storm of November 8-10, 1969", compiled by Dale B. Bucknam and J. Virginia Lincoln, World Data Center A, Upper Atmosphere Geophysics, NOAA, May 1971, single copy price 50 cents.

Upper Atmosphere Geophysics Report UAG-14, "An Experimental Comprehensive Flare Index and its Derivation for 'Major' Flares 1955-1969", by Helen W. Dodson and E. Ruth Hedeman, McMath-Hulbert Observatory, University of Michigan, July 1971, single copy price 30 cents.

Upper Atmosphere Geophysics Report UAG-15, "Catalogue of Data on Solar-Terrestrial Physics", prepared by Research Laboratories, NOAA, Boulder, Colorado, July 1971, single copy price $1.50. (Supersedes Report UAG-11, June 1970.)

Upper Atmosphere Geophysics Report UAG-16, "Temporal Development of the Geographical Distribution of Auroral Absorption for 30 Substorm Events in each of IQSY (1964-65) and IASY (1969)" by F. T. Berkey, V. M. Driatskiy, K. Henriksen, D. H. Jelly, T. I. Shchuka, A. Theander and J. Yliniemi, September 1971, single copy price 70 cents.

Upper Atmosphere Geophysics Report UAG-17, "Ionospheric Drift Velocity Measurements at Jicamarca, Peru (July 1967 - March 1970)", by Ben B. Balsley, Aeronomy Laboratory, National Oceanic and Atmospheric Administration, Boulder, Colorado, and Ronald F. Woodman, Jicamarca Radar Observatory, Instituto Geofisico del Perú, Lima, Peru, October 1971, single copy price 35 cents.

Upper Atmosphere Geophysics Report UAG-18, "A Study of Polar Cap and Auroral Zone Magnetic Variations", by K. Kawasaki and S. I. Akasofu, Geophysical Institute, University of Alaska, June 1972, single copy price 20 cents.

Upper Atmosphere Geophysics Report UAG-19, "Reevaluation of Solar Flares 1967", by Helen W. Dodson and E. Ruth Hedeman of McMath-Hulbert Observatory, The University of Michigan, and Marta Rovira de Miceli, San Miguel Observatory, Argentina, June 1972, single copy price 15 cents.

Report UAG-20, "Catalogue of Data on Solar-Terrestrial Physics", prepared by Environmental Data Service, NOAA, Boulder, Colorado, October 1972, single copy price $1.50 (supersedes Report UAG-15, 1971.)

Report UAG-21, "Preliminary Compilation of Data for Retrospective World Interval July 26 - August 14, 1972", compiled by J. Virginia Lincoln and Hope I. Leighton, WDC-A for Solar-Terrestrial Physics, November 1972, single copy price 70 cents.

Report UAG-22, "Auroral Electrojet Magnetic Activity Indices (AE) for 1970", by Joe Haskell Allen, National Geophysical and Solar-Terrestrial Data Center, Environmental Data Service, November 1972, single copy price 75 cents.

Report UAG-23, "U.R.S.I. Handbook of Ionogram Interpretation and Reduction", Second Edition, November 1972, edited by W. R. Piggott, Radio and Space Research Station, Slough, U.K., and K. Rawer, Arbeitsgruppe für Physikalische Weltraumforschung, Freiburg, G.F.R., November 1972, single copy price $1.75.

USCOMM-NOAA-ASHEVILLE,NC-1-73-1325